University of São Paulo
"Luiz de Queiroz" College of Agriculture

Emerging technologies to improve food drying: ultrasound and ethanol on convective and infrared drying

Meliza Lindsay Rojas Silva

Thesis presented to obtain the degree of Doctor in Science. Area: Food Science and Technology

Piracicaba
2019

Meliza Lindsay Rojas Silva
Agroindustrial Engineering

Emerging technologies to improve food drying: ultrasound and ethanol on convective and infrared drying

Advisor:
Prof. Dr. **PEDRO ESTEVES DUARTE AUGUSTO**

Thesis presented to obtain the degree of doctor in Science. Area: Food Science and Technology

Piracicaba
2019

Dados Internacionais de Catalogação na Publicação
DIVISÃO DE BIBLIOTECA – DIBD/ESALQ/USP

Rojas Silva, Meliza Lindsay

Emerging technologies to improve food drying: ultrasound and ethanol on convective and infrared drying / Meliza Lindsay Rojas Silva. - - Piracicaba, 2019.

160 p.

Tese (Doutorado) - - USP / Escola Superior de Agricultura “Luiz de Queiroz”.

1. Secagem convectiva 2. Secagem por infravermelho 3. Ultrassom 4. Etanol. 5. Propriedades dos alimentos I. Título

A mis seres queridos,

Dedico.

ACKNOWLEDGMENTS

First, I would like to thank the institutions, laboratories and financing agencies that made the development of this Thesis possible.

To the University of São Paulo (USP) - Luiz de Queiroz College of Agriculture (ESALQ) - Department of Agri-food Industry, Food and Nutrition (LAN). For allowing me to do my postgraduate studies in the Food Process Engineering Research Group ($\mathrm{Ge}^2\vec{\mathrm{P}}$).

To the Universitat Politècnica de València (UPV)- Departamento de Tecnología de Alimentos. For allowing me to do my doctoral mobilization period in the “Grupo de Análisis y Simulación de Procesos Agroalimentarios (ASPA)”.

To the Technology Center of Cereal and Chocolate, Food Technology Institute (ITAL), and to the “Laboratório de Análise de Imagens” (LPV-ESALQ/USP) for the provided support.

Special thanks to my doctoral studies scholarship provided by FONDECYT (Fondo Nacional de Desarrollo Científico, Tecnológico y de Innovación Tecnológica), through the Contract 087-2016-FONDECYT, Perú.

To the São Paulo Research Foundation (FAPESP, Brasil) for funding grant nº 2016/18052-5.

To the National Council for Scientific and Technological Development (CNPq, Brasil) for funding grant nº 401004/2014-7.

To the Coordination for the Improvement of Higher Education Personnel (CAPES), for the provided support through the daily aid funds that made it possible to participate in scientific events.

Next, I would like to express my thanks to all professionals who helped me directly or indirectly.

My very special thanks to my advisor Prof. Pedro Esteves Duarte Augusto for allowing me to be part of the $\mathrm{Ge}^2\vec{\mathrm{P}}$ research group, for the confidence provided, constant academic support, patience, for his enthusiasm and constant motivation. Thank you for being a personal and professional example, to you my consideration, gratitude, respect and admiration.

To the Prof. Juan Andrés Cárcel Carrion, for receiving me in his research group (ASPA), for the trust placed and for all the academic support provided. Thanks to all the members of the ASPA group, especially to Beatriz, Ramón and Virginia for the support provided. And, to all the foreign members with whom I had the pleasure of agreeing, especially to Carlota, Ingrid, Liliana and Silvana.

To all my co-authors for their important contributions to this research.

To all actual and past members of my research group ($\mathrm{Ge}^2\vec{\mathrm{P}}$), specially to Carlota, Claudio, Dâmaris, Gisandro, Isabela, Jaqueline, Karla, Karoline, Manoel, Mirian, Nanci and Stephanie.

My special thanks to Claudio for being the first person to invite me to come to Brazil, for all their support and friendship provided. And to Nanci Castanha for being the best friend I could have found here, thanks for talking to me even when I didn't speak Portuguese, for helping me whenever I needed and for sharing good and bad times. Nancy Castañita, always remember that in the end “tudo da certo”.

To all the “Peruanitos” because despite being from the same country it was here that we were able to meet and share very pleasant moments these years. Thank you Carmencita, Darío, Erick, Fernando, Melina and Rafael, it has been a pleasure, his companionship and friendship made me feel at home, in our Perú.

To my parents Felipcina Silva and Luis Rojas, for their trust, sacrifice, motivation and love. And to my whole family, especially to my grandparents, aunts and uncles for all their provided support since I was born until now.

”Nothing in life is to be feared, it is only to be understood.

Now is the time to understand more, so that we may fear less”

Maria Skłodowska-Curie (1867 – 1934)

SUMMARY

RESUMO

Tecnologias emergentes para melhoria da secagem de alimentos: ultrassom e etanol na secagem convectiva e por infravermelho

Apesar da secagem ser um dos métodos mais antigos de conservação, ainda há diversas limitações relacionadas à qualidade dos alimentos secos (propriedades físicas, químicas e nutricionais), bem como relacionadas à qualidade dos processos (consumo energético e custos). A presente Tese teve como objetivo estudar a aplicação de tecnologias emergentes para melhorar a secagem de alimentos. Para esse fim, diferentes abordagens, como análises de microestrutura, avaliação de cinéticas e análises físico-químicas foram utilizadas para descrever o processo, as propriedades e a composição dos alimentos. Em primeiro lugar, a influência dos elementos que compõem a microestrutura de vegetais foi estudada em relação à transferência de água e às propriedades físicas. Com base nos resultados obtidos, avaliou-se o efeito das aplicações de tecnologias emergentes (etanol, ultrassom e perfurações mecânicas), como pré-tratamentos do processo de secagem (por convecção, infravermelho e secagem assistida por ultrassom), bem como nas propriedades físicas dos alimentos e sua composição. Finalmente, os pré-tratamentos utilizados para melhorar a secagem foram empregados para incorporar nutrientes microencapsulados (hidrofílicos e lipofílicos) nos produtos a serem secos, com objetivo de melhorar o conteúdo nutricional. Os resultados mostraram que os alimentos, devido à sua estrutura complexa, são materiais não isotrópicos e que seus elementos microestruturais influenciam os fenômenos de transferência de água. Os pré-tratamentos propostos diminuíram o tempo de secagem convencional. Possíveis mecanismos responsáveis pelas melhorias observadas foram formulados, com base em observações macro e microestruturais, bem como nos parâmetros cinéticos que descrevem a secagem. Além disso, outros resultados foram destacados, como diminuição do consumo energético, melhoria na reidratação sem alterações negativas na viscoelasticidade e deformação, melhor retenção e incorporação de nutrientes. Em resumo, o presente trabalho pretende contribuir com a compreensão da secagem de alimentos e suas implicações, além de fornecer alternativas para sua possível melhoria.

Palavras-chave: Secagem convectiva, Secagem por infravermelho, Ultrassom, Etanol, Propriedades dos alimentos

ABSTRACT

Emerging technologies to improve food drying: ultrasound and ethanol on convective and infrared drying

Although food drying is one of the oldest preservation methods, there are still several limitations related with the quality of dried products (physical, chemical and nutritional properties), as well as related to the quality of processes (energy consumption and costs). The present thesis studied the application of different emerging technologies to improve food drying. For this purpose, different approaches such as microstructural study, kinetic evaluation, and physicochemical analyses were used to describe the process, food properties and composition. Firstly, the influence of elements that compose the plant microstructure was studied on relation to water transfer and physical properties. Based on the obtained results, it was evaluated the effect of emerging technologies (ethanol, high-power ultrasound and mechanical perforations) application as pre-treatments to the drying process (convective, infrared and ultrasound-assisted drying), as well as, on the food physical properties and composition. Finally, the pre-treatments used to improve drying was also used to incorporate microencapsulated nutrients (both hydrophilic and lipophilic) into the products to be dried, thus obtaining dry vegetable with improved nutritional content. The results show the complex structure of foods make them non-isotropic materials, where its microstructural elements influence the water transfer phenomena. The proposed pre-treatments reduced the conventional drying time. Different mechanisms responsible for improvements through the application of pre-treatments were formulated, based on macro and microstructural observations, as well as in the kinetic parameters describing the drying behaviour. Besides, other notable results were obtained, such as the decrease in energy consumption, improvements in the rehydration properties without negative changes in viscoelasticity and deformation, as well as better retention and incorporation of nutrients. Summarizing, this work intends to be a contribution to the better understanding of food drying and its implications, as well as to provide alternatives for its possible improvement.

Keywords: Convective drying, Infrared drying, Ultrasound, Ethanol, Food properties

RESUMEN

Tecnologías emergentes para mejorar el secado de alimentos: ultrasonido y etanol en el secado convectivo e infrarrojo

El secado de alimentos, a pesar de ser uno de los métodos de conservación más antiguo, aún presenta diversas limitaciones relacionadas a la calidad de los productos (propiedades físicas, químicas y nutricionales) y a la calidad del proceso (consumo energético y costos). En la presente tesis se estudió la aplicación de tecnologías emergentes para mejorar el secado de alimentos. Para ello, se utilizó diferentes enfoques tales como el estudio de microestructura, evaluación de cinéticas, y análisis fisicoquímicos, para describir el proceso, las propiedades y composición de los alimentos. En primer lugar, se estudió la influencia de elementos que conforman la microestructura de los alimentos vegetales en la transferencia de agua y en las propiedades físicas. Teniendo en cuenta los resultados, se evaluó el efecto de la aplicación de tecnologías emergentes (etanol, ultrasonido de alta potencia y perforaciones mecánicas) como pre-tratamientos del proceso de secado (convectivo, infrarrojo y secado asistido por ultrasonido), así como el efecto en las propiedades físicas y en la composición de los alimentos. Finalmente, los pre-tratamientos utilizados para mejorar el secado, se utilizaron también para realizar la incorporación de nutrientes microencapsulados en los productos a ser secados. Los resultados demostraron que la estructura compleja de los alimentos hace que sean materiales no-isotrópicos, donde sus elementos microestructurales influencian en el transporte de agua. Los pre-tratamientos propuestos redujeron el tiempo de secado convencional. Diferentes mecanismos de mejora mediante la aplicación de dichos pre-tratamientos fueron formulados basados en observaciones de macro y microestructura, así como en los parámetros cinéticos que describieron el comportamiento de secado. Además, otros resultados sobresalientes fueron obtenidos, como disminución del consumo energético, mejoras en las propiedades de rehidratación sin cambios negativos en la viscoelasticidad y deformación, mejor retención e incorporación de nutrientes también fueron obtenidos. Este trabajo pretende ser una contribución a la comprensión del secado de alimentos y sus implicaciones, así como brindar alternativas para su posible mejora.

Palabras clave: Secado convectivo, Secado por infrarrojo, Ultrasonido, Etanol, Propiedades de los alimentos

RESUM

Tecnologies emergents per a millorar l'assecat d'aliments: ultrasò i etanol en l'assecat convectiu i infraroig

L'assecat d'aliments, malgrat ser un dels mètodes de conservació més antic, encara presenta diverses limitacions relacionades a la qualitat dels productes (propietats físiques, químiques i nutricionals) i a la qualitat del procés (consum energètic i costos). En la present tesi es va estudiar l'aplicació de tecnologies emergents per a millorar l'assecat d'aliments. Per a això, es va utilitzar diferents enfocaments tals com l'estudi de microestructura, avaluació de cinètiques, i anàlisis fisicoquímiques, per a descriure el procés, les propietats i composició dels aliments. En primer lloc, es va estudiar la influència d'elements que conformen la microestructura dels aliments vegetals en la transferència d'aigua i en les propietats físiques. Tenint en compte els resultats, es va avaluar l'efecte de l'aplicació de tecnologies emergents (etanol, ultrasò d'alta potència i perforacions mecàniques) com pre-tractaments del procés d'assecat (convectiu, infraroig i assecat assistit per ultrasò), així com l'efecte en les propietats físiques i en la composició dels aliments. Finalment, els pre-tractaments utilitzats per a millorar l'assecat, es van utilitzar també per a realitzar la incorporació de nutrients microencapsulats en els productes a ser assecats. Els resultats van demostrar que l'estructura complexa dels aliments fa que siguen materials no-isotròpics, on els seus elements microestructurals influencien en el transport d'aigua. Els pre-tractaments proposats van reduir el temps d'assecat convencional. Diferents mecanismes de millora mitjançant l'aplicació de dits pre-tractaments van ser formulats basats en observacions de macro i microestructura, així com en els paràmetres cinètics que van descriure el comportament d'assecat. A més, altres resultats excel·lents van ser obtinguts, com la disminució del consum energètic, millores en les propietats de rehidratació sense canvis negatius en la viscoelasticitat i deformació, millor retenció i incorporació de nutrients també van ser obtinguts. Aquest treball pretén ser una contribució a la comprensió de l'assecat d'aliments i les seues implicacions, així com brindar alternatives per a la seua possible millora.

Paraules clau: Assecat convectiu, Assecat infraroig, Ultrasò, Etanol, Propietats dels aliments

FIGURE LIST

1. CONTEXTUALIZATION

The topic of this Thesis initiate when I was coursing the Master degree on the “Grupo de Estudos en Engenharia de Processos” (Ge²P) at ESALQ – USP, which was focused on study the application of high-power ultrasound technology (US) to improve the physical and enzymatic stability of peach juice and coconut water.

Although the topic of my master’s degree was not directly related to the current one, during this period I had the opportunity to participate in other studies from the group, one of them related to food drying (in fact, the first study of the group with this unit operation, as a prospection). Then, my first contact with drying process was the study conducted using the ultrasound as pre-treatment of carrot slices immersed in distilled water and then convectively dried (Ricce, Rojas, Miano, Siche, & Augusto, 2016).

Until that moment I mistakenly believed that drying was a simple and easy process to describe. However, I really perceived that drying is a complex process, with many phenomena occurring simultaneously in which influences both external factors and the food structure itself. This motivates us to go further and turning to dry as a focus of our research.

Food drying is an ancient method of food preservation. Basically, the climatic conditions have been used appropriately to obtain stable products available in times of scarcity. From then until today, drying is widely applied to obtain food products with longer shelf life, new forms of consumption, low cost of transportation and storage. However, the conventional drying methods based on using hot-air for a long time can deteriorate the quality of the final product (physicochemical and nutritional), as well as consuming a high amount of energy, with both economic and environmental impact.

Consequently, by combining the demand of obtaining dried foods of high quality, the need for improving the drying process, and our experience with the US technology, when I was finishing my master's degree (in September 2016), together with my advisor, we had the perfect subject to continue my doctorate: exploring food drying.

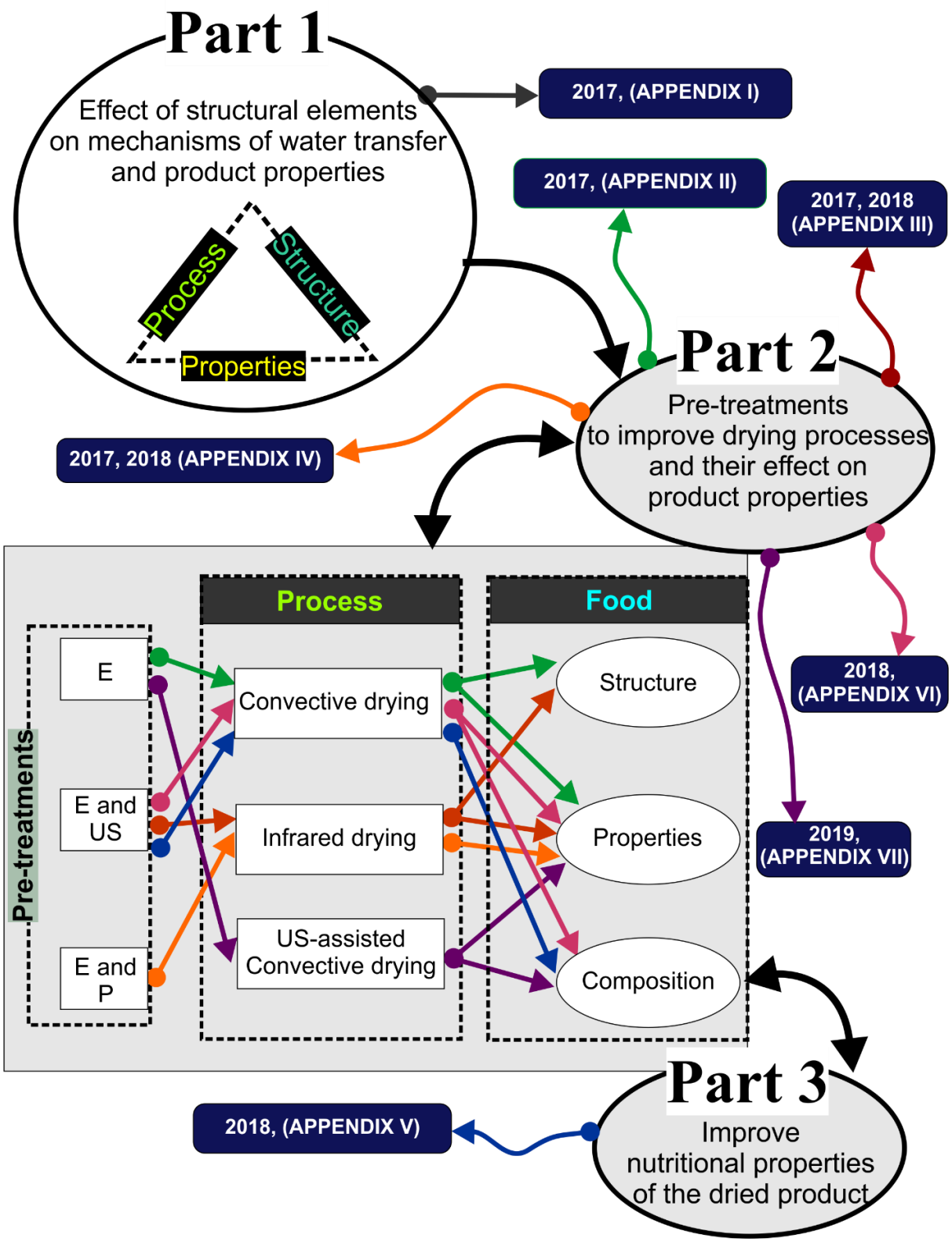

Figure 1. Thesis structure, the covered aspects and their resulting studies described in the appendixes from I to VII.

From our experience acquired during the master period regarding the US application and effects, the use of US during my doctorate thesis was also considered. In fact, there were many studies regarding the US to improve drying; however, the description of the involved mechanisms was still incomplete. For example, in that first work (Ricce, et al. (2016), the samples changed their structure and gained moisture during US pre-treatment. However, contrary to the expectations, the water inlet in the product did not negatively influence the drying, it improved the process by increasing the drying rate. From this experience, this finding opened other possibilities, such as take advantage of the liquid inlet for the nutrient incorporation and changing aqueous medium to another compound able to enhance the following drying process.

However, not only the US application was planned from the beginning of this thesis. On any given day, my advisor gave me a briefcase with some impressed articles related to drying and mass transfer topics; among them, some captured our special interest. They described the use of drying process accelerators, such as ethanol (Braga, Pedroso, Augusto, & Silva, 2009; Braga, Silva, Pedroso, Augusto, & Barata, 2010; Funebo, et al., 2002), specially the article of (Silva, Braga, & Santos, 2012), in which for first time the Marangoni Effect (at that time, a mass transfer phenomenon unknown to me) seems to be of high importance during the use of drying accelerators. However, only these four works were available at that time and there was still necessary more descriptions to better understand the involved mechanisms of how the food structure and composition interacted with the drying accelerators application and its influence on the drying process and product properties.

Based on these challenges; this thesis arises to be a contribution to better understand the food drying to improve the process and the obtained food product. The thesis was structured according to Figure 1, which shows the three main parts of this thesis, the aspects that each one covered and their respective studies (Appendix I to VII). The sequence of the studies was defined in order to take advantage of the knowledge acquired, although, as is observed in Figure 1, the studies have not been carried out in chronological order.

2. INTRODUCTION AND OBJECTIVES

Drying process, contrary to what is in general perceived, is a complex operation that describes the process of removing moisture, where the latent heat has to be supplied to the material to vaporise the water (Hawlader, Perera, & Tian, 2006).

When a whet raw material is subjected to drying, two phenomena occur simultaneously (Chen & Mujumdar, 2008; Mujumdar & Menon, 1995; Rodríguez, et al., 2019):

- (1) Energy transfer of (heat) from the surrounding to vaporize the surface moisture. It depends on the external conditions of temperature, air humidity and flow, area of the exposed surface, and pressure, which are related to the external resistance to water transfer. These conditions are especially important during initial stages of drying when unbound surface moisture is being removed.
- (2) Mass transfer. The internal moisture is transferred to the solid surface with subsequent vaporization, as a consequence of (1). It depends on the physical nature and composition of the solid, the temperature, and its moisture content, which are related to the internal resistance to water transfer. The migration of moisture from within the solid to the surface occurs through different mechanisms, namely, diffusion, capillary flow, internal pressures set up by shrinkage during drying, among others. These conditions are especially important during the final stages of drying.

Therefore, the mechanism of drying involves combined heat and mass transfer, where the drying process conditions, the composition and microstructure of the food materials are particularly relevant. In this regard, the parts that compound this Thesis were oriented to make a correlation among process, and food (structure, properties and composition). To start, Part 1 was oriented to evaluate the correlation among structure-process-properties (Figure 1). For this, the effects of microstructural elements that compose the food matrix were evaluated on mechanisms of water transfer and rehydration properties (Figure 2; Appendix I).

Moreover, the success of a drying process is determined by the balance between the quality of the obtained product and quality of the process (Chou & Chua, 2001). However, at present, the conventional methods are not necessarily optimal about that balance. Among the main challenges related to the conventional methods are energy

consumption, and environmental impact due to the combustion of fossil fuels used to provide energy for drying. In fact, the industrial drying process itself competes with distillation as the most energy-intensive unit operation (Kudra & Mujumdar, 2009), where the high-temperature industrial dryers are powered especially by propane and electricity (EIA, 2018). Therefore, the energy consumption is the main concern related to the process, and there is a demand for minimal environmental impact (Kudra, et al., 2009).

On the other hand, the properties of the dried products depend directly on how the drying process is conducted. In many processes, improper drying may lead to irreversible damage to product quality (Mujumdar & Devahastin, 2000). For example, due to the elevated temperatures and long times, conventional drying processes can reduce the quality of food products. Therefore, physical (shrinkage, poor rehydration, changes of texture), chemical (colour and aroma losses, browning and oxidative reactions) and nutritional (vitamin and volatile losses) problems of quality are still observed (Chou, et al., 2001).

Consequently, the drying processes improvement is highly desirable to both increase the quality of food products and reduce the process impact. For a decade ago until today, scientists and innovative food centres increased their interest for emerging food processing technologies to enable the introduction of new, safer, quality foods with longer shelf life (De la Fuente-Blanco, Riera-Franco de Sarabia, Acosta-Aparicio, Blanco-Blanco, & Gallego-Juárez, 2006).

Therefore, it is necessary to deeply understand, from a technical-scientific point of view, the phenomena and mechanisms involved during the drying process with the emerging technologies use. Therefore, Part 2 of this thesis was focused on improving the drying processes and product quality by applying the high-power ultrasound (US), ethanol (E), and mechanical perforations (P) (Figures 1,2; Appendix II-VI) as pre-treatments of both convective and infrared drying. The proposed emerging technologies are briefly described below.

2.1. Drying process accelerators: application of ethanol

The application of drying accelerators comprises the use of biologically degradable agents which will form an azeotrope and are partially or completely miscible with water.

The ethanol and ethyl acetate are the preferred agents since residual amounts of these may be harmless to humans, and show the highest moisture removal capacity (Bohrer, 1967; Das, Srimani, & Ghosh, 1984).

Further, Leenaars, Huethorst, and Van Oekel (1990) corroborate that the Marangoni effect is involved in the drying process when an organic vapour (2-propanol vapour) is used. It is important to note that this study was conducted in non-food materials, which do not present adsorbed water. The Marangoni Effect is a mass transfer phenomenon promoted by the surface tensions gradients formed between two liquids with different surface tensions. The surface tension gradient can be maintained by continuous vaporization of the more volatile component, which has the lowest surface tension (Fanton & Cazabat, 1998; Gugliotti & Todd, 2004). The mechanism of this phenomenon was described for first time by Thomson (1855) in his article “On certain curious motions observable at the surfaces of wine and other alcoholic liquors” – although the phenomenon adopted the name of the physicist Carlo Marangoni after his work “About the spread of the drops of a liquid on the surface of another” (Marangoni, 1871). The phenomenon was also well described in the articles “tears of wine” (Fournier & Cazabat, 1992; Vuilleumier, Ego, Neltner, & Cazabat, 1995).

The Marangoni effect was introduced at the drying of fruits (pineapple, banana and apple slices) by Silva, et al. (2012) as an explanation for the shorter drying time when samples are superficially treated with ethanol. Until then, in previous works from (Braga, et al., 2009; Corrêa, Braga, Hochheim, & Silva, 2012; Funebo, et al., 2002; Tatemoto, Mizukoshi, Ehara, & Ishikawa, 2015), this effect was not described but it was observed that the ethanol accelerates the process, changes the product properties and preserves sensible and volatile food compounds. Further, it was demonstrated that the effect of ethanol directly applied in the product surface is even better than when it is applied in the drying atmosphere.

Therefore, when I start this thesis in 2017, only four studies were exploring the use of mass transfer accelerators (focusing on ethanol) to enhance food drying and product properties. From them, in addition to our published works related to this Thesis in the two last years (2018-2019), there are other four studies published whit the ethanol use as pre-treatment for the convective drying of guaco leaves (Silva, Celeghini, & Silva, 2018), roto-aerated drying assisted by infrared of acerola residues (Silva, Nogueira, Duarte, & Barrozo, 2018), infrared hot-air drying of scallion (Wang, et al., 2019), and

infrared drying of garlic slices (Feng, et al., 2019). It is important to mention that these publications began after our first works being published (Rojas & Augusto, 2018a; Rojas & Augusto, 2018b; Rojas & Augusto, 2018d; Rojas, Silveira, & Augusto, 2019b).

It means that the use of ethanol as pre-treatment to improve the drying process and product quality is gaining more interest in food engineers and scientists, and it is interesting to observe that this Thesis contributed to this.

2.2. High-power ultrasound technology application as pre-treatment and assisting the drying process

The ultrasound (US) technology is based on the propagation of mechanical waves throughout the product at frequencies over 20 kHz, where the high-power ultrasound corresponds to frequencies between 20-50 kHz. Depending on the US application and if the US mechanical waves need to be propagated in solids, liquids, or gases, different US devices can be used (Miano, Rojas, & Augusto, 2017; Michael, Lu, & Kathryn, 2005; Rastogi, 2011).

The US can be applied as a pre-treatment in a liquid media (by using ultrasonic baths or ultrasonic probes) or simultaneously with convective drying process (by using contact or contactless transducer systems for airborne applications) (Rodríguez, et al., 2019). This technology demonstrated capacity to modify the product structure and accelerate the mass transfer phenomena, reducing the processing time and temperature of the conventional drying process.

When food is immersed in distilled water with US as a pre-treatment to drying, two mechanisms occurs: Firstly, there are water gain and solid loss in the food, due to the direct US effects (sponge effect and inertial flux)(Fernandes, Gallão, & Rodrigues, 2008; Ricce, et al., 2016); secondly, the US indirect effects take place, causing structural changes, cell flattening (needle-shaped cells) and/or cell disruption creating microscopic channels (De la Fuente-Blanco, et al., 2006; Miano, Ibarz, & Augusto, 2016; Miano, Rojas, & Augusto, 2018). The structural changes make the moisture removal easier, reducing the internal resistance during drying since water has more pathways to exit the food. On the other hand, the same mechanisms could occur when the food to be dried is immersed in ethanol instead of water. However, until this thesis started, no studies were found on this topic.

On the other hand, when the US is applied simultaneously with drying (US-assisted drying), it can reduce both the internal and external resistance to mass transfer. The internal resistance is reduced by the sponge effect and acoustic cavitation, which mechanisms causes structural changes improving the water mobility from inside the food. With regard the external resistance reduction, the US improve the vapour transfer from the surface to the air by reduction of the boundary layer thickness between solid-gas interface and increase the convection heat transfer coefficient (Corrêa, Rasia, Mulet, & Cárcel, 2017). This occurs because when the acoustic energy is dissipated on the system, pressure variations occur, microstirring on the solid-gas interface, and gradients in momentum promoting the turbulence (Rodríguez, et al., 2019).

For both cases of US application (as pre-treatment or assisting drying), an improvement of the US effects is desirable to accelerate the drying process without compromising the properties of the food. Our purpose here was using ethanol as the medium to immerse the food simultaneously applying US as pre-treatment. On the other hand, perform pre-treatments with ethanol before the US-assisted drying. It was proposed since the combination of US and ethanol effects could enhance the water transfer and, consequently, the drying process. It was not evaluated before, and we propose it here for the first time.

In addition, the US technology assisting or as pre-treatment of some processes was used to incorporate nutrients. Deng and Zhao (2008) studied the incorporation of calcium in apples with the application of pulsed vacuum and US pre-treatments prior to drying using osmotic solutions based on calcium lactate and gluconate. On the other hand, Ojha, et al. (2017) evaluated the incorporation of microencapsulated fatty acids into pork meat, Mashkour, Maghsoudlou, Kashaninejad, and Aalami (2018) evaluated the iron fortification of potato tubers using the US pre-treatment before to vacuum impregnation. The authors observed that the US use leads to a higher iron impregnation. Recently, by taking advantage of the hydration process assisted by US, iron was incorporated in grains where US improve both the hydration process and iron uptake (Miano & Augusto, 2018).

In fact, the FAO has food fortification and/or enrichment programs with vitamin A or β–carotene, Vitamin D, calcium, iodine, protein, amino acids, ascorbic acid, thiamine, riboflavin, niacin, folic acid (Crane, et al., 1995), iron (Hurrell, 1997) also a

wide range of nutrients. Further, different food products could be used as vehicles for fortification (Latham, 2002), where dried foods seems an excellent option.

Therefore, after having evaluated the improvement of the drying process, an interesting way to incorporate nutrients into the food is by taking advantage of the processes. Consequently, the last part of this thesis was focused on applying ethanol and US pre-treatments to incorporate iron and carotenoid-rich microcapsules on vegetables, (Figure 1,2; Appendix VII), thus obtaining food products with enhanced nutritional properties.

2.3. Objectives

Each development part that composed this Thesis were defined based on three main objectives. To achieve these main objectives, different specific objectives were considered. In Figure 2, the main objectives are found in grey ellipses, while specific objectives are found in the green boxes.

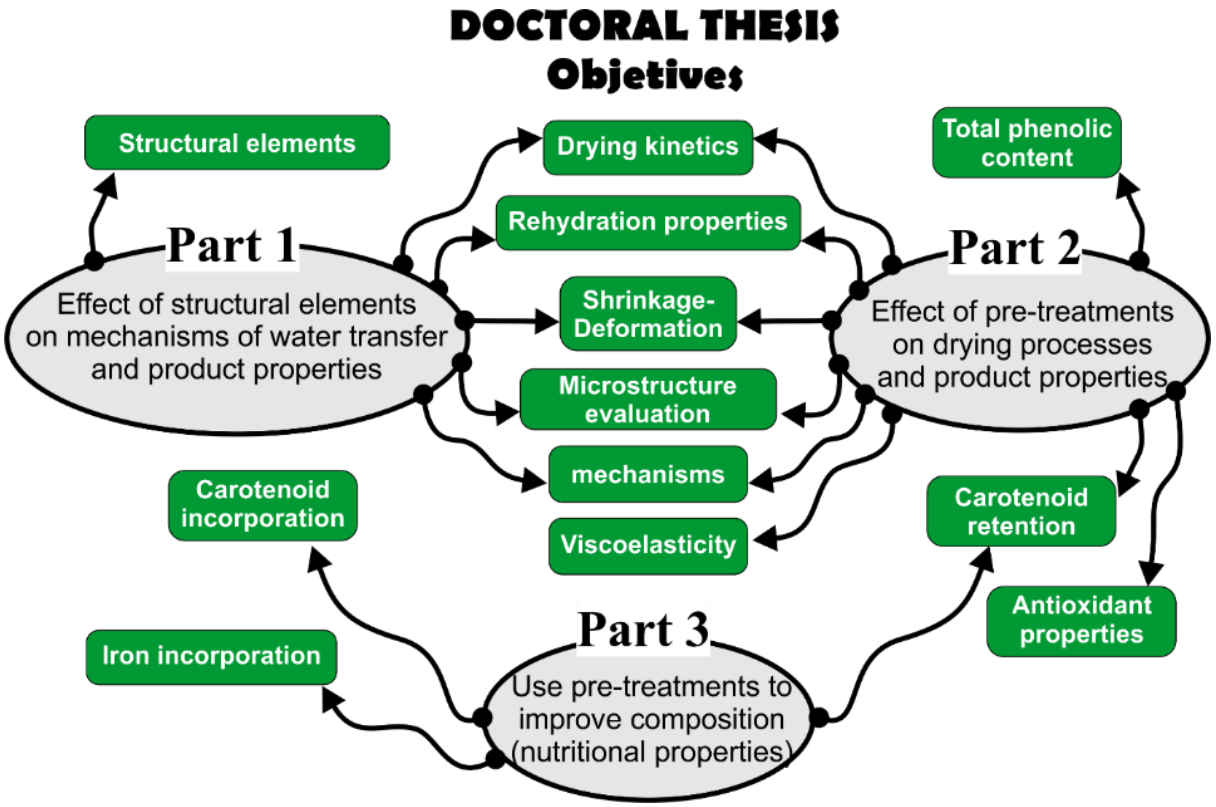

Figure 2: Main objectives (grey ellipses) and specific objectives (green boxes) of the present doctoral thesis

The main objective of Part 1 was to evaluate the effects of structural elements that compose the food matrix on mechanisms of water transfer and also on the product properties. For this the structural elements that conform the plant tissue were firstly identified, then the mechanisms of water transfer during processes and product properties effects were evaluated through the drying kinetics, microstructure evaluations, rehydration, and shrinkage.

The objective of Part 2 was to evaluate the effect of the pre-treatment application on drying processes and on the product properties. As observed in Figure 1, this part includes the application of ethanol (E), mechanical perforations (P) and/or US pre-treatments on three drying methods (convective drying, infrared drying and US-assisted convective drying). In addition, to evaluating the effects of pre-treatments on drying processes and product properties, the product composition was also studied through the evaluation of total phenolic content, antioxidant capacity and carotenoid retention.

Finally, Part 3 had as objective improve the food nutritional properties by taking advantage of the performed pre-treatments to improve drying processes. For this, it was evaluated the iron and carotenoid-rich microcapsules incorporation using ethanol and ultrasound, as well as the retention of these nutrients after drying.

3. DEVELOPMENT AND RESULTS

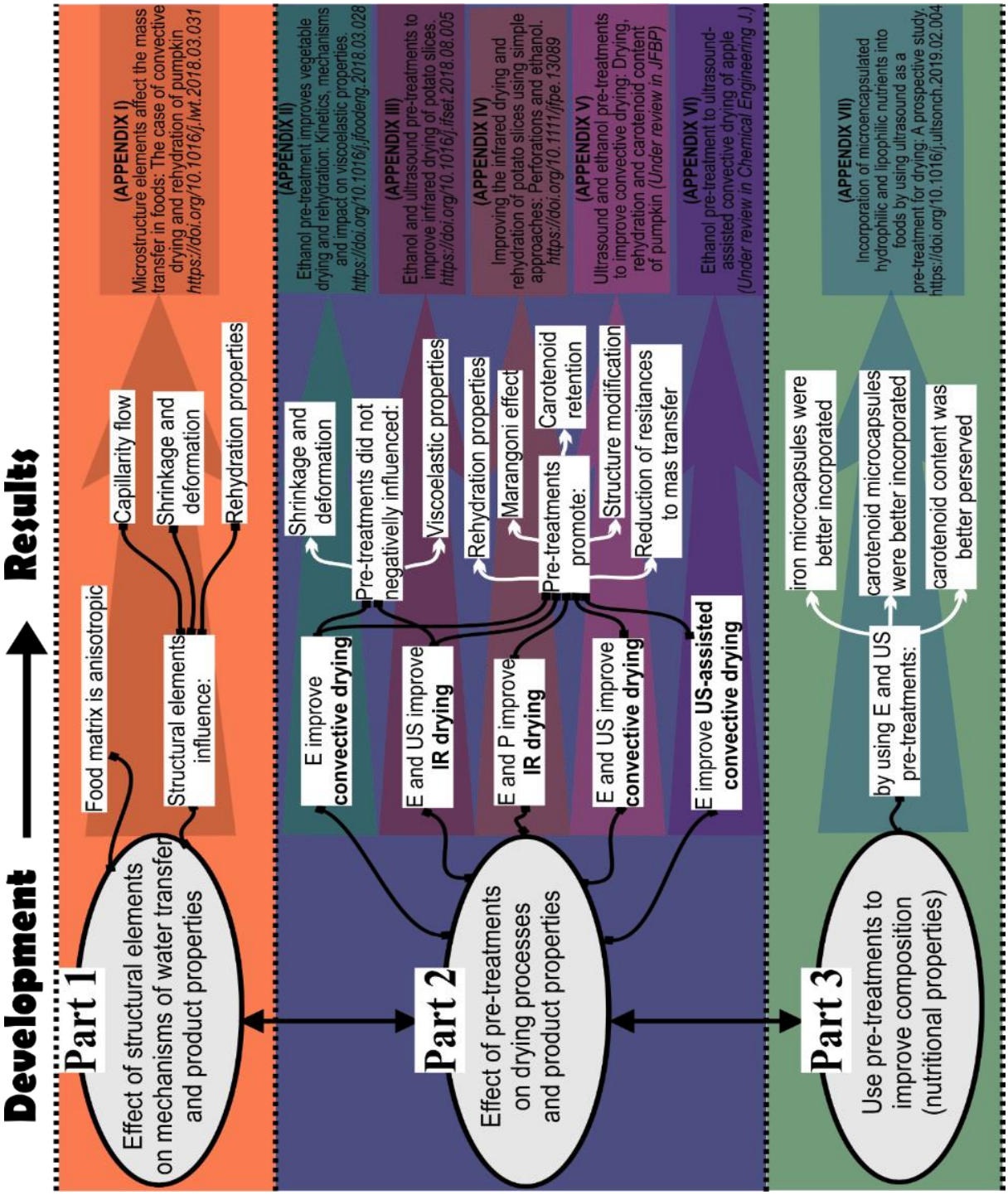

Figure 3. Thesis development with the remarkable results, which gave rise to the different publications shown in Appendix I-VII.

As stated, this thesis was developed following three parts organized according to the reasoning order. Figure 3 shows the parts of this thesis development with the remarkable results obtained in the seven studies, which gave rise to the different publications shown in the Appendix section.

The development of each part of this thesis, with their respective studies and obtained results, is better explained below.

3.1. Understanding the effects of plant structural elements on water transfer mechanisms and product properties

This Thesis was developed with vegetable food. Therefore, as a first step, it was necessary to know the representative elements of plant microstructure and understand how these elements influence on the water transfer mechanisms during the drying process and the product properties, such as rehydration and shrinkage.

For this study, pumpkin cylinders extracted from the edible part were used, as observed in Figure 4. The main tissues that compose this material are parenchyma (p) and the vascular tissue (v), specifically xylem. In fact, these tissue types mainly compose the edible part of different types of plant tissues (Aguilera & Stanley, 1999).

Then, we designed a protocol to understand and describe the influence of these structural elements during drying and rehydration, as well as their role in the mass-transfer mechanisms of water outlet-inlet. For this, cylinders were obtained considering a transversal (Tc) and longitudinal (Lc) cut orientation that allowed to obtain different tissues orientation (Figure 4). A combination of kinetics (during drying and rehydration), microscopical and x-ray evaluations were needed to achieve that objective.

The drying kinetics was described by using the Page Model (Page, 1949). Although the Page Model is an empirical model, Simpson, Ramírez, Nuñez, Jaques, and Almonacid (2017) demonstrated that the anomalous diffusion approach, based on fractional calculus, can attribute phenomenological meanings to it. We judged it useful and we have been using this interpretation to reinforce our hypothesis. In this interpretation, the Page drying rate constant (k) is associated with the diffusion coefficient and the geometry of the sample, while the dimensionless drying constant (n) describes the “type of diffusion” ($n>1$ super-diffusion and $n<1$ sub-diffusion). Therefore, we interpreted n can be related to the food microstructure and when $n \neq 1$ it

could indicate that other mechanisms than diffusion are important. For example, the "super-diffusional process" (n>1) may indicate the importance of capillarity. This approach was, in fact, useful during this Thesis development.

As the main results, the orientation of the structural elements did not affect the drying kinetics, which was described by using the Page Model (Page, 1949). However, after drying, it was observed that the tissue orientation (of the xylem vessels) had a significant impact on deformation and rehydration.

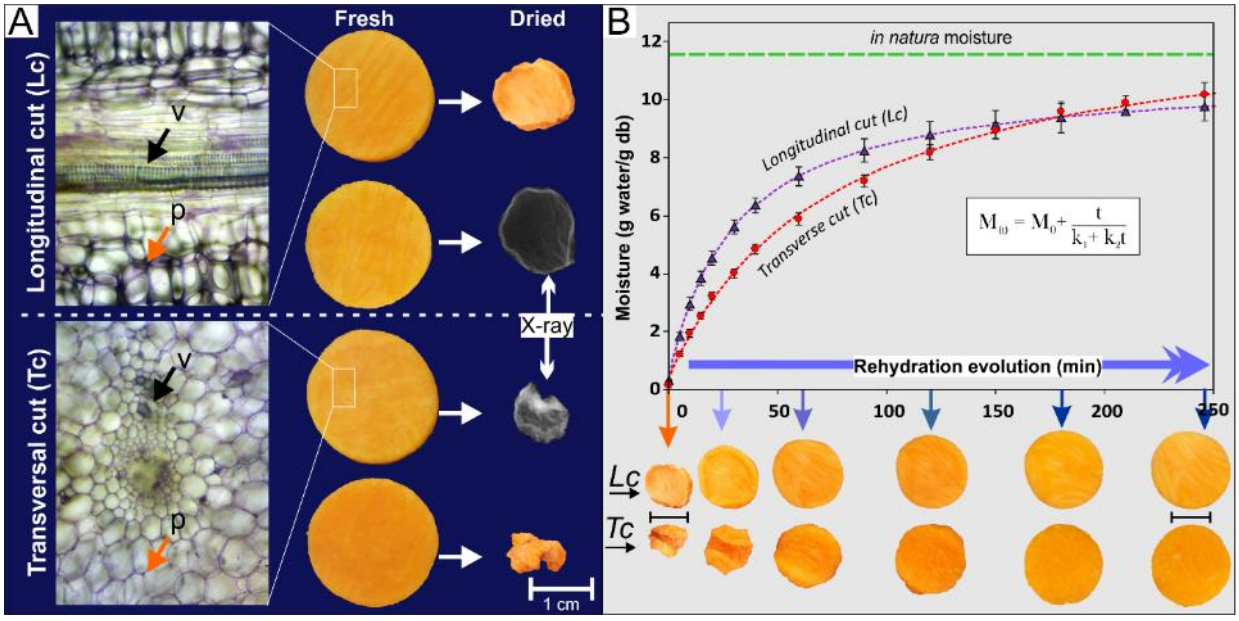

Figure 4. (A) Fresh and dried samples obtained for both transverse cut (Tc) and longitudinal cut (Lc). In details, the X-ray performed in dried samples and the optical microscopy of fresh samples shows the vascular and parenchymatic (p) tissues orientation**. (B)** Up: Rehydration kinetics for both transverse cut (Tc) and longitudinal cut (Lc) samples. Down: Evolution of rehydration of samples (1 cm scale images) taken at different times of the rehydration process.

The Lc-samples showed a more uniform appearance than the Tc ones (Figure 4.A). The shrinkage and deformation of these samples were indirectly but effectively evaluated using the greyscale histogram and the X-ray analysis. In these analyses, the Tc-samples showed a tendency towards black in the grey intensity histogram and higher density in the X-ray analysis, reflecting its highest deformation and shrinkage.

During the rehydration kinetics, evaluated through the Peleg model (Peleg, 1979), the Lc-samples presented the highest rehydration rate (lower k_1 value). In contrast, higher equilibrium moisture (lower k_2 value) was observed in the Tc-samples. These behaviours were related to water absorption mechanisms and the shrinkage effects (Figure 4.B).

Through several observations of drying and rehydration process at microscopical level, the water transport mechanism by capillarity through the xylem vessels during drying and hydration was demonstrated. Moreover, the water flow from the xylem vessels to the other tissues was observed. The mechanism was registered in an interesting video by Rojas and Augusto (2017b), available at https://youtu.be/o5vbxs1G81s.

This study was important to demonstrate that vegetable tissues are anisotropic, and how their structural elements can affect the water flow during processing. Consequently, it is described in the article "Microstructure elements affect the mass transfer in foods: The case of convective drying and rehydration of pumpkin." published in the LWT-Food Science and Technology journal (Rojas & Augusto, 2018c), showed in Appendix I.

The results here obtained were useful for the next studies, which are described as follows.

3.2. Pre-treatments applied to improve drying processes and product properties

This part consists of five studies were the main objective was to evaluate the effect of emerging technologies applied as pre-treatments on different drying processes and their effect on product properties and composition.

3.2.1. Ethanol pre-treatment to improve convective drying

This study had as objective to evaluate the ethanol (E) pre-treatment applied to improve the convective drying. The effect of ethanol pre-treatment on microstructure modifications, convective drying kinetics (Page model, (Page, 1949)), rehydration kinetics (Peleg model (Peleg, 1979)) and viscoelastic properties (generalized Maxwell model (Rao & Steffe, 1992)) was evaluated.

Firstly, the structural modifications after ethanol application, drying and rehydration were evaluated. It is important to highlight that, although ethanol was previously applied to enhance food drying (Braga, et al., 2009; Corrêa, et al., 2012; Funebo, et al., 2002; Silva, et al., 2012; Tatemoto, et al., 2015), this was the first study where the effect of this compound on food structure was evaluated. In fact, many drying studies are still being conducted considering an approach of isotropic material - and we tried to go further this proposal during my Thesis.

For this purpose, pumpkin samples were immersed in ethanol with dye, being further evaluated and processed in different ways.

Immediately after the samples were placed in contact with the ethanol, small air bubbles come out of the tissues. After pre-treatment with ethanol, the cylinders were cut in half, where it was observed macroscopically that the ethanol penetrates the surface layer of the samples. Modifications in the microstructure were observed through microscopy in regions where ethanol had an influence and where it did not. It was verified that ethanol extracts intercellular air and affects cell walls by thinning them and extracting some compounds (Figure 5-1). It is important to mention that these microstructural modifications were observed mainly in the parenchymatic tissue. However, it was also demonstrated that the ethanol travels longer into the cylinders through the xylem vessels, which could improve their effects during drying. For more detail, this microstructural modifications were described through the video shown by Rojas and Augusto (2017a), available at https://youtu.be/VcsJ5WWp--0.

As observed in Figure 5 (2,3), ethanol accelerated the drying (high drying rate) and rehydration (high rehydration rate and water retention) processes. Moreover, the mechanisms for improving the drying process due to the application of ethanol had not been described and explained until this study.

Improvements were attributed mainly to structure and composition modifications, which increased the cell wall permeability favouring both drying and rehydration. Additionally, the improvement mechanism was related to the characteristics of ethanol and interaction with food water. For this, one of the possible reasons was the higher vapour pressure of the mixture formed. However, after using different compounds, Silva, et al. (2012) verified that more than the difference in vapour pressure, the surface tension has a greater influence, introducing the concept of flow due to the Marangoni Effect.

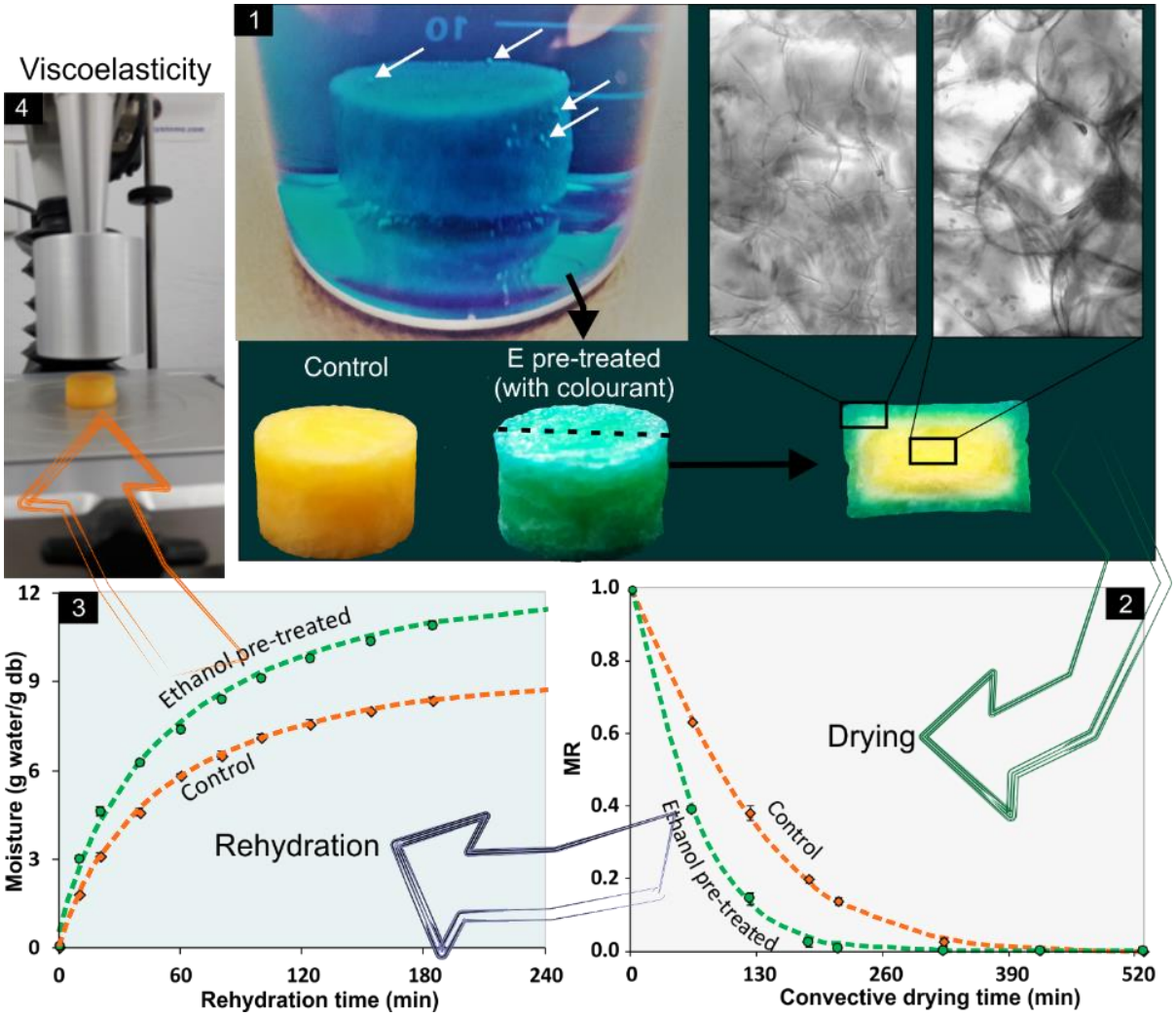

Figure 5. Representation of the sequence performed in this study. (**1)** microstructure evaluation after pre-treatment with coloured ethanol, white arrows indicate the air bubbles being expelled. The ethanol pre-treated samples were cut in half evidencing the ethanol entrance. Optical microscopy shows the superficial effects of ethanol on cell walls thinning and wrinkling. **(2)** drying kinetics of the control and E pre-treated samples described by Page model (dotted lines). **(3)** rehydration kinetics of the control and E pre-treated samples described by Peleg model (dotted lines), and **(4)** stress-relaxation test to evaluate the viscoelasticity.

Therefore, considering the Marangoni Effect principles, explained by Bird (2002); Gugliotti, et al. (2004); Thomson (1855), a possible explanation for the mass transfer mechanism during drying was proposed in this study as follows: During pre-treatment, ethanol enters to the sample and water flows out the sample to the ethanol. Therefore, the sample surface was composed of a mixture of ethanol and water. During drying,

since ethanol vaporizes faster, more water than ethanol remains in the sample surface. This region with higher water than ethanol concentration has a higher surface tension, pulling strongly the liquid from the next sample layer were a surface tension gradient between the water and the remained ethanol is now generated. The process is repeated, promoting the flow from the inside of the sample to its surface, as many times as necessary to achieve a balance in the surface tension. Furthermore, the flow promoted by the Marangoni Effect could be improved through the xylem vessels, which act like capillaries (Tyree & Zimmermann, 2002).

Finally, regarding viscoelastic properties, the stress relaxation data of rehydrated pumpkin cylinders were well fitted to a generalized Maxwell model. Each Maxwell element was correlated with a determined structure of the tissue and its parameters described its pure solid or liquid-like behaviour. The rehydrated samples showed slight differences between them but showed different viscoelastic properties (decrease the initial stress and residual relaxation with variations among the elastic and viscous modulus) compared whit those of the *in-natura* samples.

The main importance of this study was discuss and propose the mechanisms by how ethanol enhances food drying, which is described in the article "Ethanol pre-treatment improves vegetable drying and rehydration: Kinetics, mechanisms and impact on viscoelastic properties" published in the Journal of Food Engineering (Rojas, et al., 2018b), shown in Appendix II.

Consequently, this work was the basis for all the other studies using ethanol, as described below.

3.2.2. Ethanol and ultrasound pre-treatment to improve infrared drying

This study had as objective to describe the ethanol (E) and ultrasound (US) application as pre-treatments to improve the infrared (IR) drying of potato slices, evaluating the effect of each pre-treatment on drying and rehydration kinetics, on the product microstructure, and viscoelastic properties.

We selected this method and pre-treatments since, on the one hand, the IR drying was proposed as an effective and economical process that facilitates the removal of moisture on sample surface, increase the heat transfer and drying rates, reducing the processing time (Datta & Ni, 2002; Onwude, et al., 2018; Torki-Harchegani,

Ghanbarian, Maghsoodi, & Moheb, 2017). However, the use of pre-treatments to improve infrared drying has not been sufficiently explored. On the other hand, we had the hypothesis that ultrasound technology creates microchannels in the sample tissue, where the Marangoni Effect (because of adding ethanol to the system) can be promoted.

Consequently, the combination of these technologies appeared to be effective to enhance the food IR drying.

Performed pre-treatments included Control samples (Without any pre-treatment), samples immersed in ethanol (Ethanol treated), and treated with US using ethanol (Ethanol + US) or water (Water + US) as immersion media and wave transmission. The US equipment used in this study was an ultrasonic tip (ECO-SONIC, QR1000 Model, Brazil, 20 kHz and 68 W/L of actual volumetric power).

The microscopic evaluation showed that pre-treatments changed the *in-natura* potato microstructure in diverse ways. The ethanol mainly affected the cell wall membrane, similar to the observed in pumpkin in our previous study (Rojas, et al., 2018b). When US was applied using water as the medium, it mainly acted intracellularly, dispersing the intracellular compounds, such as the starch granules. However, higher inter and intracellular modifications were observed when US was applied using the ethanolic medium (Ethanol + US) (Figure 6).

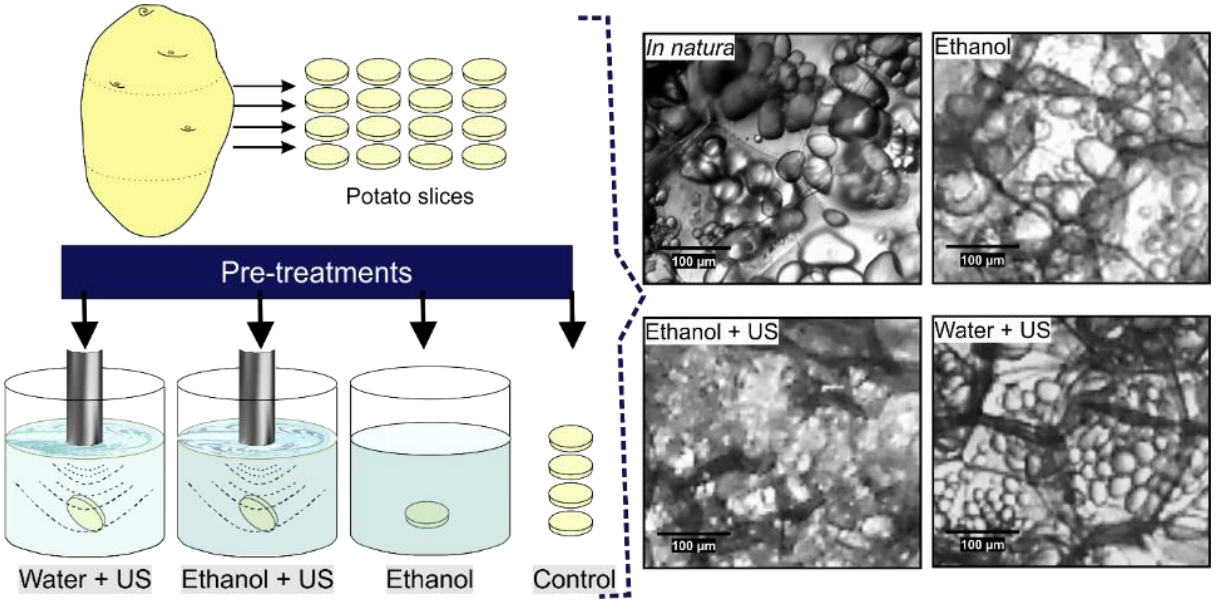

Figure 6. Performed pre-treatments on potato slices and their effects on microstructure.

The observed microstructure and composition modifications influenced the subsequent drying and product properties.

Compared to the Control, all pre-treatments decreased the drying time, while Ethanol + US provided the highest reduction. In contrast, a slight decrease in water absorption and retention capacity was observed for the Ethanol + US treated samples, which can be a consequence of the highest structural modifications produced during this pre-treatment, which exposed the starch granules to temperature effects and resulting in crust formation. Additionally, the viscoelastic properties of rehydrated samples differed significantly of those of the fresh potato *(in-natura)*, which presented more elastic properties. It reflects that the tissue lost its original viscoelastic and rehydration properties during pre-treatments and drying.

This study applied for the first time the ethanol and ultrasound (in water or ethanol medium) pre-treatments to improve infrared drying, describing and correlating the structural modifications with the drying kinetics and product properties. Consequently, it is described in the article "Ethanol and ultrasound pre-treatments to improve infrared drying of potato slices", published in the Innovative Food Science & Emerging Technologies Journal (Rojas, et al., 2018a), showed in Appendix III.

Based on these results, other pre-treatments using simple approaches were used to improve both infrared drying and rehydration, as described in the next study.

3.2.3. Using simple approaches to improve infrared drying: ethanol and mechanical perforations

This study arises based on the US and E effects demonstrated in the previous study (Rojas, et al., 2018a), where the water flow was promoted through the channels created by US and the E application improving IR drying. However, although interesting and effective, the US technology can be expensive in some contexts, or even it could result in negative effects in starchy products (such as potato, where negative result on drying properties was observed), limiting their application. Consequently, a hypothesis arises: is it possible to obtain microchannels with similar results of using ultrasound, but in a simple way, such as performing mechanical perforations by a needle?

This study was designed to test this hypothesis.

Therefore, the objective of this study was to use ethanol (E) and mechanical perforations (P) as simple approaches to improve the infrared drying and rehydration of potato slices. Perforations were performed to study the effect of promoting routes to water flow, while ethanol to evaluate the effect of Marangoni flow. They were made using a simple needle, considering an organized pattern as shown in Figure 7.

As results (Figure 7), all pre-treatments reduced the drying time compared to control treatment. However, a great time reduction was observed with the P+E pre-treatment application. In the same manner, to observed in the previous study (Rojas, et al., 2018a), the pre-treated samples with ethanol show poor rehydration properties. However, the samples with perforations (P) and even with ethanol application (P+E) increased their rehydration rate as well as the water retention capacity. Possible mechanisms were discussed based on the fact that perforations reduced the internal resistances and promoted the ethanol effects.

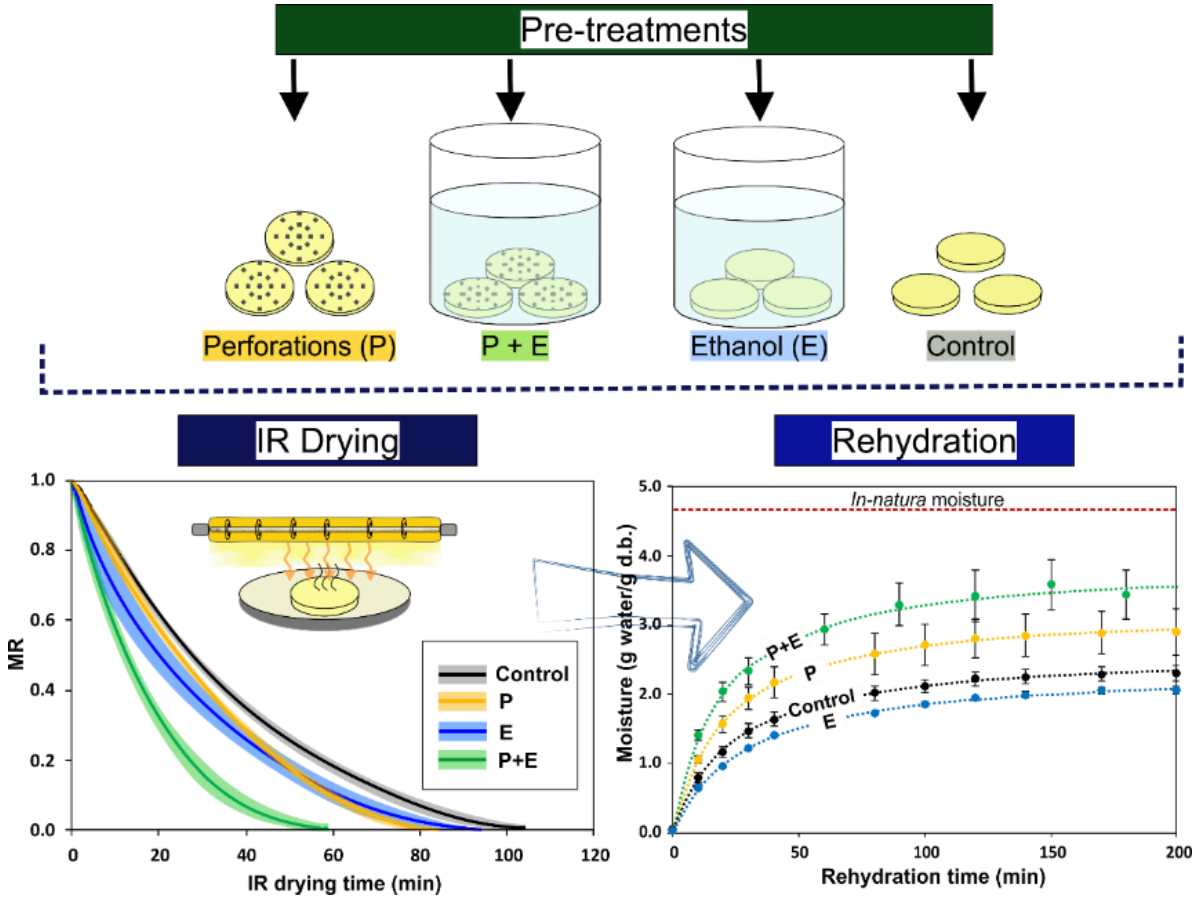

Figure 7. Performed pre-treatments in potato slices and the obtained IR drying kinetics and rehydration behaviour.

Therefore, results show that simple operations could be performed to create routes to water flow (through mechanical perforations) combined with drying accelerator (ethanol), improving both drying and rehydration of potato slices.

This study is described in the article "Improving the infrared drying and rehydration of potato slices using simple approaches: Perforations and ethanol" published in the Journal of Food Process Engineering (Rojas, et al., 2019b), showed in Appendix III.

3.2.4. Ethanol and ultrasound pre-treatment to improve convective drying and product properties

In our previous study (Rojas, et al., 2018a), the combined application of ethanol (E) and ultrasound (US) was evaluated for the first time as pre-treatments to improve infrared drying. However, the effect of this combination on convective drying had not yet been studied. Considering that convective drying is a method with higher relevance than infrared drying, this study should be conducted.

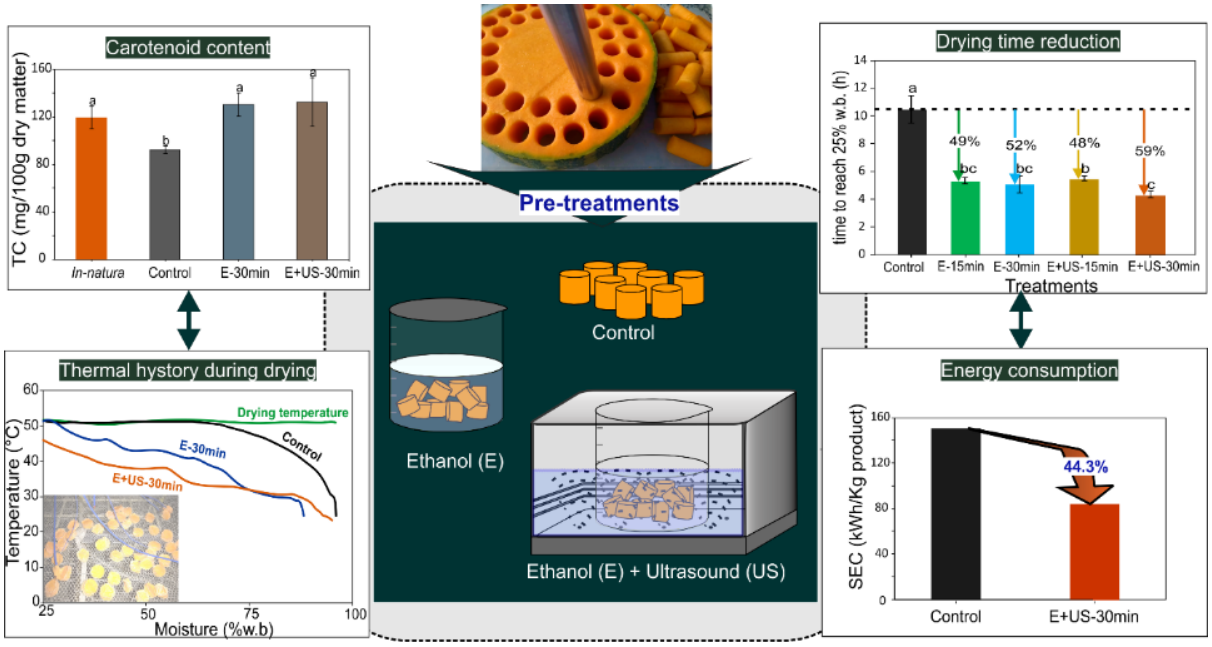

Figure 8. Performed pre-treatments on pumpkin cylinders, their effect on drying time reduction and the consequent energy consumption; thermal history registered during drying and the relation with carotenoid content are also shown.

Therefore, we evaluated for the first time the combined application of ethanol (E) and ultrasound (US) pre-treatments to improve convective drying, also evaluating the product properties and an estimative of energy consumption. Compared to our previous studies, apart from the drying method, the ultrasound equipment used in this study was also different. The ultrasound (US) equipment used was an ultrasound bath (68 W/L of actual volumetric power), which better corresponds to a possible industrial application. The effects on drying and rehydration kinetics, as well as on the energy consumption and carotenoid preservation in pumpkin samples, were studied (Figure 8).

Compared to the Control, all pre-treatments decreased the drying time, but the combination of ethanol and ultrasound presented the greatest reduction in both drying time (59%) and energy consumption (44%). The pre-treatments also enhanced the rehydration rate and increased water retention.

Additionally, in this study, the food composition, reflecting its nutritional aspects, started to be evaluated. The carotenoid content was determined for the fresh pumpkin *(in-natura)* and for each pre-treatment. Compared to fresh pumpkin, the extraction of carotenoids due to pre-treatments was negligible. During drying, while the Control samples presented partial degradation (23%), the pre-treated samples preserved ~100% of the carotenoid content, which is an interesting result. This was correlated with the thermal history registered inside the samples during drying: compared to the pre-treated samples, the control samples showed a longer exposition to higher temperatures, whose negative effects were evidenced by reducing the carotenoid content.

The results open new perspectives about an innovative method to not only improve the convective drying process, but also the product quality by combining ethanol and ultrasound. This study is described in the article "Ultrasound and ethanol pre-treatments to improve convective drying: Drying, rehydration and carotenoid content of pumpkin", which was published in the Food and Bioproducts Processing Journal (Rojas, Silveira, & Augusto, 2020), shown in Appendix V.

Therefore, in this point, ethanol and ultrasound technologies were evaluated as pre-treatments to enhance both convective and infrared drying. However, the effect of ultrasound assisting the convective drying had not been evaluated. Consequently, the next study was carried out.

3.2.5. Ethanol pre-treatment to improve ultrasound-assisted convective drying and product properties

This study was chronologically the last to be done since it was developed during a PhD mobilization period (6 months) at the *Universitat Politècnica de València* (UPV), Spain, in the “Grupo de Análisis y Simulación de Procesos Agroalimentarios (ASPA)”, through a co-guardianship with Prof. Dr. Juan A. Cárcel. In fact, ASPA is one of the few groups that study the system of ultrasound coupled to the convective drying, being Prof. Cárcel an international reference in this field. In fact, in this period, in addition to the work presented here, I made other experiments and learn other US applications during drying. For example, I made assays with the use of US-assisted drying at low temperatures (~ -10 °C), and the study of natural colourant (rich in anthocyanins from black carrot) incorporation during pre-treatments and its preservation during drying, the results of the last are being analysed and will be published. I consider that the PhD mobilization period was productive and allowed me to know new approaches in terms of analysis, systems and, above all, to learn other ways of applying US technology

For the US-assisted convective drying (50 °C, 1 m/s), the used system was a contactless vibrating cylinder that was driven by a piezoelectric transducer that generates a high ultrasonic field inside the cylinder, in which the samples were distributed, and the air passed through (Figure 9, C).

In this study, the application of ethanol (E) was evaluated as a pre-treatment to the US-assisted convective drying. Apple slices were obtained and used as model food. Pre-treatments were performed by immersion in ethanol for different periods. After that, pre-treated samples were convectively dried without and with US application (Figure 9).

The effects of pre-treatments and US during drying were evaluated on drying kinetics, described using the IR-model (which considers the internal resistance to mass transfer), the IER-model (which considers both internal and external resistances to mass transfer), and the Page Model. In addition, the rehydration kinetics; shrinkage; viscoelastic properties through stress-relaxation assays; antioxidant capacity (AC); and total phenolic content (TPC) were also evaluated.

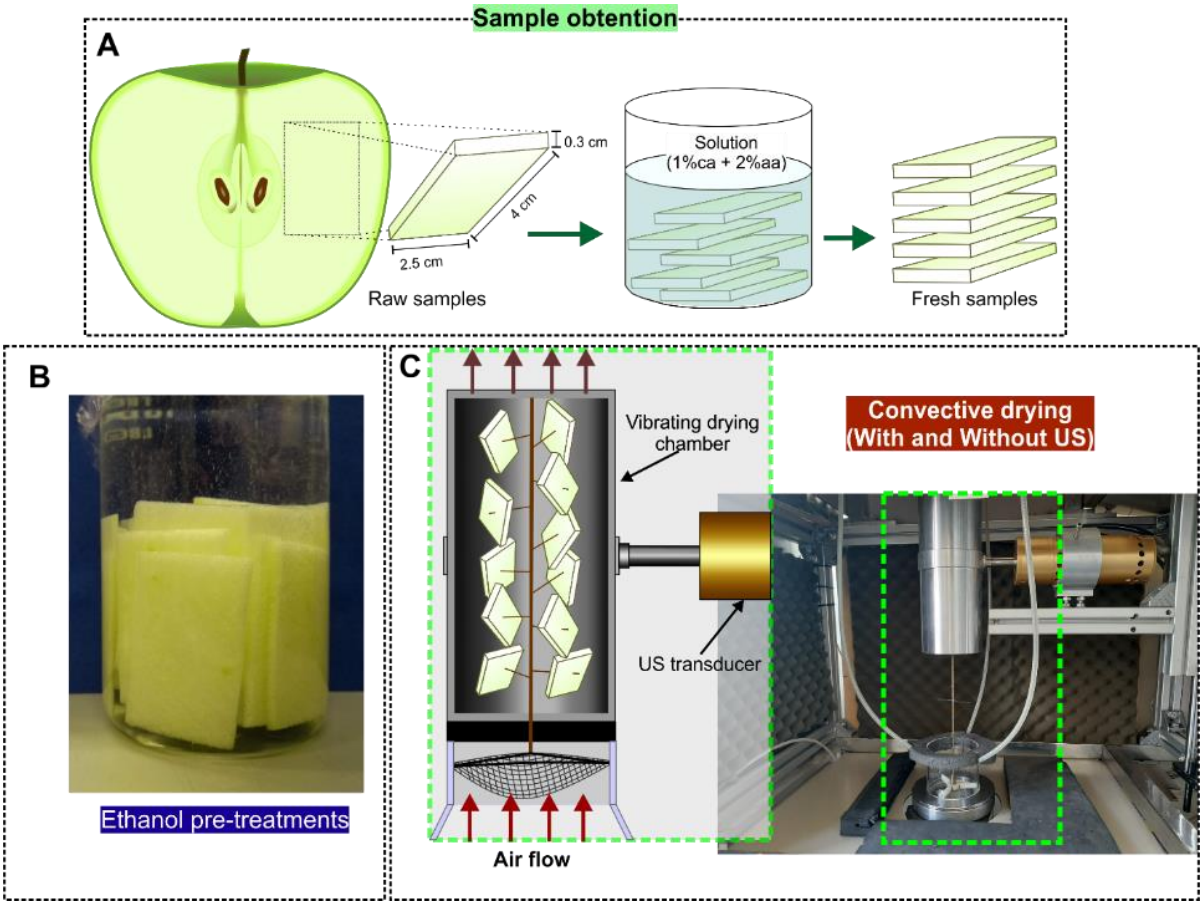

Figure 9. (A) Sample obtention and preparation, **(B)** ethanol pre-treatments by immersion of samples for 0, 10, 20 and 30 min, **(C)** Detail of sample location inside the drying chamber during convective drying without and with US (electrical input of 20.5 kW/m^3 and 21.77 kHz).

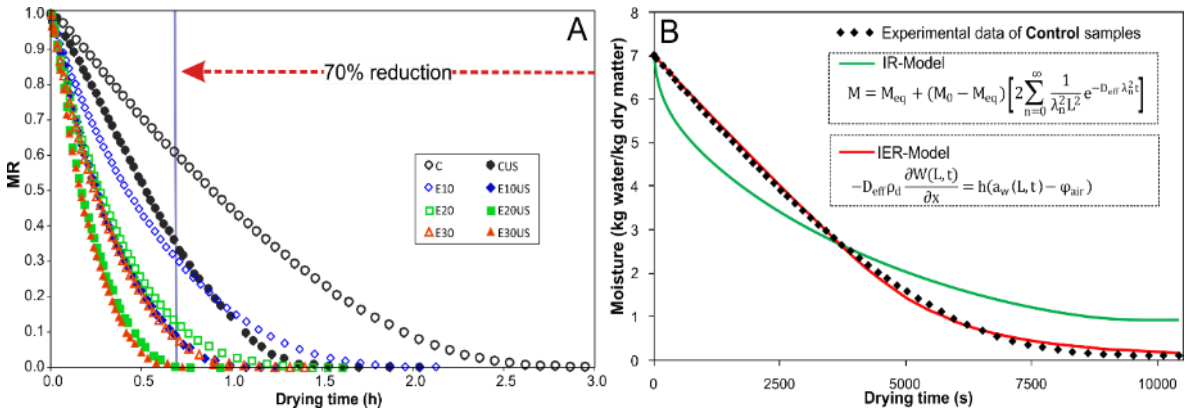

Figure 10. (A) dimensionless moisture ratio showing the highest drying time reduction, **(B)** an example of the IR and IER models fitting to experimental drying data of the control samples.

The conventional drying time was reduced 55% when US was applied, while if both ethanol pre-treatment and US-assisted drying were considered, drying time reduction reached 70% (Figure 10, A), showing this option was very effective to accelerate the process. The identified drying kinetics parameters from the different model application were correlated with possible mechanisms occurring during pre-treatments and drying.

A considerable lack of fit was obtained when the IR model was used, especially in the Control samples (Figure 10, B). This suggests the water transport was not only controlled by internal resistance, but also by influence of external resistance. Therefore, the IER-Model was used.

The convective mass transfer coefficient (h) increased for all treatments compared to control. However, the highest h values were found in the ethanol pre-treated samples, which means that the ethanol made easier the moisture transfer from the sample surface to the air phase. These effects were related, as follows, to improvement mechanisms occurring in the sample surface at the beginning of the drying process – when the external resistance influence is more important.

The external resistance is dependent on boundary layer thickness, which is affected by the sample shape, size and by the fluid circulation regime and properties (Blasco, García-Pérez, Bon, Carreres, & Mulet, 2006; Mulet, 1994). In this work, the air velocity, sample size and shape were the same for all treatments at the beginning of the drying process. However, the fluid properties were different in the ethanol pre-treated samples.

When ethanol is applied, different phenomena (related to structure and composition modifications) occurs, especially in the sample surface. The intercellular air is removed, the cell wall is thinning, some compounds are extracted and part of ethanol enters the sample (Feng, et al., 2019; Rojas, et al., 2018a; Rojas, et al., 2018b; Rojas, et al., 2019b; Wang, et al., 2019). Since the ethanol vapour pressure is higher than that of the water, the vaporization of ethanol could start almost instantly during drying. Then, the initial fluid (ethanol-water mixture) present on the sample surface became richer in water, but as it is a sequential process, there is still ethanol in the next layer of the tissue surface. A gradient surface tension is formed between the ethanol and water interface inside the sample, which promotes the water flow from inside the tissue and/or cells through the Marangoni Effect (Rojas, et al., 2018b). At

the same time, the flow is easier from the surrounding surface, since the cell wall is thinner, and intercellular air is absent offering lower resistance to flow. Then, the fluid can be fast transferred to the sample surface, and the vaporization to air phase occurred at higher rates. In fact, at the beginning of drying process, the vaporization rate of ethanol pre-treated samples for 30 min (0.95 g of fluid vaporized/min) was two times higher than the rate of vaporization of Control samples (0.4 g water vaporized/min).

This is the first time the effect of ethanol pre-treatment on the external mass transfer coefficient was described.

As the drying processing time increased, the influence of the structural modifications becomes significant in the diffusivity parameter (D_{eff}). Compared to control, the obtained D_{eff} parameter from IER-Model was similar ($p>0.05$) for every kinetics carried out with ethanol pre-treatments. However, this value highly increased for the treatments that included the US use. This demonstrates that US has an important effect in decreasing the internal resistance to mass transfer.

To complement the discussion, the Page Model parameters suggested that the lower n values, observed in ethanol pre-treatments, can be correlated with mechanisms associated to external mass transfer. In contrast, high n values when US was applied can be correlated with effects in the internal structure.

On the other hand, the shrinkage was evaluated after pre-treatments where slight area reductions were observed in the longest ethanol pre-treatments, while in dried samples the shrinkage tends to decrease as the ethanol pre-treatment time increased. Rehydration capacity was also greater in the pre-treated samples, containing even more water than the raw samples. After rehydration, samples showed a decrease in both elastic and viscous characteristics, compared to raw samples. The AC and TPC were better retained in samples dried with ultrasound application. In contrast, the AC and TPC decreased after ethanol pre-treatments and after drying; even so, the retention percentages were higher than those reported by other studies.

This study is described in the article “Ethanol pre-treatment to ultrasound-assisted convective drying of apple”, to be soon submitted, shown in Appendix VI.

Therefore, in this point, ethanol and ultrasound technologies were evaluated as pre-treatments to enhance both convective and infrared drying, as well ultrasound was also studied to assist the convective drying of ethanol pre-treated samples. Both

ethanol and ultrasound demonstrated to be interesting alternatives not only to enhance food drying but also the properties of the obtained products. In special, nutritional quality retention was highlighted. Based on that, the next step was to study the nutritional enhancement by incorporation of selected compounds, using different approaches.

3.3. Using pre-treatments to incorporate microencapsulated nutrients into the food matrix

Since in previous studies it has been shown that pre-treatments with ultrasound and/or ethanol improve the drying process and the properties of the product, in this work we expected to take advantage of these pre-treatments to incorporate nutrients.

This work was based on the following hypothesis: ultrasound not only changes the product structure but also incorporate liquids (the medium of wave transmission) into the product; therefore, through this mechanism, it is possible to incorporate nutrients in the sample.

Therefore, this study had as objective to use the ultrasound technology to incorporate microencapsulated nutrients. Both hydrophilic and lipophilic nutrients were evaluated: incorporation of iron-rich microcapsules (obtained by spray drying using maltodextrin as wall material and ferrous sulphate as the active) and carotenoid-rich microcapsules (obtained by hot emulsification and solidification using hydrogenated palm oil as wall material and paprika oleoresin as the active). The ultrasound pre-treatment was applied using two different media: water (were the carotenoid microcapsules were dispersed, but the wall material was not dissolved) and ethanol (where the iron microcapsules were dispersed, but the wall material was not dissolved). Pumpkin and apple were selected as suitable food material to perform the iron and carotenoid incorporation (Figure 11), respectively, based on nutritional considerations: due to its high carotenoid content, pumpkin was selected to perform the iron incorporation experiments (once carotenoids help the iron incorporation in human body); on the other hand, green apple present low carotenoid content, thus being selected to perform carotenoid incorporation.

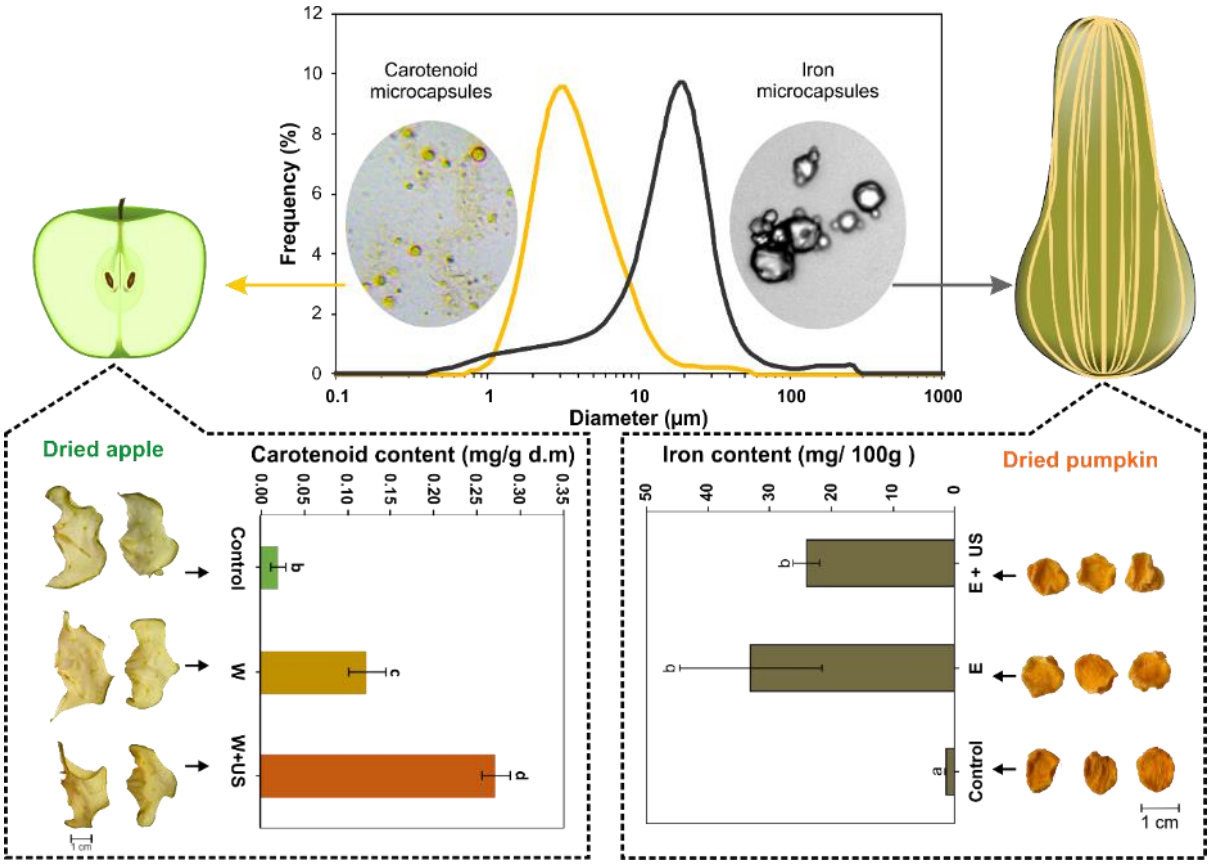

Figure 11. Up: Carotenoid and iron particle size distribution and microscopy, which dispersions were incorporated in apple and pumpkin samples respectively, by using ultrasound as pre-treatment to convective drying. Down: Carotenoid and iron content after drying with their respective images of the final obtained product

The ultrasound allowed more homogeneous iron incorporation in pumpkin. The iron content increased more than 1000% in pre-treated samples compared to control. In the same manner, carotenoid content increased when ultrasound pre-treatment was applied in pumpkin. Moreover, good carotenoid retention was obtained after drying the ultrasound processed samples (Figure 11).

The results show that pre-treatment with ultrasound can be used to incorporate microencapsulated nutrients into the food matrix, even considering a structured plant material, increasing not only the incorporated quantity but also promoting nutrient preservation. This study is described in the article "Incorporation of microencapsulated hydrophilic and lipophilic nutrients into foods by using ultrasound as a pre-treatment for drying: A prospective study." published in the Ultrasonics Sonochemistry (Rojas, Alvim, & Augusto, 2019a), shown in Appendix VI.

4. CONCLUSIONS

This PhD Thesis evaluated different aspects of food drying, focusing on emerging technologies and approaches to enhance both processing and product properties.

Plant tissue was remarkably demonstrated as complex materials and mass transfer mechanisms were demonstrated to go beyond diffusion. The orientation of the structural elements (xylem vessels) influenced the quality of the dried products and the mass transfer mechanisms. Capillarity through the xylem vessels was demonstrated during both drying and rehydration. Therefore, contrary to what is typically considered, the results showed that biological materials are anisotropic, and their structural elements affect the water flow during processing. This work is a contribution and a motivation to start looking for other alternatives and change the traditional thinking and assumptions about the food structure and mechanisms of mass transport, especially during drying.

The ethanol uses as pre-treatment to convective drying improved both drying and rehydration processes of pumpkin, without negatively impact their viscoelastic properties, when compared with the control treatment. In addition, it was demonstrated that ethanol influences mainly the parenchymatic tissue, by modifying its structure and composition, while the xylem vessels act as capillaries showing an important role during the pre-treatments by transporting ethanol.

The ethanol and US pre-treatments to infrared drying resulted in potentiated microstructure modifications in potato slices. Although the use of ethanol and/or US application is appropriate to improve the potato infrared drying, it did not have a positive impact during rehydration. On the other hand, improvement of infrared drying, and potato rehydration was obtained by using two simple techniques: the use of ethanol and mechanical perforations.

On the other hand, the ethanol and US pre-treatments to the convective drying of pumpkin improved both the process (reducing processing time and energy consumption) and product quality properties (good rehydration properties and carotenoid preservation).

It was suggested that the ethanol pre-treatments mainly contributed to reducing the external resistance to mass transfer during drying, while US-assisted drying had a

greater influence on reducing the internal ones. This result highlights the complementary effects of both technologies here proposed.

Finally, by using US pre-treatments with different media (ethanol and water), it was possible to incorporate both microencapsulated hydrophilic and lipophilic nutrients into complex structured foods. That is, the pre-treatment with US can be used with a double purpose: both to improve drying as well as to incorporate nutrients and obtain a high-quality product.

The studies described in this Thesis, therefore, contribute to better understand the food drying process, demonstrated possible alternatives to obtain better products and processes, as well as open new perspectives for future studies and product development.

5. FUTURE STUDIES

From the results of this PhD Thesis, new hypotheses arise for future studies. Therefore, some possibilities are here described.

Firstly, different plant and animal materials must be evaluated, once each microstructure can respond differently to the processes here evaluated. The contribution of structural elements to mass transfer and the correlation among them, physical mechanisms, process efficiency and product properties must be considered.

Then, other emerging technologies must be studied, including their combination. For instance, by using pulsed electric field (PEF) pre-treatments, structural modifications similarly to ultrasound can be achieved. Furthermore, infrared radiation can be used assisting convective drying, considering their complementary mechanisms. Moreover, microwave radiation can also be used, although the effectiveness in intermediate and final products must be evaluated (more specifically, the effect of ethanol and drying on dielectric properties of food products).

Next, different quality parameters must be evaluated, including nutritional markers and their bioavailability and bioaccessibility. Different ways of consuming the obtained products must be considered, such as directly dried; dried, but formulating products; or rehydrated (in different ways).

Further, a mechanistic deepening is needed in drying studies, considering different structural scales (micro, meso and macro-scales), transport phenomena, physical mechanisms and mathematical modelling.

Finally, the possibility of incorporation of microencapsulated nutrients into plant materials was demonstrated. However, further studies are necessary considering other nutrients, wall materials, microencapsulation techniques, processing conditions, food products and also evaluating the final bioavailability and bioaccessibility.

REFERENCES

Bird, R. B. (2002). Transport phenomena. *Applied Mechanics Reviews, 55*(1), R1-R4.

Blasco, M., García-Pérez, J. V., Bon, J., Carreres, J. E., & Mulet, A. (2006). Effect of Blanching and Air Flow Rate on Turmeric Drying. *Food Science and Technology International, 12*(4), 315-323.

Bohrer, B. B. (1967). Azeotropic drying process. In: Google Patents.

Braga, A. M. P., Pedroso, M. P., Augusto, F., & Silva, M. A. (2009). Volatiles Identification in Pineapple Submitted to Drying in an Ethanolic Atmosphere. *Drying Technology, 27*(2), 248-257.

Braga, A. M. P., Silva, M. A., Pedroso, M. P., Augusto, F., & Barata, L. E. S. (2010). Volatile Composition Changes of Pineapple during Drying in Modified and Controlled Atmosphere. *International Journal of Food Engineering, 6*(1), pp.

Corrêa, J., Rasia, M., Mulet, A., & Cárcel, J. (2017). Influence of ultrasound application on both the osmotic pretreatment and subsequent convective drying of pineapple (Ananas comosus). *Innovative Food Science & Emerging Technologies, 41*, 284-291.

Corrêa, J. L. G., Braga, A. M. P., Hochheim, M., & Silva, M. A. (2012). The Influence of Ethanol on the Convective Drying of Unripe, Ripe, and Overripe Bananas. *Drying Technology, 30*(8), 817-826.

Crane, N. T., Wilson, D. B., Cook, D. A., Lewis, C. J., Yetley, E. A., & Rader, J. I. (1995). Evaluating food fortification options: general principles revisited with folic acid. *American Journal of Public Health, 85*(5), 660-666.

Chen, X. D., & Mujumdar, A. S. (2008). *Drying technologies in food processing*. Oxford: Blackwell Publishing.

Chou, S. K., & Chua, K. J. (2001). New hybrid drying technologies for heat sensitive foodstuffs. *Trends in Food Science & Technology, 12*(10), 359-369.

Das, M., Srimani, B. N., & Ghosh, D. N. (1984). Solvent dehydration of potato: selection of solvent and processing conditions. *International Journal of Food Science & Technology, 19*(5), 615-622.

Datta, A. K., & Ni, H. (2002). Infrared and hot-air-assisted microwave heating of foods for control of surface moisture. *Journal of Food Engineering, 51*(4), 355-364.

De la Fuente-Blanco, S., Riera-Franco de Sarabia, E., Acosta-Aparicio, V. M., Blanco-Blanco, A., & Gallego-Juárez, J. A. (2006). Food drying process by power ultrasound. *Ultrasonics, 44, Supplement*, e523-e527.

Deng, Y., & Zhao, Y. (2008). Effect of pulsed vacuum and ultrasound osmopretreatments on glass transition temperature, texture, microstructure and calcium penetration of dried apples (Fuji). *LWT - Food Science and Technology, 41*(9), 1575-1585.

EIA. (2018). Energy Information Administration: Today in Energy. In (Vol. 2018). Washington DC.

Fanton, X., & Cazabat, A. (1998). Spreading and instabilities induced by a solutal Marangoni effect. *Langmuir, 14*(9), 2554-2561.

Feng, Y., Zhou, C., ElGasim A. Yagoub, A., Sun, Y., Owusu-Ansah, P., Yu, X., Wang, X., Xu, X., Zhang, J., & Ren, Z. (2019). Improvement of the catalytic infrared drying process and quality characteristics of the dried garlic slices by ultrasound-assisted alcohol pretreatment. *LWT*, 108577.

Fernandes, F. A. N., Gallão, M. I., & Rodrigues, S. (2008). Effect of osmotic dehydration and ultrasound pre-treatment on cell structure: Melon dehydration. *LWT - Food Science and Technology, 41*(4), 604-610.
Fournier, J., & Cazabat, A. (1992). Tears of wine. *EPL (Europhysics Letters), 20*(6), 517.
Funebo, T., Ahrné, L., Prothon, F., Kidman, S., Langton, M., & Skjöldebrand, C. (2002). Microwave and convective dehydration of ethanol treated and frozen apple – physical properties and drying kinetics. *International Journal of Food Science & Technology, 37*(6), 603-614.
Gugliotti, M., & Todd, S. (2004). Tears of Wine. *Journal of Chemical Education, 81*(1), 67.
Hawlader, M. N. A., Perera, C. O., & Tian, M. (2006). Comparison of the Retention of 6-Gingerol in Drying of Ginger Under Modified Atmosphere Heat Pump Drying and other Drying Methods. *Drying Technology, 24*(1), 51-56.
Hurrell, R. F. (1997). Preventing Iron Deficiency through Food Fortification. *Nutrition Reviews, 55*(6), 210-222.
Kudra, T., & Mujumdar, A. S. (2009). *Advanced drying technologies*: CRC Press.
Latham, M. C. (2002). *Nutrición humana en el mundo en desarrollo* (Vol. 29): Fao.
Leenaars, A. F. M., Huethorst, J. A. M., & Van Oekel, J. J. (1990). Marangoni drying: A new extremely clean drying process. *Langmuir, 6*(11), 1701-1703.
Marangoni, C. (1871). Ueber die Ausbreitung der Tropfen einer Flüssigkeit auf der Oberfläche einer anderen. *Annalen der Physik, 219*(7), 337-354.
Mashkour, M., Maghsoudlou, Y., Kashaninejad, M., & Aalami, M. (2018). Effect of ultrasound pretreatment on iron fortification of potato using vacuum impregnation. *Journal of Food Processing and Preservation*, e13590.
Miano, A. C., & Augusto, P. E. D. (2018). The ultrasound assisted hydration as an opportunity to incorporate nutrients into grains. *Food Research International, 106*, 928-935.
Miano, A. C., Ibarz, A., & Augusto, P. E. D. (2016). Mechanisms for improving mass transfer in food with ultrasound technology: Describing the phenomena in two model cases. *Ultrasonics Sonochemistry, 29*, 413-419.
Miano, A. C., Rojas, M. L., & Augusto, P. E. D. (2017). Chapter 15 - Other Mass Transfer Unit Operations Enhanced by Ultrasound. In D. Bermudez-Aguirre (Ed.), *Ultrasound: Advances for Food Processing and Preservation* (pp. 369-389): Academic Press.
Miano, A. C., Rojas, M. L., & Augusto, P. E. D. (2018). Structural changes caused by ultrasound pretreatment: direct and indirect demonstration in potato cylinders. *Ultrasonics Sonochemistry*.
Michael, J. M., Lu, W., & Kathryn, L. M. (2005). Ultrasound Properties. In *Engineering Properties of Foods, Third Edition*: CRC Press.
Mujumdar, A. S., & Devahastin, S. (2000). *Fundamental principles of drying*. Exergex, Brossard, Canada.
Mujumdar, A. S., & Menon, A. S. (1995). *Drying of solids: principles, classification, and selection of dryers* (Vol. 1).
Mulet, A. (1994). Drying modelling and water diffusivity in carrots and potatoes. *Journal of Food Engineering, 22*(1), 329-348.
Ojha, K. S., Perussello, C. A., García, C. Á., Kerry, J. P., Pando, D., & Tiwari, B. K. (2017). Ultrasonic-assisted incorporation of nano-encapsulated omega-3 fatty

acids to enhance the fatty acid profile of pork meat. *Meat Science, 132*, 99-106.
Onwude, D. I., Hashim, N., Abdan, K., Janius, R., Chen, G., & Kumar, C. (2018). Modelling of coupled heat and mass transfer for combined infrared and hot-air drying of sweet potato. *Journal of Food Engineering, 228*, 12-24.
Peleg, M. (1979). Characterization of the stress relaxation curves of solid foods. *Journal of Food Science, 44*(1), 277-281.
Rao, M. A., & Steffe, J. F. (1992). *Viscoelastic Properties of Foods*: Elsevier Applied Science.
Rastogi, N. K. (2011). Opportunities and Challenges in Application of Ultrasound in Food Processing. *Critical Reviews in Food Science and Nutrition, 51*(8), 705-722.
Ricce, C., Rojas, M. L., Miano, A. C., Siche, R., & Augusto, P. E. D. (2016). Ultrasound pre-treatment enhances the carrot drying and rehydration. *Food Research International, 89*, 701-708.
Rodríguez, Ó., Eim, V., Rosselló, C., Femenia, A., Cárcel, J. A., & Simal, S. (2019). Application of power ultrasound on the convective drying of fruits and vegetables: effects on quality. *Journal of the Science of Food and Agriculture, 99*(2), 966-966.
Rojas, M. L., Alvim, I. D., & Augusto, P. E. D. (2019a). Incorporation of microencapsulated hydrophilic and lipophilic nutrients into foods by using ultrasound as a pre-treatment for drying: A prospective study. *Ultrasonics Sonochemistry, 54*, 153-161.
Rojas, M. L., & Augusto, P. E. D. (2017a). Effect of ethanol treatment on pumpkin microstructure. In. Brazil: Ge2P.
Rojas, M. L., & Augusto, P. E. D. (2017b). Water flowing by capillarity through xylem vessels. In.
Rojas, M. L., & Augusto, P. E. D. (2018a). Ethanol and ultrasound pre-treatments to improve infrared drying of potato slices. *Innovative Food Science & Emerging Technologies, 49*, 65-75.
Rojas, M. L., & Augusto, P. E. D. (2018b). Ethanol pre-treatment improves vegetable drying and rehydration: Kinetics, mechanisms and impact on viscoelastic properties. *Journal of Food Engineering, 233*, 17-27.
Rojas, M. L., & Augusto, P. E. D. (2018c). Microstructure elements affect the mass transfer in foods: The case of convective drying and rehydration of pumpkin. *LWT, 93*, 102-108.
Rojas, M. L., & Augusto, P. E. D. (2018d). Microstructure elements affect the mass transfer in foods: The case of convective drying and rehydration of pumpkin. *LWT-Food Science and Technology, 93*, 102-108.
Rojas, M. L., Silveira, I., & Augusto, P. E. D. (2019b). Improving the infrared drying and rehydration of potato slices using simple approaches: Perforations and ethanol. *Journal of Food Process Engineering, 42*(5), e13089.
Rojas, M. L., Silveira, I., & Augusto, P. E. D. (2020). Ultrasound and ethanol pre-treatments to improve convective drying: Drying, rehydration and carotenoid content of pumpkin. *Food and Bioproducts Processing, 119*, 20-30.
Silva, M. A., Braga, A. M. P., & Santos, P. H. S. (2012). Enhancement of fruit drying: the ethanol effect. In *Proceedings of the 18th International Drying Symposium (IDS 2012)*. Xiamen.

Silva, M. G., Celeghini, R. M. S., & Silva, M. A. (2018). Effect of ethanol on the drying characteristics and on the coumarin yield of dried guaco leaves (Mikania laevigata SCHULTZ BIP. EX BAKER). *Brazilian Journal of Chemical Engineering, 35*, 1095-1104.

Silva, P., Nogueira, G., Duarte, C., & Barrozo, M. (2018). Drying of acerola residues in a roto-aerated dryer assisted by infrared heating. In *IDS 2018. 21st International Drying Symposium Proceedings* (pp. 1527-1534): Editorial Universitat Politècnica de València.

Simpson, R., Ramírez, C., Nuñez, H., Jaques, A., & Almonacid, S. (2017). Understanding the success of Page's model and related empirical equations in fitting experimental data of diffusion phenomena in food matrices. *Trends in Food Science & Technology, 62*, 194-201.

Tatemoto, Y., Mizukoshi, R., Ehara, W., & Ishikawa, E. (2015). Drying characteristics of food materials injected with organic solvents in a fluidized bed of inert particles under reduced pressure. *Journal of Food Engineering, 158*(Supplement C), 80-85.

Thomson, J. (1855). XLII. On certain curious motions observable at the surfaces of wine and other alcoholic liquors. *Philosophical Magazine Series 4, 10*(67), 330-333.

Torki-Harchegani, M., Ghanbarian, D., Maghsoodi, V., & Moheb, A. (2017). Infrared thin layer drying of saffron (Crocus sativus L.) stigmas: Mass transfer parameters and quality assessment. *Chinese Journal of Chemical Engineering, 25*(4), 426-432.

Tyree, M. T., & Zimmermann, M. H. (2002). *Xylem structure and the ascent of sap* (2 ed.): Springer.

Vuilleumier, R., Ego, V., Neltner, L., & Cazabat, A. (1995). Tears of wine: the stationary state. *Langmuir, 11*(10), 4117-4121.

Wang, X., Feng, Y., Zhou, C., Sun, Y., Wu, B., Yagoub, A. E. A., & Aboagarib, E. A. A. (2019). Effect of vacuum and ethanol pretreatment on infrared-hot air drying of scallion (Allium fistulosum). *Food Chemistry, 295*, 432-440.

APPENDIX I: Microstructure elements affect the mass transfer in foods: The case of convective drying and rehydration of pumpkin

ROJAS, M. L., & AUGUSTO, P. E. D. (2018).
LWT-FOOD SCIENCE AND TECHNOLOGY, 93, 102-108.

LWT - Food Science and Technology 93 (2018) 102–108

Contents lists available at ScienceDirect

LWT - Food Science and Technology

journal homepage: www.elsevier.com/locate/lwt

Microstructure elements affect the mass transfer in foods: The case of convective drying and rehydration of pumpkin

Meliza Lindsay Rojas, Pedro E.D. Augusto*

Department of Agri-food Industry, Food and Nutrition (LAN), Luiz de Queiroz College of Agriculture (ESALQ), University of São Paulo (USP), Piracicaba, SP, Brazil

ARTICLE INFO

Keywords:
Water flow
Food drying
Plant microstructure
Xylem vessels
Shrinkage

ABSTRACT

Drying is typically evaluated considering a pure diffusional process in an isotropic sample. However, biological materials are anisotropic, and their structural elements can affect the water flow during processing. In this work, the effect of microstructure elements on sample deformation, drying and rehydration processes (kinetics and mechanisms) was evaluated, using pumpkin cylinders (formed mainly of parenchyma and xylem tissues). The cylinders were obtained considering a transversal (Tc) and longitudinal (Lc) cut orientation. The orientation of the xylem vessels did not affect the drying kinetics (both orientations showed similar k and *n* parameters of Page model). However, it had a significant impact on deformation. The Lc-samples showed more uniform appearance than the Tc ones. Tc showed a tendency towards black in the grey intensity histogram and higher density in the X-ray analysis. The Lc-samples presented the highest rehydration rate (k_1 of Peleg model: $2.87 \pm 0.16\ min\ d\ b^{-1}$). In contrast, higher equilibrium moisture was observed in samples with Tc (k_2 of Peleg model: $0.078 \pm 0.003\ d\ b^{-1}$). The results showed the anisotropicity of biological materials, and how the microstructural elements affect the mass transfer. Additionally, a water transport mechanism by capillarity through the xylem vessels during drying and hydration was demonstrated.

1. Introduction

Drying is a complex process involving simultaneous transport phenomenon (momentum, mass and energy) throughout a system. The drying of foods allows food products with longer shelf life, new forms of consumption, low cost of transportation and storage to be obtained.

The mass transfer process during drying is typically evaluated following Fick's Second Law (Fick, 1855) for regular geometries and considering many assumptions. Among these, the samples are considered isotropic materials. However, the complex structures of biological materials formed by different tissues and cells cause them to deviate from this isotropic state. In fact, there is evidence that the tissue of biological materials strongly influences the behaviour of mass transfer. For example, the transport of water and salts is favoured or limited depending on the orientation of muscle fibre, demonstrating that there is an anisotropic behaviour of diffusion (Gómez, Sanjuán, Arnau, Bon, & Clemente, 2017; Zhang, Xiong, Liu, Xu, & Zhao, 2011). In the case of plant material, the same could occur. Consequently, it is important to better understand the mechanisms involved in the water flow phenomenon during the drying of biological material with complex structures, such as those of plant origin.

In fact, many studies have been carried out into the effect of drying conditions and/or initial geometry of samples on the quality of drying and changes in food structure (shrinkage, deformation), properties and composition (Lewicki, 1998; López-Méndez et al., 2018; Mayor & Sereno, 2004; Parthasarathi & Anandharamakrishnan, 2014; Ramos, Brandao, & Silva, 2003; Ratti, 2001; Sagar & Kumar, 2010). However, the effect and contributions of the food microstructure elements on the drying process, the rehydration properties and the final characteristics of the dried product have not yet been adequately studied.

Consequently, it is important from both the academic and industrial (for the food industry, for example) points of view to study how the microstructural elements influence the process and properties of the product.

1.1. Theory: microstructure elements of food materials from plant origins

This study does not intend to discuss the theory of plant histology, or the structure and functions of their tissues, but to consider the basic aspects in order to better understand and explain the results. This study aims to be a contribution to:

- Demonstrating the anisotropic nature of food materials: The complex structures of biological materials, whose properties depend on

* Corresponding author. Avenida Pádua Dias, 11, Piracicaba, SP, 13418-900, Brazil.
E-mail addresses: mrojas@usp.br (M.L. Rojas), pedro.ed.augusto@usp.br (P.E.D. Augusto).

https://doi.org/10.1016/j.lwt.2018.03.031
Received 2 November 2017; Received in revised form 12 March 2018; Accepted 13 March 2018
Available online 14 March 2018
0023-6438/

the tissues and direction in which they are examined, cause them to deviate from an isotropic state.

- Correlating the structure with the process and properties of the product: The structure in living tissue has been amply described. However, very few published studies have used this information to correlate and explain how structure elements influence on the process or vice versa. As well as how this influences on the product properties.

Therefore, it is important to know the main type of microstructural elements in the edible fleshy part of the plants. The function they perform during plant growth, and which could remain, influence or change during processing.

Food materials of plant origin have an intricate microstructure formed by cells, intercellular spaces, capillaries and pores, organized into different tissues. Among the different types of plant tissues, only two of these contribute to the microstructure of edible parts: Parenchyma and the conducting tissue (Aguilera & Stanley, 1999).

On the one hand, the fleshy tissue of fruit is mostly made up of parenchymatic tissue, physiologically active in the synthesis, transport and storage of metabolic products. On the other hand, the conducting tissue, specifically xylem, conducts large quantities of water and solutes from the root to all parts of the plant and also provides mechanical support (Dickinson, 2000).

The xylem is a complex tissue composed of diverse types of cells. After an intricate process of differentiation, these lose their nuclei and cell contents, leaving behind a central lumen surrounded by secondary cell walls which together form tracheids (in conifers) or vessels elements (in angiosperms) (Appezzato-da-Glória & Carmello-Guerreiro, 2006; Dickinson, 2000; Fukuda, 1997; Kim, Park, & Hwang, 2014). According to Tyree and Zimmermann (2002b), one of the main mechanisms for the transport and storage of water around the living plant through the xylem is attributed to the phenomenon of capillarity. The flow of water through vessels can be compared to flow through smooth walled capillaries, where water molecules adhere to the cellulose microfibrils and other hydrophilic components of the wall (Oda & Hasezawa, 2006; Somerville et al., 2004).

Considering the above, using different cut directions in the sample, the aim of the present work was to describe the influence of xylem vessels on the drying and rehydration kinetics as well as on sample deformation. The second target was to propose an association between the microstructure and the water inlet and outlet mechanisms during drying and rehydration (an important, but little-studied topic, as described here) using pumpkin cylinders as representative material for plant foods.

2. Material and methods

2.1. Raw material

Pumpkin (*Cucurbita moschata* Duch.) samples were obtained from the local market (Piracicaba, SP, Brazil), and used in this study as a representative model for plant foods due to its microstructure. Cylinders with different cutting orientation were obtained, always considering the same pulp region using the skin as reference. Cylinders 0.5 cm thick and 2 cm in diameter were obtained through longitudinal (Lc) and transverse cuts (Tc) of the pumpkin samples. The longitudinal cut (Lc) was made parallel to the longest part of the pumpkin. The transverse cut (Tc) was made perpendicular to the longitudinal section. Then, the samples with Lc presented long xylem vessels (2 cm) orientated horizontally, while the samples with Tc presented short xylem vessels (0.5 cm) orientated vertically (see the images in Fig. 1). The comparison between samples with different vascular tissue orientation allowed the discussion of the anisotropy of biological materials.

2.2. Drying process

The drying process was performed at 40 °C using an air stream with a relative moisture of 25–27% and velocity of 0.8 ± 0.1 m s^{-1}, in an oven with circulation and air renewal (MA 035, Marconi, São Paulo, Brazil). The pumpkin cylinders were placed on a metal net to allow the free movement of warm air over the entire surface of the samples. The samples were dried to a constant weight. The sample weight was recorded using a precision scale (Mark 2200, TECNAL, Piracicaba, Brazil) coupled to the oven. For this, the scale was placed on top of the oven, and programmed to carry out the weighing underneath. A hook was attached to the bottom of the scale. This suspended hook was used inside the oven, which supported the metal net with the samples. The initial (*in-natura* samples) and final (after drying) moisture contents were measured by completely drying crushed samples at 105 °C using a moisture analyser (MX-50, A&D Company, Tokyo, Japan). Three replicates of the process were performed, each using 10 cylinders per cut direction.

All the moisture data over drying time was calculated by mass balance. Therefore, the moisture content along the drying process (M_t) was calculated according the Eq. (1), where W_{pt} is the amount of water remained at certain time of drying (t) and m_t is the sample weight at that time.

$$M_t\ \% = \frac{w_t}{m_t}.100 \tag{1}$$

Drying curves were plotted as a function of the dimensionless moisture ratio (MR) over the processing time, computed according to Eq. (2), where M_t is the moisture content during the drying process time (t), M_e is the equilibrium moisture and M_0 is the initial moisture of *in-natura* sample.

$$MR(t) = \frac{M_t - M_e}{M_0 - M_e} \tag{2}$$

2.3. Rehydration process

Rehydration was carried out by immersion in distilled water at 25 °C. To avoid limiting the process because of water availability, approximately 1 L of water was used for each 3 g of dry pumpkin. The evolution of the sample moisture over time was determined by mass balance. For this, the slices were removed from the water, superficially dried with absorbent paper, weighed and returned to the water. Three replicates of the process were performed, each using 10 cylinders.

2.4. Qualitative analyses of dried samples: grey scale image and X-ray

The shape deformation and shrinkage in the dried samples were evaluated indirectly by using the grey-scale image analysis and X-ray analysis.

The grey-scale image analysis was applied in studies with granulated minerals (Bjørk, 2006; Bjørk, Mair, & Austrheim, 2009), using the grey scale from 0 (black) to 255 (white) from images obtained in a controlled environment. The number of pixels corresponding to a specific grey intensity of the image are grouped forming the histogram of grey scale intensity. Therefore, this is specific to each image analysed. In this study, the images of dried samples were placed on a dark and uniform background and captured from the same distance using a 9.6-megapixel camera. The images were then processed using the COREL PHOTO-PAINT Home & student X7 (Corel Corporation, Ottawa), where the background of the images was extracted, and it was converted from the colour mode to an 8-Bit colour grayscale (256 colours) with a resolution of 300 × 300 dpi. Then the histogram was generated, showing the number of pixels corresponding to each level of the grey-scale range. Different grey values mean different distances from an arbitrary plane, thus indicating sample deformation.

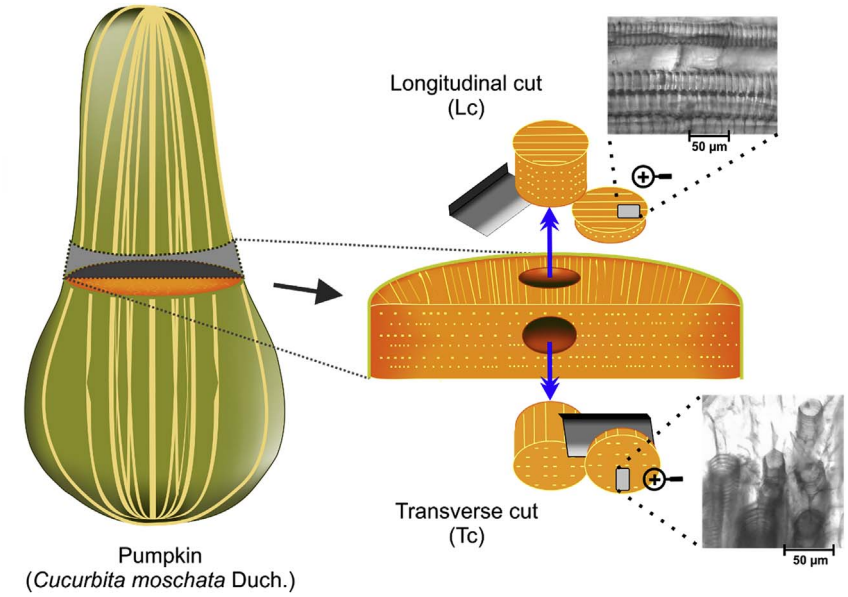

Fig. 1. Schematic representation of the sample preparation for posterior processing and analyses. In the details, optical microscopy of xylem vessels orientation as result of each longitudinal and transverse cut.

For the X-ray analysis, the dried samples were evaluated using an MX-20 Cabinet X-ray System with a DC-12 digital camera (MX-20 DC-12, Faxitron X-ray, Chicago, USA), connected to a computer, exposing the samples to the radiation at 20 kV for 10 s. The radiographs obtained allow the interpretation of different densities through the samples.

2.5. Microstructure analyses

The sample microstructure was analysed using the L1000 optical microscopy model (Bioval, Curitiba, Brazil) with a 20-W halogen lamp coupled to a portable camera of 1.3 megapixels. The samples were cut into ~8 µm dishes using a manual microtome (Ancap, São Paulo, Brazil), and observed with a 10× magnification lens. In some cases, methylene blue solution was used as a colorant. The images were captured after guaranteeing a representative field.

2.6. Mathematical description: drying and rehydration kinetics

The drying data was fitted using the Page Model (Eq. (3)) (Page, 1949), where MR(t) is the dimensionless moisture at drying time (t), k is the drying rate constant and n the dimensionless drying constant. Although the Page Model is an empirical model, successfully applied to drying process (Doymaz, 2005; Simal, Femenia, Garau, & Rosselló, 2005), Simpson, Ramírez, Nuñez, Jaques, and Almonacid (2017) recently demonstrated that the anomalous diffusion approach, based on fractional calculus, can attribute phenomenological meanings to it. Therefore, the drying rate constant (k) is associated with the diffusion coefficient and the geometry of the sample, while the dimensionless drying constant (n) describes the "type of diffusion", related to the food microstructure ($n > 1$ super-diffusion and $n < 1$ sub-diffusion). This could indicate that when $n \neq 1$, other mechanisms than diffusion are important. For example, the "super-diffusional process" ($n > 1$) may indicate the importance of capillarity.

$$\mathrm{MR(t)} = e^{-k.t^n} \tag{3}$$

The rehydration data was fitted using the Peleg model (Eq. (4)) (Peleg, 1979), where $M(t)$ is moisture content on a dry basis (kg water/kg dry matter (d.b.)) at time t (min), M_0 is the initial moisture content (d.b), k_1 is the rate constant (min·d.b^{-1}) and k_2 is the constant of the asymptotic level (d.b^{-1}). The reciprocal of k_1 represents the water absorption rate and the reciprocal of k_2 represents the water retention capacity.

$$M(t) = M_o + \frac{t}{k_1 + k_2.\, t} \tag{4}$$

The parameters of each models were iteratively adjusted to the experimental data by minimizing the sum of squared errors (*SSE* in Eq. (5)) between the experimental and predicted values for x experiments. A generalized reduced gradient algorithm was used, implemented in the 'Solver' tool of the Excel 2016 software (Microsoft, USA). The different initial guesses of the parameters were evaluated to detect possible convergence to local optima.

$$SSE = \sum_{i=1}^{x} ((predicted) - (experiemental))_i^2 \tag{5}$$

2.7. Statistical analysis

A completely randomised design (CRD) was conducted. All the analyses were performed at least 3 times. The analysis of variance (one-way ANOVA) was carried out with a significance level of 5%. Statistical analyses were determined using the IBM SPSS Statistics 23 software (IBM SPSS, USA).

3. Results and discussion

3.1. Pumpkin microstructure elements description

As can be seen in Fig. 2, the bright orange pumpkin pulp employed in the study was mainly composed of two types of tissue: Parenchyma and Xylem.

The parenchymatic tissue of pumpkin (Fig. 2a) presented cells of distinct size (242 ± 56 µm of diameter) with multi-shaped surface structure. The shape of a cell is the direct result of the pressure exerted upon it by neighbouring cells and the internal turgor pressure created during development. Additionally, parenchyma cells are separated by abundant intercellular space and despite their usually thin walls, fully turgid parenchymatic tissues can provide considerable stiffness to stems and resistance to local buckling (Dickinson, 2000).

Another type of tissue observed in pumpkin pulp was the vascular tissue, specifically xylem tissue (Fig. 2b). Considering the taxonomy of pumpkin (*Cucurbita moschata*) and its structural characteristics, the

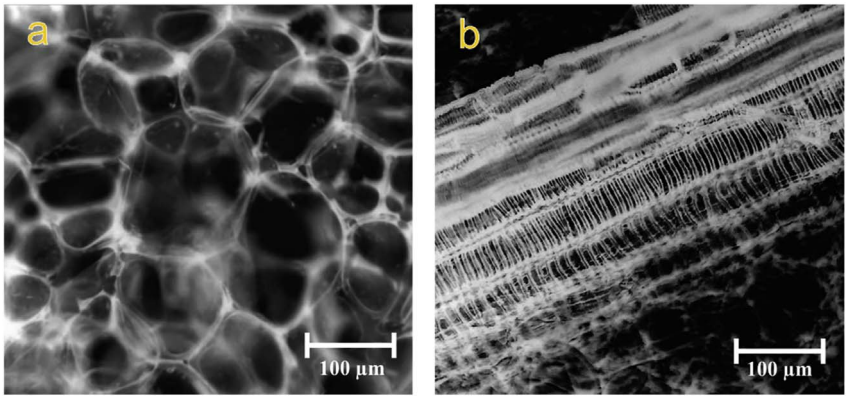

Fig. 2. Pumpkin structure elements observed by optical microscopy; a: parenchymatic tissue and b: vascular tissue (xylem vessels).

xylem observed in Fig. 2b corresponds to vessel elements and is composed of spiral vessels, 67 ± 13 µm in diameter.

As explained, the main functions of the xylem tissue during the growth of plants is mechanical support, and transport and storage of water throughout the plant (Oda & Hasezawa, 2006; Somerville et al., 2004; Tyree & Zimmermann, 2002a, pp. 175–214). The objective of the following sections was to describe the influence of the orientation of the xylem vessels during drying (3.2 section) and rehydration (3.3 section), as well as their role in the mass-transfer mechanisms of water outlet-inlet (3.4 section).

3.2. Effect of the orientation of the xylem vessels on drying kinetics and sample deformation

Fig. 3 shows the effect of the orientation of the xylem vessels on drying kinetics of pumpkin using samples with transverse (Tc) and longitudinal cuts (Lc). The drying curves were evaluated using the Page Model (Eq. (3)). The samples with transverse cuts (Tc) presented parameters of n (1.15 ± 0.02) and k (0.005 ± 0.000 min^{-1}); while for longitudinal cuts (Lc), these were n (1.18 ± 0.07) and k (0.004 ± 0.001 min^{-1}). It was observed that n was > 1 for both cuts, obtaining super-diffusive behaviour during drying according to Simpson et al. (2017) (the parameter n is related to the type of diffusion: $n > 1$ super-diffusion and $n < 1$ sub-diffusion). It reinforces the importance of other mass-transfer mechanisms – such as capillarity. However, no significant differences ($p > 0.05$) were observed between the drying parameters of both cuts. This may be because different structural modifications, such as deformation by shrinkage and tortuosity effects, occur simultaneously with the water outlet (López-Méndez et al., 2018). Furthermore, it can also indicate that any effect of the orientation of the xylem vessels is jeopardized as the resistance to water flow through the sample is small, probably due to the large surface area of the evaluated samples.

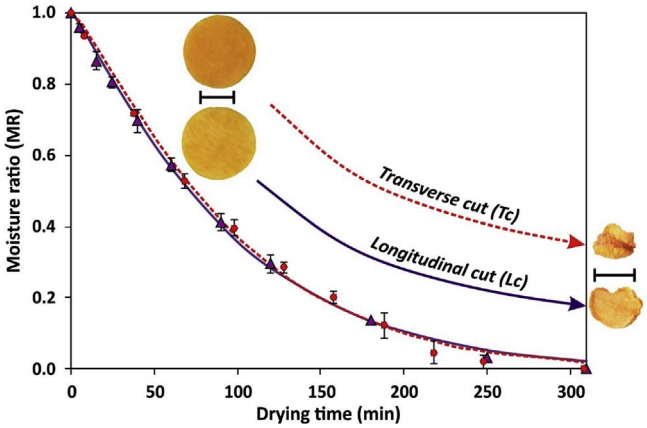

Fig. 3. Effect of the xylem vessels orientation on drying kinetics for both samples, with transverse cut (Tc) and longitudinal cut (Lc). Scale images (1 cm horizontal bar). See Fig. 1 for orientation reference. The dots are the experimental data, the vertical bars the standard deviation and the curves represent the Page Model (Eq. (3)).

To evaluate the sample deformation after drying, qualitative analyses (X-ray analysis and grey scale intensity histogram) of dried samples were done and these are shown in Figs. 4 and 5.

On the one hand, the samples with transversal cuts (Tc) deform and shrink in diameter rapidly during the drying process, while the thickness was maintained. On the other hand, the Lc samples mainly shrink in thickness while conserving their diameter. Consequently, they look more uniform – which is highly desirable. This can be shown through the X-ray analysis and grey intensity histogram (Figs. 4 and 5). When the samples have greater deformation, more shadows are generated in their images, because of their own twisting, showing a greater number of pixels distributed to the left on the graphic (tending to black, Fig. 5), as shown for samples with transverse cuts (Tc). Therefore, the opposite occurs in less deformed samples, as is the case of the Lc samples, where the histogram shifted to the right (tending to white, Fig. 5).

In addition, the X-rayed images of Tc samples showed more white regions than in the Lc samples. This indicates that after drying, the Tc samples presented a higher density due to the grouped tissues, which absorbed more X-rays as a consequence of shrinkage. This did not occur in the Lc samples, which showed a uniform appearance (Fig. 4).

The structural-related phenomena during drying are difficult to correlate and/or isolate from the mass transfer mechanisms. Many authors established that the shrinkage effect correlated with the variation of the moisture ratio. It has been reported that a higher rate of moisture removal is directly related to an increase in shrinkage ratio (Onwude, Hashim, Abdan, Janius, & Chen, 2018; Onwude, Hashim, Janius, Nawi, & Abdan, 2016). However, if shrinkage and moisture

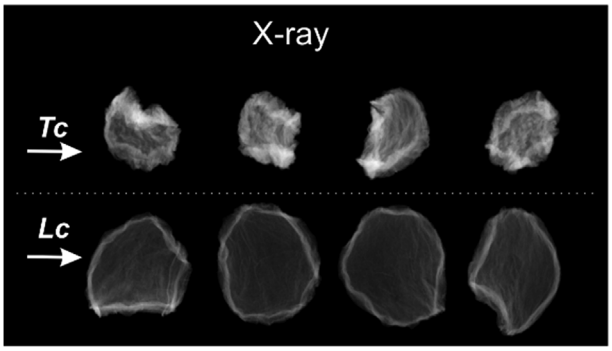

Fig. 4. X-ray radiographs to show the effect of the xylem vessels orientation on shrinkage and shape deformation of the samples with transverse cut (Tc) and longitudinal cut (Lc) at the end of drying process.

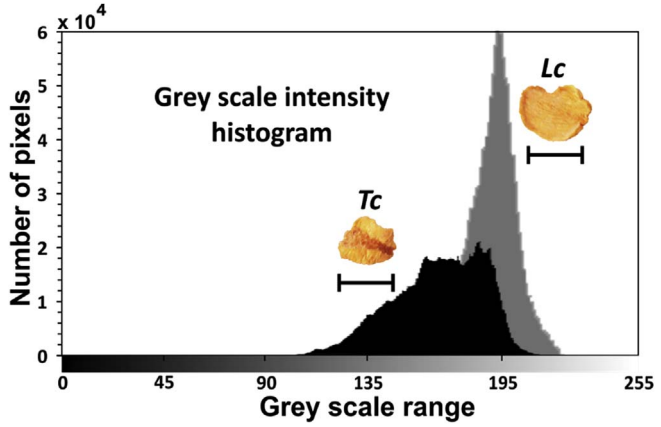

Fig. 5. Grey scale intensity histogram of the inserted sample images to show the effect of the xylem vessels orientation on shrinkage and shape deformation of the samples with transverse cut (Tc) and longitudinal cut (Lc) at the end of drying process.

removal occur simultaneously (as in fact, happens during drying), there would be a mutual interference. There was no difference between the drying rate of the Tc and Lc samples, although great differences in shrinkage and sample deformation were observed (Fig. 3). Probably these structural changes in the Tc samples interfered on its drying rate.

Furthermore, Chen and Mujumdar (2008) established that if the capillary diameter and reduction in thickness is balanced, an extended constant drying flux period is possible while the material shrinks. To corroborate that, another experiment was carried out increasing the thickness of the firsts cylinders. Then, cylinders of 2 cm in diameter and 3 cm thick were dried under the same conditions. However, once again, no significant differences in drying between the two types of cut (data not shown), and large differences in deformation between both samples were observed. The shrinkage occurred perpendicular to the orientation of the xylem vessels, as observed in Fig. 6.

In conclusion, in pumpkin samples with the same geometry, the orientation of the vessel does not show a significant effect on the drying kinetics. However, this orientation avoids the high deformation of structures parallel to them. Even so, it is important to evaluate the rehydration kinetics.

3.3. Effect of the orientation of the xylem vessels on rehydration kinetics

Unlike the drying process, noticeable differences were observed

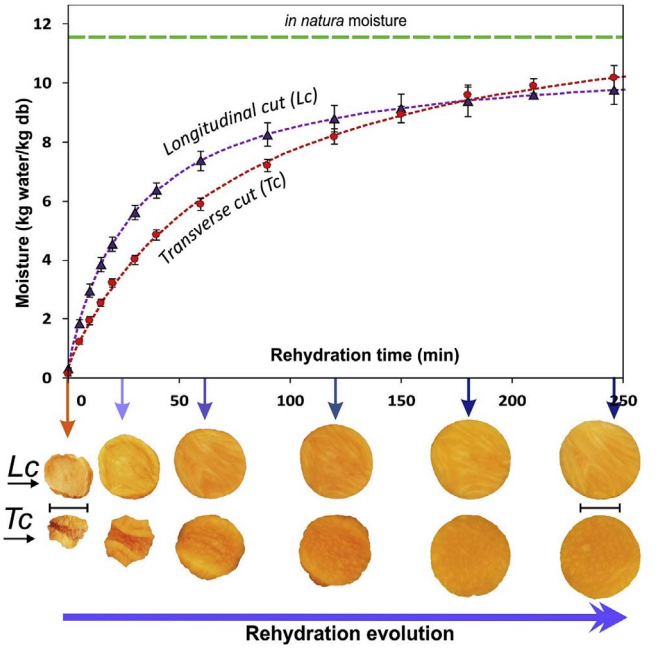

Fig. 7. Effect of the vascular tissue orientation on pumpkin rehydration. Up: Rehydration kinetics for both transverse cut (Tc) and longitudinal cut (Lc) samples. The dots are the experimental data and the curves the Peleg Model (Eq. (4)). Down: Evolution of rehydration (scale images (1 cm horizontal bar) of samples taken at different times of rehydration process are shown).

during the rehydration of samples with different vascular orientation (as can be seen from Fig. 7). The rehydration kinetics were modelled using the Peleg model (Eq. (4)), a two-term (k_1, k_2) mathematical function. The inverse of the parameter k_1 is associated with the maximum water absorption rate, while the inverse of the parameter k_2 is associated with the product equilibrium moisture content.

The k_1 parameter for the Lc samples was $2.87 \pm 0.16\ \text{min d.b}^{-1}$ and for the Tc samples, it was $5.84 \pm 0.41\ \text{min d.b}^{-1}$. The k_2 parameter for the Lc samples was $0.094 \pm 0.005\ \text{d b}^{-1}$, and $0.078 \pm 0.003\ \text{d b}^{-1}$ for the Tc. Significant differences ($p < 0.05$) between the Lc and Tc samples were observed for both k_1 and k_2. Consequently, as shown in Fig. 7, the vascular orientation affects both the water absorption rate and maximum moisture.

The Lc samples presented the highest rehydration rate (lowest k_1 value). According to Crank (1953) and Valle and Aguilera (1989) the

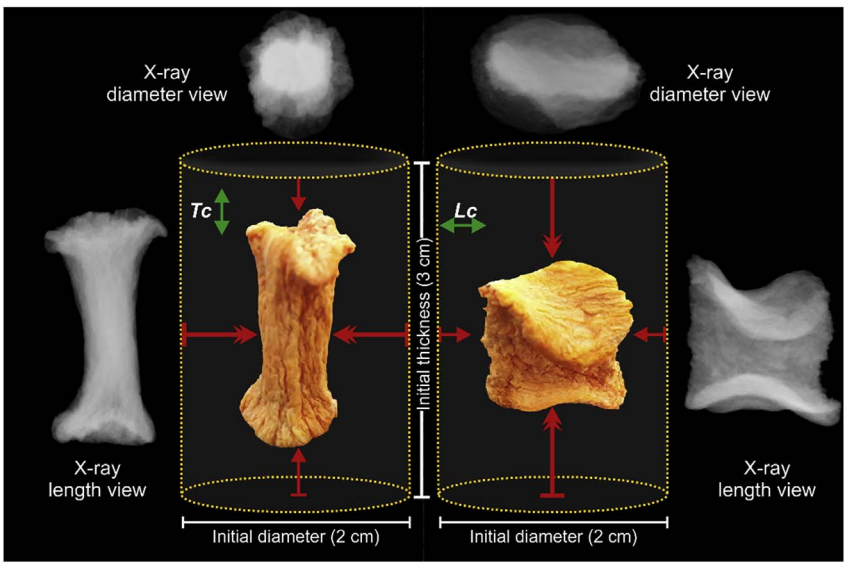

Fig. 6. Dried cylinders with transversal cut (Tc) and longitudinal cut (Lc) with their respective X-ray analysis (diameter and length views). Green arrows indicate the vascular orientation and the red arrows indicate the direction of the shrinkage/deformation. Left: Tc cylinders shown high shrinkage and deformation in diameter and low shrinkage in thickness. Right: Lc cylinders shown high shrinkage in thickness and low shrinkage and deformation in diameter. (For interpretation of the references to colour in this figure legend, the reader is referred to the Web version of this article.)

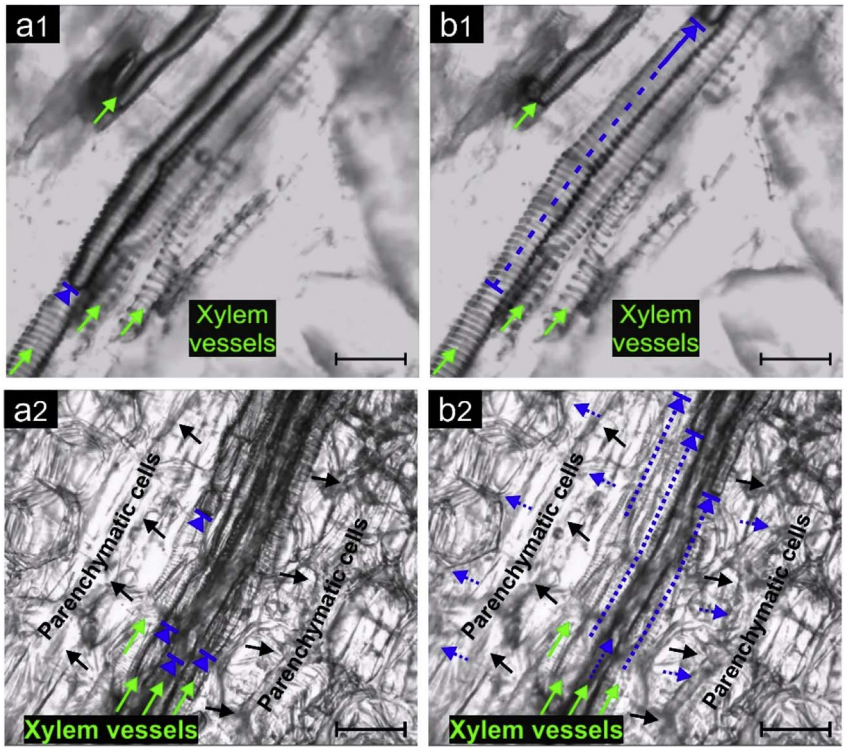

Fig. 8. Water flow through pumpkin xylem vessels during drying (1) and rehydration (2). Scale bars indicate 100 μm. The green arrows indicate the xylems vessels, the black arrows indicate parenchymatic cells and the blue arrows indicate the position and transport of the water from a to b. For more detail, this image can be better visualized through the video shown by Rojas and Augusto (2017), available at: https://youtu.be/o5vbxs1G81s.(For interpretation of the references to colour in this figure legend, the reader is referred to the Web version of this article.)

mass transfer increases in samples with low deformation during drying and is favoured by the low resistance in the internal passages. Since the internal resistance to flow depends on the width and tortuosity of channels (Cai & Yu, 2011), it could be stated that the Lc samples presented lower resistance to water flow than the Tc samples, probably due to their more uniform structure. In addition, Saguy, Marabi, and Wallach (2005) suggested that capillarity can be the primary mode of liquid transport in porous food. Therefore, the water transport by capillarity could be considered an important mechanism during rehydration. In the case of the Lc samples, the water enters quickly through the xylem vessels, favoured by their length and orientation, thus resulting in a higher hydration rate.

In contrast, the highest equilibrium moisture (lower k_2 value) was observed in the Tc samples. In fact, there is a point in the hydration process where both rehydration curves converge (at approximately 180 min), which coincides with the change in the shape of the Tc samples, as observed in the bottom part of Fig. 7. Beyond this point, the Tc samples are no longer deformed, but recover their original shape and continue to be rehydrated, surpassing the Lc samples. This indicates that in these samples, after a certain time, the short vertical xylem vessels are displaced, recovering their diameter and allowing them to contain more water.

Therefore, although non-significant differences were observed during drying, in the rehydration process, the xylem vessel orientation and the deformation level determine the rehydration rate and the amount of water retained in the samples.

3.4. Water transport mechanism during drying and rehydration

In this work, it is proposed and shown that the phenomenon of capillarity is one of the main water transport mechanisms during drying and rehydration through the xylem vessels.

By making a correlation with what happens in plants and the role played by the vascular system in the mechanisms of exit and reposition of water (Somerville et al., 2004; Tyree & Zimmermann, 2002b), the influence on water transport mechanisms during drying and rehydration can be inferred.

Therefore, during drying, as water vaporizes, the capillary forces lead the water through the xylem conduits to the surface of the sample. This is observed in Fig. 8 (1), where Image a1 shows the initial position of the water inside the xylem vessels, while Image b1 shows the route of the water transport during drying through pumpkin xylem vessels after ~30 s. Consequently, it contributes to decreasing the internal resistances by streamlining the water outlet during drying.

During rehydration, a similar mechanism occurs. When the dried material is in contact with water, the water is faster transported through the xylem vessels by capillarity. To demonstrate this, a drop of water was placed on the end of a dried sample sheet, then the water transport mechanism was microscopically observed. Fig. 8 (2) shows Image a2, which corresponds to the initial position of the water inside the xylem during rehydration, while Image b2 shows the transport and distribution of water reached after ~90 s. For more detail, the water transport by capillarity through the xylem vessels during pumpkin drying and hydration can be visualized in the video by Rojas and Augusto (2017), available at: https://youtu.be/o5vbxs1G81s.

During rehydration, the water is transported through the xylem vessel at a velocity of ~14 $\mu m\, s^{-1}$, and as the xylem vessels are filled with water, the adjacent cells are hydrated, as observed in Fig. 8 (b2). Therefore, the water is not only transported through the vessels: when vessels are filled, the water is available to be distributed through contiguous tissues, first through intercellular spaces, then it diffuses through the walls and membranes into the cell. It reinforces the importance of xylem vessels in both the drying and rehydration of the pumpkin cylinders.

Consequently, the anisotropy of biological materials was demonstrated. The *in-natura* heterogeneous structure had important effects and contributions on the observed drying and rehydration behaviour, as well as on the characteristics of the dried product (such as deformation and shrinkage). In the same way, the importance of the microstructural elements in the water flow mechanisms was demonstrated, reinforcing the idea that capillarity is an important mechanism during the drying and rehydration processes.

4. Conclusion

For the first time, the influence of the tissues and sampling orientation on the drying process, deformation and rehydration properties of a food vegetable (pumpkin) was demonstrated. The main tissues in the pumpkin structure were parenchyma and xylem. The results showed that the orientation of the xylem vessels did not show a significant effect on drying kinetics. However, it strongly affected the shrinkage and deformation of the samples (common problems in dry samples): the deformation of the samples could be minimized by making longitudinal cuts. During drying, the samples showed a super-diffusive behaviour ($n > 1$), highlighting the importance of capillarity. During rehydration, the effect of the orientation vascular tissue was shown to be important. The samples with longitudinal cuts had the highest rehydration rate (lower k_1 value). In contrast, the highest equilibrium moisture (lower k_2 value) was observed in samples with transverse cuts. It was shown that the orientation of the microstructure elements influenced the quality of the dried products and the mass transfer mechanisms.

The main limitation of this work is that only one type of sample was evaluated. Consequently, another type of food with a different structure must be studied. However, this work is a contribution and a motivation to start looking for other alternatives and change the traditional thinking and assumptions about the food structure and mechanisms of mass transport, especially during drying.

Authors' contributions

ML Rojas and PED Augusto conceived and designed the study. ML Rojas performed the experiments. ML Rojas and PED Augusto evaluated the data and wrote the manuscript.

Acknowledgements

The authors are grateful to the São Paulo Research Foundation (FAPESP, Brazil) for funding the project nº 2016/18052-5; to the National Council for Scientific and Technological Development (CNPq, Brazil) for funding the project nº 401004/2014-7; and to Cienciactiva for the M.L. Rojas Ph.D. scholarship (CONCYTEC, Peru; Contract 087-2016-FONDECYT), from the “Consejo Nacional de Ciencia, Tecnología e Innovación Tecnológica”. The authors are also grateful to the “Laboratório de Análise de Imagens” (LPV-ESALQ/USP) for the support and facilities for X-ray analysis.

Conflicts of interest

None.

References

Aguilera, J. M., & Stanley, D. W. (1999). *Microstructural principles of food processing and engineering.* Springer Science & Business Media.
Appezzato-da-Glória, B., & Carmello-Guerreiro, S. M. (2006). *Anatomia vegetal [Plant anatomy].* [Portugues](2nd ed.). Viçosa: Universidade Federal de Viçosa.
Bjørk, T. E. (2006). *Gray scale image analysis. Image analysis program for use with MATLAB.* from: http://folk.uio.no/torbjoeb/image_analysis/.
Bjørk, T. E., Mair, K., & Austrheim, H. (2009). Quantifying granular material and deformation: Advantages of combining grain size, shape, and mineral phase recognition analysis. *Journal of Structural Geology, 31*(7), 637–653.
Cai, J., & Yu, B. (2011). A discussion of the effect of tortuosity on the capillary imbibition in porous media. *Transport in Porous Media, 89*(2), 251–263.
Chen, X. D., & Mujumdar, A. S. (2008). *Drying technologies in food processing.* Oxford: Blackwell Publishing.
Crank, J. (1953). A theoretical investigation of the influence of molecular relaxation and internal stress on diffusion in polymers. *Journal of Polymer Science, 11*(2), 151–168.
Dickinson, W. C. (2000). *Integrative plant anatomy.* San Diego: Harcourt Academic Press.
Doymaz, İ. (2005). Drying characteristics and kinetics of okra. *Journal of Food Engineering, 69*(3), 275–279.
Fick, A. (1855). Ueber diffusion. *Annalen der Physik, 170*(1), 59–86.
Fukuda, H. (1997). Tracheary element differentiation. *The Plant Cell, 9*(7), 1147.
Gómez, J., Sanjuán, N., Arnau, J., Bon, J., & Clemente, G. (2017). Diffusion of nitrate and water in pork meat: Effect of the direction of the meat fiber. *Journal of Food Engineering, 214*, 69–78.
Kim, H. K., Park, J., & Hwang, I. (2014). Investigating water transport through the xylem network in vascular plants. *Journal of Experimental Botany, 65*(7), 1895–1904.
Lewicki, P. P. (1998). Effect of pre-drying treatment, drying and rehydration on plant tissue properties: A review. *International Journal of Food Properties, 1*(1), 1–22.
López-Méndez, E. M., Ortiz-García-Carrasco, B., Ruiz-Espinosa, H., Sampieri-Croda, A., García-Alvarado, M. A., Ochoa-Velasco, C. E., ... Ruiz-López, I. I. (2018). Effect of shape change and initial geometry on water diffusivity estimation during drying of gel model systems. *Journal of Food Engineering, 216*(Supplement C), 52–64.
Mayor, L., & Sereno, A. M. (2004). Modelling shrinkage during convective drying of food materials: A review. *Journal of Food Engineering, 61*(3), 373–386.
Oda, Y., & Hasezawa, S. (2006). Cytoskeletal organization during xylem cell differentiation. *Journal of Plant Research, 119*(3), 167–177.
Onwude, D., Hashim, N., Abdan, K., Janius, R., & Chen, G. (2018). The potential of computer vision, optical backscattering parameters and artificial neural network modelling in monitoring the shrinkage of sweet potato (*Ipomoea batatas* L.) during drying. *Journal of the Science of Food and Agriculture, 98*(4), 1310–1324.
Onwude, D., Hashim, N., Janius, R., Nawi, N., & Abdan, K. (2016). Modelling effective moisture diffusivity of pumpkin (Cucurbita moschata) slices under convective hot air drying condition. *International Journal of Food Engineering, 12*(5), 481–489.
Page, G. E. (1949). *Factors influencing the maximum rates of air drying shelled corn in thin layers.* Ann Arbor: Purdue University.
Parthasarathi, S., & Anandharamakrishnan, C. (2014). Modeling of shrinkage, rehydration and textural changes for food structural analysis: A review. *Journal of Food Process Engineering, 37*(2), 199–210.
Peleg, M. (1979). Characterization of the stress relaxation curves of solid foods. *Journal of Food Science, 44*(1), 277–281.
Ramos, I., Brandao, T., & Silva, C. (2003). Structural changes during air drying of fruits and vegetables. *Revista de Agroquimica y Tecnologia de Alimentos, 9*(3), 201–206.
Ratti, C. (2001). Hot air and freeze-drying of high-value foods: A review. *Journal of Food Engineering, 49*(4), 311–319.
Rojas, M. L., & Augusto, P. E. D. (2017). *Water flowing by capillarity through xylem vessels.* Retrieved from: https://youtu.be/o5vbxs1G81s.
Sagar, V., & Kumar, P. S. (2010). Recent advances in drying and dehydration of fruits and vegetables: A review. *Journal of Food Science and Technology, 47*(1), 15–26.
Saguy, I. S., Marabi, A., & Wallach, R. (2005). Liquid imbibition during rehydration of dry porous foods. *Innovative Food Science & Emerging Technologies, 6*(1), 37–43.
Simal, S., Femenia, A., Garau, M. C., & Rosselló, C. (2005). Use of exponential, Page's and diffusional models to simulate the drying kinetics of kiwi fruit. *Journal of Food Engineering, 66*(3), 323–328.
Simpson, R., Ramírez, C., Nuñez, H., Jaques, A., & Almonacid, S. (2017). Understanding the success of Page's model and related empirical equations in fitting experimental data of diffusion phenomena in food matrices. *Trends in Food Science & Technology, 62*, 194–201.
Somerville, C., Bauer, S., Brininstool, G., Facette, M., Hamann, T., Milne, J., ... Raab, T. (2004). Toward a systems approach to understanding plant cell walls. *Science, 306*(5705), 2206–2211.
Tyree, M. T., & Zimmermann, M. H. (2002a). *Hydraulic architecture of whole plants and plant performance Xylem structure and the ascent of sap.* Springer175–214.
Tyree, M. T., & Zimmermann, M. H. (2002b). *Xylem structure and the ascent of sap* (2nd ed.). Springer.
Valle, J. M., & Aguilera, J. M. (1989). Effects of substrate densification and CO2 conditions on supercritical extraction of mushroom oleoresins. *Journal of Food Science, 54*(1), 135–141.
Zhang, Q., Xiong, S., Liu, R., Xu, J., & Zhao, S. (2011). Diffusion kinetics of sodium chloride in Grass carp muscle and its diffusion anisotropy. *Journal of Food Engineering, 107*(3), 311–318.

APPENDIX II: Ethanol pre-treatment improves vegetable drying and rehydration: Kinetics, mechanisms and impact on viscoelastic properties.

ROJAS, M. L., & AUGUSTO, P. E. D. (2018)
JOURNAL OF FOOD ENGINEERING, 233, 17-27.

Journal of Food Engineering 233 (2018) 17–27

Contents lists available at ScienceDirect

Journal of Food Engineering

journal homepage: www.elsevier.com/locate/jfoodeng

Ethanol pre-treatment improves vegetable drying and rehydration: Kinetics, mechanisms and impact on viscoelastic properties

Meliza Lindsay Rojas, Pedro E.D. Augusto*

Department of Agri-food Industry, Food and Nutrition (LAN), Luiz de Queiroz College of Agriculture (ESALQ), University of São Paulo (USP), Piracicaba, SP, Brazil

ARTICLE INFO

Article history:
Available online 29 March 2018

Keywords:
Drying
PAGE model
Rehydration
PELEG model
Viscoelastic properties
Microstructure

ABSTRACT

Drying is a complex unit operation widely applied in food processing. There is still an increasing interest to enhance the process, as well as the product quality and properties. In this work, ethanol was used to enhance drying of pumpkin, which has been considered as a structurally representative material of plant foods. The effect of ethanol treatment on microstructure, convective drying kinetics (Page model), rehydration kinetics (Peleg model) and viscoelastic properties (generalized Maxwell model) was evaluated. The pre-treatment was conducted by immersing pumpkin cylinders in ethanol before convective drying. The ethanol treatment accelerated both drying and rehydration processes. Microstructure modifications were observed after the ethanol treatment, drying and rehydration. The rehydrated samples (control and ethanol treated) showed different viscoelastic properties compared with those *in natura*, which presented low stress decay and more residual elasticity. A possible mechanism was proposed. In conclusion, the ethanol improved both drying and rehydration processes, without negatively impacting on the microstructure and viscoelastic properties of pumpkin cylinders.

1. Introduction

Drying is a process widely applied to extend the shelf life, to obtain new forms of consumption and to decrease transportation and storage costs of food. However, the conventional drying methods based on using hot-air for long time can deteriorate the physicochemical and nutritional quality of the final product, as well as consuming a high amount of energy, with both economic and environmental impact (Chou and Chua, 2001; Kudra and Mujumdar, 2009; Mujumdar, 2008).

An interesting but still underexplored alternative to enhance the drying processes is the use of process accelerators agents, which must be biologically degradable and harmless to humans. In previous works, agents that form an azeotrope with water such as ethanol, acetic acid, isopropanol, n-propyl acetate and ethyl acetate, were used to accelerate the drying process and preserve the product properties and its compounds (Braga et al., 2009, 2010). When this type of agents are used, it is particularly important as the Marangoni effect seems to be of high importance for improving the drying process (Silva et al., 2012).

The drying kinetics is typically evaluated considering this unit operation as a simple diffusional process, following the Fick's Second law (Fick, 1855) through the series developed by (Crank, 1979) for regular geometries and considering many assumptions. Among these, the samples are considered as isotropic materials, which highly deviate from the complex structures of biological materials such as vegetables, formed by different tissues and cells. Consequently, the established diffusion coefficient becomes a parameter that includes the effects of the known hypotheses together with the unknown phenomena (Simal et al., 1998). This approach does not distinguish among the transport of water by liquid or vapour diffusion, capillary or hydrodynamic flow due to pressure gradients set up in the material during drying (Mujumdar, 2008). Furthermore, there are many evidences in the literature for doubting the applicability of the diffusional theory in biology (Agutter et al., 2000), especially in the drying and hydration processes. For example, Marabi and Saguy (2004) demonstrated that the food hydration behaviour deviate from the Fick's diffusive description when porosity is altered, while Goula and Adamopoulos (2009) highlighted the capillary flow during hydration. Further, Miano and Augusto (2015) demonstrated that the tissue permeability to water can change with the water activity, and that capillarity is

* Corresponding author. Avenida Pádua Dias, 11, Piracicaba, SP 13418-900, Brazil.
E-mail addresses: mrojas@usp.br (M.L. Rojas), pedro.ed.augusto@usp.br (P.E.D. Augusto).

https://doi.org/10.1016/j.jfoodeng.2018.03.028
0260-8774/

important in hydration process. Consequently, other approaches must be considered in order to adequately describe the drying process of biological material.

One emerging approach is using the concept of "non-Fickian diffusion", also called "anomalous diffusion", some Researchers used non-traditional mathematical solutions to explain the complexity of the mass transfer phenomenon (Metzler and Klafter, 2000; Pogany, 1976; Rosselló et al., 1997; Smith and Fisher, 1984). For example, the fractional calculus (Machado et al., 2011) was proposed to describe the anomalous diffusion phenomenon within materials (Simpson et al. (2013); Zhokh and Strizhak (2017). As the mass flow through capillarity can be important when ethanol is used as pre-treatment, the "anomalous diffusion" approach can be used for better understanding of the phenomena.

Pumpkin samples were used as raw material in this study. This product is appreciated due to its nutritive and functional properties (good source of carotene, water-soluble vitamins and amino acids) being used as additive in many food items (Aydin and Gocmen, 2017). Furthermore, different studies used pumpkin samples as suitable material to investigate the effect of different drying methods, as a good model (Arévalo-Pinedo and Murr, 2006; Nawirska-Olszańska et al., 2017; Nawirska et al., 2009). This study explored the use of ethanol as pre-treatment to hot-air convective drying of pumpkin cylinders. The effect of the ethanol treatment was studied on structure modifications, drying kinetics, rehydration kinetics and viscoelastic properties (thought stress-relaxation assays), being proposed a possible mechanism.

2. Material and methods

2.1. Raw material

Pumpkin (*Cucurbita moschata* Duch.) samples were obtained from local market (Piracicaba, SP, Brazil), being used in this study as a representative model of plant food due to its microstructure. Cylinders of 1.5 cm diameter and 1 cm height were obtained parallel to the longest part of the pumpkin (Fig. 1).

2.2. Ethanol pre-treatment

The pumpkin cylinders were pre-treated by immersion in ethanol 92.8% (V/V) for 1 h using 0.08:1 (w/V) of *in natura* pumpkin cylinders: ethanol ratio. After pre-treatment, both the control (C) (i.e. without pre-treatment), and the ethanol treated (E) samples were dried.

2.3. Drying process

The hot-air forced convective drying process was performed using air at 50 °C and 1 ± 0.1 m s^{-1} velocity, for this an oven with circulation and air renewal (MA 035, Marconi, São Paulo, Brazil) was used. The pumpkin cylinders were placed on a galvanized steel net to allow the free movement of warm air through the entire surface of the samples. The samples were dried until constant weight. The sample weight was recorded using a precision scale (AL 500, Marte Científica, São Paulo, Brazil). The initial (of *in natura* samples) and final (after drying) moisture content were measured by completely drying crushed samples at 105 °C using a moisture analyzer (MX-50, A&D Company, Tokyo, Japan).

It is important to mention that during the ethanol treatment the samples lose water and gain ethanol. Therefore, the moisture after ethanol treatment (M_p), include the remaining water and the gained ethanol. Being the calculated moisture after ethanol treatment according to Eq. (1).

$$M_p\% = \frac{w_p + OH_p}{m_p.100} \quad (1)$$

where w_p is the remaining water, OH_p the gained ethanol and m_p is the sample weight after ethanol treatment.

On the other hand, during drying process, the weight loss includes both the water and ethanol loss. Therefore, according to Silva

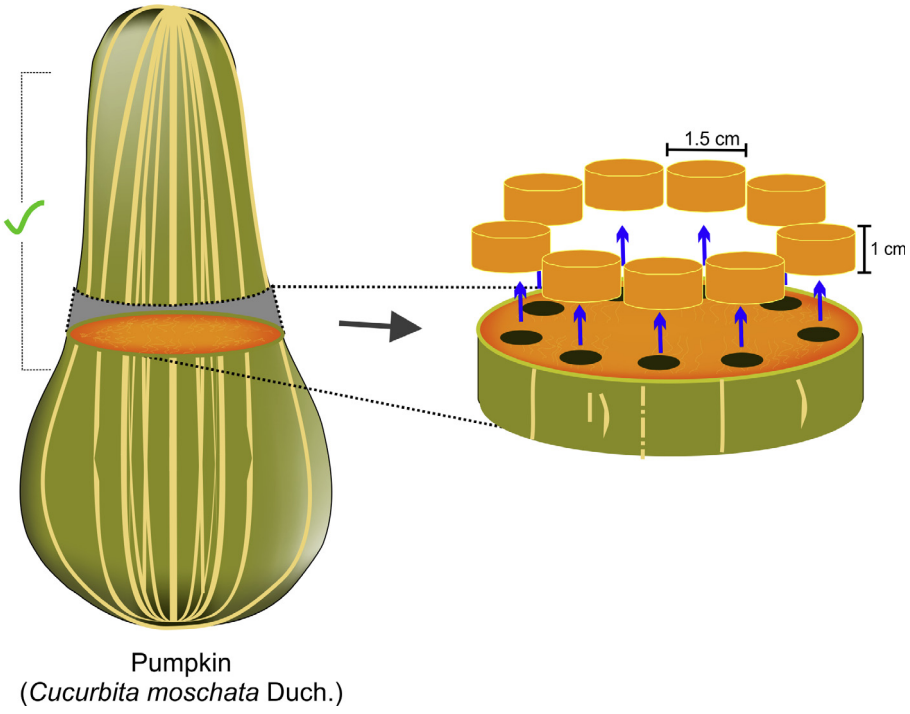

Fig. 1. Schematic representation of the pumpkin cylinders preparation for posterior processing and analyses.

et al. (2012), the moisture content (M_t) during the drying process time (t), include the water and ethanol remained at certain drying time divided by the sample weight at that time (Eq. (2)).

$$M_t\% = \frac{w_{pt} + OH_{pt}}{m_{pt}.100} \quad (2)$$

were w_{pt} is the amount of water, OH_{pt} is the amount of ethanol and m_{pt} is the sample weight at certain drying time. All the moisture data along drying time was calculated by mass balance.

Drying curves were plotted as a function of the dimensionless moisture content (MR) over the processing time, computed according to Eq. (3).

$$MR(t) = \frac{M_t - M_e}{M_p - M_e} \quad (3)$$

where M_t is the moisture content during the drying process time (t), M_e is the equilibrium moisture and M_p is the initial moisture after ethanol treatment. In the case of the control samples, the M_p is equal to the initial moisture of *in natura* sample. Therefore, the control and ethanol treated samples started the drying process with MR values equals to one.

2.4. Rehydration process

Rehydration was carried out by immersion of the drying cylinders in distilled water at 24 ± 1 °C. To avoid limiting the process because of water availability, approximately 0.003:1 of dried pumpkin: water (w/w) ratio was used. The evolution of sample moisture over the time was determined by mass balance. For this, the slices were removed from the water, superficially dried with absorbent paper, weighed and returned to the water until the end of the rehydration process, that is, until a constant mass of samples was registered.

2.5. Structure analyses

2.5.1. Microstructure analysis

The sample microstructure was analysed using the L1000 optical microscopy model (Bioval, Curitiba, Brazil) with a halogen lamp of 20 W coupled to a portable camera of 1.3 megapixels. The samples were cut into ~8 μm dishes using a manual microtome (Ancap, São Paulo, Brazil), and observed with a 10× magnification objective. The microstructure was analysed from the surface and internal tissues of the *in natura*, ethanol treated, dried and rehydrated samples. In some cases, solutions of ethanol-methylene blue or water-methylene blue were used as indicator to study the ethanol or water flow during pre-treatment, drying and rehydration processes. The images were captured after guaranteeing a representative field.

2.5.2. X-ray analysis

The ethanol effect in dried samples structure were evaluated indirectly through X-ray analysis, following the method described by Arruda et al. (2016). For this, the dried samples were evaluated using the MX-20 Cabinet X-ray System with DC-12 digital camera (Faxitron X-ray, Lincolnshire, England), connected to a computer, exposing the samples to the radiation at 20 kV for 10 s. The obtained radiographs allow the interpretation of different densities along the samples.

2.6. Viscoelastic properties: stress-relaxation analysis

The drying processes involve changes on food structure, such as the composition and structure of cell walls (Reeve, 1970), affecting their macroscopic characteristics (Mattea et al., 1989), such as texture - which can be considered an external reflection of micro and macrostructural characteristics of a food product (Aguilera and Stanley, 1999).

The stress-relaxation analysis was used to describe the viscoelastic changes on pumpkin cylinders. It consists of an instantaneous deformation to a sample, maintaining the strain constant and then evaluating the related stress over the time (Rao and Steffe, 1992). The stress-relaxation analyses of the *in natura* and rehydrated samples (C and E) were evaluated using a Texture Analyzer (TA.XT Plus, Stable Micro Systems Ltd., Surrey, UK) with a load cell of 50 kg-f (490.03 N) and a 35 mm aluminium cylindrical probe (P/35R). The cylinders were firstly compressed until a strain of 0.3 with 1 mm s^{-1} velocity. Then, the deformation was maintained constant for 15 s, being the data of force (N) versus time (s) recorded every 0.005 s to detailing analysing the relaxation curves and the model adjustment.

2.7. Mathematical description: viscoelastic properties, drying and rehydration kinetics

2.7.1. Viscoelastic properties (stress-relaxation behaviour)

To describe the viscoelastic properties, the data was fitted using the Generalized Maxwell Model (Rao and Steffe, 1992). Each Maxwell Element (ME) is composed by a Hookean spring (representing the solid, elastic behaviour) and a Newtonian dashpot (representing the fluid, viscous behaviour) organized in series. The Maxwell Elements are organized in parallel with an isolated Hookean spring, which contributes to the residual elasticity (ξ_e). The stress decay along the time ($\sigma(t)$) during the stress-relaxation evaluation can thus be described as a function of the constant strain (ε), the relaxation time (τ) and the elastic modulus (ξ) (Eq. (4)) (Rao and Steffe, 1992). From the relaxation time and the elastic modulus, the viscous modulus was obtained according to Eq. (5) (Rao and Steffe, 1992).

$$\sigma(t) = \varepsilon.\left(\xi_e + \xi_1.\exp\left(-\frac{t}{\tau_1}\right) + \xi_2.\exp\left(-\frac{t}{\tau_2}\right) + \ldots + \xi_i.\exp\left(-\frac{t}{\tau_i}\right)\right) \quad (4)$$

$$\eta_i = \tau_i.\xi_i \quad (5)$$

2.7.2. Drying and rehydration kinetics

The drying data was fitted using the Page Model (Eq. (6)), where MR(t) is the dimensionless moisture at drying time (t), k is the drying rate constant and n the dimensionless drying constant. Although the Page Model is an empirical model, successfully applied to drying process (Doymaz, 2005; Simal et al., 2005), recently Simpson et al. (2017) demonstrated that the anomalous diffusion approach, based on fractional calculus, can attribute phenomenological meanings to it: the drying rate constant (k) is associated with the diffusion coefficient and the geometry of the sample, while the dimensionless drying constant (n) describes the "type of diffusion", related to the food microstructure ($n > 1$ super-diffusion and $n < 1$ sub-diffusion). Our interpretation is that when $n \neq 1$, other mechanisms than diffusion are important. For example, the "super-diffusional process" ($n > 1$) may indicate the importance of capillarity.

$$MR(t) = \exp(-k.t^n) \quad (6)$$

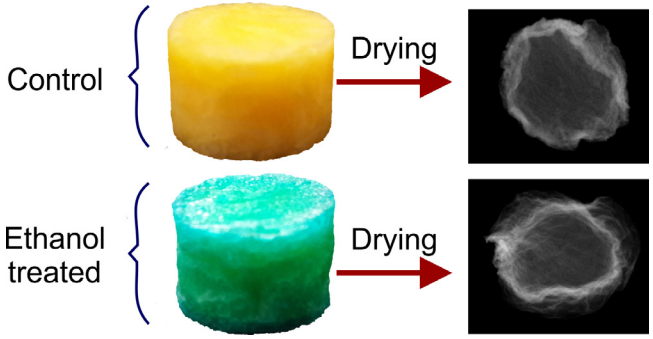

Fig. 2. X-ray images of the control and ethanol treated (ethanol and colourant) samples after drying process.

The rehydration data was fitted using the Peleg's model (Eq. (7)) (Peleg, 1979), where $M(t)$ is moisture content in dry basis (d.b) (g water/g dry matter) at time t (min), M_0 is initial moisture content (d.b), k_1 is the rate constant (min·d.b^{-1}) and k_2 is the constant of asymptotic level (d.b^{-1}). The reciprocal of k_1 represent the water absorption rate and the reciprocal of k_2 represent the water retention capacity.

$$M(t) = M_o + \frac{t}{k_1 + k_2.t} \tag{7}$$

The parameters of each models were iteratively adjusted to the experimental data by minimizing the sum of squared errors (*SSE* in Eq. (8)) between the experimental and the predicted values for the x experiements. A generalized reduced gradient algorithm was used, implemented in the 'Solver' tool of software Excel 2016 (Microsoft, USA). The different initial guesses of the parameters were evaluated to detect possible convergence to local optima.

$$SSE = \sum_{i=1}^{x} ((predicted) - (experiemental))_i^2 \tag{8}$$

2.8. Statistical analysis

A completely randomised design (CRD) was conducted. All the analyses were performed at least 3 times. The analysis of variance (ANOVA one way) was carried out with a significance level of 5%. Statistical analyses were determined using IBM SPSS Statistics 23 software (IBM SPSS, USA).

3. Results and discussion

3.1. Effect of ethanol treatment on pumpkin structure

Results and discussion on the structure modifications after ethanol application, drying and rehydration are presented in this section. This will allow a better understanding of the differences described in the following sections (drying and rehydration kinetics).

Fig. 2 shows the X-ray images of the dried cylinders, considering both treatments: control and ethanol treated (ethanol with colourant, immersed for 1 h). The X-ray images show that the ethanol treated samples present an external region less dense when compared to the control dried samples. This region includes the extent to which ethanol entered during pre-treatment, whose changes are best described in Figs. 3 and 4.

Fig. 3 show the pumpkin microstructure changes during the ethanol treatment. It is observed that the *in natura* samples present intercellular air (a), while when a drop of ethanol was placed on the

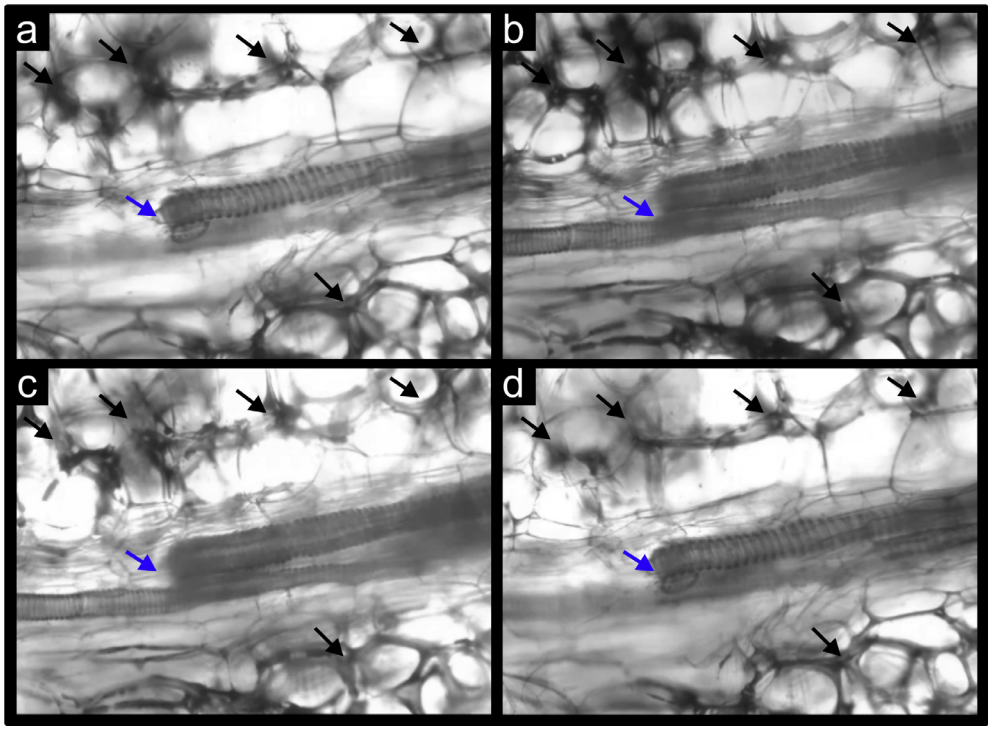

Fig. 3. Pumpkin microstructure during ethanol treatment. (a) *in natura* samples, (b) samples at the instant of ethanol application, (c) samples 10 s after ethanol application and (d) samples after 30 s ethanol application. The black arrows indicate the intercellular air of parenchymatic tissue and the blue arrow the xylems vessels. For more detail, this image can be better visualized through the video shown by Rojas and Augusto (2017), available at: https://youtu.be/VcsJ5WWp–0.(For interpretation of the references to colour in this figure legend, the reader is referred to the web version of this article)

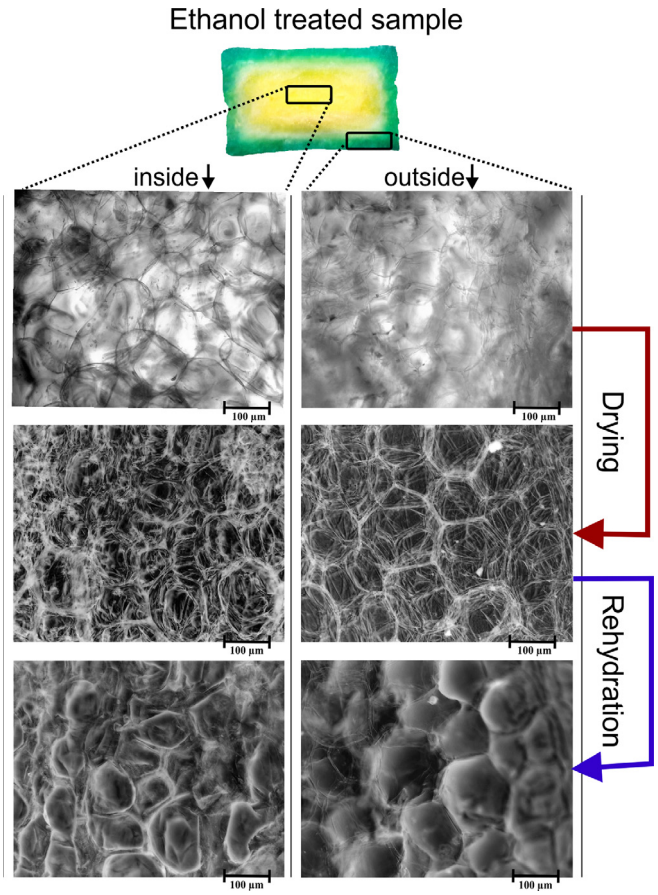

Fig. 4. Pumpkin structural changes during ethanol treatment, drying and rehydration. The upper image shows a longitudinal cut of a cylinder treated with ethanol and colourant. The green/blue region (outside) corresponds to the approximated distance to where the ethanol entered the sample. The orange colour is the central region to which ethanol did not enter. Each region was microscopically analysed: before drying, after drying and after rehydration.(For interpretation of the references to colour in this figure legend, the reader is referred to the web version of this article)

sample surface (b), it was evidenced that, along the time, the xylem vessels filled with ethanol and the intercellular air is expelled from inside the samples (c). As a result, there is less air between the cells of the parenchymatic tissue, the cell walls look slightly thinned, while no significant change is observed in the xylem vessels (d). For more detail, this image was better described through the video shown by Rojas and Augusto (2017), available at: https://youtu.be/VcsJ5WWp–0. It is important to emphasize that these changes are shown for a short time of sample exposition to ethanol, so when the samples were pre-treated for 1 h, the observed changes here probably were intensified.

Since no representative structural differences were observed on vascular tissue (xylem vessels) after ethanol treatment, drying and rehydration. It is probably due to its double cellulose and lignified walls, which confers a rigid structure. Therefore, Fig. 4 shows only the microstructural changes for the parenchymatic tissue, which show important changes.

Fig. 4 shows a longitudinally cut of an ethanol with colourant treated pumpkin cylinder. The external green/blue region corresponds to the distance where the ethanol entered during the pre-treatment, while the centre of orange colour, evidenced the region where the ethanol did not reach. The external and internal regions of the cylinders were microscopically analysed before drying (i.e. after ethanol treatment), after drying and after rehydration.

After ethanol treatment, it is observed that the cells show a compacted appearance with thin walls in the external part of the cylinder (Fig. 4). This is explained by the loss of turgidity caused by the exit of air, water and some solutes during the ethanol treatment. On the other hand, the tissue inside the cylinder (which remained the same characteristics of the control sample) present a defined cell wall structure (Fig. 4).

After drying, the internal tissue of the cylinder shows wrinkled and contracted cells, with thick walls and a large amount of entrained air, while the tissue on the outside of the cylinder shows wrinkled cells with thinner walls. This supports the statement above that during the ethanol treatment, apart from extracting water and solutes, there is also an intercellular air outlet. The small presence or even the absence of air inside tissues of alcohol treated samples was also evidenced by Shipman et al. (1972).

Finally, after rehydration, it was observed that the cells on the cylinder outside presented a more bloated appearance than those of the internal tissue, evidencing that the cell walls become more permeable, allowing more water to enter the cell. Similar explanation was stated by Funebo et al. (2002). This suggest that the ethanol treated samples present better absorption and retention of water than the control samples, as will be evidenced in section 3.2.2.

3.2. Ethanol treatment to improve the drying and rehydration processes

3.2.1. Impact of ethanol treatment on drying kinetics

Fig. 5 shows that the ethanol treated samples (E) dried faster than the control samples (C). For example, the drying time to reach a MR of 0.02 was 49.5% shorter for the ethanol treated samples than the required by the control samples.

Analysing the kinetic parameters obtained from Page Model, the control samples presented n parameter value of 1.233 ± 0.030 and the k value was 0.003 ± 0.000 min^{-1}, which is consistent with the literature. For example, Junqueira et al. (2017) convective dried pumpkin slices, obtaining n values greater than 1.240.

According to Simpson et al. (2017), the parameter n are related to the type of diffusion ($n > 1$ super-diffusion and $n < 1$ sub-diffusion). Therefore, both treatments showed a super-diffusive behaviour ($n > 1$) during drying, reinforcing the importance of other mass transfer mechanisms – such as capillarity.

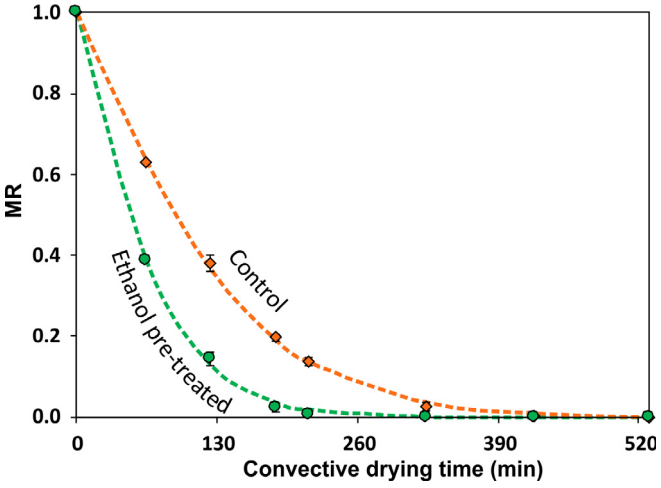

Fig. 5. Convective drying (50 °C and 1 ± 0.1 m·s^{-1} air velocity) kinetics of control (without treatment) and ethanol treated pumpkin cylinders. Dots are the experimental data; vertical bars are the standard deviation and the curves are the Page Model (Eq. (6)).

The n parameter was 1.197 ± 0.001 for the ethanol treated sample, with no significant differences ($p > 0.05$) with the control sample. It indicates that the microstructure changes during ethanol treatment and drying were not sufficiently differentiable between treatments (this will be better explained in the following sections).

However, significant differences ($p < 0.05$) were obtained for the k values between the control (0.003 ± 0.000 min^{-1}) and ethanol treated (0.006 ± 0.000 min^{-1}.) samples, where the high value obtained for ethanol treated samples reflects a faster drying process.

To date, few work has been carried out with the application of alcohols as treatment to accelerate the drying process of foods. Among them, celery soaked in glycerol (Shipman et al., 1972); apple slices immersed in ethanol (Funebo et al., 2002); pineapple slices dried in a ethanolic atmosphere (Corrêa et al., 2012); bananas surface treated with ethanol (Corrêa et al., 2012) and in ethanol-injected structured balls (mixed rice and soybean powders) samples (Tatemoto et al., 2015). Higher drying rates, when compared to the drying of control samples, were reported in all of them.

Different explanations for the drying enhancement due to alcohol application were proposed. It was proposed that the ethanol vaporizes early from inside to the surface forming flow channels and pores in the sample that promoted the drying process during the falling drying rate period (Tatemoto et al., 2015). In the obtained results (Fig. 5), however due to the different form of ethanol application, the faster drying can be seen even at the early drying stages and the formation of the mentioned channels was not observed. Further the existence of these channels probably would be evidenced in a significant change in the value of n, but this also did not occur.

Furthermore, it was assumed that being ethanol an organic solvent, which dissolves the cell wall compounds, the permeability through cell walls should be high for both dehydration and rehydration of ethanol treated food (Funebo et al., 2002). In fact, this effect was evidenced in the microstructure analyses, as demonstrated on section 3.1.

Additionally, it is known that ethanol-aqueous solutions present lower intermolecular forces and higher vapour pressure than the pure water, which could reduce the sample drying time (Corrêa et al., 2012). However, by using different compounds, Silva et al. (2012) verified that the observed improvement on drying by using different substances (ethanol, acetone, acetic acid and water) could not be related with their vapour pressure, but could be related with their surface tension. Consequently, the concept of flow due to the Marangoni effect was introduced by Silva et al. (2012) at the food drying area. In fact, previous studies conducted in non-food materials, which do not present absorbed water, corroborated that the Marangoni effect is involved in the drying process when alcohol is used (Leenaars et al., 1990; Schultz and Schlünder, 1990).

The Marangoni effect, also called Gibbs-Marangoni effect, is the mass transfer along an interface between two fluids with different surface tensions, being promoted by the formed surface tension gradient (Bird, 2002; Leenaars et al., 1990; Silva et al., 2012). It was first identified in the “tears of wine” by Thomson (1855). The general mechanism is based on that a liquid with high surface tension pulls more strongly on the surrounding liquid than one with low surface tension. The formed gradient in surface tension will naturally induce the liquid to flow away from regions of low surface tension (Gugliotti and Todd, 2004; Thomson, 1855).

In this work, a possible explanation for the mass transfer mechanism during drying promoted by the Marangoni Effect is proposed.

During ethanol treatment, the samples are placed in contact with ethanol, whose surface tension is lower than that of water. Consequently, the ethanol enters to the matrix, displacing the superficial water of samples.

Considering the Marangoni effect principles, explained by Bird (2002); Gugliotti and Todd (2004); Thomson (1855), a possible mass transfer mechanism during drying is described as follows.

During drying the ethanol superficially remained on the sample is rapidly vaporized. Consequently, a surface tension gradient is generated inside the samples. Therefore, since ethanol vaporizes faster, more water than ethanol is remained in the sample surface. This region with higher water than ethanol concentration has a higher surface tension, pulling strongly the water from the inside of the cylinder. As a result, the water is pulled up. The process is repeated, promoting the flow from the inside of the sample as many times as necessary to achieve a balance in the surface tension.

Furthermore, the flow promoted by the Marangoni Effect could be improved through the xylem vessels, which act like capillaries (Tyree and Zimmermann, 2002). In fact, by using ethanol with colourant during pre-treatment, it was observed that the xylem ducts inside the cylinders were blue painted after drying (Fig. 6), while the parenchymatic cells did not. This demonstrates that the ethanol travels longer into the cylinder through the xylem vessels, which could improve the Marangoni effect during drying.

3.2.2. Impact of ethanol treatment on rehydration kinetics

Fig. 7 shows the rehydration kinetics of control and ethanol treated pumpkin cylinders, which were described by the Peleg Model (Eq. (7)). The k_1 parameter was 4.84 ± 0.14 $min \cdot d.b^{-1}$ for the control samples and it was 4.05 ± 0.23 $min \cdot d.b^{-1}$ for the ethanol treated sample. The parameter k_2 was 0.094 ± 0.001 $d\,b^{-1}$ for the control sample and 0.074 ± 0.001 $d\,b^{-1}$ for ethanol treated samples. Both k_1 and k_2 values between treatments had significant differences ($p < 0.05$). Therefore, as observed in Fig. 7, the ethanol treatment enhanced the pumpkin cylinders rehydration by increasing both water absorption rate and the equilibrium moisture content. Both results are of great interest, since the rehydration process aims to restore the properties of the raw material. The results reflect that the ethanol treated samples have the best restoration properties that approximate the rehydrated samples to those of an *in natura* product.

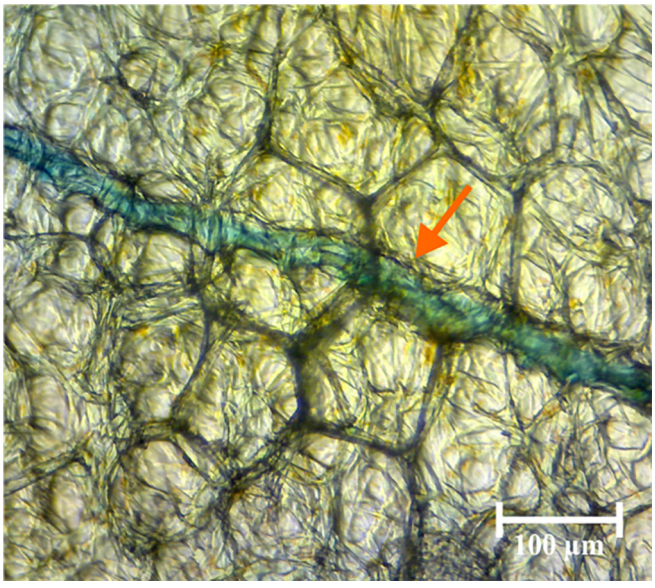

Fig. 6. Optical microscopy of dried pumpkin showing ethanol incorporation. The arrow shows the xylem vessel painted of blue due to the ethanol with colourant entrance.(For interpretation of the references to colour in this figure legend, the reader is referred to the web version of this article)

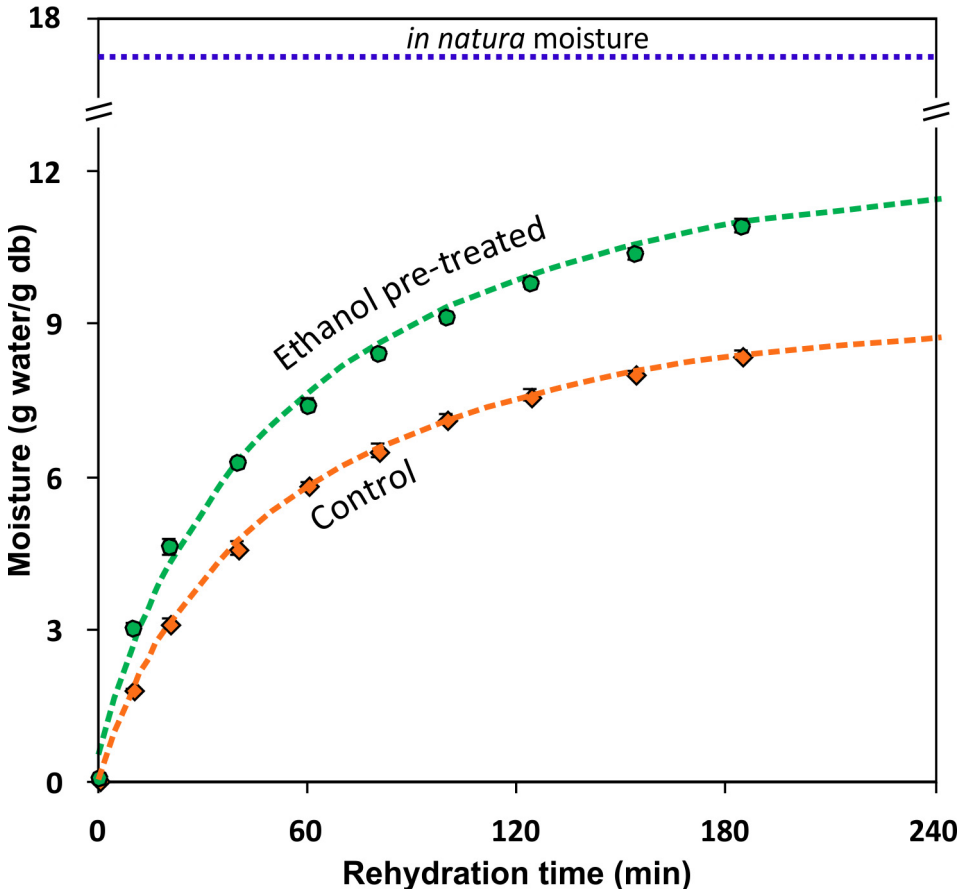

Fig. 7. Rehydration kinetics at 24 ± 1 °C of control and ethanol treated pumpkin cylinders after convective drying at 50 °C and 1 ± 0.1 m s^{-1} air velocity. Dots are the experimental data; vertical bars are the standard deviation and curves are the Peleg Model (Eq. (7)).

Furthermore, the *in natura* moisture content was 94.5% (17.08 g water. g dry matter^{-1}). The nearest moisture content after rehydration was reached by the ethanol treated samples, with 93% (12.4 g water. g dry matter^{-1}), compared with 90% (9.4 g water. g dry matter^{-1}) of the control sample at the end of rehydration process. Similar results were obtained in dehydrated apples (ethanol treated), which were attributed to the increased permeability of the thinned cell walls as a result of the ethanol treatment (Funebo et al., 2002). Consequently, the water is easier to enter inside the samples through the cell walls, improving the rehydration. In fact, the thinner cell walls in the ethanol pumpkin treated samples was evidenced in the previous microstructure section 3.1.

3.3. Impact of ethanol treatment on viscoelastic properties

The drying, pre-drying treatments and rehydration processes induce changes in food microstructure and composition (Krokida et al., 2001; Krokida and Philippopoulos, 2005; Lewicki, 1998). Consequently, it affects their macroscopic characteristics, such as viscoelastic properties.

3.3.1. Stress-relaxation behaviour

The stress-relaxation experimental data was well fitted ($R^2 > 0.99$) using the Generalized Maxwell Model with 2 Mx Elements (ME-1; ME-2) and a residual spring (Elastic Element (EE)) organized in parallel. In fact, the greater are the number of Maxwell elements in the model, better adjustment is obtained. However, this makes it difficult to interpret the parameters and their correlation with the food structure.

Each Maxwell Elements (ME-1 and ME-2) were composed by an elastic modulus (ξ), represented by the spring, and a viscous modulus (η), represented by the dashpot. This representation is shown in Fig. 8a.

Fig. 8b show the stress-relaxation behaviour of the *in natura* and rehydrated samples after drying with and without the ethanol treatment. It was observed that the *in natura* samples show low stress decay and more residual elasticity. It suggests that the *in natura* samples presented more elastic characteristics when compared with both control and ethanol treated rehydrated samples.

Table 1 show the GMM parameters obtained for *in natura* and rehydrated control (C) and ethanol treated (E) samples. The relaxation times (τ_1 and τ_2), modulus of elasticity (ξ_1 and ξ_2), viscosity (η_1 and η_2) of each Maxwell element and the residual elasticity (ξ_e) values are presented.

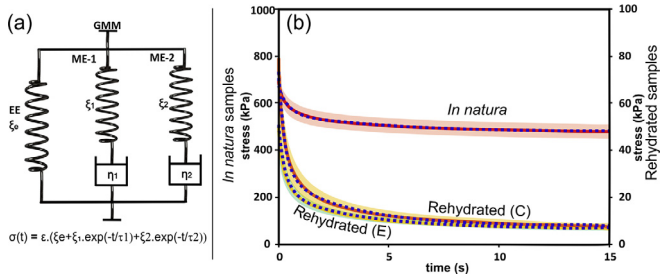

Fig. 8. (a) Representation of the applied General Maxwell Model (GMM). (b) Stress-relaxation curves: Continuous curves represent experimental averages; dotted lines represent model predictions and shaded regions represent the confidence bands of the experimental data (α = 5%).

Table 1
General Maxwell Model parameters for *in natura* and rehydrated samples (control and ethanol treated).[a]

GMM Parameters	*In natura*	Control (C)	Ethanol treated (E)
τ_1 (s)	4.67 ± 0.18^{A}	3.09 ± 0.02^{B}	3.34 ± 0.16^{B}
τ_2 (s)	0.39 ± 0.02^{A}	0.29 ± 0.01^{B}	0.31 ± 0.02^{B}
ξ_e (kPa)	1594.78 ± 110.58^{A}	27.40 ± 5.17^{B}	22.92 ± 3.64^{B}
ξ_1 (kPa)	268.05 ± 19.22^{A}	86.04 ± 14.88^{B}	62.26 ± 6.75^{B}
ξ_2 (kPa)	386.22 ± 24.08^{A}	175.62 ± 32.65^{B}	113.68 ± 14.37^{C}
η_1 (kPa.s)	1253.74 ± 116.34^{A}	265.58 ± 45.59^{B}	207.74 ± 25.38^{B}
η_2 (kPa.s)	150.70 ± 13.68^{A}	51.14 ± 10.85^{B}	34.89 ± 5.30^{B}

[a] Average ± standard deviation is presented. Different letters, indicate significant statistical differences ($p < 0.05$) among treatments.

It was observed that the *in natura* samples presented relaxation times (τ_1 and τ_2) higher than the relaxation times of the rehydrated samples. It reflects that during drying and rehydration, the tissue loses its original properties and characteristics. In fact, when compared with *in natura* samples, the τ_1 decreased 34% and 28% in the control and ethanol treated samples respectively, while the τ_2 decreased 26% and 21% in the control and ethanol treated samples respectively.

On the other hand, it was observed that the elastic modulus (ξ_e, ξ_1 and ξ_2) of both rehydrated samples presented significant reduction compared to the *in natura* elastic modulus. The elastic modulus for the *in natura* samples was higher due to cell-bonding and high turgor pressure of cells compared to elastic modulus of the rehydrated samples, reflecting cell wall damage and disruption during drying, losing its elasticity. The control samples presented a ξ_e reduction of 98%, 68% for ξ_1 and 52% for ξ_2, while the ethanol treated presented ξ_e, ξ_1 and ξ_2 modulus reduction of 99%, 77% and 71% respectively. In fact, the loss of elasticity in pumpkin tissue was also observed after osmotic dehydration (Mayor et al., 2007).

Finally, the viscous modulus (η) of *in natura* samples was higher than the rehydrated samples. The viscous modulus of the rehydrated samples was principally influenced by the composition and the water distribution changes inside the samples as a result of the structural damages during drying. It was reported that the fibres get more separated in pumpkin after water soaking due to the entrance of water in the intercellular spaces; as a consequence, the material fails at lower deformation and stress (Mayor et al., 2007). Therefore, the structure modifications conferred low resistance to flow, reflecting also the low value of viscous modulus in rehydrated samples.

It is important to mention that the elastic and viscous modulus of the ethanol treated samples were slightly lower than that of the rehydrated control samples. This could be attributed to structure modifications produced by the ethanol, which extracted and solubilized some components of their structures (reinforcing the assertion in section 3.1).

3.3.2. *Possible correlation between the Generalized Maxwell model parameters and structure elements*

Few works have proposed an association of viscoelastic model parameters with food structure elements. For example, Miano et al. (2017) described an association between the Generalized Maxwell model parameters and the melon structure and Augusto et al. (2013) described the Burger model in tomato juice.

A proposal is here presented to correlate each GMM elements and their parameters with the parenchymatic microstructure of pumpkin.

The parenchymatic microstructure is the majority tissue of the plant edible part (Aguilera and Stanley, 1999; Dickinson, 2000). Consequently, it was considered that this structure is the most important to describe the sample viscoelastic properties. The parenchymatic tissue is formed by intercellular spaces and cells which walls are cemented by a pectin layer (middle lamella) (Aguilera and Stanley, 1999; Dickinson, 2000). Therefore, a possible association of each structural element with the GMM elements is explained as follows.

Firstly, to better understand the contributions and behaviour of each component of the General Maxwell Model (GMM) (blue dotted line curve), the stress relaxation curves were discomposed in each of their components: The Elastic Element (EE, red line), the Maxwell Element 1 (ME-1, purple curve) and the Maxwell Element 2 (ME-2, green curve) (Fig. 9). It is observed, for all samples, that each GMM components present different behaviour. Therefore,

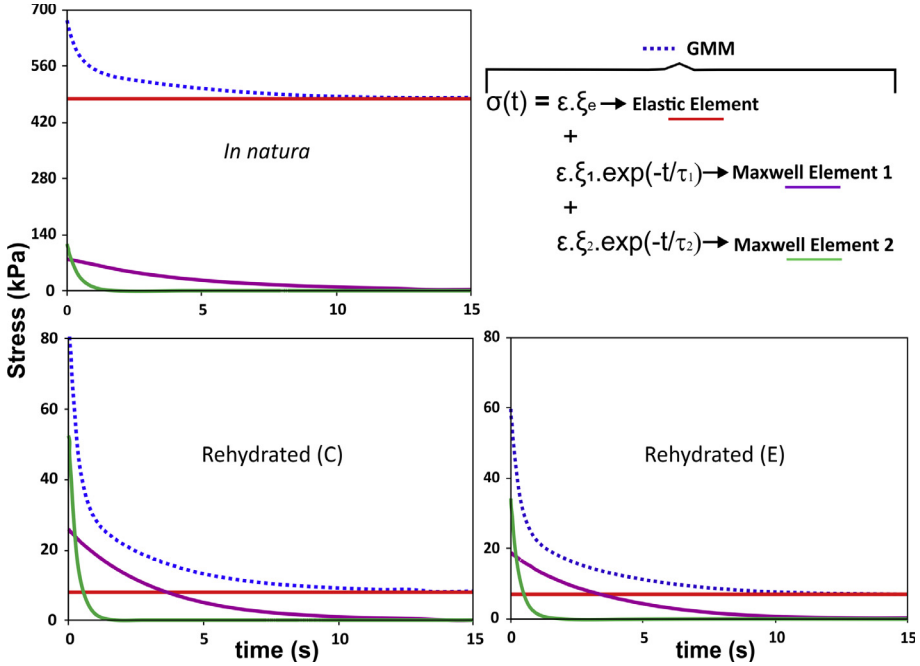

Fig. 9. General Maxwell Model (GMM) components for each sample. The Elastic Element (red line), the Maxwell Element 1 (purple curve) and the Maxwell Element 2 (green curve).(For interpretation of the references to colour in this figure legend, the reader is referred to the web version of this article)

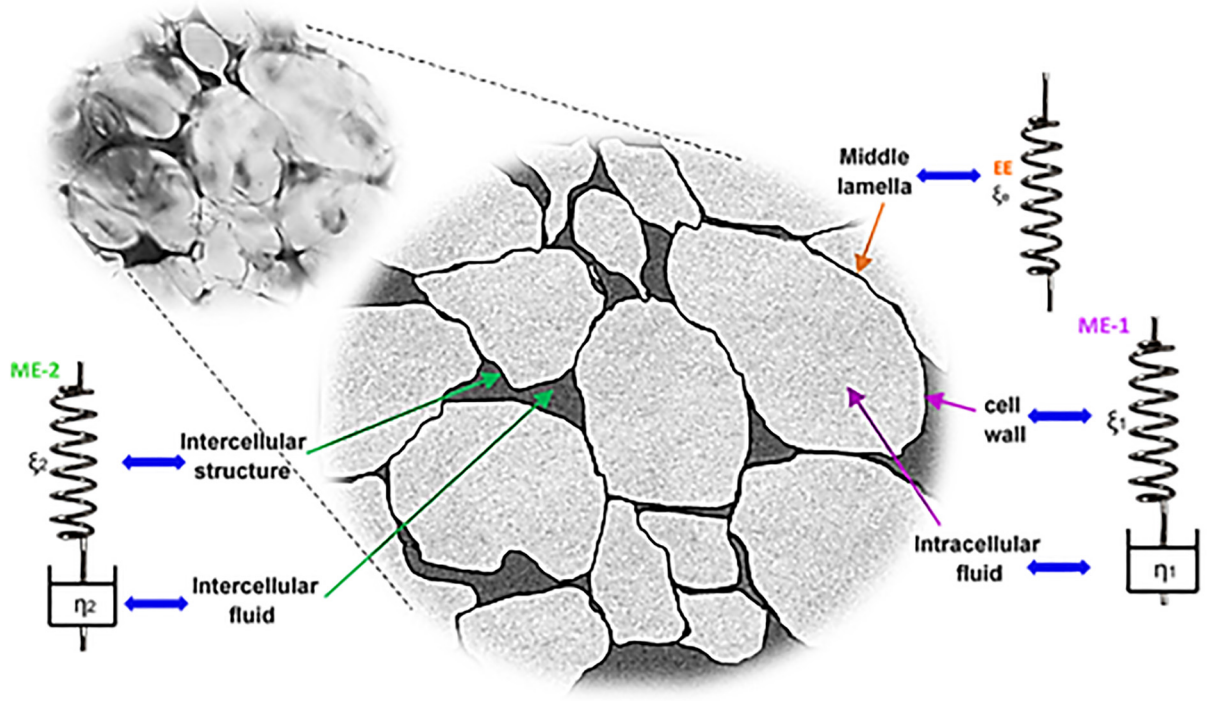

Fig. 10. General Maxwell Model elements correlated with pumpkin microstructure (represented by a microscopy). Maxwell Element 1 (ME-1); Maxwell Element 2 (ME-2) and residual spring (Elastic Element (EE)).

there is three structural elements (cells, intercellular structure and middle lamella) that could be correlated with the GMM elements (ME-1, ME-2 and EE) presented in Fig. 10.

The elastic element (EE) (red line, Fig. 9), with its parameter (ξe, constant of elasticity) would be associated with the middle lamella, since it presents only elastic behaviour. As observed in Fig. 9, the plot of the elastic element presents a horizontal constant behaviour, which value in the *in natura* samples was higher than that of the rehydrated samples, reflecting its greater elasticity.

As observed in Fig. 9, the ME-2 show a faster decay than the ME-1 for all samples. The ME-1 behaviour reflected the higher relaxation time (τ) observed in Table 1. Therefore, this suggest that the structure related to the ME-1 should be more rigid than the structure associated with the ME-2.

Considering that there are two options (cells and intercellular structure) to be correlated with ME-1 and ME-2, the characteristics of these structures must be evaluated. The cell rigidity is attributed to the cell wall and internal pressure (turgor), which are the major contributors to determining the mechanical properties of cells (Lin and Pitt, 1986; Smith et al., 2003). The turgor pressure keeps the cells and thereby tissues rigid (turgid) (Smith et al., 2003). The turgor of the cells depends on the integrity of their walls and their intracellular aqueous content (quantity and composition). Therefore, to produce turgor pressure, the elasticity of cell acts in conjunction with the cellular influx of water (Smith et al., 2003), and its water retention (Briggs, 1967; Frey-Wyssling, 1952). On the other hand, the intercellular structure is principally composed by water and air, which makes the structure more compressible than cells. Consequently, considering that the cells are more rigid than the intercellular spaces, the ME-1 would be associated with the cell structure and the ME-2 would be associated with the intercellular space structure and composition (Fig. 10). This makes sense since the relaxation times of the cells (τ_1) was higher than the relaxation times of the intercellular spaces (τ_2), reflecting that the cells are more rigid than the intercellular spaces.

After having associated each structure with each Maxwell element, the specific correlation between the ME parameters with the structure and composition of the cell and intercellular space could be made.

The ME-1 parameters are the ξ_1 and η_1, which would be correlated with the cell wall and the intracellular fluid. Therefore, the elastic modulus (ξ_1) was correlated to the cell wall, which is composed of cellulose and other polysaccharides that envelops the cell (Mattea et al., 1989) and confers elasticity (Smith et al., 2003). The η_1 modulus was correlated to intracellular fluid (mainly composed by high molecular weight constituents).

On the other hand, the ME-2 parameters are ξ_2 and η_2, which would be correlated with the intercellular structure and composition. Therefore, the ξ_2 modulus were correlated with the intercellular structure (mainly composed by hemicellulose and pectin), whose form depends on the shape of adjacent cells, and the η_2 was correlated to the intercellular fluid (mainly composed by air and water).

Finally, as general mode, after drying and rehydration the cell loses its *in natura* intracellular composition, decreasing the η_1 and η_2 in both rehydrated samples. In the same way, the cell wall structure was affected, decreasing its elasticity (ξ_1). Additionally, as reported by Lin and Pitt (1986) and Mattea et al. (1989), the cell-debonding mechanism (reduction of the contact area between cells) in dehydrated samples decrease the intercellular bond strength. Consequently, it decreased both the middle lamella elasticity (ξ_e) and the intercellular structure elasticity (ξ_2).

It is important to highlight that the given description was only a probable explanation of the mechanical behaviour changes considering some simplifications. Even so, it contributes for future studies to deepen in this complex association between the mechanical models and the biological structure.

4. Conclusion

Ethanol pre-treatment improved the drying process reducing 49.5% of the required time to reach MR < 0.02, when compared with control samples. Both treatments showed a super-diffusive behaviour (n > 1) during pumpkin drying, highlighting the importance of capillarity, and a higher drying rate (k) was obtained for ethanol treated samples. The ethanol effect was attributed to dissolution of cell wall compounds and to the Marangoni effect during drying. Additionally, the ethanol treatment improved the rehydration process, obtaining higher rehydration rate and water retention. The microstructure analyses evidenced that ethanol treatment, drying and rehydration process have higher impact on the parenchymatic tissue than in the vascular tissue. Finally, the stress-relaxation behaviour was evaluated using the General Maxwell Model (GMM), whose elements were correlated with the microstructure elements (cells and intercellular structures). The rehydrated samples showed different viscoelastic properties compared with those of the *in natura* sample, reflecting that during drying and rehydration, several modifications occurs in the structure and composition affecting the mechanical properties. Therefore, the obtained results shown an important option as the ethanol treatment to improve the drying and rehydration process without significant negative impacts in microstructure and viscoelastic properties.

Conflicts of interest

None.

Acknowledgements

The authors are grateful to the São Paulo Research Foundation (FAPESP, Brazil) for funding the project nº 2016/18052-5; to the National Council for Scientific and Technological Development (CNPq, Brazil) for funding the project nº 401004/2014-7; and to Cienciactiva for the M.L. Rojas Ph.D. scholarship (CONCYTEC, Peru; Contract 087-2016-FONDECYT), from the "Consejo Nacional de Ciencia, Tecnología e Innovación Tecnológica". The authors are also grateful to the "Laboratório de Análise de Imagens" (LPV-ESALQ/USP) for the support and facilities of X-ray analysis.

Nomenclature

C	Control samples, i.e. without pre-treatment
d.b	dry basis, i.e. g water/g dry matter
E	Ethanol pre-treated samples
EE	Elastic Element composed by ξ_e, and represented by an isolated spring
ε	constant strain [ ] (Eq. (4))
ξ	elastic modulus of the Maxwell element [kPa] (Eq. (4))
ξ_1	Elastic modulus of the Maxwell element 1 [kPa] (Table 1)
ξ_2	Elastic modulus of the Maxwell element 2 [kPa] (Table 1)
ξ_e	residual elasticity (kPa) (Eq. (4), Table 1)
GMM	Generalized Maxwell Model
In natura	cylinders of fresh pumpkin without any processing
k	drying rate constant [min^{-1}] (Eq. (6))
k_1	rate constant [$min \cdot d.b^{-1}$] (Eq. (7))
k_2	constant of asymptotic level [$d.b^{-1}$] (Eq. (7))
ME	Maxwell Element composed by an elastic modulus (ξ), represented by a spring, and a viscous modulus (η), represented by a dashpot
ME-1	Maxwell Element 1
ME-2	Maxwell Element 2
M_e	equilibrium moisture [%] (Eq. (3))
M_p	moisture after ethanol treatment [%] (Eq. (1))
m_{pt}	sample weight at certain drying time (t) [g] (Eq. (2))
MR(t)	dimensionless moisture at drying time (t) [ ] (Eq. (3) and (6))
M_t	moisture content during the drying process time (t) [%] (Eq. (2))
$M(t)$	moisture content during rehydration process [g water/g dry matter] (Eq. (7))
M_0	initial moisture content of dried samples [g water/g dry matter] (Eq. (7))
n	dimensionless drying constant [ ] (Eq. (6))
η	viscous modulus [kPa.s] (Eq. (5))
η_1	Viscous modulus of the Maxwell element 1 [kPa.s] (Table 1)
η_2	Viscous modulus of the Maxwell element 2 [kPa.s] (Table 1)
OH_p	amount of ethanol gained after ethanol treatment [g] (Eq. (1))
OH_{pt}	ethanol remained at certain drying time (t) [g] (Eq. (2))
$\sigma(t)$	stress decay along the stress-relaxation evaluation time [kPa] (Eq. (4))
SSE	sum of squared errors (Eq. (8))
t	time of stress-relaxation evaluation [s] (Eq. (4))
τ	relaxation time [s] (Eq. (4))
τ_1	relaxation time of the Maxwel element 1 [s] (Table 1)
τ_2	relaxation time of the Maxwel element 2 [s] (Table 1)
w_p	amount of remaining water after ethanol treatment [g] (Eq. (1))
w_{pt}	water remained at certain drying time (t) [g] (Eq. (2))

References

Aguilera, J.M., Stanley, D.W., 1999. Microstructural Principles of Food Processing and Engineering. Springer Science & Business Media.
Agutter, P.S., Malone, P.C., Wheatley, D.N., 2000. Diffusion theory in biology: a relic of mechanistic materialism. J. Hist. Biol. 33 (1), 71–111.
Arévalo-Pinedo, A., Murr, F.E.X., 2006. Kinetics of vacuum drying of pumpkin (Cucurbita maxima): modeling with shrinkage. J. Food Eng. 76 (4), 562–567.
Arruda, N., Cicero, S.M., Guilhien Gomes-Junior, F., 2016. Radiographic analysis to assess the seed structure of Crotalaria juncea L. J. Seed Sci. 38 (2), 161–168.
Augusto, P.E.D., Ibarz, A., Cristianini, M., 2013. Effect of high pressure homogenization (HPH) on the rheological properties of tomato juice: creep and recovery behaviours. Food Res. Int. 54 (1), 169–176.
Aydin, E., Gocmen, D., 2017. Bioaccessible phenolics, phenolic bioaccessibility and antioxidant activity of pumpkin flour. World Academy of Science, Engineering and Technology Int. J. Nutr. Food Eng. 4 (4).
Bird, R.B., 2002. Transport phenomena. Appl. Mech. Rev. 55 (1), R1–R4.
Braga, A.M.P., Pedroso, M.P., Augusto, F., Silva, M.A., 2009. Volatiles identification in pineapple submitted to drying in an ethanolic atmosphere. Dry. Technol. 27 (2), 248–257.
Braga, A.M.P., Silva, M.A., Pedroso, M.P., Augusto, F., Barata, L.E.S., 2010. Volatile composition changes of pineapple during drying in modified and controlled atmosphere. Int. J. Food Eng. 6 (1).
Briggs, G.E., 1967. Movement of Water in Plants. Movement of water in plants).
Corrêa, J.L.G., Braga, A.M.P., Hochheim, M., Silva, M.A., 2012. The influence of ethanol on the convective drying of unripe, ripe, and overripe bananas. Dry. Technol. 30 (8), 817–826.
Crank, J., 1979. The Mathematics of Diffusion. Oxford university press.
Chou, S.K., Chua, K.J., 2001. New hybrid drying technologies for heat sensitive foodstuffs. Trends Food Sci. Technol. 12 (10), 359–369.
Dickinson, W.C., 2000. Integrative Plant Anatomy. Harcourt Academic Press, San Diego.
Doymaz, İ., 2005. Drying characteristics and kinetics of okra. J. Food Eng. 69 (3), 275–279.
Fick, A., 1855. Ueber diffusion. Ann. Phys. 170 (1), 59–86.
Frey-Wyssling, A., 1952. Deformation and Flow in Biological Systems. Deformation and Flow in biological systems.
Funebo, T., Ahrné, L., Prothon, F., Kidman, S., Langton, M., Skjöldebrand, C., 2002. Microwave and convective dehydration of ethanol treated and frozen apple – physical properties and drying kinetics. Int. J. Food Sci. Technol. 37 (6), 603–614.
Goula, A.M., Adamopoulos, K.G., 2009. Modeling the rehydration process of dried

tomato. Dry. Technol. 27 (10), 1078–1088.
Gugliotti, M., Todd, S., 2004. Tears of wine. J. Chem. Educ. 81 (1), 67.
Junqueira, J.R.d.J., Corrêa, J.L.G., Ernesto, D.B., 2017. Microwave, convective, and intermittent microwave–convective drying of pulsed vacuum osmodehydrated pumpkin slices. J. Food Process. Preserv., e13250 n/a).
Krokida, M.K., Maroulis, Z.B., Saravacos, G.D., 2001. The effect of the method of drying on the colour of dehydrated products. Int. J. Food Sci. Technol. 36 (1), 53–59.
Krokida, M.K., Philippopoulos, C., 2005. Rehydration of dehydrated foods. Dry. Technol. 23 (4), 799–830.
Kudra, T., Mujumdar, A.S., 2009. Advanced Drying Technologies. CRC Press.
Leenaars, A.F.M., Huethorst, J.A.M., Van Oekel, J.J., 1990. Marangoni drying: a new extremely clean drying process. Langmuir 6 (11), 1701–1703.
Lewicki, P.P., 1998. Effect of pre-drying treatment, drying and rehydration on plant tissue properties: a review. Int. J. Food Prop. 1 (1), 1–22.
Lin, T.T., Pitt, R., 1986. Rheology of apple and potato tissue as affected by cell turgor pressure. J. Texture Stud. 17 (3), 291–313.
Machado, J.T., Kiryakova, V., Mainardi, F., 2011. Recent history of fractional calculus. Commun. Nonlinear Sci. Numer. Simulat. 16 (3), 1140–1153.
Marabi, A., Saguy, I.S., 2004. Effect of porosity on rehydration of dry food particulates. J. Sci. Food Agric. 84 (10), 1105–1110.
Mattea, M., Urbicain, M.J., Rotstein, E., 1989. Computer model of shrinkage and deformation of cellular tissue during dehydration. Chem. Eng. Sci. 44 (12), 2853–2859.
Mayor, L., Cunha, R., Sereno, A., 2007. Relation between mechanical properties and structural changes during osmotic dehydration of pumpkin. Food Res. Int. 40 (4), 448–460.
Metzler, R., Klafter, J., 2000. The random walk's guide to anomalous diffusion: a fractional dynamics approach. Phys. Rep. 339 (1), 1–77.
Miano, A.C., Augusto, P.E.D., 2015. From the sigmoidal to the downward concave shape behavior during the hydration of grains: effect of the initial moisture content on Adzuki beans (Vigna angularis). Food Bioprod. Process. 96 (Suppl. C), 43–51.
Miano, A.C., da Costa Pereira, J., Miatelo, B., Augusto, P.E.D., 2017. Ultrasound assisted acidification of model foods: kinetics and impact on structure and viscoelastic properties. Food Res. Int. 100 (Part 1), 468–476.
Mujumdar, A.S., 2008. Drying: principles and practice. In: Albright, L.F. (Ed.), Albright's Chemical Engineering Handbook. CRC Press, pp. 1667–1716.
Nawirska-Olszańska, A., Stępień, B., Biesiada, A., 2017. Effectiveness of the fountain-microwave drying method in some selected pumpkin cultivars. LWT 77, 276–281.
Nawirska, A., Figiel, A., Kucharska, A.Z., Sokół-Łętowska, A., Biesiada, A., 2009. Drying kinetics and quality parameters of pumpkin slices dehydrated using different methods. J. Food Eng. 94 (1), 14–20.
Peleg, M., 1979. Characterization of the stress relaxation curves of solid foods. J. Food Sci. 44 (1), 277–281.
Pogany, G., 1976. Anomalous diffusion of water in glassy polymers. Polymer 17 (8), 690–694.
Rao, M.A., Steffe, J.F., 1992. Viscoelastic Properties of Foods. Elsevier Applied Science.
Reeve, R., 1970. Relationships of histological structure to texture of fresh and processed fruits and vegetables. J. Texture Stud. 1 (3), 247–284.
Rojas, M.L., Augusto, P.E.D., 2017. Effect of Ethanol Treatment on Pumpkin Microstructure. Ge2P, Brazil.
Rosselló, C., Simal, S., SanJuan, N., Mulet, A., 1997. Nonisotropic mass transfer model for Green bean drying. J. Agric. Food Chem. 45 (2), 337–342.
Schultz, P., Schlünder, E.U., 1990. Influence of additives on crust formation during drying. Chem. Eng. Process: Process Intensificat. 28 (2), 133–142.
Shipman, J.W., Rahman, A., Segars, R., Kapsalis, J., Westcott, O., 1972. Improvement of the texture of dehydrated celery by glycerol treatment. J. Food Sci. 37 (4), 568–571.
Silva, M.A., Braga, A.M.P., Santos, P.H.S., 2012. Enhancement of fruit drying: the ethanol effect. In: Proceedings of the 18th International Drying Symposium (IDS 2012), Xiamen.
Simal, S., Femenia, A., Garau, M.C., Rosselló, C., 2005. Use of exponential, Page's and diffusional models to simulate the drying kinetics of kiwi fruit. J. Food Eng. 66 (3), 323–328.
Simal, S., Rosselló, C., Berna, A., Mulet, A., 1998. Drying of shrinking cylinder-shaped bodies. J. Food Eng. 37 (4), 423–435.
Simpson, R., Jaques, A., Nunez, H., Ramirez, C., Almonacid, A., 2013. Fractional calculus as a mathematical tool to improve the modeling of mass transfer phenomena in food processing. Food Eng. Rev. 5 (1), 45–55.
Simpson, R., Ramírez, C., Nuñez, H., Jaques, A., Almonacid, S., 2017. Understanding the success of Page's model and related empirical equations in fitting experimental data of diffusion phenomena in food matrices. Trends Food Sci. Technol. 62, 194–201.
Smith, A.C., Waldron, K.W., Maness, N., Perkins-Veazie, P., 2003. Vegetable texture: measurement and structural implications. Postharvest Physiol. Pathol. Veg. 2, 297–329.
Smith, P.M., Fisher, M.M., 1984. Non-Fickian diffusion of water in melamine-formaldehyde resins. Polymer 25 (1), 84–90.
Tatemoto, Y., Mizukoshi, R., Ehara, W., Ishikawa, E., 2015. Drying characteristics of food materials injected with organic solvents in a fluidized bed of inert particles under reduced pressure. J. Food Eng. 158 (Suppl. C), 80–85.
Thomson, J., 1855. XLII. On certain curious motions observable at the surfaces of wine and other alcoholic liquors. Phil. Mag. Series 4 10 (67), 330–333.
Tyree, M.T., Zimmermann, M.H., 2002. Xylem Structure and the Ascent of Sap, 2 ed. Springer.
Zhokh, A., Strizhak, P., 2017. Non-Fickian diffusion of methanol in mesoporous media: geometrical restrictions or adsorption-induced? J. Chem. Phys. 146 (12), 124704.

APPENDIX III: Ethanol and ultrasound pre-treatments to improve infrared drying of potato slices

ROJAS, M. L., & AUGUSTO, P. E. D. (2018).
INNOVATIVE FOOD SCIENCE & EMERGING TECHNOLOGIES, 49, 65-75.

Innovative Food Science and Emerging Technologies 49 (2018) 65–75

Contents lists available at ScienceDirect

Innovative Food Science and Emerging Technologies

journal homepage: www.elsevier.com/locate/ifset

Ethanol and ultrasound pre-treatments to improve infrared drying of potato slices

Meliza Lindsay Rojas, Pedro E.D. Augusto*

Department of Agri-Food Industry, Food and Nutrition (LAN), Luiz de Queiroz College of Agriculture (ESALQ), University of São Paulo (USP), Piracicaba, SP, Brazil

ARTICLE INFO

Keywords:
Drying
Rehydration
Microstructure
Viscoelastic properties
Texture

ABSTRACT

Ethanol and ultrasound (US) were applied as pre-treatments to improve the infrared (IR) drying of potato slices. Pre-treatments included Control samples (Without any pre-treatment), samples immersed in ethanol (Ethanol treated) and treated with US using ethanol (Ethanol + US) and water medium (Water + US). Effects on microstructure, drying, rehydration, and viscoelasticity were studied. Microstructure analyses suggested that ethanol affected the potato cell wall. The Water + US pre-treatment impacted the starch granules dispersion inside cells. However, higher modifications were observed when Ethanol + US was applied. Compared to the Control, all pre-treatments decreased the drying time, while Ethanol + US provided the highest reduction. In contrast, a slight decrease in rehydration properties was observed. The dried and rehydrated samples presented similar viscoelasticity among them but differed significantly with the *in-natura* (fresh potato) samples. Possible mechanisms were discussed. The results open new perspectives about an innovative method to improve drying.

1. Introduction

Drying is a complex unit operation that implies simultaneous heat and mass transfer to remove moisture from a product. The heat transfer during drying of agricultural materials can be obtained as result of conduction, convection or radiation, as well as their combination (Mongpraneet, Abe, & Tsurusaki, 2004; Ratti & Mujumdar, 2006). Conventionally, industrial food drying is performed using the convective hot-air drying technique, in which air acts as the heat and moisture carrier (Onwude, Hashim, & Chen, 2016). However, there is a growing interest for other technologies focusing on the reduction of drying time and energy consumption, an increase of overall efficiency and products quality.

This study will focus on study the application of ethanol and ultrasound (US) as pre-treatments to improve infrared (IR) drying of potato slices. In fact, there are different thermal (such as blanching by hot water or vapour, microwave assisted drying) and non-thermal (such as osmotic pre-treatments, ultrasound and pulsed electric fields) methods or technologies that are being studied to improve the conventional drying process. However, there are few studies focused on improving IR drying of food by combining other technologies.

During IR drying, the product is heated directly by absorption of infrared energy in the form of electromagnetic waves, rather than by transfer of heat from the hot air (Afzal & Abe, 1998; Mongpraneet et al., 2004). The ability of a product to absorb this energy depends on the source wavelength, porosity and the composition of the surface (Lampinen, Ojala, & Koski, 1991; Pawar & Pratape, 2017). Generally, solid materials absorb infrared radiation in a thin surface layer (Lampinen et al., 1991). Several authors applied the IR for drying agricultural products. For example, it was used in combination with convective hot-air drying or to completely replace it for different products, such as, sweet potato (Onwude et al., 2018), citrus press-cakes (Senevirathne et al., 2010), saffron stigmas (Torki-Harchegani, Ghanbarian, Maghsoodi, & Moheb, 2017), kiwifruit (Özdemir, Aktaş, Şevik, & Khanlari, 2017), grape by-products (Celma, López-Rodríguez, & Blázquez, 2009) and strawberry (Adak, Heybeli, & Ertekin, 2017). IR drying was also used by combining with other technologies, such as microwave heating, hot-press drying, freeze drying, vibration and vacuum (Datta & Ni, 2002; Mongpraneet et al., 2004; Oh, Ramachandraiah, & Hong, 2017; Pawar & Pratape, 2017; Riadh, Ahmad, Marhaban, & Soh, 2015). Among the reported advantages, IR drying was proposed as an effective and economical process that facilitates the removal of moisture on sample surface, increase the heat transfer and drying rates, reducing the processing time and the degradation of food compounds with nutritive and functional properties. However, the use of pre-treatments to improve infrared drying has not been sufficiently explored.

To date, different works have been developed with the application

* Corresponding author: Avenida Pádua Dias, 11, Piracicaba, SP 13418-900, Brazil.
E-mail addresses: mrojas@usp.br (M.L. Rojas), pedro.ed.augusto@usp.br (P.E.D. Augusto).

https://doi.org/10.1016/j.ifset.2018.08.005
Received 10 April 2018; Received in revised form 28 June 2018; Accepted 3 August 2018
Available online 04 August 2018
1466-8564/

of ultrasound (US) as a pre-treatment to enhance convective drying of biological materials (Fan, Zhang, & Mujumdar, 2017; Kowalski & Rybicki, 2017; Magalhães et al., 2017; Mothibe, Zhang, Nsor-atindana, & Wang, 2011; Rodríguez et al., 2018). When ultrasound travels across a food product immersed in a liquid medium (usually water), the compression and decompression cycles can result in two phenomena inside the product: the cavitation of fluid, producing changes on the product structure, and the absorption of the liquid by the product due to the so-called "sponge effect", as the product structure is compared to a sponge squeezed and released repeatedly. Both phenomena have been demonstrated to enhance food drying (Ricce, Rojas, Miano, Siche, & Augusto, 2016). In fact, the ultrasound pre-treatment was able to reduce the infrared drying time of apple slices (Brncic et al., 2010) and pear slices (Dujmić et al., 2013).

On the contrary, only few works have been carried out with the application of alcohols as a pre-treatment to accelerate the drying process of foods: celery soaked in glycerol (Shipman, Rahman, Segars, Kapsalis, & Westcott, 1972); apple (Funebo et al., 2002) and pumpkin (Rojas & Augusto, 2018a) slices immersed in ethanol; pineapple slices dried in a ethanolic atmosphere (Braga, Pedroso, Augusto, & Silva, 2009); bananas surface treated with ethanol (Corrêa, Braga, Hochheim, & Silva, 2012) and structured balls samples (mixed rice and soybean powders) with injection of ethanol (Tatemoto, Mizukoshi, Ehara, & Ishikawa, 2015). Higher drying rates, when compared to the drying of control samples, were reported in all of them.

Different explanations have been proposed for the improvement of drying by ethanol. Being ethanol an organic solvent, (Funebo et al., 2002) proposed that it dissolves the cell wall compounds, increasing the permeability through this structure during dehydration and rehydration. In fact, Rojas and Augusto (2018a) demonstrated the changes on cell wall thickness due to this treatment. Additionally, by using different compounds (ethanol, acetone, acetic acid and water), Silva, Braga, and Santos (2012) verified that the observed improvement could be related with their surface tension. Consequently, the concept of flow due to the Marangoni Effect was introduced by Silva et al. (2012) at the food drying area. The Marangoni Effect is promoted by the formed surface tension gradient between two fluids (for example between the water and an alcohol). The general mechanism is based on that the formed surface tension gradient will naturally induce the liquid to flow away from regions of low to regions of high surface tension (Bird, 2002; Gugliotti & Todd, 2004; Leenaars, Huethorst, & Van Oekel, 1990; Silva et al., 2012; Thomson, 1855).

Ultrasound, ethanol application and drying using infrared radiation is being proposed here for first time, where capillarity can be an important mechanism for water flow. Our hypothesis is that the ultrasound technology changes the food product structure, creating microchannels where the capillarity flow could occur. The Marangoni Effect because of adding ethanol to the system can be promoted by the formed microchannels. Finally, the infrared drying promotes the heating of sample surface, with vapourization of water and ethanol on the top surface, thus promoting the upward flow through capillarity. Consequently, the combination of these three technologies seems to be effective to enhance food drying.

The objective of the present work was to describe the ethanol and ultrasound application as pre-treatments to improve the infrared drying of potato slices, evaluating the effect of each pre-treatment on drying and rehydration kinetics and on the product microstructure and viscoelastic properties.

2. Material and methods

2.1. Raw material

Fresh potato tubers were obtained from a local market (Piracicaba, SP, Brazil). As shown in Fig. 1, the central part of potato tubers was employed to extract cylinders from the perimedullary zone using a sharp stainless-steel tube (diameter of 2.0 cm). Then, the potato slices (2.0 cm diameter × 0.5 cm thickness) were obtained from the cutting of extracted cylinders. Before pre-treatments, the obtained slices were immersed for 30 s in a solution of sodium bisulphite (0.1% m/v) to prevent browning.

2.2. Pre-treatments to drying

The evaluated pre-treatments include the Control samples (which were the potato slices without any pre-treatment) and those that were pre-treated with ethanol and/or ultrasound as follows:

2.2.1. Ethanol application

Each potato slice, hereafter called "Ethanol treated samples", was previously weighted and then immersed for 3 min in 125 mL of ethanol with 92.8°INPM (% m/m) or 95.0°GL (%v/v). After this period, the excess of ethanol was removed and dried with paper towels. This process was conducted at least in three replicates.

2.2.2. Ultrasound (US) application in ethanol and water medium

Each potato slice was immersed in 125 mL of ethanol (hereafter called "Ethanol + S treated samples") or water ("Water + US treated samples") and then processed with US for 3 min. The temperature during processing was kept at 25–27 °C using a jacketed reactor. The process was conducted at least in three replicates.

The ultrasound processing was carried out using an ultrasonic tip (nominal maximum power of 1000 W, 20 kHz - ECO-SONIC, QR1000 Model, Brazil) with a 1.26 cm^2 titanium probe, which was kept at 3 mm depth in the medium where the potato slice was immersed (ethanol or water). By adjusting the equipment to 30% of its capacity, the acoustic density and acoustic intensity were calculated by the calorimetric method, according to the described by Fonteles et al. (2012); O'Donnell, Tiwari, Bourke, and Cullen (2010). For this, the rate of temperature increasing were measured during the first 120 s of sonication using 125 of water as propagation medium, resulting in an acoustic density of 68 W/L and, considering the area of the probe, an acoustic intensity of 6.75 W/cm^2.

2.3. Infrared drying process

The samples were dried using a multispectral halogen lamp (QIR240V400W/140) of a moisture analyzer (AND MX-50, A&D company, Tokyo, Japan) with set temperature of 100 °C. The lamp wave range emission is showed in Fig. 1, which 95% of emission corresponds to IR radiation (Near IR and Medium IR radiation). The initial (of *in-natura* or fresh samples) and final (after drying) moisture contents were measured by completely drying crushed samples at 105 °C. The moisture loss data were calculated based on the sample mass over the time during IR drying, which was recorded every second using a WinCT-Moisture V2.41 Windows communication (A&D company, Japan).

It is important to mention that during the ethanol pre-treatment the samples lose water, solids and gain ethanol. Therefore, according to Silva et al. (2012) and Rojas and Augusto (2018a), the sample "moisture" after ethanol pre-treatment (M_p %) include the two volatile liquids, there is, it includes the remaining water and the gained ethanol.

The (M_p %) calculation could be represented according to Eq. (1). Where w_p is the remaining water, OH_p the gained ethanol and m_p is the sample mass after ethanol pre-treatment. Since the OH_p and m_p mass are difficult to calculate separately, in this work they considered together as a lumped parameter (L_p) that include the mass of both liquids after pre-treatment.

$$M_p\% = \frac{w_p + OH_p}{m_p}.\ 100 = \frac{L_p}{m_p}.\ 100 \quad (1)$$

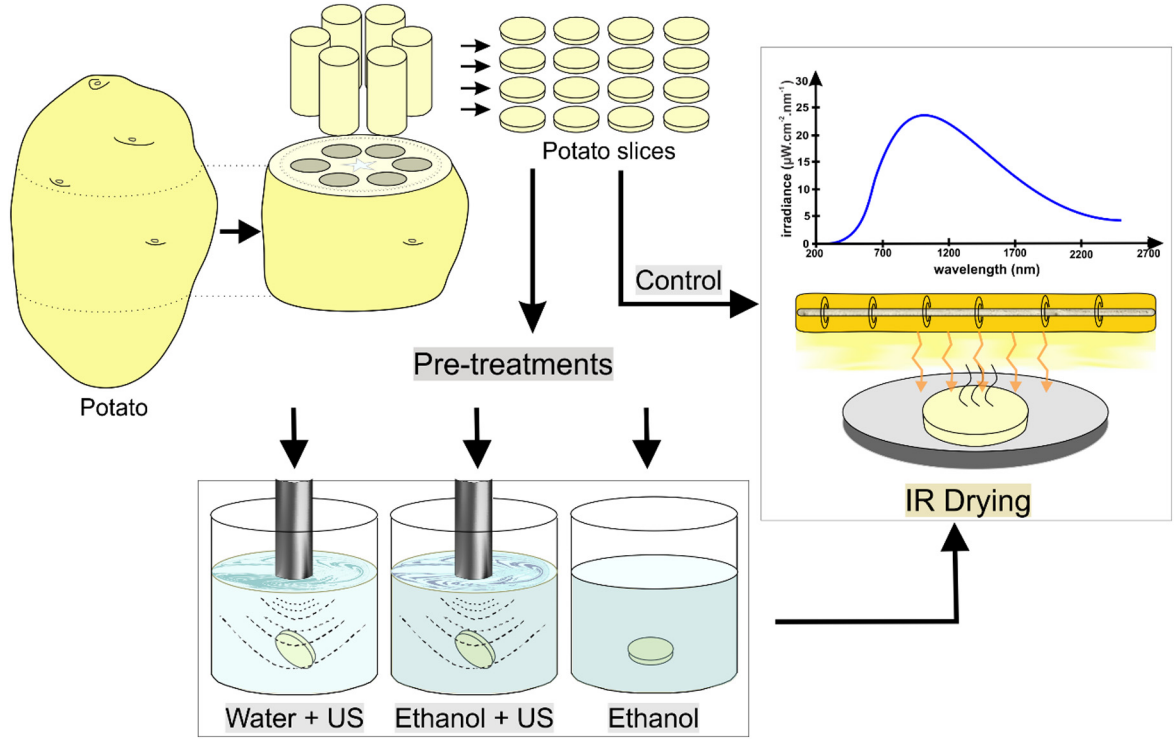

Fig. 1. Representation of the method to obtain potato slices from the perimedullary zone of potato tuber. The pre-treatments and IR drying method also are represented.

During drying process, the mass loss also includes both volatile liquids, there is, it includes both the water and ethanol loss. Therefore, the moisture content (M_t) over the drying process time is calculated according to (Eq. 2). In the same manner, it was calculated by considering a lumped parameter (L_{pt}) that includes the mass of both liquids at certain drying time (t).

$$M_t\% = \frac{w_{pt} + OH_{pt}}{m_{pt}}.\ 100 = \frac{L_{pt}}{m_p}.\ 100 \quad (2)$$

where w_{pt} is the mass of water, OH_{pt} is the mass of ethanol and m_{pt} is the sample mass at certain drying time (t).

Drying curves were plotted as a function of the moisture content (M_t%) (Eq. 2) and dimensionless moisture ratio (MR) (Eq. 3) over the drying process time.

$$MR(t) = \frac{M - M_e}{M_0 - M_e} \quad (3)$$

where M is the moisture content in dry basis (d.b.) (i.e. kg of water/kg dry matter) at a given time (t) of drying process, M_e is the equilibrium moisture and M_0 is the initial moisture (d.b.) after pre-treatment. In the case of the control samples, M_0 is equal to the initial moisture of *in-natura* sample. Therefore, the Control and Ethanol treated samples started the drying process with MR values equals to one.

2.4. Rehydration process

Each dried slice was immersed in 50 mL of distilled water at 24 ± 1 °C for rehydration. The evolution of sample moisture over the time was then determined by mass balance. For this, the slices were periodically removed from the water, superficially dried with absorbent paper, weighed and returned to the water until water absorption stabilization.

2.5. Viscoelastic properties: stress-relaxation behaviour

The stress-relaxation analysis was used to describe the viscoelastic changes of samples after pre-treatments and processes, compared with those of the *in-natura* samples. It consists of an instantaneous deformation to a sample, maintaining the strain constant and then evaluating the related stress over the time (Rao & Steffe, 1992). The stress-relaxation of the *in-natura*, and rehydrated samples (Control, Ethanol, Ethanol + US and Water + US) was evaluated using a Texture Analyzer (TA.XT Plus, Stable Micro Systems Ltd., Surrey, UK) with a load cell of 50 kg-f (490,03 N) and a 35 mm aluminium cylindrical probe (P/35R). The cylinders were firstly compressed until a strain of 0.3 with 0.2 mm·s^{-1} velocity. Then, the deformation was maintained constant for 30 s, being the data of force (N) versus time (s) recorded every 0.005 s to detailing analysing the relaxation curves and the model adjustment. From 4 to 8 replicates were evaluated.

2.6. Microstructure evaluation

The sample microstructure was evaluated using an optical microscopy (model L1000, Bioval, Brazil) with a 10× magnification objective, and a microscopy stereoscopy (model XTD-30-LED, NOVA, Brazil) with 15× magnification, both coupled to a portable camera of 1.3 megapixels. The microstructure was analysed from the surface and internal tissues of the samples, which were cut into ~8 μm dishes using a manual microtome (Ancap, São Paulo). In some cases, iodine (0.1% in ethanol) and toluidine blue solution (0.1% in water) were used as colorant to enhance the images. The images were captured after guaranteeing a representative field after several visualizations.

2.7. Mathematical description

2.7.1. Drying and rehydration kinetics

The drying data was fitted using the Page Model (Eq. 4) (Page, 1949), where MR(t) is the dimensionless moisture at drying time (t), k

is the drying rate constant and n the dimensionless drying constant. Although the Page Model is an empirical model, it was successfully applied to drying process over the years (Doymaz, 2005; Simal, Femenia, Garau, & Rosselló, 2005). Recently, Simpson, Ramírez, Nuñez, Jaques, and Almonacid (2017) demonstrated that the anomalous diffusion approach, based on fractional calculus, can attribute phenomenological meanings to the Page Model: the drying rate constant (k) is associated with the diffusion coefficient and the geometry of the sample, while the dimensionless drying constant (n) describes the "type of diffusion": when $n > 1$, the drying is characterized by super-diffusion, while it is characterized by sub-diffusion when $n < 1$. Our interpretation (Rojas & Augusto, 2018b) is that when $n \neq 1$, other mechanisms than diffusion are important. For example, the "super-diffusional process" ($n > 1$) may indicate the importance of capillarity.

$$MR(t) = exp(-k.\ t^n) \tag{4}$$

The rehydration data was fitted using the Peleg Model (Eq. 5) (Peleg, 1979), where $M(t)$ is moisture content in dry basis (d.b) at time t (min), M_0 is initial moisture content (d.b), k_1 is the rate constant (min·kg dry matter/kg water) and k_2 is the constant of asymptotic level (kg dry matter/kg water). Although the Peleg Model is an empirical model, it was successfully applied to hydration process over the years (Doymaz, 2005; Miano & Augusto, 2018; Simal et al., 2005). The reciprocal of k_1 represent the water absorption rate and the reciprocal of k_2 represent the water retention capacity.

$$M(t) = M_o + \frac{t}{k_1 + k_2.\ t} \tag{5}$$

2.7.2. Viscoelastic properties (stress-relaxation behaviour)

To describe the viscoelastic properties, the data was fitted to the Guo-Campanella Model (Guo & Campanella, 2017), described on Eq. 6, and to the Peleg Model (Peleg, 1979), described on Eq. 7. The Peleg Model has already been used to successfully describe the viscoelastic behaviour of different materials. On the other hand, the Guo-Campanella model presents parameters that allow an adequate and comprehensible interpretation of the viscoelastic properties. Therefore, these two models were used in order to achieve an adequate interpretation and description of the viscoelastic properties of the *in-natura* and rehydrated potato samples.

The Guo-Campanella model is based on fractional calculus, developed until Eq. 6, which express the material viscoelastic behaviour:

$$\sigma(t) = k\frac{\varepsilon_0}{\Gamma(1-\alpha)}t^{-\alpha} \tag{6}$$

where, $\sigma(t)$ is the compression stress over the compression time, k is a parameter that represents the viscoelastic modulus, ε_0 is the strain (which is constant in the stress relaxation test), t is the compression time, α is the fractional order and Γ is the gamma function. When $\alpha = 0$, k represents the elastic modulus (i.e., pure elastic/solid behaviour). On the other hand, when $\alpha = 1$, k represents the viscosity (i.e., pure viscous/fluid behaviour). Finally, when $0 < \alpha < 1$, Eq. 4 represents the viscoelastic behaviour, being the parameter k, the viscoelastic modulus (Augusto, Miano, & Rojas, 2018; Guo & Campanella, 2017).

On the other hand, the Peleg Model (Eq. 7) is an empirical model with only two parameters (k_1, k_2), but excellent fitting for different materials. The reciprocal of k_1 represents the initial decay rate, while the reciprocal of k_2 represents the hypothetical asymptotic level of the normalized relaxation curve (Peleg, 1979; Peleg & Normand, 1983).

$$\frac{\sigma_0 - \sigma(t)}{\sigma_0} = \frac{t}{k_1 + k_2.\ t} \tag{7}$$

The obtained data was fitted by nonlinear regression to the Guo-Campanella Model (Eq. 6) and the Peleg Model (Eq. 7) as described below.

2.7.3. Regressions

The parameters of each models (Eqs. 4 to 7) were iteratively adjusted to the experimental data by minimizing the sum of squared errors (*SSE* in Eq. 8) between the experimental and the predicted values for the x experiements. The Generalized Reduced Gradient algorithm (GRG Nonlinear Solving method), implemented in the 'Solver' tool of software Excel 2010 (Microsoft, USA) was used. The parameters of each model were considered valid when Solver reported that the GRG method found a locally optimal solution (to a set convergence of 0.00001). That is, there was no other set of values for the parameters close to the current values that yields a better value for the objective function (*SSE*).

$$SSE = \sum_{i=1}^{x} ((predicted) - (experiemental))_i^2 \tag{8}$$

2.8. Statistical analysis

A completely randomised design (CRD) was conducted. All the processes and analyses were performed at least 3 times. The analysis of variance (ANOVA) was carried out with a significance level of 10%. To determine differences among means of pre-treatments, Tukey test was used. Statistical analyses were performed using IBM SPSS Statistics 23 software (IBM SPSS, USA).

3. Results and discussion

3.1. Microstructure evaluation

Fig. 2 shows the microstructure of the potato slices surface, allowing a global vision of the tissue in the *in-natura* and treated samples. Fig. 3 shows the cellular microstructure of the samples *in-natura* and after pre-treatments. Representative images were also included to the right of Fig. 3, with our interpretation based on the observed structures and literature descriptions about the effect of ultrasound and ethanol on the microstructure of plant tissue (Rajewska & Mierzwa, 2017; Rojas & Augusto, 2018a; Rojas, Miano, & Augusto, 2017). As described previously, the potato samples were obtained from the perimedullary zone of mature potatoes. According to Reeve, Hautala, and Weaver (1969) the perimedullary zone of the mature potato tuber is formed mainly by starch-storage parenchyma cells. In fact, a large amount of starch granules was observed inside the cells, which were grouped together next to the cell membrane in the *in-natura* samples (Fig. 3).

After Ethanol pre-treatment, it was observed that the surface of the Ethanol treated samples showed slightly wrinkled cells with thin walls and low intercellular air, if compared to the microstructure of the *in-natura* samples (Fig. 2). Probably the ethanol had greater impact on intercellular spaces and on the cell wall and a lower impact on cell membrane. In fact, the cell membrane permeability of potato cells to water is at least three orders lower than the permeability of the intercellular space and of the cell wall (Halder, Datta, & Spanswick, 2011). Therefore, when samples were in contact with ethanol, it enters firstly to the intercellular spaces, where the intercellular air and water naturally present were expelled from inside. In the same manner, there was extraction of some solutes from cell walls. As a consequence, the cell wall remained tinned, the cells lose turgidity, changing its initial shape and then looking more compact (Figs. 2 and 3). Similar results, when alcohols were used as treatment to improve drying, were reported and evidenced by Shipman et al. (1972) for celery, by Funebo et al. (2002) for apple and by Rojas & Augusto, 2018afor pumpkin. Additionally, it is interesting to notice that the starch granules conserved its initial position inside the cells and continued grouped (Fig. 3).

The Ethanol + US samples showed cell disruption and micro-channels formation in some parts of the tissue, additionally to the wrinkled cells (Figs. 2 and 3). In fact, during pre-treatment with US,

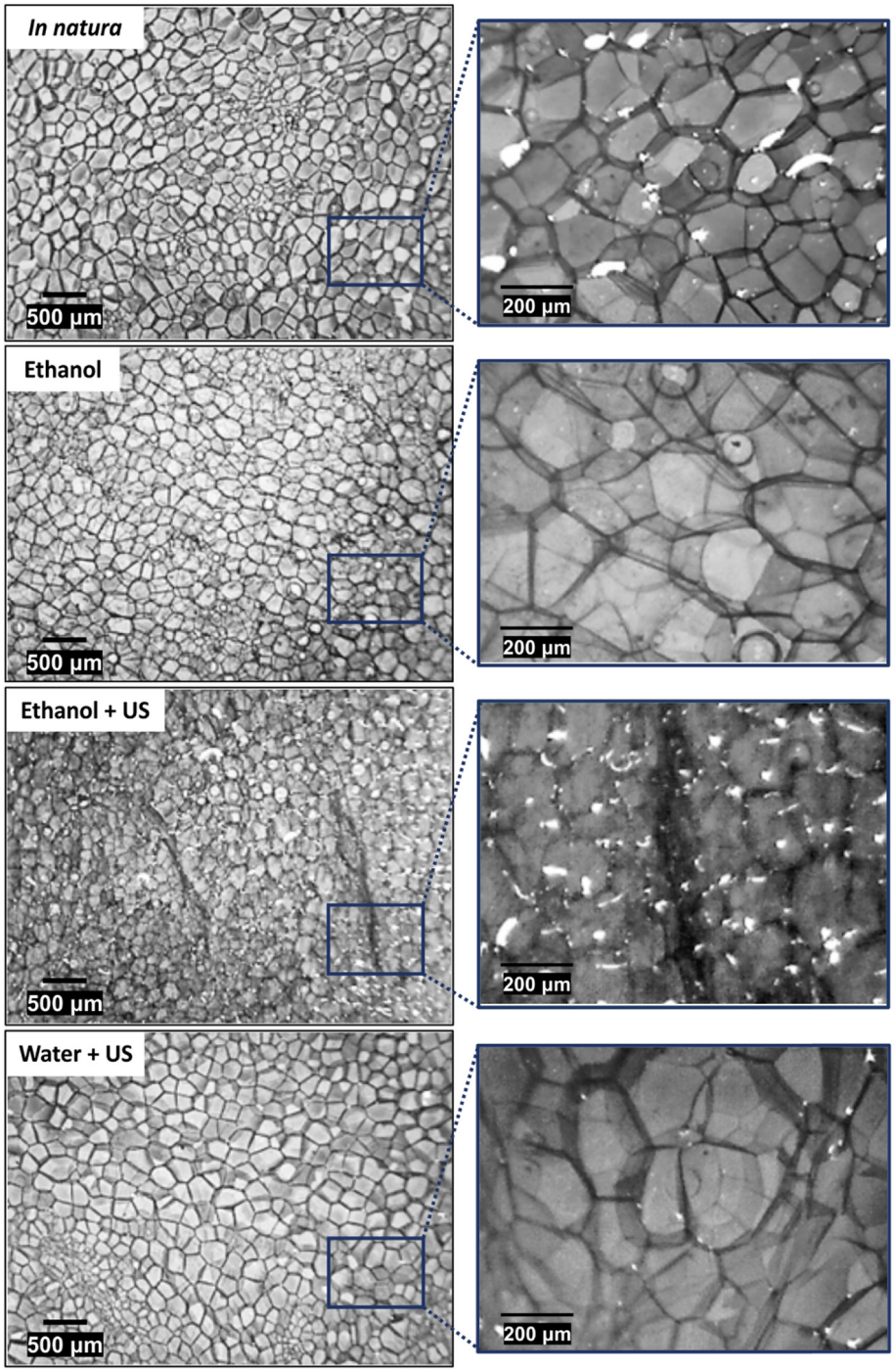

Fig. 2. Surface microstructure of the *in-natura* potato sample and those after pre-treatments (with Ethanol, Ethanol + US and Water + US). Toluidine blue solution was used to mark the cell walls. (For interpretation of the references to colour in this figure legend, the reader is referred to the web version of this article.)

many works demonstrated the tissues and cells disruption and micro-channels formation due to the acoustic cavitation (Fernandes, Linhares Jr, & Rodrigues, 2008b; Fernandes & Rodrigues, 2007, 2008; Miano, Ibarz, & Augusto, 2016; Ricce et al., 2016). Consequently, as the cell membrane and cell wall were disrupted with the US application, the starch granules were expelled from inside the cells (Fig. 3).

To better understand the ethanol effect combined with the ultrasound technology, water was used for comparison in similar process conditions (Water + US samples). These samples showed cells that seem more bloated than the Control and Ethanol treated samples (Fig. 2). The water influx phenomenon was previously observed at short time of ultrasound application (Fernandes, Gallão, & Rodrigues, 2008a; Miano et al., 2016; Mulet, Cárcel, Sanjuán, & Bon, 2003; Ricce et al., 2016), and it has been attributed to a direct effect of ultrasound called "sponge effect" (rapid alternative compression and expansion of the food matrix). Furthermore, the starch granules initially grouped inside the cells (as observed in the *in-natura* samples), were scattered and distributed inside the cell after ultrasound pre-treatment (Fig. 3). Similar phenomenon was also observed and described by Rojas, Leite, Cristianini, Alvim, and Augusto (2016) in peach juice cells, where at short ultrasound processing time, the intercellular plastids are firstly disrupted, releasing its internal compounds inside the cell. In the present study, probably the amyloplasts were firstly disintegrated with the ultrasound and then the starch granules were distributed inside the cell.

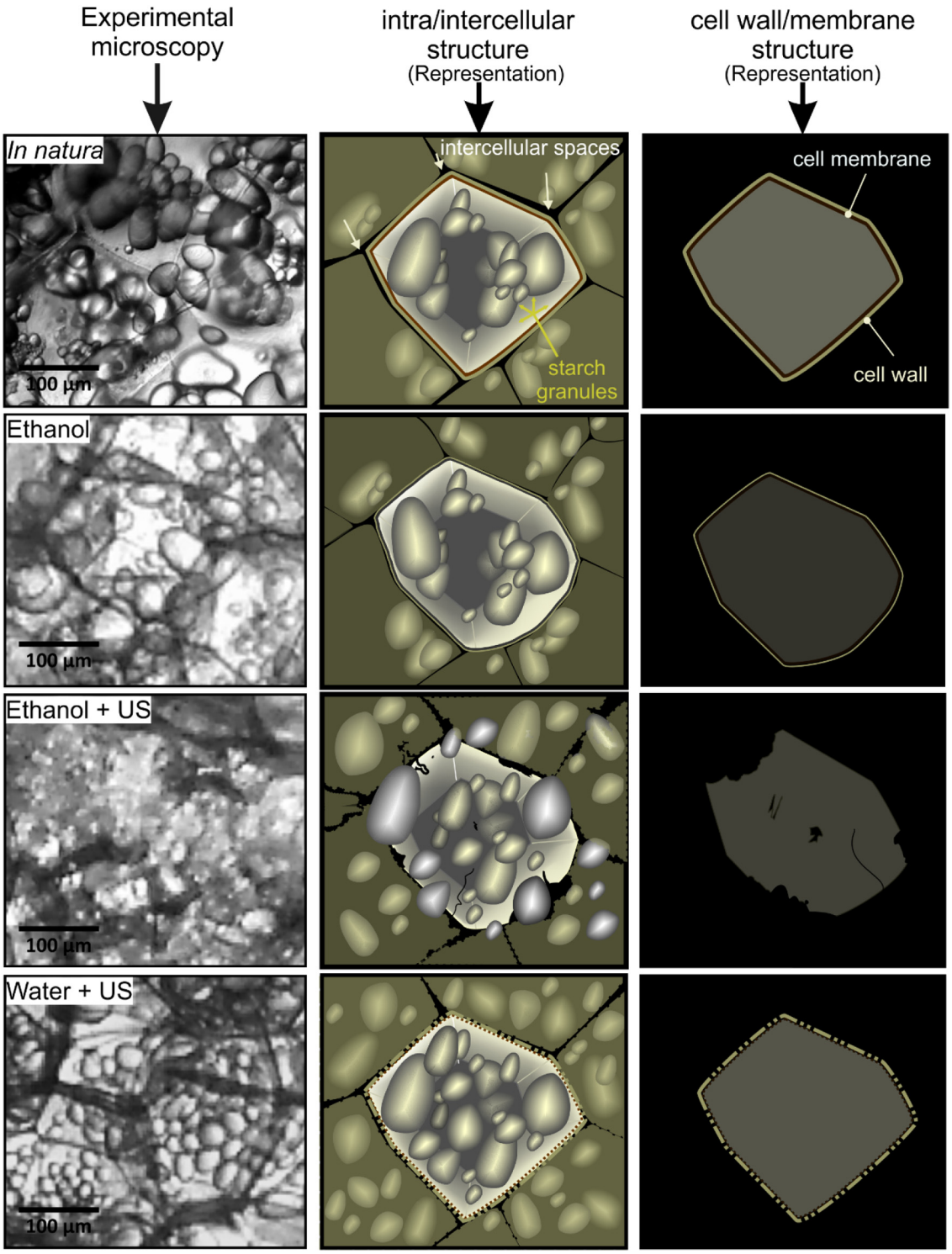

Fig. 3. Internal tissue microstructure of the *in-natura* potato samples and those after pre-treatments (Ethanol, Ethanol + US and Water + US). A representation of the possible changes in the intercellular and intracellular structure, as well as in the cell wall and membrane, is also presented, based on the microscopic experimental observations and bibliography.

Even though the Water + US samples were processed under the same ultrasonic conditions than the Ethanol + US, the microchannels formation was not evidenced when water was the medium. This result suggests that when ethanol was used instead of water, the effects of the US on the sample structure were intensified, which can be attributed to two mechanisms. Firstly, the occurrence and the intensity of cavitation are different in both cases, once vapour pressure, viscosity and surface tension of ethanol are different from water (Sujka, 2017). Secondly, due to the different dissolution properties of components in water and ethanol, as well as a possibly different spatial disposition of macromolecules in these two solvents, the cell and tissue structure are expected to be different in both pre-treatments (i.e. Water + US and Ethanol + US), leading to different behaviours - as observed in Fig. 3.

The microstructure results suggest that all the evaluated pre-treatment can result in different drying and rehydration properties, as will be evidenced in the next sections.

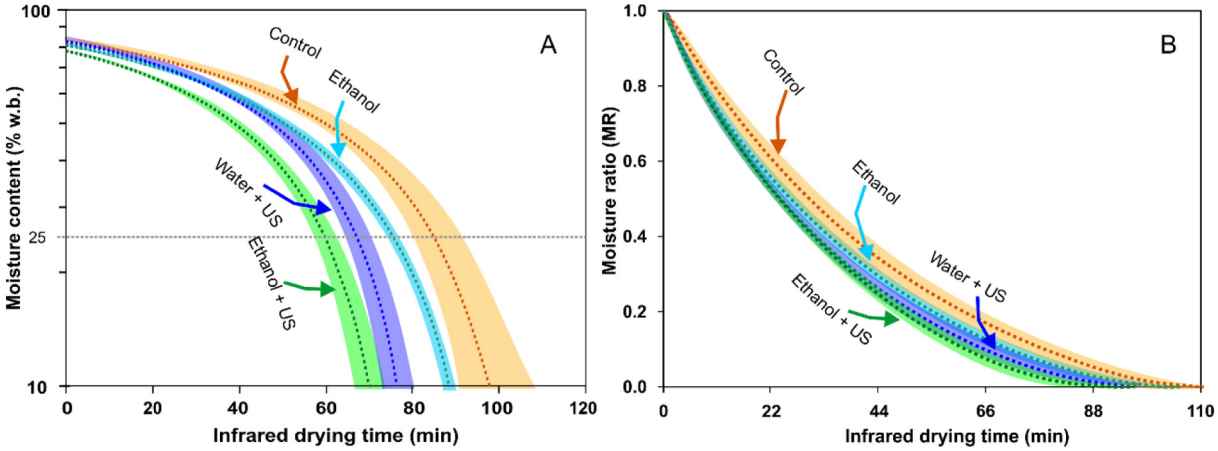

Fig. 4. Infrared drying of control and treated samples. Moisture content on wet basis (log-scale) (A) and moisture ratio (Eq. 3) (B), along infrared drying time. Doted lines are the mean of the experimental data and the shaded areas represent the confidence bands (95%) of the experimental data. For comparison, a horizontal line at 25% of moisture content on wet basis (w.b.) is provided on (A).

3.2. Effect on drying process

Fig. 4A and B allowed to describe the drying kinetics. Fig. 4A shows the moisture content reduction of the Control, Ethanol, Ethanol + US and Water + US treated samples until 10% w.b. (this moisture was selected only for visualization effects in the graph) as a function of the infrared drying time. Additionally, Fig. 4B shows the normalized moisture or moisture ratio (Eq. 3), this data was used to perform the regressions using the Page model (Eq. 4), whose parameters (n and k), are showed in Table 1. As observed, the control samples presented $n = 1.214 \pm 0.068$ and $n = 0.012 \pm 0.004\ \text{min}^{-1}$. According to Simpson et al. (2017), the parameter n on Page Model is related to the type of diffusion ($n > 1$ super-diffusion and $n < 1$ sub-diffusion). Therefore, all pre-treatments showed a super-diffusive behaviour ($n > 1$) during drying, which is expected due to the importance of capillarity. As shown in Table 1, a small variation was observed for the parameter n. On the other hand, significant differences among all pre-treatments were observed for the k parameter, associated with the drying rate – thus confirming that all the pre-treatments enhanced the drying process, being the Ethanol + US pre-treatment the most efficient (Fig. 4).

Fig. 5 shows the time required for each pre-treatment to reach a moisture of 25% w.b. (horizontal line in Fig. 4A). According to Jay, Loessner, and Golden (2005), a moisture < 25% w.b. are necessary for dried (or low-moisture) foods. Therefore, this was considered as a reference of maximum moisture in vegetable dry products to make comparisons among pre-treatments. The drying time to reach a moisture of 25% w.b. was reduced in an average of 30% with Ethanol + US application when compared to Control.

According to Motevali, Minaei, and Khoshtagaza (2011) the energy consumption during IR drying can be calculated directly by the radiation energy consumed by IR lamps multiplied by the drying time. Considering the same parameters for all pre-treatments (such as, distance between lamps and product, temperature and drying surface), the reduced drying time with Ethanol + US application could reduce the consumed energy in the same proportion (i.e. ~30% of energy consumed reduction). It is noteworthy that this result is highly interesting.

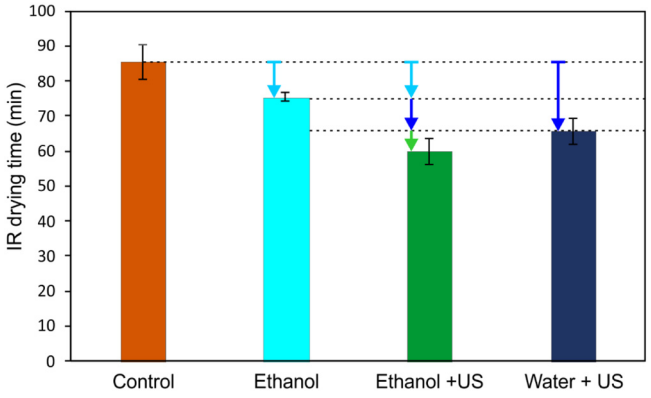

Fig. 5. Time required for the different treatments to reach a sample moisture content of 25% w.b. Down arrows indicate drying time reduction whit respect to the Control.

The drying time reduction obtained with US + Ethanol was higher than the reduction obtained separately for both Ethanol (~12% reduction) and US + Water (~23% reduction) pre-treatments. In fact, it is difficult to determine if the effect of US + Ethanol is synergistic or additive, since it is difficult to isolate their effects individually. Even so, a better effect by combining these two technologies is demonstrated, in

Table 1
Drying and rehydration kinetics parameters*.

Pre-treatment	Drying kinetics		Rehydration kinetics	
	Page Model parameter (Eq. 4)		Peleg Model parameter (Eq. 5)	
	n	k (min^{-1})	k_1 (min kg dry matter/kg water)	k_2 (kg dry matter/kg water)
Control	1.214 ± 0.068^{a}	0.012 ± 0.004^{b}	9.474 ± 0.936^{b}	0.264 ± 0.015^{b}
Ethanol	1.135 ± 0.032^{b}	0.018 ± 0.002^{a}	9.111 ± 0.143^{b}	0.302 ± 0.025^{ab}
Ethanol + US	1.201 ± 0.025^{a}	0.016 ± 0.001^{a}	12.098 ± 0.704^{a}	0.339 ± 0.023^{a}
Water + US	1.149 ± 0.048^{ab}	0.018 ± 0.003^{a}	9.175 ± 1.579^{b}	0.277 ± 0.019^{b}

*Mean ± standard deviation. Differences among letters indicate significant differences ($p < 0.1$) among Pre-treatments.

relation to using each one individually.

The possible mechanisms that explain the improvement of the drying process with the applied pre-treatments are described below.

In the Ethanol pre-treatment, the drying time decreased probably due to the increase in the permeability of the cell walls, since some solutes are extracted by ethanol, in accordance with the description made on Section 3.1. Furthermore, as detailed by Silva et al. (2012) and by Rojas and Augusto (2018a) ethanol result in a gradient of surface tension, promoting the Marangoni flow. This effect pulls up the water from inside the sample, thus decreasing the drying time compared to the *in-natura* samples.

When ultrasound is used as a pre-treatment, different effects could occur.

On the one hand, in the case of the Water + US pre-treatment, the cell disruption and microchannel formation was not evidenced (Figs. 2 and 3), even though the drying time was reduced if compared to control (Fig. 5). In fact, other effects occurred inside the cells previously to its disruption, and all of them influenced the obtained results. Based on what was evidenced on Section 3.1, two effects probably were responsible for the observed behaviour during drying of the Ultrasound treated samples. Firstly, since the compounds inside the cell (as the starch granules) were redistributed, it suggests that the water mobility was changed. Secondly, the cells appeared bloated (Fig. 2). This indicated that water was forced to enter inside the cells during ultrasound process, suggesting that there were modifications on permeability of the cell wall and membrane. Consequently, during drying, the Water + US samples experienced a rapid exit of water mainly at the beginning of the process. In fact, due to this, the Water + US samples showed a slightly higher k value (Table 1).

On the other hand, in the case of Ethanol + US pre-treatment, the drying time was reduced in a higher percentage (Fig. 5). According to Halder et al. (2011) any change in the cell and intercellular structure will affect the water exit pathway. Additionally, the authors stablished that 90–95% of the total potato water is located intracellularly (at 22 °C). Therefore, the intracellular and intercellular structure changes as consequence of Ethanol + US application, highly impacted the water mobility, also allowed that the water experiences less resistances to flow, accelerating the drying process. In contrast, in the Control samples, the water flow probably followed an intracellular pathway (Halder et al., 2011), where water flow through cell membranes ⟶ cell walls ⟶ intercellular spaces, making the drying process slower.

The observed drying improvement when Ethanol + US was used indicates that the process is also influenced by the occurrence and the intensity of cavitation, in addition to the effects produced by ethanol when it was used alone. When compared with water properties at 25 °C, ethanol present high vapour pressure and viscosity, and low surface tension. Hemwimol, Pavasant, and Shotipruk (2006) affirm that small surface tension requires lower energy to produce cavitation bubbles; thus, the compression and decompression mechanism to achieving cavitation occurs readily. In fact, Crum (1984) reported that the rate cavitation bubbles growth is increased by a factor of about five when the surface tension was lowered by a factor of about two. Therefore, when Ethanol + US was used, the structural changes due to cavitation are the responsible for shortening drying time.

As conclusions, the low surface tension of ethanol could be the property responsible for intensifying the cavitation effect when ultrasound is being applied. After that, the modified structure of the Ethanol + US pre-treatment promoted extracellular routes to water flow during drying by capillarity, which could also have favoured by the Marangoni effect. Furthermore, it is worth mentioning that further studies are needed, to evaluate other variables such as ethanol concentration, ultrasound time, frequency and power, temperature, among others.

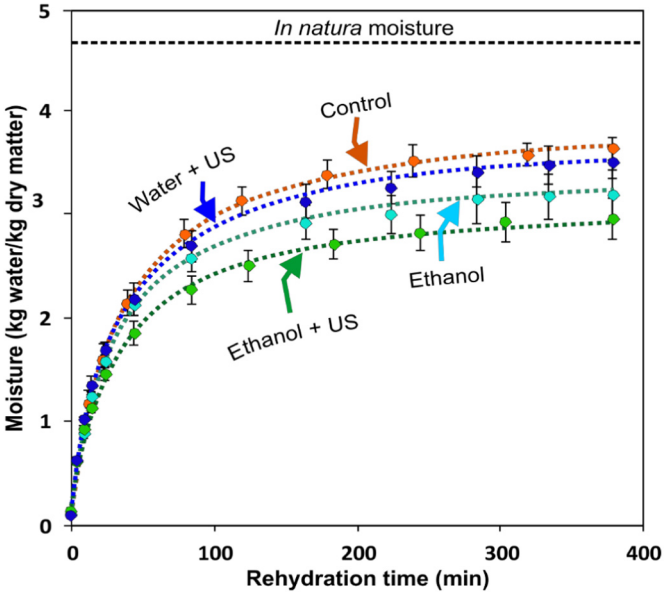

Fig. 6. Rehydration kinetics of control and treated samples. Dots are the mean values and vertical bars are the standard deviation of experimental data. Dotted curves correspond to the Peleg Model (Eq. 5).

3.3. Effect on rehydration properties

Fig. 6 shows the rehydration kinetics of control and treated samples, which were described by the Peleg Model (Eq. 5). The lower the value of k_1 and k_2, the higher the water absorption rate and the higher equilibrium moisture content, respectively. Table 1 shows the Peleg Model k_1 and k_2 parameters value. For the k_1 parameter, significant differences ($p < 0.1$) among of the Ethanol + US treated and the other samples were found. For the k_2 parameter, no significant differences ($p > 0.1$) were observed between the Ethanol and Ethanol + US treated but significantly differed ($p < 0.1$) from the other samples.

Although the rehydration process aims to restore the properties of the raw material, the potato samples after pre-treatments and drying lost part of its capacity of holding water. The *in-natura* moisture content was 82.5% (4.7 kg water/kg dry matter). After 380 min of rehydration, the Control reached 78.3% (3.6 kg water/kg dry matter), the Ethanol treated reached 76.0% (3.2 kg water/kg dry matter), the Ethanol + US reached 74.6% (2.9 kg water/kg dry matter) and the water + US reached 77. 7% (3.5 kg water/kg dry matter) of moisture content.

As observed in Fig. 6, the Control and Water + US pre-treatments have similar rehydration behaviour, while the other pre-treatments (Ethanol and Ethanol + US) have lower rehydration properties. The Ethanol + US pre-treatment caused higher structure modifications on samples (Figs. 3 and 4), which could be directly related with the lower rehydration rate (high k_1 value) and water retention capacity (high k_2 value) of these samples, as observed in Fig. 7 and Table 1. The rehydration behaviour in turn was influenced directly by the structural modifications during drying.

Regarding the modifications during drying, it is important to highlight that the set temperature for the IR dryer equipment was 100 °C, but the temperature at the sample surface has reached the maximum of 80 °C. As previously evidenced, the cells are composed by considerable amounts of starch granules (Figs. 2 and 3). The potato starch gelatinization temperature is close to 66 °C (Castanha, da Matta Junior, & Augusto, 2017). Therefore, at 80 °C, it is expected that the starch in the sample surface was gelatinized, contributing for creating crust. This phenomenon was more important when Ethanol + US was used, because the starch granules that were released from inside the cells, probably were more susceptible to gelatinize. Furthermore, the heat could penetrate deeper into the sample tissue due to the formed

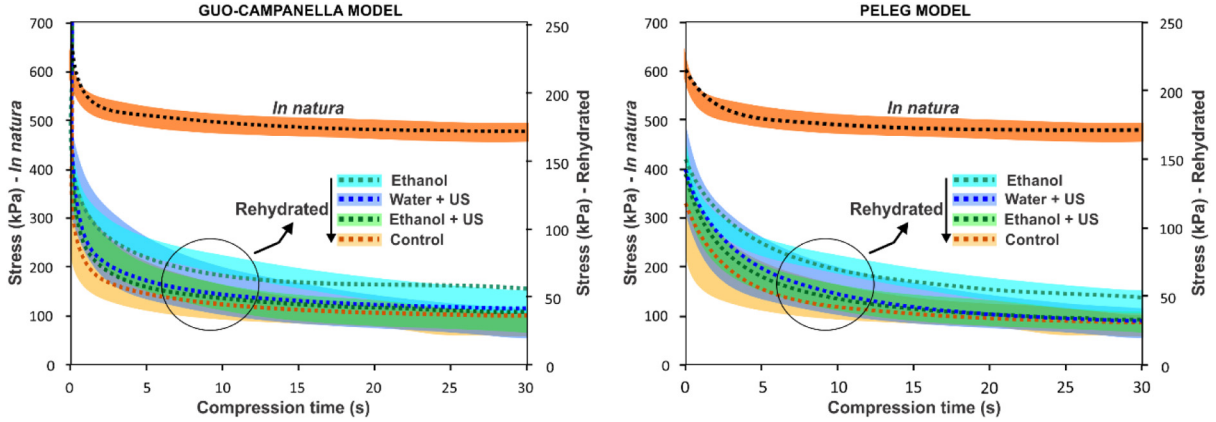

Fig. 7. Stress-relaxation profile of the *in-natura* and rehydrated potato samples. The dashed lines represent the values of each model fitting, while the shaded areas represent the confidence bands of the experimental data (95%). Note that each figure has an axis for the *in-natura* samples and other for the processed samples.

microchannels.

Consequently, in the case of Ethanol + US samples, the structure modifications during pre-treatments and the modifications during drying increased the resistance for the water enters the sample due to the external resistance offered by crust (reflected in the high k_1 value), as well as it was difficult to the cells retain the water due to their broken walls and membranes (reflected in the high k_2 value).

Summarizing, the application of Ethanol + US had a positive impact during drying, reducing the needed time. However, improvements on the rehydration properties were not evidenced due to the severe modifications in the structure. It would be required to apply this pre-treatment in other materials with different structures and composition to better describe the effects during drying and rehydration.

3.4. Effect on viscoelastic properties

The stress-relaxation profile of the *in-natura* and processed potato samples is shown in Fig. 7. As observed, the *in-natura* samples show low stress decay and more residual elasticity in comparison with the processed samples. It suggests that the *in-natura* samples presented more elastic characteristics when compared with the rehydrated samples.

The experimental data was well fitted to the Guo-Campanella and the Peleg models. However, the Guo-Campanella Model fitted the stress-relaxation data of *in-natura* samples better than the data of processed samples. This coincides with the description of Augusto et al. (2018). On contrary, the Peleg Model fitted well all the samples.

Table 2 shows the parameters and fit criteria for both models. It was observed that the values of the parameters obtained for the *in-natura* samples were significantly different from those obtained for the rehydrated samples. It reflects that the structural modifications during pre-treatments and drying cause the tissue to lose its original viscoelastic properties.

In the Guo-Campanella Model, the α parameter (the fractional order) represents the sample "degree of viscoelasticity". When $\alpha = 0$, the product behaviour is purely elastic (solid). On the other hand, when $\alpha = 1$, the product behaviour is purely viscous (fluid) (Guo & Campanella, 2017). Table 2 shows that the α value increased for all rehydrated samples, for example it increased about 376% for the Ethanol and 498% for the US rehydrated samples when compared to the *in-natura*, indicating that the rehydrated samples were more viscous/fluid. This is because the elasticity of the *in-natura* samples is higher due to cell-bonding and high turgor pressure (Mayor, Cunha, & Sereno, 2007). Therefore, the cell wall damage and cell disruption during pre-treatments and drying reduce the samples elasticity. Further, it was observed in Table 2 that the values of α for all treated, dried and rehydrated samples were higher compared to *in-natura* samples. However, statistically there are no differences ($p > 0.1$) among the control and treated samples. This means that the pre-treatments have no greater influence than the drying process itself has on the sample viscoelasticity.

The k_2 parameter in the Peleg Model can also be considered as "a representation of the solidity degree": for fluids, $k_2 = 1$, while for solids $k_2 \rightarrow \infty$ (Peleg & Normand, 1983). Although statistically significant differences were not evidenced ($p > 0.1$), as in the Guo-Campanella model, the samples that were processed with ultrasound show a tendency to have more viscous than elastic character, probably with higher ultrasound process time it could be evidenced.

The viscoelastic properties depend on the composition and structure of the sample, which in turn depend on the performed process. After any process is required that viscoelastic characteristics result like those of *in-natura* (i.e. low stress decay and high residual elasticity). As general mode, all the rehydrated samples presented similar characteristics. Consequently, the evaluated pre-treatments did not negatively influence the viscoelastic properties of the products since these remained like those of the control samples, which is an interesting result.

Table 2
Parameters of the Guo-Campanella Model and Peleg Model for describe the viscoelastic properties of the different potato samples*.

Sample	Guo-Campanella Model parameters (Eq. 6)			Peleg Model parameters (Eq. 7)		
	k (kPa)	α	R^2	k_1 (s)	k_2 (1/s)	R^2
In-natura	1844.13 ± 70.17^{a}	0.04 ± 0.00^{c}	0.99	7.44 ± 0.89^{a}	4.67 ± 0.08^{a}	0.95
Rehydrated control	281.97 ± 76.28^{b}	0.21 ± 0.01^{ab}	0.83	3.27 ± 0.62^{c}	1.25 ± 0.05^{b}	0.97
Rehydrated ethanol	413.83 ± 17.83^{b}	0.19 ± 0.01^{b}	0.80	5.64 ± 1.03^{b}	1.31 ± 0.11^{b}	0.97
Rehydrated ethanol + US	337.78 ± 28.60^{b}	0.24 ± 0.03^{a}	0.84	3.28 ± 1.05^{c}	1.20 ± 0.08^{b}	0.99
Rehydrated water + US	364.45 ± 85.47^{b}	0.24 ± 0.01^{a}	0.81	4.09 ± 1.10^{bc}	1.15 ± 0.03^{b}	0.99

*Means ± standard deviation. Differences among letters indicate significant defences among the *in-natura* and processed samples ($p < 0.1$).

4. Conclusions

For the first time the application of ethanol and ultrasound (in water or ethanol medium) was studied as pre-treatments to improve the infrared drying. The microstructure evaluation showed that pre-treatments changed the *in-natura* potato microstructure in diverse ways. The ethanol mainly affected the cell wall membrane. When US was applied using water as medium, it mainly acted intercellularly, dispersing the intracellular compounds, such as the starch granules. However, great structural modifications were observed when Ethanol + US was applied. Comparing with the control sample, ethanol decreased the drying time. However, ethanol combined with ultrasound provides the high drying time reduction, as both pre-treatments favourable the capillarity flow. In contrast, a slight decrease in water absorption and retention capacity was observed for the Ethanol + US treated samples due to high structural modifications. Therefore, it is recommended to apply this pre-treatment in other samples with a different structure and composition to better describe the effects during drying and rehydration. Additionally, the viscoelastic properties of rehydrated samples differed significantly of those of the *in-natura* samples, which presented more elastic properties. It reflects that during pre-treatments and drying the tissue lost its original viscoelastic and rehydration properties. These results show an important contribution because while the pre-treatment of US technology combined with ethanol is appropriate to improve the potato infrared drying, it did not have a positive impact during its rehydration, probably due to the potato sample composition and the structural modifications produced during pre-treatment.

Declarations of interest

None.

Acknowledgments

The authors are grateful to the São Paulo Research Foundation (FAPESP, Brazil) for funding the project n° 2016/18052-5; to the National Council for Scientific and Technological Development (CNPq, Brazil) for funding the project n° 401004/2014-7 and the productivity grant of P.E.D. Augusto (306557/2017-7); and to Cienciactiva for the M.L. Rojas Ph.D. scholarship (CONCYTEC, Peru; Contract 087-2016-FONDECYT), from the “Consejo Nacional de Ciencia, Tecnología e Innovación Tecnológica”.

References

Adak, N., Heybeli, N., & Ertekin, C. (2017). Infrared drying of strawberry. *Food Chemistry, 219*, 109–116.
Afzal, T. M., & Abe, T. (1998). Diffusion in potato during far infrared radiation drying. *Journal of Food Engineering, 37*(4), 353–365.
Augusto, P. E., Miano, A. C., & Rojas, M. L. (2018). Evaluating the Guo–Campanella viscoelastic model. *Journal of Texture Studies, 49*(1), 121–128.
Bird, R. B. (2002). Transport phenomena. *Applied Mechanics Reviews, 55*(1), R1–R4.
Braga, A. M. P., Pedroso, M. P., Augusto, F., & Silva, M. A. (2009). Volatiles identification in pineapple submitted to drying in an ethanolic atmosphere. *Drying Technology, 27*(2), 248–257.
Brncic, M., Karlovic, S., Rimac, B. S., Bosiljkov, T., Ježek, D., & Tripalo, B. (2010). Textural properties of infra red dried apple slices as affected by high power ultrasound pre-treatment. *African Journal of Biotechnology, 9*(41), 6907–6915.
Castanha, N., da Matta Junior, M. D., & Augusto, P. E. D. (2017). Potato starch modification using the ozone technology. *Food Hydrocolloids, 66*, 343–356.
Celma, A. R., López-Rodríguez, F., & Blázquez, F. C. (2009). Experimental modelling of infrared drying of industrial grape by-products. *Food and Bioproducts Processing, 87*(4), 247–253.
Corrêa, J. L. G., Braga, A. M. P., Hochheim, M., & Silva, M. A. (2012). The influence of ethanol on the convective drying of unripe, ripe, and overripe bananas. *Drying Technology, 30*(8), 817–826.
Crum, L. (1984). Acoustic cavitation series: Part five rectified diffusion. *Ultrasonics, 22*(5), 215–223.
Datta, A. K., & Ni, H. (2002). Infrared and hot-air-assisted microwave heating of foods for control of surface moisture. *Journal of Food Engineering, 51*(4), 355–364.
Doymaz, İ. (2005). Drying characteristics and kinetics of okra. *Journal of Food Engineering, 69*(3), 275–279.
Dujmić, F., Brnčić, M., Karlović, S., Bosiljkov, T., Ježek, D., Tripalo, B., & Mofardin, I. (2013). Ultrasound-assisted infrared drying of pear slices: Textural issues. *Journal of Food Process Engineering, 36*(3), 397–406.
Fan, K., Zhang, M., & Mujumdar, A. S. (2017). Application of airborne ultrasound in the convective drying of fruits and vegetables: A review. *Ultrasonics Sonochemistry, 39*, 47–57.
Fernandes, F. A. N., Gallão, M. I., & Rodrigues, S. (2008a). Effect of osmotic dehydration and ultrasound pre-treatment on cell structure: Melon dehydration. *LWT - Food Science and Technology, 41*(4), 604–610.
Fernandes, F. A. N., Linhares, F. E., Jr., & Rodrigues, S. (2008b). Ultrasound as pre-treatment for drying of pineapple. *Ultrasonics Sonochemistry, 15*(6), 1049–1054.
Fernandes, F. A. N., & Rodrigues, S. (2007). Ultrasound as pre-treatment for drying of fruits: Dehydration of banana. *Journal of Food Engineering, 82*(2), 261–267.
Fernandes, F. A. N., & Rodrigues, S. (2008). Application of ultrasound and ultrasound-assisted osmotic dehydration in drying of fruits. *Drying Technology, 26*(12), 1509–1516.
Fonteles, T. V., Costa, M. G. M., de Jesus, A. L. T., de Miranda, M. R. A., Fernandes, F. A. N., & Rodrigues, S. (2012). Power ultrasound processing of cantaloupe melon juice: Effects on quality parameters. *Food Research International, 48*(1), 41–48.
Funebo, T., Ahrné, L., Prothon, F., Kidman, S., Langton, M., & Skjöldebrand, C. (2002). Microwave and convective dehydration of ethanol treated and frozen apple – Physical properties and drying kinetics. *International Journal of Food Science & Technology, 37*(6), 603–614.
Gugliotti, M., & Todd, S. (2004). Tears of wine. *Journal of Chemical Education, 81*(1), 67.
Guo, W., & Campanella, O. H. (2017). A relaxation model based on the application of fractional calculus for describing the viscoelastic behavior of potato tubers. *Transactions of the ASABE, 60*(1), 259.
Halder, A., Datta, A. K., & Spanswick, R. M. (2011). Water transport in cellular tissues during thermal processing. *AICHE Journal, 57*(9), 2574–2588.
Hemwimol, S., Pavasant, P., & Shotipruk, A. (2006). Ultrasound-assisted extraction of anthraquinones from roots of *Morinda citrifolia*. *Ultrasonics Sonochemistry, 13*(6), 543–548.
Jay, J. M., Loessner, M. J., & Golden, D. A. (2005). Protection of foods by drying. *Modern food microbiology* (pp. 443–456). Boston, MA: Springer US.
Kowalski, S. J., & Rybicki, A. (2017). Ultrasound in wet biological materials subjected to drying. *Journal of Food Engineering, 212*, 271–282.
Lampinen, M. J., Ojala, K. T., & Koski, E. (1991). Modeling and measurements of infrared dryers for coated paper. *Drying Technology, 9*(4), 973–1017.
Leenaars, A. F. M., Huethorst, J. A. M., & Van Oekel, J. J. (1990). Marangoni drying: A new extremely clean drying process. *Langmuir, 6*(11), 1701–1703.
Magalhães, M. L., Cartaxo, S. J. M., Gallão, M. I., García-Pérez, J. V., Cárcel, J. A., Rodrigues, S., & Fernandes, F. A. N. (2017). Drying intensification combining ultrasound pre-treatment and ultrasound-assisted air drying. *Journal of Food Engineering, 215*, 72–77.
Mayor, L., Cunha, R., & Sereno, A. (2007). Relation between mechanical properties and structural changes during osmotic dehydration of pumpkin. *Food Research International, 40*(4), 448–460.
Miano, A. C., & Augusto, P. E. D. (2018). The hydration of grains: A critical review from description of phenomena to process improvements. *Comprehensive Reviews in Food Science and Food Safety, 17*(2), 352–370.
Miano, A. C., Ibarz, A., & Augusto, P. E. D. (2016). Mechanisms for improving mass transfer in food with ultrasound technology: Describing the phenomena in two model cases. *Ultrasonics Sonochemistry, 29*, 413–419.
Mongpraneet, S., Abe, T., & Tsurusaki, T. (2004). Kinematic model for a far infrared vacuum dryer. *Drying Technology, 22*(7), 1675–1693.
Motevali, A., Minaei, S., & Khoshtagaza, M. H. (2011). Evaluation of energy consumption in different drying methods. *Energy Conversion and Management, 52*(2), 1192–1199.
Mothibe, K. J., Zhang, M., Nsor-Atindana, J., & Wang, Y.-C. (2011). Use of ultrasound pretreatment in drying of fruits: Drying rates, quality attributes, and shelf life extension. *Drying Technology, 29*(14), 1611–1621.
Mulet, A., Cárcel, J. A., Sanjuán, N., & Bon, J. (2003). New food drying technologies - Use of ultrasound. *Food Science and Technology International, 9*(3), 215–221.
O'Donnell, C. P., Tiwari, B. K., Bourke, P., & Cullen, P. J. (2010). Effect of ultrasonic processing on food enzymes of industrial importance. *Trends in Food Science & Technology, 21*(7), 358–367.
Oh, S., Ramachandraiah, K., & Hong, G.-P. (2017). Effects of pulsed infra-red radiation followed by hot-press drying on the properties of mashed sweet potato chips. *LWT-Food Science and Technology, 82*, 66–71.
Onwude, D. I., Hashim, N., Abdan, K., Janius, R., Chen, G., & Kumar, C. (2018). Modelling of coupled heat and mass transfer for combined infrared and hot-air drying of sweet potato. *Journal of Food Engineering, 228*, 12–24.
Onwude, D. I., Hashim, N., & Chen, G. (2016). Recent advances of novel thermal combined hot air drying of agricultural crops. *Trends in Food Science & Technology, 57*, 132–145.
Özdemir, M. B., Aktaş, M., Şevik, S., & Khanlari, A. (2017). Modeling of a convective-infrared kiwifruit drying process. *International Journal of Hydrogen Energy, 42*(28), 18005–18013.
Page, G. E. (1949). *Factors influencing the maximum rates of air drying shelled corn in thin layers.* Ann Arbor: Purdue University.
Pawar, S. B., & Pratape, V. M. (2017). Fundamentals of infrared heating and its application in drying of food materials: A review. *Journal of Food Process Engineering, 40*(1), e12308.
Peleg, M. (1979). Characterization of the stress relaxation curves of solid foods. *Journal of Food Science, 44*(1), 277–281.
Peleg, M., & Normand, M. D. (1983). Comparison of two methods for stress relaxation data presentation of solid foods. *Rheologica Acta, 22*(1), 108–113.

Rajewska, K., & Mierzwa, D. (2017). Influence of ultrasound on the microstructure of plant tissue. *Innovative Food Science & Emerging Technologies, 43*, 117–129.
Rao, M. A., & Steffe, J. F. (1992). *Viscoelastic properties of foods.* Essex: Elsevier Applied Science.
Ratti, C., & Mujumdar, A. S. (2006). Infrared drying. In A. S. Mujumdar (Ed.). *Handbook of industrial drying* (pp. 423–438). New York: Marcel Dekker.
Reeve, R. M., Hautala, E., & Weaver, M. L. (1969). Anatomy and compositional variation within potatoes. *American Potato Journal, 46*(10), 361–373.
Riadh, M. H., Ahmad, S. A. B., Marhaban, M. H., & Soh, A. C. (2015). Infrared heating in food drying: An overview. *Drying Technology, 33*(3), 322–335.
Ricce, C., Rojas, M. L., Miano, A. C., Siche, R., & Augusto, P. E. D. (2016). Ultrasound pre-treatment enhances the carrot drying and rehydration. *Food Research International, 89*, 701–708.
Rodríguez, Ó., Eim, V., Rosselló, C., Femenia, A., Cárcel, J. A., & Simal, S. (2018). Application of power ultrasound on the convective drying of fruits and vegetables: Effects on quality. *Journal of the Science of Food and Agriculture, 98*(5), 1660–1673.
Rojas, M. L., & Augusto, P. E. D. (2018a). Ethanol pre-treatment improves vegetable drying and rehydration: Kinetics, mechanisms and impact on viscoelastic properties. *Journal of Food Engineering, 233*, 17–27.
Rojas, M. L., & Augusto, P. E. D. (2018b). Microstructure elements affect the mass transfer in foods: The case of convective drying and rehydration of pumpkin. *LWT, 93*, 102–108.
Rojas, M. L., Leite, T. S., Cristianini, M., Alvim, I. D., & Augusto, P. E. D. (2016). Peach juice processed by the ultrasound technology: Changes in its microstructure improve its physical properties and stability. *Food Research International, 82*, 22–33.
Rojas, M. L., Miano, A. C., & Augusto, P. E. (2017). Ultrasound processing of fruit and vegetable juices. *Ultrasound: advances for food processing and preservation* (pp. 181–199). Elsevier.
Senevirathne, M., Kim, S.-H., Kim, Y.-D., Oh, C.-K., Oh, M.-C., Ahn, C.-B., ... Jeon, Y.-J. (2010). Effect of far-infrared radiation drying of citrus press-cakes on free radical scavenging and antioxidant activities. *Journal of Food Engineering, 97*(2), 168–176.
Shipman, J. W., Rahman, A., Segars, R., Kapsalis, J., & Westcott, O. (1972). Improvement of the texture of dehydrated celery by glycerol treatment. *Journal of Food Science, 37*(4), 568–571.
Silva, M. A., Braga, A. M. P., & Santos, P. H. S. (2012). Enhancement of fruit drying: The ethanol effect. *Proceedings of the 18th international drying symposium (IDS 2012)* (Xiamen).
Simal, S., Femenia, A., Garau, M. C., & Rosselló, C. (2005). Use of exponential, Page's and diffusional models to simulate the drying kinetics of kiwi fruit. *Journal of Food Engineering, 66*(3), 323–328.
Simpson, R., Ramírez, C., Nuñez, H., Jaques, A., & Almonacid, S. (2017). Understanding the success of Page's model and related empirical equations in fitting experimental data of diffusion phenomena in food matrices. *Trends in Food Science & Technology, 62*, 194–201.
Sujka, M. (2017). Ultrasonic modification of starch – Impact on granules porosity. *Ultrasonics Sonochemistry, 37*, 424–429.
Tatemoto, Y., Mizukoshi, R., Ehara, W., & Ishikawa, E. (2015). Drying characteristics of food materials injected with organic solvents in a fluidized bed of inert particles under reduced pressure. *Journal of Food Engineering, 158*(Supplement C), 80–85.
Thomson, J. (1855). XLII. On certain curious motions observable at the surfaces of wine and other alcoholic liquors. *Philosophical Magazine Series 4, 10*(67), 330–333.
Torki-Harchegani, M., Ghanbarian, D., Maghsoodi, V., & Moheb, A. (2017). Infrared thin layer drying of saffron (*Crocus sativus* L.) stigmas: Mass transfer parameters and quality assessment. *Chinese Journal of Chemical Engineering, 25*(4), 426–432.

APPENDIX IV: Improving the infrared drying and rehydration of potato slices using simple approaches: Perforations and ethanol

ROJAS, M. L., SILVEIRA, I., & AUGUSTO, P. E. D. (2019).
JOURNAL OF FOOD PROCESS ENGINEERING, 42(5), e13089

Received: 1 February 2019 | Revised: 17 March 2019 | Accepted: 21 April 2019

DOI: 10.1111/jfpe.13089

ORIGINAL ARTICLE

Journal of Food Process Engineering WILEY

Improving the infrared drying and rehydration of potato slices using simple approaches: Perforations and ethanol

Meliza L. Rojas[1] | Isabela Silveira[1] | Pedro E. D. Augusto[1,2]

[1]Department of Agri-food Industry, Food and Nutrition (LAN), Luiz de Queiroz College of Agriculture (ESALQ), University of São Paulo (USP), Piracicaba, SP, Brazil

[2]Food and Nutrition Research Center (NAPAN), University of São Paulo (USP), São Paulo, SP, Brazil

Correspondence
Meliza L. Rojas and Pedro E. D. Augusto, Avenida Pádua Dias, 11, Piracicaba, SP 13418-900, Brazil.
Emails: mrojas@usp.br (M. L. R.) and pedro.ed.augusto@usp.br (P. E. D. A.)

Funding information
Conselho Nacional de Desenvolvimento Científico e Tecnológico, Grant/Award Number: 306557/2017-7; Fondo Nacional de Desarrollo Científico y Tecnológico, Grant/Award Number: 087-2016-FONDECYT; Fundação de Amparo à Pesquisa do Estado de São Paulo, Grant/Award Number: 2016/18052-5

Abstract

The objective of this work was use ethanol and perforations as simple approaches to improve the infrared drying and rehydration of potato slices. Perforations were performed to study the effect of promoting routes to capillarity flow, while ethanol was impregnated in the samples to evaluate the effect of Marangoni flow. All pretreatments reduced the drying time compared to control treatment. However, a great time reduction was observed with *P* + *E* pretreatment: The synergistic combination of both treatments increased the drying rate in more than four times, reducing both drying time and the necessary energy by 44%. The samples with perforations (*P* and *P* + *E*) increased their rehydration rate as well as the water retention capacity. However, the pretreated samples with ethanol shows poor rehydration properties. Possible mechanisms were discussed. These results show simple approaches to enhance food drying and rehydration.

Practical Applications

Drying is an ancient unit operation to obtain safe and stable food products. However, some challenges still face food process engineers, such as the long processing time and the low rehydration capacity. Consequently, different technologies have been explored to enhance food drying, such as pulsed electric fields, high pressure, and ultrasound. However, although interesting and effective, some of that approaches can be complicated or even expensive when considering the reality of drying vegetables such as fruits and starchy products, limiting their application. Therefore, this work purposes a simple but efficient technique based on the use of ethanol and the creation of channels through perforations to improve the infrared drying of potato slices, also evaluating the rehydration properties. Our results show that simple operations could be performed to create routes to water flow (through mechanical perforations) combined with drying accelerator (ethanol), improving both drying and rehydration of food products.

1 | INTRODUCTION

Drying is a physical unit operation that involves both heat and mass transfer, where the last is usually the rate-limiting factor (Saravacos, 2014). Compared to conventional convective drying, infrared (IR) drying present some advantages, such as the uniform heating, rapid water vaporization and considerable reduction of drying time. Moreover, it can be carried out in conditions were the use of hot air is limited or undesirable, such as on future long-term space missions. However, it presents some inconvenient such as the ticker of samples is limited, and the crust formation due to excessive surface heating, inhibit the heat and mass transfer and decreasing the water flux

(Krishnamurthy, Khurana, Soojin, Irudayaraj, & Demirci, 2008; Supmoon & Noomhorm, 2013).

Most drying of food materials takes place during the falling rate period. A characteristic of this period is that the moisture loss is an internally controlled mechanism, that is, the complex structure and elements of food tissue provide resistance to water flow (Halder, Datta, & Spanswick, 2011; Srikiatden & Roberts, 2007). Therefore, the drying rate is limited by the water transfer from the interior toward the surface (internal resistance).

This internal resistance is lower in food products whose structure naturally present intercellular or capillary spaces (Molz & Ikenberry, 1974; Shi & Le Maguer, 2002), pores, capillaries (Aguilera, 2005), or structural elements such as xylem vessels (Rojas & Augusto, 2018c). All these are the routes to water flow. Although in these products it is desired to preserve the initial structure during drying, to promote the water flow through these channels, an interesting approach is form artificial channels to enhance drying.

In fact, different pretreatments have been explored to improve heat and water flow during drying (Liu & Lee, 2015; Sagar & Kumar, 2010; Witrowa-Rajchert, Wiktor, Sledz, & Nowacka, 2014; Yang, Zhang, Mujumdar, Zhong, & Wang, 2018), some of them by forming a porous structure to facilitate the mass transfer. For example, in freeze-dried foods, a directional freezing process was developed to produce aligned channels (Qian & Zhang, 2011), which promote the water sublimation and allow obtaining foods with highly porous structure. Pulsed electric fields (Lebovka, Shynkaryk, & Vorobiev, 2007), and high pressure technology (Oliveira, Tribst, Leite Júnior, Oliveira, & Cristianini, 2015) have been used as alternatives for structural modification, enhancing drying. Among other emerging technologies, the ultrasound technology enhances the mass transfer during drying and rehydration due unclogging and/or creation of cavities and microchannels (Fernandes, Rodrigues, Law, & Mujumdar, 2011; Yao, 2016).

A promising technique to accelerate the drying process, preserve physical properties, and sensible food compounds is the use of ethanol pretreatment (Braga, Pedroso, Augusto, & Silva, 2009; Braga, Silva, Pedroso, Augusto, & Barata, 2010; Corrêa, Braga, Hochheim, & Silva, 2012; Corrêa, Rasia, Mulet, & Cárcel, 2017; Rojas & Augusto, 2018b; Tatemoto, Mizukoshi, Ehara, & Ishikawa, 2015). Among the possible mechanisms to improve food drying, the Marangoni effect is important, in special considering the capillarity flow (Rojas & Augusto, 2018b; Silva, Braga, & Santos, 2012). Therefore, based on the ultrasound and ethanol effects, one interesting possibility was their combined application, where the ethanol promoted the water flow through the channels created by ultrasound (Rojas & Augusto, 2018a).

However, although interesting and effective, some of that approaches can be complicated or even expensive when considering the reality of drying vegetables such as fruits and starchy products, limiting their application.

Therefore, this work purposes a simple but efficient technique based on the use of ethanol and the creation of channels through perforations to improve the IR drying of potato slices, also evaluating the rehydration properties.

2 | MATERIAL AND METHODS

2.1 | Raw material

Potato slices were obtained from fresh potato tubers (Piracicaba, SP, Brasil). Figure 1 shows the sample obtention process. For this, cylinders were extracted from the central part of potato tubers (perimedullary zone) using sharp stainless-steel tube (diameter of 2.0 cm). The extracted cylinders were cut obtaining slices of 0.5 cm thickness. To prevent browning slices were immersed for 30 s in sodium bisulphite (0.1% m/v).

2.2 | Pretreatments

Four pretreatments to IR drying were performed in potato slices:

- Samples without any treatment (control).
- Perforated samples using a needle with 1.2 mm of diameter (*P*). In each potato slice 17 perforations were performed, these were uniformly distributed following the circular geometry and perpendicularly oriented in relation to the circular surface.
- Non-perforated samples immersed in ethanol (95% v/v) for 15 min (*E*). To assure that all the surface was exposed to ethanol, each potato slice was completely immersed in 60 mL of ethanol.
- Samples firstly perforated and then immersed in ethanol for 15 min (*P* + *E*).

2.3 | IR drying process

Drying process was performed at a set temperature of 100°C using a multispectral halogen lamp (QIR240V400W/140). The lamp emission range is showed in Figure 1, which 95% of that corresponds to near and medium IR radiation. The potato slices mass over drying time was recorded every second using the WinCT-Moisture (V2.41, Windows communication, A&D Company, Japan). Based on this data and by taking into account the initial moisture, the moisture at each time during drying was calculated by mass balance. The initial and final moisture content was measured by completely drying crushed samples at 105°C.

During ethanol pretreatments, some considerations should be observed, once samples simultaneously lose water and solids, as well as they absorb ethanol (Rojas & Augusto, 2018a, 2018b; Silva et al., 2012). Therefore, the sample "moisture" after pretreatments includes both the mass of the remaining water and the gained ethanol, which are considered together as a lumped parameter (L_p). The sample "moisture" after pretreatments (M_p%) is calculated, thus, through Equation (1), considering the lumped parameter (L_p) additionally to the sample mass (m_p):

$$M_p\% = \frac{L_p}{m_p} \cdot 100 \quad (1)$$

In the same manner, during drying, the mass loss includes the volatilization of both liquids (water and ethanol). Therefore, the moisture content (M_t) over the drying process (Equation 2) is calculated by

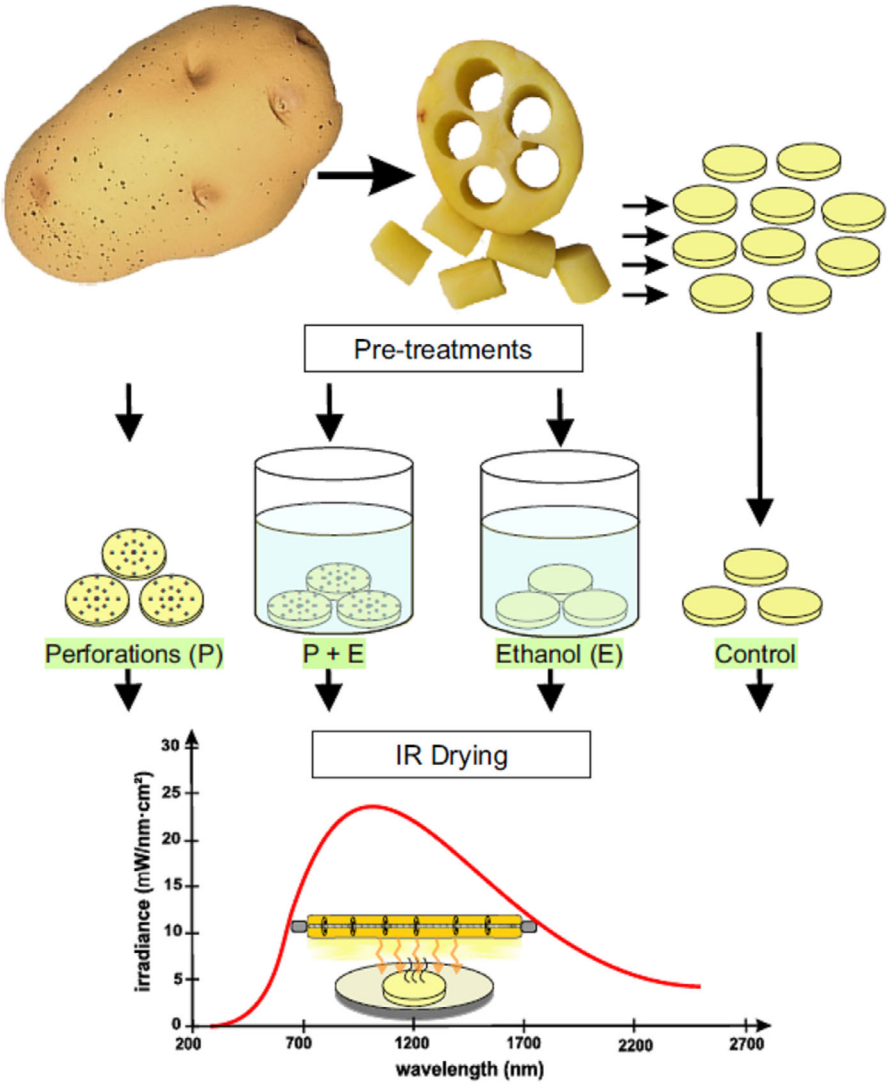

FIGURE 1 Representation of sample obtention, pretreatments, and infrared (IR) drying

considering the mass of both liquids (L_{pt}) at a given drying time (t), where m_{pt} is the sample mass at that time (t).

$$M_t\% = \frac{L_{pt}}{m_{pt}} \cdot 100 \quad (2)$$

The dimensionless moisture ratio (MR; Equation 3) data were used to construct the drying curves (where M is the moisture content at a given drying process time (t), M_e is the equilibrium moisture and M_0 is the initial moisture after pretreatment, all expressed in dry basis (d.b.; i.e., g of water/g dry matter)). In the case of the control samples, M_0 is the *in-natura* sample moisture. Therefore, the control and samples with different pretreatment started the drying process with MR = 1.

$$MR(t) = \frac{M - M_e}{M_0 - M_e} \quad (3)$$

2.4 | Rehydration process

Each dried potato slice was rehydrated at 25°C by immersion in 50 mL of distilled water. The mass gain was registered during process. For this, the slices were removed form water, the surface excess of water removed, the slices were weighed, and returned to the same water. The process was performed until water absorption was stabilized. From the mass gain data and the sample initial moisture, by mass balance, the moisture content over the rehydration time was determined.

2.5 | Mathematical description: Drying and rehydration kinetics

The Page model (Equation 4; Page, 1949), was used to fit the drying data, where MR(t) is obtained using Equation (3), k is the drying rate constant and n the dimensionless drying constant. Although originally empiric, the Peleg model was recently studied by Simpson, Ramírez, Nuñez, Jaques, and Almonacid (2017) with a phenomenological interpretation: According to the authors, n is related to the "type of diffusion," defining the conditions of super-diffusion ($n > 1$), and subdiffusion ($n < 1$). Therefore, when $n \neq 1$, other mechanisms of water transport than diffusion are important (Rojas & Augusto, 2018a, 2018c):

$$MR(t) = e^{-k \cdot t^n} \quad (4)$$

The potato slices rehydration was described using the Peleg model (Equation 5; Peleg, 1988), where $M(t)$ is the moisture (d.b.) at a rehydration time t (min), M_0 is the initial moisture (d.b), the reciprocal of k_1 (min d.b^{-1}), and k_2 (d.b^{-1}) represents the maximum water absorption rate and the water retention capacity, respectively:

$$M(t) = M_0 + \frac{t}{k_1 + k_2 \cdot t} \quad (5)$$

The parameters of Equations (4) and (5) were varied iteratively in order to adjust the Models to the experimental data. The best fit was achieved by minimizing the sum of squared errors (SSE in Equation 6) using the generalized reduced gradient algorithm (GRG), through a nonlinear solving method (implemented in the "Solver" tool of Excel 2016, Microsoft). The parameters value of each model was considered valid when the GRG method found a locally optimal solution (using a set convergence of 0.000001). The regressions were conducted for each replicate.

$$\text{SSE} = \sum_{i=1}^{x} ((\text{predicted}) - (\text{experiemental}))_i^2 \quad (6)$$

2.6 | Experimental design and statistical analysis

The study was developed through a completely randomized design, with at least three replicates of processes and analyses. The analysis of variance and Tukey test were conducted when relevant to determine which treatments differ from each other (significance level of 5%, IBM SPSS Statistics 23 software, IBM SPSS).

3 | RESULTS AND DISCUSSION

Figure 2 shows the drying kinetics of the control and pretreated samples. All pretreatments reduced the drying time to reach the equilibrium moisture. The *P* samples needed 19% less time, *E* samples needed 10%, and the *P* + *E* needed 44% less time, compared to the control samples. Considering the same conditions for all pretreatments and drying process (such as, distance between lamps and product, temperature, and drying surface), the observed drying time reduction can be directly correlated with a reduction in the energy consumed in the same proportion. Therefore, a synergistic effect of combining both treatments (*P* + *E*) was achieved, which can reduce both time of processing and the necessary energy by ~44%. It is worth mentioning this reduction is significative, in special by combining simple and cost-effective approaches.

As observed in Figure 2, *E* samples improve the initial stage of drying. This behavior could be attributed at the Marangoni effect (Silva et al., 2012), which is based on the surface tension gradient formed between the ethanol remained on samples surface and their water: This effect promotes the water flow from the sample core to the surface, then accelerating the drying process (Rojas & Augusto, 2018b).

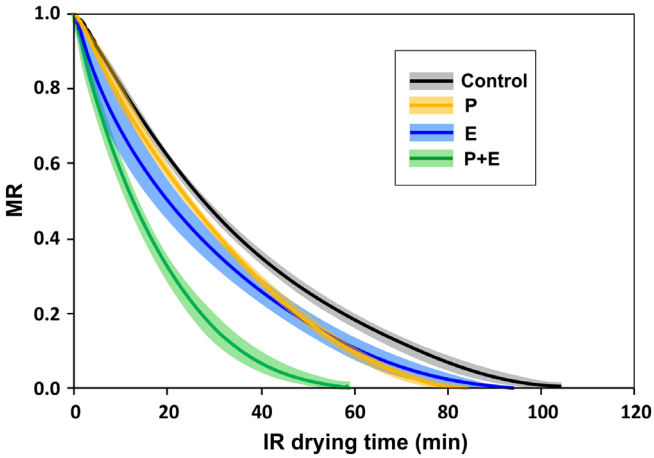

FIGURE 2 Experimental values of moisture ratio (MR) as a function of infrared (IR) drying time for all pretreatments. Bands indicate confidence interval (95%)

However, as the drying time passes, the ethanol is vaporized and the water of the sample decrease. Consequently, the effects of this phenomenon probably decrease. In the *P* + *E* treatment, the Marangoni effect can be facilitated through the formed channels (perforations), which can explain the observed synergistic effect.

Another important observation is that *E* samples reached the equilibrium when moisture is still higher (~20% w.b) when compared to other samples (~10% w.b), although in a moisture level generally considered adequate (Jay, Loessner, & Golden, 2005). This behavior is probably a consequence of crust formation. In fact during IR drying crust formation was reported in products such as banana slices (Pan, Shih, McHugh, & Hirschberg, 2008). This phenomenon occurs due to phase transition and surface overheating, that depends on drying conditions, structure and composition of food material (Mayor & Sereno, 2004; Rahman, 2001).

During ethanol pretreatment structural modifications occurs, mainly on the cell wall composition and structure (intercellular air expelling, extraction of superficial compounds, and cell thinning; Rojas & Augusto, 2018a). These modifications make the tissue and components (in special starch) more exposed and susceptible to heat effects such as crust formation.

On the other hand, compared to ethanol treated (*E*), perforated samples improve principally the last stage of drying process, suggesting the reduction on internal resistance. This could be attributed at the fact that perforations increased the sample drying area, and, more important, perforations are routes to water flow from inside the potato tissue, which is more important and notorious at the last stage of drying.

Therefore, a proposal to promote the drying improvement on their initial and final stages was the use of the *P* + *E* pretreatment. Effectively, this treatment allowed obtaining the highest drying time reduction. This means that the combination of the ethanol and perforations promoted different mechanism to improve the IR drying. In the first time, the Marangoni effects as consequence of ethanol promotes the water flow by capillarity through the created channels (perforations),

highly accelerating the drying process. Finally, when ethanol loss their effect, the perforations even promote the water exit.

In fact, this can be a simple but clever approach to enhance potato drying. Although similar results were obtained by combining ultrasound and ethanol (Rojas & Augusto, 2018a), it is worth mentioning how simple and practical the perforation approach is in relation to the ultrasound technology. In fact, it can be a promising technique, from small farmers/producers, to the most elaborate possibilities—such as food processing outside the Earth.

Experimental drying data were mathematically modeled using the Page model (Equation 4), obtaining the *n* and *k* parameters, whose values were presented on Table 1. The *P* + *E* treated samples showed the highest drying rate (*k*), with synergism in relation to the other treatments, which corroborate the faster drying of these samples observed on Figure 2. In all cases the *n* value was higher than 1. Therefore, as expected, all samples showed a super-diffusive behavior (Simpson et al., 2017) it means that other water transfer phenomena than diffusion are important, such as capillarity.

Rehydration behavior is related with the performed pretreatments, the severity of drying process and the consequent structural modifications. It was observed (Figure 3) that *E* treatment resulted in lower rehydration properties. In fact, Table 1 shows the *E* samples showed lower water absorption rate and retention capacity (higher k_1 and k_2 values, respectively). Therefore, although ethanol improves the IR drying (Figure 2), this pretreatment present negative effects during potato slices rehydration. The observed behavior can be due to the mentioned structure modifications during ethanol pretreatment that caused a more compacted surface structure. In fact, a dense or collapsed structure reduce the ability to imbibe and retain the water (Prothon, Ahrné, & Sjöholm, 2003). For this product, the same rehydration behavior was observed by Rojas and Augusto (2018a) being attributed to crust formation during IR drying. When crust remains intact, it can act as an impermeable layer (Rahman, 2001). However, in other products, such as pumpkin, ethanol pretreatment not only improved drying but also rehydration (Rojas & Augusto, 2018b). Therefore, the type of product highly influences on the obtained results. In the case of potatoes, probably due to their natural high starch content and structure, under the studied conditions, ethanol treatment did not present positive rehydration characteristics.

On the contrary, the perforation treatment whit and without ethanol application improved rehydration behavior. The best rehydration

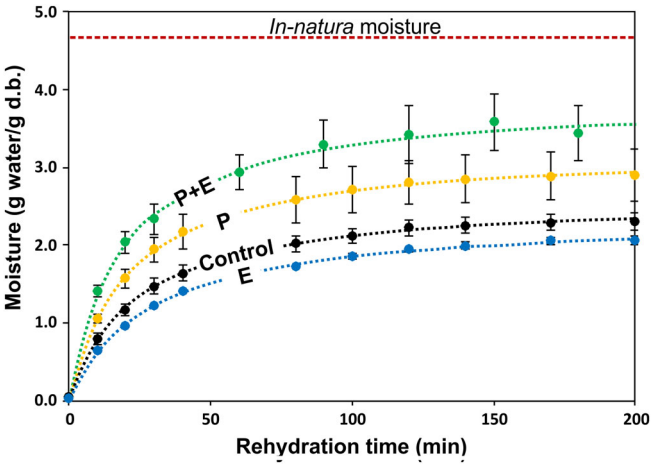

FIGURE 3 Rehydration kinetics. Horizontal dashed line represents the initial moisture of *in-natura* potato samples. Dots are the experimental data and vertical bars are *SD*. Curves are the Peleg model (Equation 5)

properties were presented by the *P* + *E* samples, which showed lower k_1 (higher water absorption rate). Therefore, the created channels promote the water absorption by capillarity that is quickly distributed to surrounded tissue. These demonstrated that not only natural pores, cavities and capillaries promote the water uptake due to capillarity (Lewicki, 1998), but that artificial channels can be easily created facilitating enhancing both drying and rehydration. In addition, Mayor and Sereno (2004) observed that high rehydration rate reflect more interconnected porous structure. Another important fact is that perforations did not negatively impact the retention of the absorbed water, which is reflected in the lower k_2 (higher water retention capacity—i.e., higher equilibrium moisture; Table 1).

Consequently, as demonstrated, a manner to avoid the negative effects of drying during rehydration is through perforations. Using this simple technique not only drying is highly improved but also the rehydration properties.

4 | CONCLUSIONS

This work explored the use of ethanol and perforations individually and combined to improve both IR drying and rehydration of potato slices. The use of ethanol had positive effects on drying process, but

TABLE 1 Drying and rehydration model parameters obtained for each pretreatment

	Drying process Page model parameters		Rehydration process Peleg model parameters	
Pretreatment	***n***	***k***	k_1	k_2
Control	1.201 ± 0.072^{A}	0.014 ± 0.005^{B}	10.051 ± 1.282^{B}	0.397 ± 0.018^{A}
P	1.234 ± 0.110^{AB}	0.018 ± 0.012^{B}	6.528 ± 0.328^{C}	0.313 ± 0.037^{B}
E	1.039 ± 0.106^{B}	0.033 ± 0.012^{AB}	12.691 ± 0.493^{A}	0.424 ± 0.011^{A}
P + *E*	1.032 ± 0.129^{B}	0.062 ± 0.030^{A}	5.037 ± 0.079^{C}	0.261 ± 0.032^{B}

Note. Average ± *SD*; different letters indicate significant differences ($p < .05$) among pretreatments.

not during rehydration. The use of perforations improves both processes. When the pretreatment combining both ethanol and perforations were applied (*P* + *E*), a synergistic effect was achieved reducing 44% the drying time. Therefore, improvement of drying and rehydration was obtained by using simple techniques.

ACKNOWLEDGMENTS

The authors are grateful to the São Paulo Research Foundation (FAPESP, Brazil) for funding the project No. 2016/18052-5; to the National Council for Scientific and Technological Development (CNPq, Brazil) for the productivity grant of P. E. D. Augusto (306557/2017-7); and to FONDECYT-CONCYTEC (Peru) for the M.L. Rojas Ph.D. scholarship (grant contract number 087-2016-FONDECYT).

ORCID

Meliza L. Rojas https://orcid.org/0000-0001-5750-8399
Pedro E. D. Augusto https://orcid.org/0000-0001-7435-343X

REFERENCES

Aguilera, J. M. (2005). Why food microstructure? *Journal of Food Engineering*, *67*(1), 3–11. https://doi.org/10.1016/j.jfoodeng.2004.05.050

Braga, A. M. P., Pedroso, M. P., Augusto, F., & Silva, M. A. (2009). Volatiles identification in pineapple submitted to drying in an ethanolic atmosphere. *Drying Technology*, *27*(2), 248–257. https://doi.org/10.1080/07373930802606097

Braga, A. M. P., Silva, M. A., Pedroso, M. P., Augusto, F., & Barata, L. E. S. (2010). Volatile composition changes of pineapple during drying in modified and controlled atmosphere. *International Journal of Food Engineering*, *6*(1), 12. https://doi.org/10.2202/1556-3758.1835

Corrêa, J., Rasia, M., Mulet, A., & Cárcel, J. (2017). Influence of ultrasound application on both the osmotic pretreatment and subsequent convective drying of pineapple (*Ananas comosus*). *Innovative Food Science & Emerging Technologies*, *41*, 284–291.

Corrêa, J. L. G., Braga, A. M. P., Hochheim, M., & Silva, M. A. (2012). The influence of ethanol on the convective drying of unripe, ripe, and overripe bananas. *Drying Technology*, *30*(8), 817–826. https://doi.org/10.1080/07373937.2012.667469

Fernandes, F. A. N., Rodrigues, S., Law, C. L., & Mujumdar, A. S. (2011). Drying of exotic tropical fruits: A comprehensive review. *Food and Bioprocess Technology*, *4*(2), 163–185. https://doi.org/10.1007/s11947-010-0323-7

Halder, A., Datta, A. K., & Spanswick, R. M. (2011). Water transport in cellular tissues during thermal processing. *AICHE Journal*, *57*(9), 2574–2588. https://doi.org/10.1002/aic.12465

Jay, J. M., Loessner, M. J., & Golden, D. A. (2005). Protection of foods by drying. In *Modern food microbiology* (pp. 443–456). Boston, MA: Springer.

Krishnamurthy, K., Khurana, H. K., Soojin, J., Irudayaraj, J., & Demirci, A. (2008). Infrared heating in food processing: An overview. *Comprehensive Reviews in Food Science and Food Safety*, *7*(1), 2–13. https://doi.org/10.1111/j.1541-4337.2007.00024.x

Lebovka, N. I., Shynkaryk, N. V., & Vorobiev, E. (2007). Pulsed electric field enhanced drying of potato tissue. *Journal of Food Engineering*, *78*(2), 606–613. https://doi.org/10.1016/j.jfoodeng.2005.10.032

Lewicki, P. P. (1998). Effect of pre-drying treatment, drying and rehydration on plant tissue properties: A review. *International Journal of Food Properties*, *1*(1), 1–22.

Liu, X., & Lee, D.-J. (2015). Some recent research and development in drying technologies: Product perspective. *Drying Technology*, *33*(11), 1339–1349. https://doi.org/10.1080/07373937.2015.1026986

Mayor, L., & Sereno, A. M. (2004). Modelling shrinkage during convective drying of food materials: A review. *Journal of Food Engineering*, *61*(3), 373–386. https://doi.org/10.1016/S0260-8774(03)00144-4

Molz, F. J., & Ikenberry, E. (1974). Water transport through plant cells and cell walls: Theoretical development 1. *Soil Science Society of America Journal*, *38*(5), 699–704.

Oliveira, M. M. d., Tribst, A. A. L., Leite Júnior, B. R. d. C., Oliveira, R. A. d., & Cristianini, M. (2015). Effects of high pressure processing on cocoyam, Peruvian carrot, and sweet potato: Changes in microstructure, physical characteristics, starch, and drying rate. *Innovative Food Science & Emerging Technologies*, *31*, 45–53. https://doi.org/10.1016/j.ifset.2015.07.004

Page, G. E. (1949). *Factors influencing the maximum rates of air drying shelled corn in thin layers*. Ann Arbor: Purdue University.

Pan, Z., Shih, C., McHugh, T. H., & Hirschberg, E. (2008). Study of banana dehydration using sequential infrared radiation heating and freeze-drying. *LWT-Food Science and Technology*, *41*(10), 1944–1951. https://doi.org/10.1016/j.lwt.2008.01.019

Peleg, M. (1988). An empirical model for the description of moisture sorption curves. *Journal of Food Science*, *53*(4), 1216–1217. https://doi.org/10.1111/j.1365-2621.1988.tb13565.x

Prothon, F., Ahrné, L., & Sjöholm, I. (2003). Mechanisms and prevention of plant tissue collapse during dehydration: A critical review. *Critical Reviews in Food Science and Nutrition*, *43*, 447–479.

Qian, L., & Zhang, H. (2011). Controlled freezing and freeze drying: A versatile route for porous and micro-/nano-structured materials. *Journal of Chemical Technology & Biotechnology*, *86*(2), 172–184. https://doi.org/10.1002/jctb.2495

Rahman, M. S. (2001). Toward prediction of porosity in foods during drying: A brief review. *Drying Technology*, *19*(1), 1–13. https://doi.org/10.1081/DRT-100001349

Rojas, M. L., & Augusto, P. E. D. (2018a). Ethanol and ultrasound pretreatments to improve infrared drying of potato slices. *Innovative Food Science & Emerging Technologies*, *49*, 65–75. https://doi.org/10.1016/j.ifset.2018.08.005

Rojas, M. L., & Augusto, P. E. D. (2018b). Ethanol pre-treatment improves vegetable drying and rehydration: Kinetics, mechanisms and impact on viscoelastic properties. *Journal of Food Engineering*, *233*, 17–27. https://doi.org/10.1016/j.jfoodeng.2018.03.028

Rojas, M. L., & Augusto, P. E. D. (2018c). Microstructure elements affect the mass transfer in foods: The case of convective drying and rehydration of pumpkin. *LWT*, *93*, 102–108. https://doi.org/10.1016/j.lwt.2018.03.031

Sagar, V., & Kumar, P. S. (2010). Recent advances in drying and dehydration of fruits and vegetables: A review. *Journal of Food Science and Technology*, *47*(1), 15–26.

Saravacos, G. D. (2014). Mass transfer properties of foods. In *Engineering properties of foods* (3rd ed., pp. 349–402). Boca Raton, Florida: CRC Press.

Shi, J., & Le Maguer, M. (2002). Osmotic dehydration of foods: Mass transfer and modeling aspects. *Food Reviews International*, *18*(4), 305–335. https://doi.org/10.1081/FRI-120016208

Silva, M. A., Braga, A. M. P., & Santos, P. H. S. (2012). *Enhancement of fruit drying: The ethanol effect*. Paper presented at the Proceedings of the 18th International Drying Symposium (IDS 2012), Xiamen.

Simpson, R., Ramírez, C., Nuñez, H., Jaques, A., & Almonacid, S. (2017). Understanding the success of Page's model and related empirical equations in fitting experimental data of diffusion phenomena in food matrices. *Trends in Food Science & Technology*, *62*, 194–201.

Srikiatden, J., & Roberts, J. S. (2007). Moisture transfer in solid food materials: A review of mechanisms, models, and measurements. *International*

Journal of Food Properties, *10*(4), 739–777. https://doi.org/10.1080/10942910601161672

Supmoon, N., & Noomhorm, A. (2013). Influence of combined hot air impingement and infrared drying on drying kinetics and physical properties of potato chips. *Drying Technology*, *31*(1), 24–31.

Tatemoto, Y., Mizukoshi, R., Ehara, W., & Ishikawa, E. (2015). Drying characteristics of food materials injected with organic solvents in a fluidized bed of inert particles under reduced pressure. *Journal of Food Engineering*, *158*(Suppl. C), 80–85. https://doi.org/10.1016/j.jfoodeng.2015.03.006

Witrowa-Rajchert, D., Wiktor, A., Sledz, M., & Nowacka, M. (2014). Selected emerging technologies to enhance the drying process: A review. *Drying Technology*, *32*(11), 1386–1396. https://doi.org/10.1080/07373937.2014.903412

Yang, F., Zhang, M., Mujumdar, A. S., Zhong, Q., & Wang, Z. (2018). Enhancing drying efficiency and product quality using advanced pretreatments and analytical tools—An overview. *Drying Technology*, *36*(15), 1824–1838. https://doi.org/10.1080/07373937.2018.1431658

Yao, Y. (2016). Enhancement of mass transfer by ultrasound: Application to adsorbent regeneration and food drying/dehydration. *Ultrasonics Sonochemistry*, *31*, 512–531. https://doi.org/10.1016/j.ultsonch.2016.01.039

How to cite this article: Rojas ML, Silveira I, Augusto PED. Improving the infrared drying and rehydration of potato slices using simple approaches: Perforations and ethanol. *J Food Process Eng*. 2019;e13089. https://doi.org/10.1111/jfpe.13089

APPENDIX V: Ultrasound and ethanol pre-treatments to improve convective drying: Drying, rehydration and carotenoid content of pumpkin

ROJAS, M.L., ISABELA. S., AUGUSTO, P.E.D

Reprinted with permission from: https://doi.org/10.1016/j.fbp.2019.10.008

Contents lists available at ScienceDirect

Food and Bioproducts Processing

journal homepage: www.elsevier.com/locate/fbp

Ultrasound and ethanol pre-treatments to improve convective drying: Drying, rehydration and carotenoid content of pumpkin

Meliza Lindsay Rojas[a], *Isabela Silveira*[a], *Pedro Esteves Duarte Augusto*[a,b,*]

[a] *Department of Agri-food Industry, Food and Nutrition (LAN), Luiz de Queiroz College of Agriculture (ESALQ), University of São Paulo (USP), Piracicaba, SP, Brazil*

[b] *Food and Nutrition Research Center (NAPAN), University of São Paulo (USP), São Paulo, SP, Brazil*

ARTICLE INFO

Article history:
Received 24 June 2019
Received in revised form 29 August 2019
Accepted 12 October 2019
Available online 19 October 2019

Keywords:
Drying
Rehydration
Ultrasound
Ethanol
Food properties
Carotenoids

ABSTRACT

Among different effects, both ultrasound and ethanol technologies change the product structure and promote mass transfer when used as pre-treatments to improve the food drying. For the first time, their combined application was evaluated as pre-treatment to improve convective drying, as well as the properties of the dried food. Pumpkin cylinders were used as model food, being dried using air at 50 °C and 0.8 ± 0.1 m s^{-1}. Effects on drying and rehydration kinetics, as well as on the energy consumption and carotenoid preservation, were studied. Compared to the Control, all pre-treatments decreased the drying time in more than 48%. The combination of ethanol and ultrasound presented the greatest reduction in both drying time (59%) and energy consumption (44%). The pre-treatments also enhanced the rehydration properties in more than 28%: higher rehydration rate and an increase of water retention were achieved. Possible mechanisms, involving structure modification and mass transfer during pre-treatment and drying process were discussed. Additionally, the extraction of carotenoids due to pre-treatments was negligible when compared to the remarkable effect in avoiding this nutrient degradation during drying. Pre-treated samples preserved ~100% of the carotenoid content, while the Control samples presented partial degradation (23%). This was explained by the negative effects evidenced by sample thermal history during drying. The results open new perspectives about an innovative method to improve the drying process and product quality by combining ethanol and ultrasound.

1. Introduction

Although drying is an ancient unit operation in food processing, many conventional methods still need improvement concerning the quality of the dried products – being this particularly true for convective drying (Kudra and Mujumdar, 2009). In fact, the properties of the final products highly depend on how the drying process is conducted. Improper drying may lead to irreversible damage to product physical, chemical and nutritional quality (Chou and Chua, 2001; Mujumdar and Devahastin, 2000). Additionally, the drying process requires high energy consumption, which is in general provided by the use of fossil fuels or electricity (E.I.A., 2018). It is a real problem related to the process, and there is an increasing demand for minimal costs and environmental impact (Chou and Chua, 2001; Kudra and Mujumdar, 2009).

The use of emerging technologies is very promising to face these challenges (Moses et al., 2014). In fact, different technologies are being evaluated worldwide with this purpose, such as pulsed electric fields (Lebovka et al., 2007), high pressure technology (de Oliveira et al., 2015) and microwave energy (Monteiro et al., 2016). This work is focused on the use of high-power ultrasound technology (US) and ethanol (E) as pre-treatments to convective drying.

* Corresponding author at: Avenida Pádua Dias, 11, Piracicaba, SP 13418-900, Brazil.
E-mail addresses: mrojas@usp.br (M.L. Rojas), pedro.ed.augusto@usp.br (P.E.D. Augusto).
https://doi.org/10.1016/j.fbp.2019.10.008

The US technology can be used as a pre-treatment to improve the drying process (Rodríguez et al., 2019). Mechanisms of improvement are related to mass transfer phenomena (influx and outflux of water and/or solutes and movement of intercellular compounds, for example) and structural modifications (such as microchannel formation) (De la Fuente-Blanco et al., 2006; Fernandes et al., 2008; Miano et al., 2017; Ricce et al., 2016). The pre-treatment with this technology has already demonstrated the capacity to reduce the internal resistance to water flow during drying, being necessary shorter processing times and/or lower temperatures. However, in some cases, to obtain a relevant drying time reduction, longer pre-treatments with US are required.

Therefore, there are still many aspects and mechanisms to be understood, described and improved, regarding the use of US. One of these is related to the US effects on nutritional compounds. During convective drying, depending on the product matrix and the process conditions. For example, the effect of acoustic cavitation on bioactive compounds and vitamins maybe either beneficial or detrimental (Aguilar et al., 2017; Campoli et al., 2018; Rodríguez et al., 2018). Therefore, it is important to evaluate the effect of US application on food compounds to determine if its application is advantageous, in special considering sensitive components.

Additionally, the pre-treatment with drying accelerators (such as ethanol), has been shown as a promising technique to improve drying. This technology can be used to accelerate the drying process, preserve physical properties and preserve sensible and volatile food compounds (Braga et al., 2009, 2010; Corrêa et al., 2012; Rojas and Augusto, 2018b; Tatemoto et al., 2015; Wang et al., 2019). Some possible effects and mechanisms by how ethanol improve food drying are structure modifications (in special in the cell walls), changes on vapour pressure and the Marangoni effect, which is important considering the capillarity flow (Rojas and Augusto, 2018b; Silva et al., 2012).

Based on the ultrasound and ethanol individual effects, one interesting possibility is their combined application. Until now, there is only two works in the literature related to the use of US and E as pre-treatments. One of these are focused on the incorporation of an hydrophilic nutrient (microparticles of maltodextrin containing iron) in apple slices (Rojas et al., 2019), but without evaluating the drying process. The other (Rojas and Augusto, 2018a) was carried out with potato slices, but using infrared drying (whose mechanisms are different from convective drying). Results demonstrated that pre-treatment combining E and US greater affect both potato structure and drying time. In contrast, a slight decrease in rehydration properties was observed. However, the convective and the infrared drying are very different technologies, as well as each food matrix has its typical structure and composition. Therefore, the application of these technologies in other products using other drying methods and conditions is still necessary to deeply understand and explain their effect on the process and the quality of dry products. Furthermore, convective drying is a technique much more important from an industrial point of view than the infrared drying, highlighting the necessity of evaluating it.

Consequently, the objective of the present work was to describe the combined application of US and E as pre-treatments to convective drying of pumpkin cylinders, evaluating their effect on drying kinetics, energy consumption and rehydration kinetics. Additionally, the effect of these technologies on carotenoid preservation (a sensitive compound naturally present on the pumpkin) was studied.

2. Material and methods

2.1. Raw material

Pumpkin (*Cucurbita moschata* Duch.) samples were obtained from the local market (Piracicaba, São Paulo, Brazil). They were stored for maximum 1 week at 4 °C, after that, new pumpkin with similar characteristics (colour, size and region) was obtained and used. Pumpkin was selected as a structural representative model for plant foods due to its tissue type, principally parenchymatic and vascular tissue (Rojas and Augusto, 2018c). Pumpkin cylinders (1 cm thick and 1.5 cm in diameter) were obtained just previously to processing using a sharp stainless-steel tube considering a longitudinal cut from the same pulp region (Fig. 1).

Table 1 – Pre-treatments performed using ethanol with and without US aplication.

Independent variable		Pre-treatment Code
Ethanol processing time (min)	US treatment	
0	Without US	Control
15		E-15 min
30		E-30 min
15	With US	E + US-15 min
30		E + US-30 min

2.2. Pre-treatments to drying

The performed drying pre-treatments include the Control samples (which were the pumpkin cylinders without any pre-treatment, i.e., the cylinders obtained from the *in-natura* pulp were directly dried) and those that were pre-treated with ethanol (99.5% v/v) and US as observed in Table 1 and Fig. 2. The conditions of each pre-treatment were based on pre-tests and our previous works (Rojas and Augusto, 2018a,b). Pre-treatments and analyses were conducted at least in three replicates.

2.2.1. Ethanol (E) application

Pumpkin cylinders were immersed in ethanol in a mass ratio of 0.37. For this, each replicate was composed by 80 cylinders (~145 g), which were immersed in 500 mL of ethanol for 15 min and 30 min (conditions defined after pre-tests). After this period, the excess of ethanol was removed with paper towels and then samples were placed to dry.

2.2.2. Ultrasound (US) and ethanol (E) application

The same pumpkin cylinders:ethanol mass ratio was used for all pre-treatments. Pumpkin cylinders were immersed in a glass beaker containing the 500 mL of ethanol under US application for 15 min and 30 min. The ethanol volume was selected in order to cover the pumpkin cylinders and, at the same time, coincide with the level of distilled water used in the US bath for the transmission of ultrasound waves.

The ultrasound processing was carried out using an ultrasonic bath (Q13/25, Ultronique Brazil; frequency of 25 kHz, volumetric power of 68 W/L – measured by the calorimetric method (Jambrak et al., 2007; Mason and Peters, 2004)) containing 6 L of distilled water. The process temperature was kept at 24–26 °C by an auxiliary thermostatic water bath (Cold-Lab CL 16–40 - Brazil) and a heat exchanger recirculating a cold ethanol–water solution. To assure the highest ultrasonic intensity, and taking into account the good practices described by Vinatoru (2015), the location of the vessel with samples inside the ultrasonic bath was above ultrasound transducers (this location was selected using the aluminium foil cavitation activity). The same location was used for all processes.

The cylinders were removed from the ethanol and superficially dried with a paper towel for then being analysed (10 cylinders) and dried (70 cylinders).

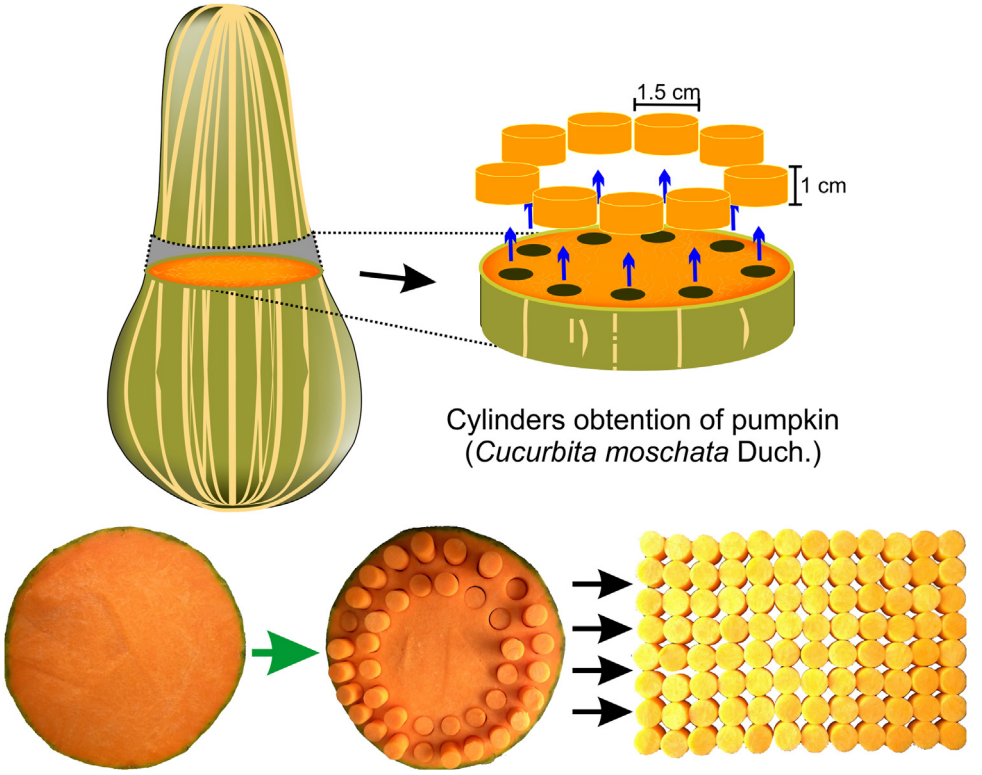

Fig. 1 – Schematic representation (up) and real images (down) of the pumpkin cylinders obtention.

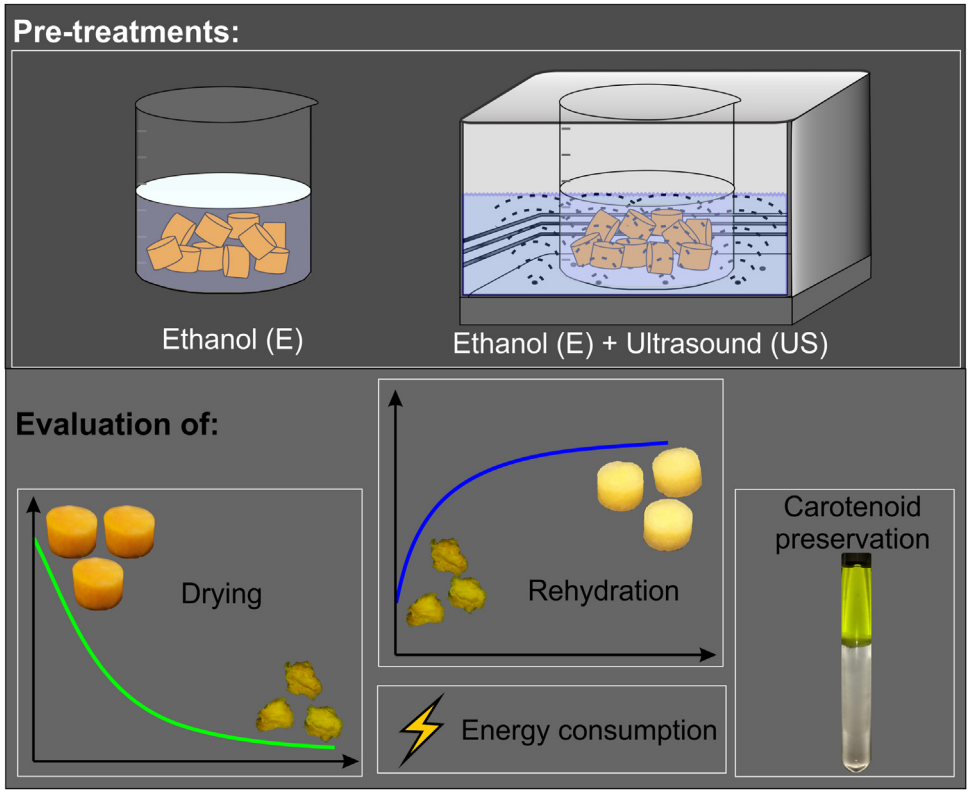

Fig. 2 – Schematic representation of E and E + US pre-treatments performed and the evaluation of drying, energy consumption, rehydration and carotenoid preservation.

2.3. *Convective drying process*

The drying process was performed similarly to the reported by Rojas and Augusto (2018b,c), using air at 50 °C and $0.8 \pm 0.1\ m\ s^{-1}$ velocity (measured parallelly to sample surface, in the direction of the diameter), using an oven with circulation and air renewal (MA 035, Marconi, São Paulo, Brazil). The pumpkin samples (70 cylinders) were placed on a metal net to allow the free movement of warm air over the entire surface of the samples.

During drying, the sample temperature history was registered by a thin thermocouple (type T, AWG-30, Omega, USA),

placed on the cylinder central point and connected to a data logger (Almemo 2890-9, Ahlborn, Germany). For each process, the samples with thermocouples were distributed in all the area (0.086 m^2) used for drying in order to be representative.

The samples were dried in two conditions: (1) until "constant" weight, for evaluating the drying kinetics; and (2) up to a moisture of 25%, in samples that were rehydrated. This moisture value was selected as the maximum reference for low-moisture products (which present a_w up to 0.6), according to Jay et al. (2005). The sample weight was automatically recorded each 30 min for Control samples and each 10 min for treated samples by using a precision scale (Mark 2200, TECNAL, Piracicaba, Brazil) coupled to the oven. The initial (*in-natura* samples and after ethanol treatments) and final (after drying) moisture contents were measured at 105 °C by drying crushed samples (until moisture variation was <0.01%/min) using a moisture analyser (MX-50, A&D Company, Tokyo, Japan). Three replicates of the drying process and moisture analyses were performed.

It is important to mention that during ethanol pre-treatments the samples lose water and solids and gain ethanol. Therefore, according to Rojas and Augusto (2018b), the sample "moisture" after ethanol pre-treatment include the two volatile liquids, there is, it includes the remaining water and the gained ethanol. Consequently, the mass loss in samples being dried also includes both volatile liquids. Therefore, the moisture content over drying processing time (M_t) is calculated by considering a lumped parameter (L_t) that include the mass of both liquids at certain drying time (t).

$$M_t\% = \frac{w_t + OH_t}{m_t}.100 = \frac{L_t}{m_t}.100 \quad (1)$$

where w_t is the mass of water, OH_t is the mass of ethanol and m_t is the sample mass at certain drying time (t).

Drying curves were plotted as a function of the dimensionless moisture ratio (MR) (Eq. (2)) over the drying processing time.

$$MR(t) = \frac{M - M_e}{M_0 - M_e} \quad (2)$$

where M is the moisture content in dry basis (%d.b) (i.e. g water/100 g dry matter) at a given time (t) during drying process, M_e is the equilibrium moisture (considered as the last moisture obtained from samples which mass variation was <0.04 g in the last seven registered points) and M_0 is the initial moisture (%d.b) before drying. For the Control samples, M_0 is equal to the initial moisture of *in-natura* sample, and in the case of ethanol treated samples, M_0 was considered as the sample moisture after pre-treatments. Therefore, the Control and ethanol treated samples started the drying process with MR values equals to one.

2.4. Estimative of the total energy consumption

An estimative of the total energy consumption (TEC) during processing (including pre-treatment and drying) was calculated according considering 1 kg of fresh product by using Eq. (3). E_{US} represents the energy consumption during US pre-treatment (Eq. (4)), and E_D represents the energy consumption during convective drying process (Eq. (5)), calculated based on Motevali et al. (2011) and Onwude et al. (2019).

$$TEC = \frac{E_{US} + E_D}{m_p} \quad (3)$$

$$E_{US} = \frac{W.V.t_P}{m_p} \quad (4)$$

where m_p is the mass of fresh product to be dried, W is the US volumetric power (W/L) determined by the calorimetric method, V is the volume of water (L) used in the US bath, t_P is the time of US pre-treatment (s).

$$E_D = \frac{A.v.\rho_a.Cp_a.\Delta T.t_D}{m_p} \quad (5)$$

where A is the cross-sectional area of drying (m^2), v is the air velocity (m/s), ρ is the ambient air density, Cp is the specific heat capacity of ambient air (J/kg K) at a temperature of 25 °C, ΔT is the temperature difference between the ambient air and drying air, and t_D is the drying time needed to the samples reach a moisture 25% w.b. It is important to mention this approach is a first estimative of energy consumption by considering the performed pre-treatments, which is useful for comparison purposes, but does not consider the strict energy consumption during processing (in special because the actual value is a function of process particularities, such as equipment and process optimization).

2.5. Rehydration process

Rehydration was evaluated similarly to performed by Rojas and Augusto (2018b). For this, ~2 g of dried pumpkin cylinders (10 cylinders) were immersed in 120 mL of distilled water maintained at 25 °C. The cylinders were removed from the water periodically, superficially dried with absorbent paper, weighed and returned to the water. The cylinders were weighed each 5 min during the first 15 min of rehydration, each 10 min until 40 min of rehydration, each 20 min until 100 min of rehydration and finally each 30 min. The sample moisture over rehydration time was determined by mass balance by considering the moisture of dried samples and the mass registered at each period of rehydration. Three replicates of the rehydration process were performed.

2.6. Mathematical description: drying and rehydration kinetics

The drying data were fitted using the Page Model (Eq. (6)) (Page, 1949), where MR(t) is the dimensionless moisture at drying time (t), k is the drying rate constant and n the dimensionless drying constant. The Page Model has been successfully applied to describe the drying kinetics of different food products. Moreover, this model was recently studied by Simpson et al. (2017) using the anomalous diffusion concept and the fractional calculus approach, obtaining a phenomenological interpretation. In this interpretation, the drying rate constant (k) is associated with the "diffusion" coefficient and the geometry of the sample, while the dimensionless drying constant (n) is related to the "type of diffusion" and food microstructure (>1 super-diffusion and $n < 1$ subdiffusion). Our interpretation

(Rojas and Augusto, 2018a,c) is that when $n \neq 1$, other mechanisms than diffusion are important.

$$MR(t) = e^{-k.t^n} \quad (6)$$

The rehydration data was fitted using the Peleg model (Eq. (7)) (Peleg, 1988), where $M(t)$ is moisture content on a dry basis (g water/100 g dry matter (%d.b)) at time t (min), M_0 is the initial moisture content (%d.b), k_1 is the rate constant (min d.b^{-1}) and k_2 is the constant of the asymptotic level (d.b^{-1}). The reciprocal of k_1 represents the water absorption rate and the reciprocal of k_2 represents the water retention capacity.

$$M(t) = M_o + \frac{t}{k_1 + k_2.t} \quad (7)$$

The obtained data were fitted by nonlinear regression to the Page and Peleg Models as described below.

2.6.1. Regressions

The parameters of each model (Eqs. (6) and (7)) were iteratively adjusted to the experimental data by minimizing the sum of squared errors (*SSE* in Eq. (8)) between the experimental and the predicted values for the x experiments. The Generalized Reduced Gradient algorithm (GRG Nonlinear Solving method), implemented in the 'Solver' tool of software Excel 2016 (Microsoft, USA) was used. The parameters of each model were considered valid when Solver reported that the GRG method found a locally optimal solution (to a set convergence of 0.000001). That is, there was no other set of values for the parameters close to the current values that yield a better value for the objective function (*E* minimization). The regressions were conducted for each replicate.

$$SSE = \sum_{i=1}^{x} ((predicted) - (experiemental))_i^2 \quad (8)$$

2.7. Carotenoid determination

The degradation of nutrients is one of the main concerns of conventional drying. In this work, the carotenoid preservation or degradation was evaluated by using the proposed pre-treatments and the convective drying process. For this, the carotenoid content was determined in the *in-natura* samples and after the drying and rehydration process.

Important points before the carotenoid determination

- To prevent effects of overdrying and compare only pre-treatment effects, all samples were dried to controlled moisture of ~25% w.b.
- After drying the samples were rehydrated for 250 min at 25 °C to facilitate the carotenoid extraction.

2.7.1. Carotenoid determination

The total carotenoid content was determined according to the spectrophotometric method described by Ordoñez-Santos and Ledezma-Realpe (2013) and Potosí-Calvache et al. (2017) with some modifications. The solvent used for carotenoid extraction was a solution composed by ethanol (99.5%, Êxodo Científica, São Paulo) and hexane (98.5%, Labsynth, São Paulo) in a proportion of 4:3 ethanol:hexane.

Approximately 0.25 g of the samples were placed in a glass tube (tightly capped and lined with aluminium foil for protecting it from oxygen and light). Then, 21 mL of the solvent solution was added. The samples with the solvent solution were crushed for 1 min using a rotor-stator homogenizer (Superohm, São Paulo) and the tube was removed from the homogenizer. Then, another glass tube containing 21 mL of solvent solution was poured in the homogenizer to wash its probe, and the solution was stored.

The tubes containing the sample and the solvent were stirred at 250 rpm for 30 min using an orbital shaker cold bath (2 °C, DUBNOFF MA 095/CFRE, Marconi, Brazil). After this, the solvent was separated from the sample and poured in another vessel protected from light and oxygen. The solution used for washing the homogenizer probe was then mixed with the remained sample, and this tube was stirred for 30 min at the same conditions. Similarly, the solvent was separated from the remained sample and added to the vessel containing the solvent from the first extraction. 5 mL of distilled water was added to this vessel, which was stirred for 5 min and left at rest for 5 min to separate the phases (aqueous phase and hexanoic phase).

The hexanoic phase, which contained the extracted carotenoid (Fig. 2), was collected using a micropipette and its volume was registered. Then, 2.5 mL of this phase were transferred into a quartz cuvette of 1 cm light path. Then, the absorbance was read at 450 nm (FEMTO 600 S, São Paulo) using hexane to calibrate. The carotenoid content of the extracts was calculated according to Eq. (9) and expressed as $\beta-$carotene equivalents (mg)/100 g of dry matter.

$$TC\left(\frac{mg}{100g\,d.m}\right) = \frac{A_{450}\,x\,536.85\,x\,V x 10^{-1}}{m_{dm}\,x\,137.4} \quad (9)$$

where 536.85 g/mol is the molecular weight of $\beta-$carotene, V is the volume (mL) of hexanoic phase measured after separation from the aqueous phase, 10^{-1} is the conversion unit factor, m_{dm} is the dry matter of sample (g), and 137.4 mM^{-1} is the extinction coefficient for $\beta-$carotene in hexane.

2.8. Experimental design and statistical analysis

A completely randomised design (CRD) was conducted. All processes of each treatment and analyses were performed at least 3 times. The analysis of variance (ANOVA) and Tukey test were conducted when relevant to determine which treatments differ from each other (significance level of 5%). Statistical analyses were determined using the IBM SPSS Statistics 23 software (IBM SPSS, USA).

3. Results and discussion

3.1. Drying kinetics

The fresh pumpkin presented high water content (moisture >88% w.b) requiring a long drying time. For example, to reach a moisture level lower than 25%, the Control samples required more than 10 h of drying (Fig. 3), similarly to reported by Doymaz (2007) for pumpkin samples convectively dried at 50 °C and 1 m s^{-1}.

Compared to the Control, all the pre-treatments reduced the convective drying time in 49% for E-15 min, 52% for E-30 min, 48% for E + US-15 min and 59% for E + US-30 min treatments (Fig. 3B). If the time of pre-treatments (15 and 30 min) are included in the calculi of total processing, a reduction of 47% was obtained for E-15 and E-30, 45% for E + US-15 min and 54% for E + US-30 min pre-treated samples.

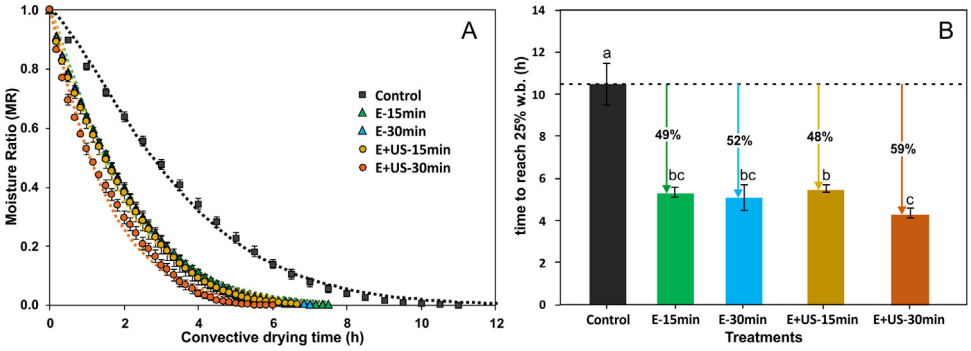

Fig. 3 – (A) Convective drying kinetics for the five treatments (Control, ethanol pre-treated samples with and without ultrasound application for 15 and 30 min). Dots are experimental data; dotted lines are the predicted data using Page Model (Eq. (6)). (B) Drying time reduction for the five treatments. Vertical bars are the standard deviation obtained from the three replicates. Different letters indicate significant differences among treatments ($p < 0.05$).

These time reductions during convective drying are similar or higher superior than the results obtained in previous studies. The use of ethanol (92.8% v/v) pre-treatment (for 1 h) reduced in 50% the convective drying time of pumpkin (Rojas and Augusto, 2018b), while US as pre-treatment reduced in 11–58% the drying time in apple convective drying or US assisted convective drying (Magalhães et al., 2017). In fact, the obtained time reduction with E + US pre-treatment is comparable to when the US was employed assisting the drying processes. For example, 28% of time reduction was reported for osmotic pre-treated pineapple samples after convective drying assisted with US (40 °C, 1.0 ± 0.1 m s^{-1}) (Corrêa et al., 2017), 67% for eggplant after US assisted atmospheric freeze drying 10.3 kW m^{-3}, −10 °C, 2 m s^{-1}) (Colucci et al., 2018), 41–53% for carrot slices dried with ultrasonic vacuum drying (USV) (Chen et al., 2016), and 54% in raspberries dried using convective US assisted drying (55 °C, 0.4 m s^{-1}, US-100 W) (Szadzińska et al., 2018). Moreover, even considering only the use of ethanol application, at short pre-treatment time (15 min), the drying process was drastically accelerated. Compared to treatments only with ethanol for 15 min, the use of US had no significant effects in the percentage of drying time reduction. However, when ultrasound was applied for 30 min, a considerable drying time reduction was obtained, which will be discussed in the following paragraphs.

Experimental drying data were mathematically described using the Page model, whose parameters (k and n) are presented in Table 2. The n value was always >1 indicating a super-diffusive behaviour. This behaviour was also reported by Rojas and Augusto (2018c) during pumpkin drying.

The n value decreased with all pre-treatments ($p < 0.05$). Considering that US application generates microchannels in sample structure, it could be expected an increase in n value (i.e. a super-diffusive behaviour due to capillarity) in samples processed with US. However, this was not observed. The increase in n can be explained by the diverse phenomena (structural and compositional) occurring simultaneously during pre-treatments, which directly influences the drying behaviour.

According to Simpson et al. (2017) the n parameter from Page equation could be correlated with the α (fractional-time order) parameter of the anomalous diffusion model. The α decrease is attributed to modifications produced in the sample structure, which becomes close to one as the structure is more homogeneous. For example, when electric fields (a technology that modify the structure) were applied to apple slices, it was reported that the α value decreases and becomes closer to one as the electric field becomes higher (Simpson et al., 2015).

Furthermore, as demonstrated by Miano et al. (2016), different kind of cavities and micro channels are formed during ultrasound processing of foods, such as tortuous, isolated cavities, with lack of connectivity, and with external medium connectivity. The different kind of cavities and micro channels formed have varied tortuosity, permeability and diffusion, improving or not the mass transfer in different ways (Warning et al., 2014). For instance, although thin channels promote liquid flow through capillarity, larger channels may not be able to. Furthermore, isolated cavities can reduce the rate of liquid outflow from the sample by damming it (thus representing a possible sub-diffusion system).

Therefore, it is difficult so far to directly relate the n increase or decrease only with changes in the structure. Probably, the decrease observed in n value can also be correlated with the high cell wall structure but also with composition modifications in the sample surface produced by ethanol and potentiated by the increase in US processing time.

Rojas and Augusto (2018b) explained the mechanism of drying improvement when ethanol (95%, 1 h) was used as pre-treatment, which include structural modifications (intercellular air expulsion, cell wall thinning with some compound extraction) and ethanol entrance, which promotes the water transfer phenomena by Marangoni Effect during drying. Different from that previous study, in the present work ethanol of higher concentration (99.5% v/v) was used. Therefore, a shorter time is necessary to its entrance in the sample and to reach the "maximum" structural modifications. It can also explain why there was no significant differences ($p > 0.05$) for k (min^{-1}) values among 15 min or 30 min for E or E + US pre-treatments.

On the other hand, the k increased significatively ($p < 0.05$) when both pre-treatments were applied (E + US). Compared to Control samples, the k parameter increased more than 10 times for E + US-30 min pre-treated samples, reflecting its highest drying rate (Table 2). In fact, the ethanol properties, in special their lower surface tension, promotes the formation of cavitation bubbles during US application (Crum, 1984; Hemwimol et al., 2006; Sujka, 2017), increasing the effects in the sample structure. For example, the potato tissue was greatly affected when ethanol was used as a medium to transmit the ultrasonic waves instead of water (Rojas and Augusto, 2018a). However, in the present work, the US applied for 15 min (E + US-15 min) did not differ from the samples only treated

Table 2 – Drying and rehydration kinetic parameters for the control, ethanol pre-treated samples with and without ultrasound application for 15 and 30 min*.

Pre-treatments	Drying kinetics		Rehydration kinetics	
	Page model (Eq. (6))		Peleg model (Eq. (7))	
	k (min^{-1})	n	k_1 (min $d.b^{-1}$)	k_2 ($d.b^{-1}$)
Control	0.0007 ± 0.0001^{b}	1.3500 ± 0.0160^{a}	6.219 ± 0.156^{a}	0.120 ± 0.002^{a}
E-15 min	0.0037 ± 0.0000^{b}	1.1610 ± 0.0039^{b}	–	–
E-30 min	0.0036 ± 0.0001^{b}	1.1722 ± 0.0029^{b}	4.332 ± 0.226^{b}	0.093 ± 0.003^{b}
E + US-15 min	0.0043 ± 0.0005^{ab}	1.1445 ± 0.0155^{b}	–	–
E + US-30 min	0.0076 ± 0.0024^{a}	1.0840 ± 0.0569^{b}	3.769 ± 0.446^{b}	0.094 ± 0.006^{b}

* Mean ± standard deviation, differences between letters indicate significative differences ($p < 0.05$) among pre-treatments.

with ethanol for the same time (E-15 min) (Table 2). This means that the effect of US pre-treatment applied for 15 min is negligible compared to the effect of the ethanol applied individually.

In fact, it was previously evidenced that US pre-treatment applied for a short time did not significantly reduce the convective drying time, as reported by Miano et al. (2018) and Ricce et al. (2016). US pre-treatment generally result in less than 25% of convective drying time reduction (Fijalkowska et al., 2016; Magalhães et al., 2017), including when it is used as pre-treatment for other methods such as Microwave Freeze Drying (Duan et al., 2008) and infrared drying (Rojas and Augusto, 2018a). In fact, as affirmed by Corrêa et al. (2017), the drying time reduction obtained in some cases is not enough to compensate the time used during pre-treatment. However, in the present work, the (E + US) application for 30 min had a significant effect on pumpkin drying, whose combination was better than the individual application of ethanol at the same conditions. Therefore, in terms of drying time reduction, the use of E + US for 30 min would be convenient since the additional time reduction obtained compared the other pre-treatments was more than 1 h, and it was 48 min when disregarding the 30 min used during pre-treatment.

3.2. *Estimative of the total energy consumption*

Table 3 shows an estimative of the total energy consumption (TEC), which includes the energy necessary during US pre-treatment and during convective drying process. The energy consumed to dry the samples was greatly reduced using pre-treatments. The highest TEC reduction (44%) was obtained when E + US-30 min pre-treatment was applied. These results are related to what was observed in Fig. 3, where this pre-treatment allows reducing the drying time in a high percentage. An interesting point to notice is that the energy consumed during US pre-treatments represent less than 2% of the energy consumed during drying. Even considering all the limitations and simplifications of this approach of calculi, it contributes to demonstrating that the energy consumption with the US pre-treatments application could be compensated later, during drying, in a greater proportion. This is true only if these pre-treatments are going to have a significant effect in reducing the drying time.

It is important to highlight that these results are an estimative of the energy necessary to perform the process. Certainly, the electric energy consumed will be higher, considering the equipment efficiencies, which were not considered. Even so, the magnitude of energy calculated serves to demonstrate how the application of these technologies contribute to reducing the energy consumption of the process, with possible positive impact both in cost and in the environment.

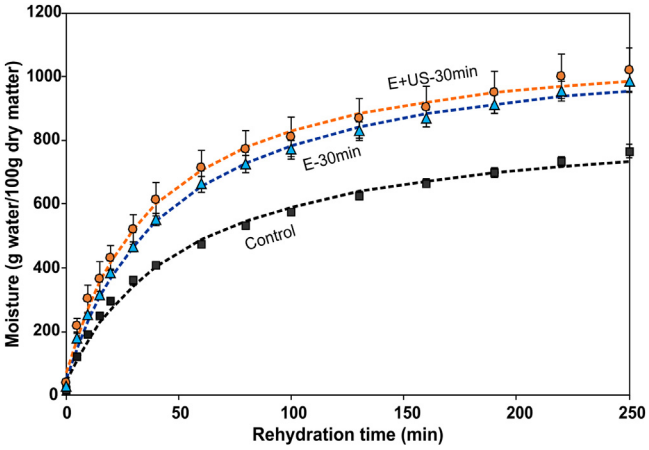

Fig. 4 – Rehydration kinetics for the Control, Ethanol pre-treated samples with and without US application for 30 min. Dots are experimental data, the vertical bars are the standard deviation and dotted lines are the predicted data using Peleg Model (Eq. (7)).

It is known that an efficient drying process is not enough, being also necessary to guarantee adequate product properties. Therefore, the pumpkin rehydration and carotenoid content were also evaluated, being described in the next sections.

3.3. *Rehydration kinetics*

Some pre-treatments (Control, E-30 min and E + US-30 min) were selected to describe the rehydration properties and the carotenoid content. These pre-treatments were selected based on drying results.

The Peleg model was used to describe rehydration behaviour (Fig. 4). The pre-treatments reflected in lower values of k_1 (reflecting high water abortion rate) and k_2 (reflecting high water retention capacity) in comparison with the control (Table 2). The ethanol pre-treatment improved the rehydration properties of pumpkin compared to Control samples. When E + US was applied, the rehydration was also improved, but without significant differences compared to E pre-treated samples.

The rehydration properties of a dried product are directly related to their pre-treatment, the employed drying conditions, and its effect on the product structure and composition. Regarding the US application, different works reported an improvement of rehydration properties of dried products

Table 3 – Estimative of energy consumption during pre-treatments and drying process[a].

Treatments	Energy consumption by US pre-treatment (Eq. (4)) (kWh/kg)	Energy consumption during drying (Eq. (5)) (kWh/kg)	Total energy consumption (TEC) (kWh/kg)	TEC reduction in relation to control
Control	–	150.9	150.9	–
E-15 min	–	90.1	90.1	40.2%
E-30 min	–	90.3	90.3	40.1%
E + US-15 min	0.7	103.0	103.8	31.2%
E + US-30 min	1.5	82.5	84.1	44.3%

[a] Results were calculated using mean values for each parameter of Eqs. (4) and (5).

(Rodríguez et al., 2018). The rehydration capacity and the level of rehydration improvement is dependent on the degree of cellular and structural disruption caused by US (Fijalkowska et al., 2016; Szadzińska et al., 2018). For example, in apple, the amount of absorbed water increased (Fijalkowska et al., 2016), and in carrot slices a great capacity to absorb water was reported due to higher porosity and micro-channels formation (Chen et al., 2016; Ricce et al., 2016; Wang et al., 2018). On the other hand, in some cases, although US cause a faster water absorption, the retention of the absorbed water could be affected due to high structure damages (Santacatalina et al., 2016).

It is important to mention that the type of fluid used as a medium to US pre-treatment influences the level of structural modification. As explained in the above section, when ethanol is used as a medium, the impact on the structure is higher when compared to water (Rojas and Augusto, 2018a). In addition, the type of raw material (natural structure and composition) highly influences how US pre-treatment affects rehydration. For example, Rojas and Augusto (2018a) reported a great structure modification in potatoes pre-treated with E + US. Consequently, the intercellular starch granules were exposed, which formed a crust during infrared drying (100 °C) in the sample surface, negatively influencing the rehydration properties.

In contrast, in the present study, the E + US pre-treatment presented positive effect during drying, and for both rehydration rate (lower k_1 value) and water retention (lower k_2 value), when compared to the Control samples. This reflects that the pre-treatment effects on rehydration properties are specific for each food material and depend on the drying method and conditions. The E + US pre-treatment seems to be effective and could be an alternative to improve convective drying and rehydration properties of pumpkin. However, it is recommended more studies about the E + US application using other food materials and under different drying conditions.

3.4. *Carotenoid content*

Raw pumpkin (*in-natura*) presented a carotenoid content of 88.08 ± 6.77 μg/g or 117.49 ± 9.113 mg/100 g dry matter, reflecting its intense orange colour. This value is in the range reported for different cultivars of this pumpkin species (*C. moschata*), which is up to 380 mg/100 g dry matter (de Carvalho et al., 2012; Nawirska-Olszańska et al., 2017) and is higher than in other vegetables rich in carotenoids, such as carrot (Rawson et al., 2011; Rodriguez-Amaya et al., 2008).

Fig. 5 shows the total carotenoid content of the *in-natura* pumpkin, as well as after drying and rehydration with different pre-treatments. It is important to mention that the extractive effect of carotenoids by the pre-treatments was negligible, due to the small contact area of the samples, contrary to when ethanol and/or ultrasound are used for solid–liquid extraction purposes. Furthermore, since the content of carotenoids in the fresh sample was very large, small variations in the content because of pre-treatments were not significant.

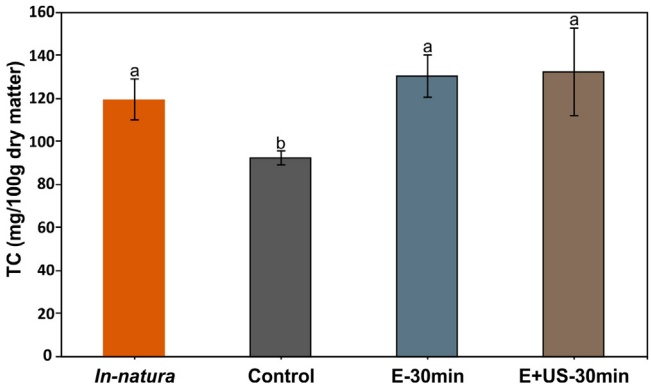

Fig. 5 – Total carotenoid content of the *in-natura*, and rehydrated samples (Control, E-30 min and E + US-30 min). Different letters indicate significant differences among treatments ($p < 0.05$).

After drying, a carotenoid reduction of about 23% was observed in the Control samples. In fact, carotenoids are sensitive compounds to factors such as heat, oxygen, light, and enzymes (Rawson et al., 2011). Consequently, a carotenoid content reduction is expected after hot-air drying. Carotenoid content reduction of 27% was also observed in carrot slices convectively dried (60 °C, 0.3 m s^{-1}) (Rawson et al., 2011).

In pumpkin, different drying methods were performed to improve carotenoid retention. Compared to convective and microwave drying methods (Nawirska-Olszańska et al., 2017; Song et al., 2017), the carotenoid content of pumpkin species after drying was better preserved using freeze-drying (Nawirska et al., 2009). However, the freeze-drying method is well known for its high costs and long processing time.

Fig. 5 shows no significant differences among the carotenoid content of the *in-natura* pumpkin and the samples dried after pre-treatments with E and US. It is interesting to notice that a recent work used ethanol and vacuum pre-treatments to infrared drying of scallion, reporting degradation of ascorbic acid even considering all the treatments (Wang et al., 2019). Therefore, it is worth mention the relevance of the present study, which demonstrated that the carotenoid content in processed pumpkin remained like to the content of the *in-natura* samples.

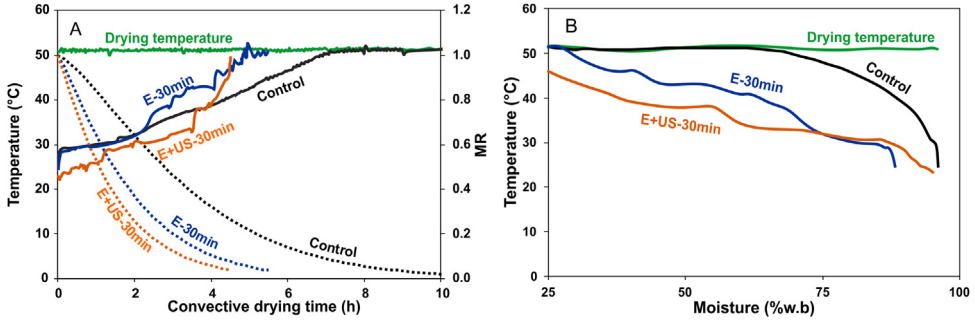

Fig. 6 – Temperature record measured inside (geometric center) of the Control and Pre-treated samples during the drying process. (A) Temperature and predicted moisture ratio (MR → until 25% w.b), as a function of the drying time. (B) Temperature as a function of the moisture content (% w.b → until 25% w.b).

Actually, when US is applied as pre-treatment to drying or assisting it, a better carotenoid retention was reported for carrot (Nowacka and Wedzik, 2016; Rawson et al., 2011; Wang et al., 2018), papaya (Azoubel et al., 2015), and tomato (Fernandes et al., 2016). The carotenoid retention by using US can be correlated with two effects. On one hand, the reduction of drying time means a reduction of the sample exposition to deteriorating factors, such as temperature and oxygen. In this case, if the carotenoid quantity after drying is similar to the *in-natura* sample, it means the carotenoid initially present is better preserved. On the other hand, an effect related to the structural modifications, such as on cell wall and chromoplasts, is expected (Campoli et al., 2018; Rojas et al., 2016). It can improve the carotenoid release, increasing their quantification. However, in this case, the extractability is improved, but it does not necessarily mean the carotenoids are better preserved after drying.

In this work, carotenoids were preserved, since no-significant differences in carotenoid content were observed among the samples processed with only E and those processed with US (Fig. 5). In addition, as described, the E and E + US application for 30 min improved the drying rate (Fig. 3) where both treatments have a considerable reduction in drying time. Furthermore, the carotenoid extraction was carried out until the samples remained completely colourless for all cases. Therefore, probably the most important reason for the obtained carotenoid content is the reduction of sample exposition to drying conditions, which allow ~100% of carotenoid preservation in pumpkin by using the proposed E + US pre-treatments.

The effect of reducing the drying time and the sample exposition to high temperature during drying is evidenced in Fig. 6. As observed in Fig. 6A, the Control samples needed longer drying time to reach a moisture lower than 25% w.b. Additionally, this samples reached the set drying temperature (50 °C) when they still had a moisture of 67% w.b (Fig. 6B), then remaining for ~3 h at that temperature to reach 25% w.b (Fig. 6A). On the other hand, the E pre-treated samples remained for 0.5 h at the set drying temperature while the E + US reach a maximum temperature of ~47 °C for less than 10 min.

During drying, both heat exchange (between the hot-air and sample) and phase change (liquid to vapor) occur. Part of the liquid inside pre-treated samples is composed by ethanol and water, whose vaporization occurs at lower temperature than the water in the Control samples. This explain the differences observed in temperature profiles of pre-treated samples compared to Control (Fig. 6).

Therefore, it was demonstrated that compared to Control, the carotenoid content was better preserved due to the short drying time and the lower high-temperature exposition during drying after pre-treatments.

4. Conclusion

Ethanol and high-power ultrasound were applied as pre-treatments to improve the convective drying. Compared to Control, the application of ethanol decreased the drying time. The highest drying time reduction (59%) was obtained when ethanol was combined with ultrasound for 30 min (E + US-30 min). The same pre-treatment allowed a lower energy consumption for the whole process. Regarding rehydration properties, pre-treated samples showed an increase in water absorption rate and water retention capacity. Additionally, the carotenoid content was preserved in pre-treated samples, despite a partial degradation (23%) in the dried pumpkins without pre-treatments. This was attributed to the drying time reduction and the consequent lower sample exposition to deteriorating conditions. These results show an important contribution because it was demonstrated that with the use of ethanol and ultrasound, it is possible to improve the convective drying process (processing time and energy consumption reduction) and improve some product quality properties (good rehydration properties and nutrient preservation). Under the studied conditions, it is recommended the used of ethanol combined with US for 30 min to obtain higher dehydration and rehydration rates, lower energy consumption and higher carotenoid preservation.

Declarations of interest

None.

Acknowledgments

The authors are grateful to the São Paulo Research Foundation (FAPESP, Brazil) for funding the project nº 2016/18052-5; to the National Council for Scientific and Technological Development (CNPq, Brazil) for funding the project nº 401004/2014-7 and the productivity grant of P.E.D. Augusto (306557/2017-7); and to FONDECYT-CONCYTEC for the M.L. Rojas Ph.D. scholarship (grant contract number 087-2016-FONDECYT).

References

Aguilar, K., Garvín, A., Ibarz, A., Augusto, P.E.D., 2017. Ascorbic acid stability in fruit juices during thermosonication. Ultrason. Sonochem. 37, 375–381.

Azoubel, P.M., da Rocha Amorim, M., Oliveira, S.S.B., Maciel, M.I.S., Rodrigues, J.D., 2015. Improvement of water transport and carotenoid retention during drying of papaya by applying ultrasonic osmotic pretreatment. Food Eng. Rev. 7, 185–192.

Braga, A.M.P., Pedroso, M.P., Augusto, F., Silva, M.A., 2009. Volatiles identification in pineapple submitted to drying in an ethanolic atmosphere. Dry. Technol. 27, 248–257.

Braga, A.M.P., Silva, M.A., Pedroso, M.P., Augusto, F., Barata, L.E.S., 2010. Volatile composition changes of pineapple during drying in modified and controlled atmosphere. Int. J. Food Eng. 6.

Campoli, S.S., Rojas, M.L., do Amaral, J.E.P.G., Canniatti-Brazaca, S.G., Augusto, P.E.D., 2018. Ultrasound processing of guava juice: effect on structure, physical properties and lycopene in vitro accessibility. Food Chem. 268, 594–601.

Colucci, D., Fissore, D., Rossello, C., Carcel, J.A., 2018. On the effect of ultrasound-assisted atmospheric freeze-drying on the antioxidant properties of eggplant. Food Res. Int. 106, 580–588.

Corrêa, J., Rasia, M., Mulet, A., Cárcel, J., 2017. Influence of ultrasound application on both the osmotic pretreatment and subsequent convective drying of pineapple (*Ananas comosus*). Innov. Food Sci. Emerg. Technol. 41, 284–291.

Corrêa, J.L.G., Braga, A.M.P., Hochheim, M., Silva, M.A., 2012. The influence of ethanol on the convective drying of unripe, ripe, and overripe bananas. Dry. Technol. 30, 817–826.

Crum, L., 1984. Acoustic cavitation series: part five rectified diffusion. Ultrasonics 22, 215–223.

Chen, Z.-G., Guo, X.-Y., Wu, T., 2016. A novel dehydration technique for carrot slices implementing ultrasound and vacuum drying methods. Ultrason. Sonochem. 30, 28–34.

Chou, S.K., Chua, K.J., 2001. New hybrid drying technologies for heat sensitive foodstuffs. Trends Food Sci. Technol. 12, 359–369.

de Carvalho, L.M.J., Gomes, P.B., Godoy, R.Ld.O., Pacheco, S., do Monte, P.H.F., de Carvalho, J.L.V., Nutti, M.R., Neves, A.C.L., Vieira, A.C.R.A., Ramos, S.R.R., 2012. Total carotenoid content, α-carotene and β-carotene, of landrace pumpkins (*Cucurbita moschata* Duch): a preliminary study. Food Res. Int. 47, 337–340.

De la Fuente-Blanco, S., Riera-Franco de Sarabia, E., Acosta-Aparicio, V.M., Blanco-Blanco, A., Gallego-Juárez, J.A., 2006. Food drying process by power ultrasound. Ultrasonics 44 (Supplement), e523–e527.

de Oliveira, M.M., Tribst, A.A.L., Júnior, B.R.D.C.L., de Oliveira, R.A., Cristianini, M., 2015. Effects of high pressure processing on cocoyam, Peruvian carrot, and sweet potato: Changes in microstructure, physical characteristics, starch, and drying rate. Innov. Food Sci. Emerg. Technol. 31, 45–53.

Doymaz, I., 2007. The kinetics of forced convective air-drying of pumpkin slices. J. Food Eng. 79, 243–248.

Duan, X., Zhang, M., Li, X., Mujumdar, A.S., 2008. Ultrasonically enhanced osmotic pretreatment of sea cucumber prior to microwave freeze drying. Dry. Technol. 26, 420–426.

E.I.A, 2018. Energy Information Administration: Today in Energy. Linda Doman, Washington DC.

Fernandes, F.A.N., Gallão, M.I., Rodrigues, S., 2008. Effect of osmotic dehydration and ultrasound pre-treatment on cell structure: melon dehydration. LWT Food Sci. Technol. 41, 604–610.

Fernandes, F.A.N., Rodrigues, S., García-Pérez, J.V., Cárcel, J.A., 2016. Effects of ultrasound-assisted air-drying on vitamins and carotenoids of cherry tomatoes. Dry. Technol. 34, 986–996.

Fijalkowska, A., Nowacka, M., Wiktor, A., Sledz, M., Witrowa-Rajchert, D., 2016. Ultrasound as a pretreatment method to improve drying kinetics and sensory properties of dried apple. J. Food Process Eng. 39, 256–265.

Hemwimol, S., Pavasant, P., Shotipruk, A., 2006. Ultrasound-assisted extraction of anthraquinones from roots of *Morinda citrifolia*. Ultrason. Sonochem. 13, 543–548.

Jambrak, A.R., Mason, T.J., Paniwnyk, L., Lelas, V., 2007. Ultrasonic effect on pH, electric conductivity, and tissue surface of button mushrooms, brussels sprouts and cauliflower. Czech J. Food Sci. 25, 90–100.

Jay, J.M., Loessner, M.J., Golden, D.A., 2005. Protection of Foods by Drying, Modern Food Microbiology. Springer, US, Boston, MA, pp. 443–456.

Kudra, T., Mujumdar, A.S., 2009. Advanced Drying Technologies. CRC Press.

Lebovka, N.I., Shynkaryk, N.V., Vorobiev, E., 2007. Pulsed electric field enhanced drying of potato tissue. J. Food Eng. 78, 606–613.

Magalhães, M.L., Cartaxo, S.J.M., Gallão, M.I., García-Pérez, J.V., Cárcel, J.A., Rodrigues, S., Fernandes, F.A.N., 2017. Drying intensification combining ultrasound pre-treatment and ultrasound-assisted air drying. J. Food Eng. 215, 72–77.

Mason, T.J., Peters, D., 2004. Practical Sonochemistry: Power Ultrasound Uses and Applications. Horwood Publishing Limited.

Miano, A.C., Ibarz, A., Augusto, P.E.D., 2016. Mechanisms for improving mass transfer in food with ultrasound technology: describing the phenomena in two model cases. Ultrason. Sonochem. 29, 413–419.

Miano, A.C., Rojas, M.L., Augusto, P.E.D., 2017. Chapter 15 – other mass transfer unit operations enhanced by ultrasound. In: Bermudez-Aguirre, D. (Ed.), Ultrasound: Advances for Food Processing and Preservation. Academic Press, pp. 369–389.

Miano, A.C., Rojas, M.L., Augusto, P.E.D., 2018. Structural changes caused by ultrasound pretreatment: direct and indirect demonstration in potato cylinders. Ultrason. Sonochem. 52, 176–183.

Monteiro, R.L., Carciofi, B.A.M., Laurindo, J.B., 2016. A microwave multi-flash drying process for producing crispy bananas. J. Food Eng. 178, 1–11.

Moses, J.A., Norton, T., Alagusundaram, K., Tiwari, B.K., 2014. Novel drying techniques for the food industry. Food Eng. Rev. 6, 43–55.

Motevali, A., Minaei, S., Khoshtagaza, M.H., 2011. Evaluation of energy consumption in different drying methods. Energy Convers. Manage. 52, 1192–1199.

Mujumdar, A.S., Devahastin, S., 2000. Fundamental Principles of Drying. Exergex, Brossard, Canada.

Nawirska-Olszańska, A., Stępień, B., Biesiada, A., 2017. Effectiveness of the fountain-microwave drying method in some selected pumpkin cultivars. LWT 77, 276–281.

Nawirska, A., Figiel, A., Kucharska, A.Z., Sokół-Łętowska, A., Biesiada, A., 2009. Drying kinetics and quality parameters of pumpkin slices dehydrated using different methods. J. Food Eng. 94, 14–20.

Nowacka, M., Wedzik, M., 2016. Effect of ultrasound treatment on microstructure, colour and carotenoid content in fresh and dried carrot tissue. Appl. Acoust. 103, 163–171.

Onwude, D.I., Hashim, N., Abdan, K., Janius, R., Chen, G., 2019. The effectiveness of combined infrared and hot-air drying strategies for sweet potato. J. Food Eng. 241, 75–87.

Ordoñez-Santos, L.E., Ledezma-Realpe, D.P., 2013. Lycopene concentration and physico-chemical properties of tropical fruits. Food Nutr. Sci. 4, 758.

Page, G.E., 1949. Factors Influencing the Maximum Rates of Air Drying Shelled Corn in Thin Layers. Purdue University, Ann Arbor.

Peleg, M., 1988. An empirical model for the description of moisture sorption curves. J. Food Sci. 53, 1216–1217.

Potosí-Calvache, D.C., Vanegas-Mahecha, P., Martínez-Correa, H.A., 2017. Convective drying of squash (*Cucurbita moschata*): influence of temperature and air velocity on effective moisture diffusivity, carotenoid content and total phenols. DYNA 84, 112–119.

Rawson, A., Tiwari, B.K., Tuohy, M.G., O'Donnell, C.P., Brunton, N., 2011. Effect of ultrasound and blanching pretreatments on polyacetylene and carotenoid content of hot air and freeze dried carrot discs. Ultrason. Sonochem. 18, 1172–1179.

Ricce, C., Rojas, M.L., Miano, A.C., Siche, R., Augusto, P.E.D., 2016. Ultrasound pre-treatment enhances the carrot drying and rehydration. Food Res. Int. 89, 701–708.

Rodriguez-Amaya, D.B., Kimura, M., Godoy, H.T., Amaya-Farfan, J., 2008. Updated Brazilian database on food carotenoids: factors affecting carotenoid composition. J. Food Compos. Anal. 21, 445–463.

Rodríguez, Ó., Eim, V., Rosselló, C., Femenia, A., Cárcel, J.A., Simal, S., 2018. Application of power ultrasound on the convective drying of fruits and vegetables: effects on quality. J. Sci. Food Agric. 98, 1660–1673.

Rodríguez, Ó., Eim, V., Rosselló, C., Femenia, A., Cárcel, J.A., Simal, S., 2019. Application of power ultrasound on the convective drying of fruits and vegetables: effects on quality. J. Sci. Food Agric. 99, 966.

Rojas, M.L., Alvim, I.D., Augusto, P.E.D., 2019. Incorporation of microencapsulated hydrophilic and lipophilic nutrients into foods by using ultrasound as a pre-treatment for drying: a prospective study. Ultrason. Sonochem. 54, 153–161.

Rojas, M.L., Augusto, P.E.D., 2018a. Ethanol and ultrasound pre-treatments to improve infrared drying of potato slices. Innov. Food Sci. Emerg. Technol. 49, 65–75.

Rojas, M.L., Augusto, P.E.D., 2018b. Ethanol pre-treatment improves vegetable drying and rehydration: kinetics, mechanisms and impact on viscoelastic properties. J. Food Eng. 233, 17–27.

Rojas, M.L., Augusto, P.E.D., 2018c. Microstructure elements affect the mass transfer in foods: the case of convective drying and rehydration of pumpkin. LWT 93, 102–108.

Rojas, M.L., Leite, T.S., Cristianini, M., Alvim, I.D., Augusto, P.E.D., 2016. Peach juice processed by the ultrasound technology: changes in its microstructure improve its physical properties and stability. Food Res. Int. 82, 22–33.

Santacatalina, J.V., Soriano, J.R., Cárcel, J.A., Garcia-Perez, J.V., 2016. Influence of air velocity and temperature on ultrasonically assisted low temperature drying of eggplant. Food Bioprod. Process. 100, 282–291.

Silva, M.A., Braga, A.M.P., Santos, P.H.S., 2012. Enhancement of fruit drying: the ethanol effect. In: Proceedings of the 18th International drying Symposium (IDS 2012), Xiamen.

Simpson, R., Ramírez, C., Birchmeier, V., Almonacid, A., Moreno, J., Nuñez, H., Jaques, A., 2015. Diffusion mechanisms during the osmotic dehydration of Granny Smith apples subjected to a moderate electric field. J. Food Eng. 166, 204–211.

Simpson, R., Ramírez, C., Nuñez, H., Jaques, A., Almonacid, S., 2017. Understanding the success of Page's model and related empirical equations in fitting experimental data of diffusion phenomena in food matrices. Trends Food Sci. Technol. 62, 194–201.

Song, J., Wang, X., Li, D., Meng, L., Liu, C., 2017. Degradation of carotenoids in pumpkin (*Cucurbita maxima* L.) slices as influenced by microwave vacuum drying. Int. J. Food Prop. 20, 1479–1487.

Sujka, M., 2017. Ultrasonic modification of starch – impact on granules porosity. Ultrason. Sonochem. 37, 424–429.

Szadzińska, J., Łechtańska, J., Pashminehazar, R., Kharaghani, A., Tsotsas, E., 2018. Microwave-and ultrasound-assisted convective drying of raspberries: drying kinetics and microstructural changes. Dry. Technol., 1–12.

Tatemoto, Y., Mizukoshi, R., Ehara, W., Ishikawa, E., 2015. Drying characteristics of food materials injected with organic solvents in a fluidized bed of inert particles under reduced pressure. J. Food Eng. 158, 80–85.

Vinatoru, M., 2015. Ultrasonically assisted extraction (UAE) of natural products some guidelines for good practice and reporting. Ultrason. Sonochem. 25, 94–95.

Wang, L., Xu, B., Wei, B., Zeng, R., 2018. Low frequency ultrasound pretreatment of carrot slices: effect on the moisture migration and quality attributes by intermediate-wave infrared radiation drying. Ultrason. Sonochem. 40, 619–628.

Wang, X., Feng, Y., Zhou, C., Sun, Y., Wu, B., Yagoub, A.E.A., Aboagarib, E.A.A., 2019. Effect of vacuum and ethanol pretreatment on infrared-hot air drying of scallion (*Allium fistulosum*). Food Chem. 295, 432–440.

Warning, A., Verboven, P., Nicolaï, B., van Dalen, G., Datta, A.K., 2014. Computation of mass transport properties of apple and rice from X-ray microtomography images. Innov. Food Sci. Emerg. Technol. 24, 14–27.

APPENDIX VI: Ethanol pre-treatment to ultrasound-assisted convective drying of apple

ROJAS, M.L., AUGUSTO, P.E.D, CÁRCEL, J.A.

Research article to be soon submitted

Ethanol pre-treatment to ultrasound-assisted convective drying of apple

Rojas, M.L.[1,2], Augusto, P.E.D[1,3], Cárcel, J.A.[2]

[1] Department of Agri-food Industry, Food and Nutrition (LAN), Luiz de Queiroz College of Agriculture (ESALQ), University of São Paulo (USP), Piracicaba, SP, Brazil
[2] Grupo de Análisis y Simulación de Procesos Agroalimentarios (ASPA), Departamento de Tecnología de Alimentos, Universitat Politècnica de València, Valencia 46022, Spain
[3] Food and Nutrition Research Center (NAPAN), University of São Paulo (USP), São Paulo, SP, Brazil

Highlights

- Ethanol treatment and US-assisted drying reduced 70% the conventional drying time
- Ethanol pre-treatment mainly reduce the external resistances to mass transfer
- US had the greater influence on reduce the internal resistances to mass transfer
- Shrinkage in dried samples decreased as the ethanol pre-treatment time increased
- Rehydration properties were improved in the ethanol pre-treated samples

Abstract

This work evaluated for the first time the combined application of ethanol as pre-treatment to the ultrasonically assisted convective drying of foods. Apple slices were used as model food. Pre-treatments were performed by immersion in ethanol for 0, 10, 20 and 30 min. After that, pre-treated samples were convectively dried (50 °C, 1 $m \cdot s^{-1}$), without and with ultrasound application (electrical input of 20.5 kW/m^3 and 21.77 kHz). The effects of pre-treatments and ultrasound during drying were evaluated on: drying kinetics, described using three mathematical models; rehydration kinetics; shrinkage; viscoelastic properties through stress-relaxation assays; antioxidant capacity (AC); and total phenolic content (TPC). The conventional drying time was reduced 55 ± 4% when ultrasound was applied, while 53 ± 4% when using the largest ethanol pre-treatment (30 min). If both ethanol pre-treatment and ultrasound-assisted drying were considered, drying time reduction reached 70 ± 2%, showing this option was very effective to accelerate the process. The identified drying kinetics parameters suggested that the ethanol pre-treatments mainly contributed to reducing the external resistance to mass transfer during drying, while ultrasound had a greater influence on reducing the internal ones. This result highlights the complementary effects of both technologies here proposed. The shrinkage in dried samples decreased as the ethanol pre-treatment time increased. Rehydration capacity was also greater in the pre-treated samples. After

rehydration, samples showed a decrease in both elastic and viscous characteristics compared to raw samples. The AC and TPC decreased after ethanol pre-treatments and after drying. In contrast, AC and TPC were better retained in samples dried with ultrasound application. The obtained results corroborate that ethanol pre-treatments and ultrasound highly accelerate the convective drying without significant negative effects on some physical properties.
Keywords: food processing, ultrasound, ethanol, convective drying, food properties

1. Introduction

The conventional drying methods based on using hot-air are the most applied process to produce dried foods. Even so, different emerging technologies or combined techniques are being used to improve conventional drying process and the obtained product properties. Some examples of emerging approaches are using infrared radiation [1, 2], microwave [3], electric pulses [4], high pressure [5], ethanol [6], ultrasound [7, 8], and some combinations, such as ethanol and ultrasound pre-treatments [9], ultrasound and vacuum [10], ethanol and vacuum [11], vacuum, ethanol and infrared radiation [12], ethanol, ultrasound and infrared radiation [2, 13]. Even so, some combination of technologies with the potential to obtain better processes were still not evaluated.

From these, interesting results were obtained by using ethanol pre-treatments. It was demonstrated that a balance on the structure and composition modifications, such as the changes on cell wall thickness and the air removal from intercellular spaces, are responsible for improving the process and product properties [2, 6, 14]. Furthermore, during pre-treatments, the entrance of ethanol occurs into the sample, forming a mixture with water. Then, during drying, the superficial ethanol vaporization promotes mechanisms to accelerate the drying process, such as the Marangoni effect [6, 15].

On the other hand, high power ultrasound technology (US) was used assisting the convective drying with very positive results on drying time reduction and improvements of product properties, such as rehydration, texture, nutritional compounds retention and availability [16-21]. Generally, the effects of applying US are more significant when drying is performed at temperatures lower than 70°C [22] and air velocities lower than 2 m/s [23], which are typical conditions for fruit drying.

The mechanisms linked to mass transfer improvements during US-assisted convective drying are related to effects not only on the solid-gas interface but also on internal structure. Effects on the solid-gas interface are related to acoustic microstreaming, pressure variations and oscillating velocities, which contribute to decrease external resistances to the mass transfer [24-26]. Therefore, these effects promote the moisture vaporization to air phase. On the other hand, the structure modifications inside the food matrix (cell wall breakdown, creation of microscopic channels) are a consequence of acoustic cavitation and the indirect effects of the mechanism known as the “sponge effect” (a series of cyclical compressions and expansions) related to acoustic waves traveling through the product [21, 27, 28]. Therefore, the structure modifications inside the food matrix promote the water transfer from inside to sample surface.

Consequently, very promissory results are expected from combining the ethanol pre-treatments with the US application during convective drying. However, this approach was not evaluated until now. In this work, apple (cv. Granny Smith) samples were used to study this combination, by applying different periods of ethanol pre-treatment with the consequent convective drying without and with US application. The effects on drying kinetics, rehydration, shrinkage, viscoelasticity, antioxidant capacity and total phenolic compounds were evaluated.

2. Material and method

2.1. Sample preparation

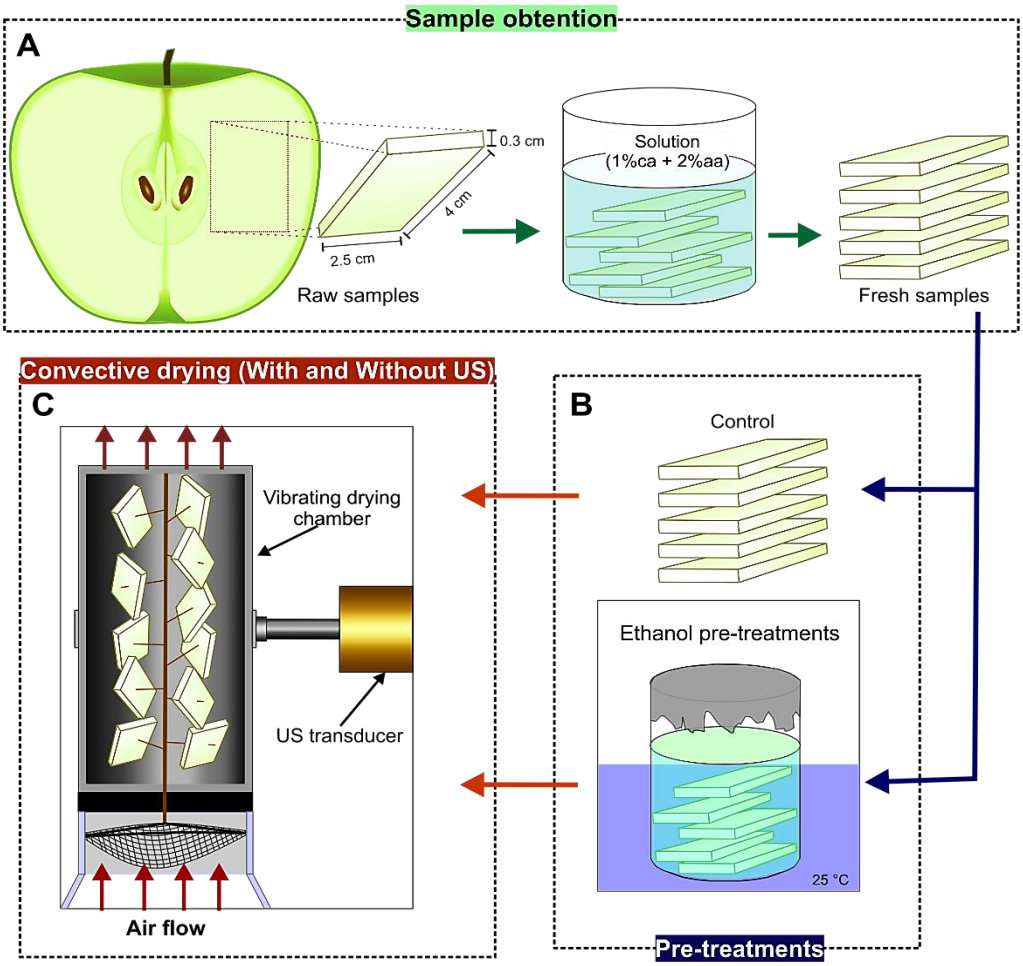

Figure 1. Schematic representation of (A) sample obtention, (B) pre-treatments with and without ethanol (Control), (C) Detail of sample location inside the drying chamber during convective drying with and without US application.

Apples (cv. Granny smith) were acquired from a local market (Valencia, Spain). They were washed, and the flesh parts were cut in order to obtain rectangular-shaped samples

of 4 cm length x 2.5 cm width x 0.3 cm height. After that, the raw samples were immersed for 10min in a solution composed by 1% citric acid and 2% ascorbic acid in a rate of 0.4 g of sample/mL of solution (ca+aa solution) to prevent browning reactions. These fresh samples were then ethanol pre-treated and, subsequently convectively dried (Fig. 1).

2.2. Ethanol pre-treatments

Ethanol pre-treatments were performed by immersion in ethanol (96% v/v) at a constant temperature of 25 °C for 0, 10, 20 and 30 min. A rate of 0.46 g of sample/g ethanol was used for all ethanol pre-treatments.

2.3. Drying

Hot-air drying experiments were performed at 50 °C and 1 $m \cdot s^{-1}$ using an ultrasonically assisted dryer, as described by García-Pérez, Cárcel, de la Fuente-Blanco and Riera-Franco de Sarabia [29]. Drying was performed without and with US application at an electrical input of 20.5 kW/m^3 and frequency of 21.77 kHz. In each drying process, 19 apple samples were randomly placed inside the drying chamber (Figure 1) using a sample holder [30], which was put inside the dryer. Sample weight was automatically recorded along the drying time. The final criterium of drying was stablished when samples showed a variation < 0.05 g in the tree last weights. The performed treatments include the Control (C, i.e. the samples without any pre-treatment conventionally dried), the different ethanol pre-treatment times with the consequent drying with and without US. Table 1 shows the code assigned to each treatment. The initial and final moisture was determined by vacuum drying at 70 °C and -0.8 bar (VACIOTEM-T, J.P. SELECTA, S.A., Barcelona).

Table 1. Treatments performed as a result of ethanol pre-treatment time and drying with and without US application.

Ethanol pre-treatment (min)	Convective drying	
	Without US	With US
0	Control (C)	CUS
10	E10	E10US
20	E20	E20US
30	E30	E30US

2.4. Projected area: an estimation of shrinkage

The shrinkage with their deformation effect was estimated from the bidimensional projected area. This was obtained by segmentation of images using the Fiji-ImageJ project (ImageJ-win64 software, USA) [31], which has been previously used to measure the shrinkage during drying [32, 33].

The process to obtain the projected area was performed according to the following steps (Fig. 2): (a) conversion of the coloured image (ci) to 8-bit grayscale; (b) set-scale in pixels/cm; (c) threshold - conversion into binary image (Black & Withe option with black background); (d) measure the area following the criteria that any interference lower than1 cm^2 will not be considered in the measurement. In addition, the options of show outlines and considerer holes were selected to evidence the areas that were considered and measured.

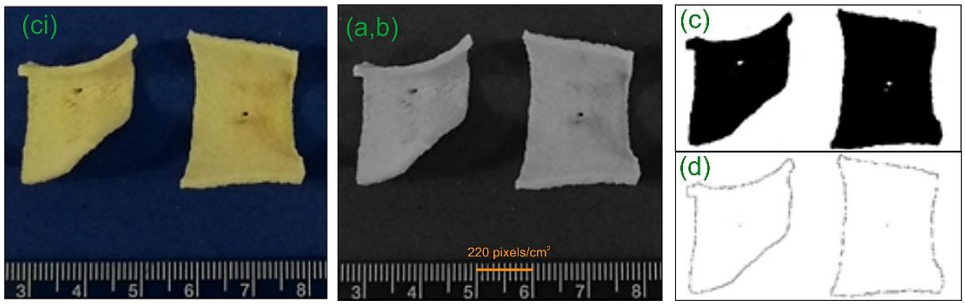

Figure 2. Example of the image segmentation process using Fiji-ImageJ project (-win64 software, USA) for evaluating the dried samples.

2.5. Rehydration

Rehydration was performed at 25 °C. Dried samples were immersed in distilled water in a rate of 0.0125 g sample/mL water. During the rehydration process, the gain of mass was registered. Then, the moisture content was determined by mass balance taking account the initial moisture and mass registered. The initial moisture of dried samples was determined by vacuum drying at 70 °C and -0.8 bar (VACIOTEM-T, J.P. SELECTA, S.A, Barcelona, Spain).

2.6. Viscoelastic properties

The stress-relaxation assay was considered to describe the viscoelastic changes on apple samples before drying and after rehydration [34] using a Texture Analyzer (TA-XT2i, Stable Micro Systems Ltd., Surrey, UK) with a load cell of 50 kg-f (490.03 N) and

a 50 mm aluminium cylindrical probe (SMS/P50). The tests were carried out cylinders of 1.5 cm diameter obtained from each apple sample. The cylinders were firstly compressed until a strain of 0.25 with 0.02 $mm.s^{-1}$ velocity. Then, the deformation was maintained constant for 50 s, being the data of force (N) versus time (s) recorded every 0.01 s to detailing analyse the relaxation curves and model fit.

2.7. Nutritional aspects

2.7.1. Obtaining sample extracts

Sample extracts from raw samples, pre-treated, and dried samples were performed to analyse the antioxidant capacity (AC) and total phenolic content (TPC). Each extract was obtained by mix 10 mL of ethanol (96%) and the sample (~1 g of raw, fresh, and ethanol pre-treated samples or ~0.2 g of ground (coffee grinder, Lauson, 120W, PRC) dried samples). The mixture was homogenized at 8000 RPM (Yellow line D1 25 basic, IKA-WERKE, Germany) for 1 min. Then it was stirred for 20 min and centrifuged at 9167 Rcfxg (Medifriger B1-5, SELECTA, Barcelona, Spain) for 5 min, both stages were performed at 4 °C. The supernatant was filtered and collected in hermetic glass flasks protected from light, then the obtained extract was stored under refrigeration until analysis.

2.7.2. Antioxidant capacity (AC)

The ABTS method, described by Vieira, Borges, Copetti, Amboni, Denardi and Fett [35] with some modifications, was used to express the antioxidant capacity (AC). The $ABTS^{\bullet+}$ radical was generated according to Re, Pellegrini, Proteggente, Pannala, Yang and Rice-Evans [36] by oxidation of ABTS (2,2′-Azino-bis (3-ethylbenzothiazoline-6-sulfonic acid) diammonium salt) (SIGMA-ALDRICH, Germany) 7mM, with potassium persulphate (SIGMA-ALDRICH, Germany) 2.45 mM (final concentration). The mixture was left in rest in dark for 16 h. Ethanol was used to dilute the $ABTS^{\bullet+}$ radical. Then, the ABTS solution work was prepared by adjusting their absorbance to 0.699 ± 0.011 at 734 nm using a spectrophotometer (Helios gamma UV-Vis spectrophotometer, Thermo electron corporation, USA). For reaction, 2 mL of ABTS solution work were used, 50 µL of extract, and 150 µL of ethanol. After performing the reaction, it was left for 20 min in the dark at room temperature and the absorbance was read at 734 nm. A calibration curve was constructed with different quantities of Trolox (6-hydroxy-2,5,7,8-tetramethylchroman-2-

carboxylic acid) (SIGMA-ALDRICH, Germany) 0.5mM (from 10 to 73 µL). The antioxidant capacity was expressed in mg of Trolox/g dry matter.

2.7.3. Total phenolic content (TPC)

The reduction of Folin-Ciocalteu's reagent method was used to express the total phenolic content (TPC). TPC was performed based on the reported by Colucci, Fissore, Rossello and Carcel [18], Rodrigues, Fernandes, García-Pérez and Cárcel [37], Moreno, Brines, Mulet, Rosselló and Cárcel [38] with some modifications. For each reaction, it was used 2.3 mL of distilled water, 100 µL of extract, 200 µL of Folin- Ciocalteu's reagent 2M (SIGMA-ALDRICH, Swithzerland) and 400 µL of sodium carbonate (Labken, Spain) 20% m/v. For this, in a glass tube were mixed the water, extract and Folin- Ciocalteu's quantities, this mixture was homogenized using a vortex shaker and after 4 min, the sodium carbonate was added to the reaction. It was left to react for 60 min in dark at ambient temperature. A calibration curve was constructed with different quantities (from 10 to 90 µL) of 250 µg/mL gallic acid (GA) (3,4,5-trihydroxybenzoic acid) (SIGMA-ALDRICH, Germany) solution. Total phenolic content was expressed in mg of GA/g dry matter.

2.8. Mathematical modelling description

2.8.1. Drying kinetics

Three models were applied to describe the apple drying.

Firstly, the drying was described considering a model based in the derivation from Fick's second law [30, 38-40], considering the diffusion model (Eq. 1).

$$\frac{\partial \mathrm{M_{x,t}}}{\partial \mathrm{t}} = \mathrm{D_{eff}} \frac{\partial^2 \mathrm{M_{x,t}}}{\partial \mathrm{x^2}} \quad (1)$$

Where t is the drying time (s); M is the moisture content (kg water/kg dry matter, d.m.) at any t; $\mathrm{D_{eff}}$ is the moisture effective diffusivity (m^2/s), and x is the distance (m) in the direction of the water transport.

It is important to highlight the moisture effective diffusivity ($\mathrm{D_{eff}}$) is a lumped constant that represent the global transport phenomena; it might include molecular diffusion, liquid diffusion through the solid pores, vapour diffusion and all other factors that affect drying characteristics [41], including capillarity and even other mass transfer mechanisms, such as the "sponge effect" during US-assisted drying.

For modelling purposes, different assumptions should be considered [42, 43]. Apple samples were considered as isotropic materials, also exhibiting an infinite slab behaviour. Negligible shrinkage was assumed during the process, as well as uniform temperature and initial moisture inside the sample. The flux of moisture was considering taking place in one direction symmetrically from the thickness centre to surface. The moisture effective diffusivity (D_{eff}) was considered constant over the process and across the sample.

Eq. (1) could be solved using the above assumptions and different initial and boundary conditions. As the initial condition, a uniform moisture content distribution ($M = M_i$) inside the sample was considered at the beginning of the process ($t = 0$). Therefore, the moisture distribution symmetry was considered as the first boundary condition. Then, if the moisture content of the solid surface achieves equilibrium when drying starts ($t > 0; x = L$), it results in the Eq. (2).

$$M(L,t) = M_{eq} \tag{2}$$

Where L is the half-thickness of the sample and M_{eq} is the equilibrium moisture content (kg water/kg d.m). The equilibrium moisture content was estimated from the desorption isotherm of apple (c.v. Granny Smith) reported by Vega-Gálvez, Miranda, Bilbao-Sáinz, Uribe and Lemus-Mondaca [44]. Therefore, in this case, it was considered that the drying kinetics was controlled by the movement of the moisture inside the solid, being Eq. (3) a purely diffusive model controlled by internal resistances (IR-Model), which results from the analytical solution integrated for the sample volume [45].

$$M = M_{eq} + (M_0 - M_{eq})\left[2\sum_{n=0}^{\infty}\frac{1}{\lambda_n^2 L^2}e^{-D_{eff}\lambda_n^2 t}\right] \tag{3}$$

$$\lambda = \frac{(2n+1)\pi}{2L} \tag{4}$$

The IR-Model (Eq. 3) model was considered as a first approach for fitting the experimental results. In another approximation, the external resistance to mass transfer was considered in the boundary conditions changing Eq. (2) by Eq. (5) (IER-Model). This last explains better the transfer of water from inside to surface sample (described by the cited moisture effective diffusivity - D_{eff}) and how that water is transferred to the air by convention (described by the convective mass transfer coefficient - h).

$$-D_{eff}\rho_d\frac{\partial W(L,t)}{\partial x} = h(a_w(L,t) - \varphi_{air}) \tag{5}$$

Where ρ_d is the density of dry sample (kg d.m/m^3); h is the convective mass transfer coefficient (kg water/m^2·s), a_w is the water activity and φ_{air} is the relative humidity of drying air.

Once other mechanisms of mass transfer further than diffusion takes place during drying, an empirical model was also used to describe the process, the Page Model [46]

(Eq. 6), which has been successfully applied to describe the drying kinetics of different food products. Simpson, Ramírez, Nuñez, Jaques and Almonacid [47], using the anomalous diffusion concept and the fractional calculus approach, provided a phenomenological interpretation of the model, where, the drying rate constant (k) is associated with the "diffusion" coefficient and the geometry of the sample, while the dimensionless drying constant (n) is related to the "type of diffusion" and food microstructure ($n > 1$ super-diffusion and $n < 1$ subdiffusion).

$$\frac{M-M_{eq}}{M_0-M_{eq}} = e^{-k.t^n} \quad (6)$$

The IR-Model (Eq. 3), and Page model (Eq. 6) were adjusted to experimental data by identifying the D_{eff} (of Eq.3), k and n (of Eq. 6) values that minimize the sum of squared errors (SSE, Eq.7) between the experimental and the predicted values for the x local moisture content (M). The Generalized Reduced Gradient algorithm (GRG Nonlinear Solving optimization method) implemented in the 'Solver' tool of software Excel 2016 (Microsoft, USA) was used. The parameter value was considered valid when Solver reported that the GRG method found a locally optimal solution (to a set convergence of 0.000001).

$$SSE = \sum_{i=1}^{x}((predicted) - (experimental))_i^2 \quad (7)$$

On the other hand, the IER model was solved by applying a numerical method (implicit finite differences) described by Ortuño, Pérez-Munuera, Puig, Riera and Garcia-Perez [24]. The fitting of this model was carried out by the simultaneous identification of both kinetic parameters, moisture effective diffusivity (D_{eff}) and convective mass transfer coefficient (h). The optimization was carried out through the SIMPLEX method available in Matlab (Fmin search function), using the Matlab R2015b (Mathworks, Inc., USA) software.

2.8.2. Rehydration kinetics

The rehydration kinetics were modelled by fitting the IR-Model (Eq. 3) to experimental rehydration data. In this case, M is moisture content on dry basis (kg water/kg d.m) at time *t* (s), M_0 is the initial moisture content (kg water/kg d.m), M_{eq} is the equilibrium moisture (considered as the last measured moisture when samples showed a weight variation <0.05 g). The diffusivity (D_{eff}) (m^2/s) during rehydration was obtained by minimizing the SSE (Eq. 5), as explained above.

2.8.3. Viscoelastic properties (stress-relaxation behaviour)

Two models were used to describe the sample viscoelastic properties: the Generalized Maxwell Model [34], described in Eq.(8), and the Peleg Model [48], described in Eq. (10).

Regarding the Generalized Maxwell Model, two Maxwell Elements were considered, organized in parallel with an isolated Hookean spring, which contributes to the residual elasticity (ξ_e). The stress decay along the time ($\sigma(t)$, Eq. 8) during the stress-relaxation evaluation can thus be described as a function of the constant strain (ε), the relaxation time (τ_i) and the elastic modulus (ξ_i). From the relaxation time and the elastic modulus, the viscous modulus was obtained according to Eq. (9) [34].

$$\sigma(t) = \varepsilon.\left(\xi_e + \xi_1.e^{\left(-\frac{t}{\tau_1}\right)} + \xi_2.e^{\left(-\frac{t}{\tau_2}\right)}\right) \quad (8)$$

$$\eta_i = \tau_i.\xi_i \quad (9)$$

The Peleg Model (Eq. 10) is a simple empirical model with only two parameters (k_1, k_2). It has already been used to successfully describe the viscoelastic behaviour of different materials. The reciprocal of k_1 represents the initial decay rate, while the reciprocal of k_2 represents the hypothetical asymptotic level of the normalized relaxation curve [48, 49].

$$\frac{\sigma_0 - \sigma(t)}{\sigma_0} = \frac{t}{k_1 + k_2.t} \quad (10)$$

The models were fitted by nonlinear regression, whose parameters were determined by minimizing the sum of squared errors (SSE in Eq. 7).

The estimation of the determination coefficient (R^2) and the percentage of explained variance (%Var), according to Eq. (11, were S_{cal}^2 is the variance of calculated data and S_{exp}^2 is the variance of the experimental data) were used to evaluate how accurately the models fit the experimental data.

$$\%\mathrm{Var} = \left(1 - \frac{S_{cal}^2}{S_{exp}^2}\right).100 \quad (11)$$

2.9. Experimental design and statistical analysis

A completely randomized design (CDR) was conducted. All processes and analysis were carried out at least in triplicate. The analysis of variance (ANOVA) and Tukey test were conducted to determine which treatments differ from each other (significance level

of 5%). Statistical analyses were determined using the IBM SPSS Statistics 23 software (IBM SPSS, USA).

3. Results and discussion

3.1. Drying

Figure 3 shows the dimensionless moisture ratio (MR) over the drying time, considering all the treatments. The drying processes were stopped when sample weight variation was lower than 0.05g in the last three registered points. At the end of the drying process, all the samples presented moisture of 0.06 ± 0.02 d.b.

The conventional drying time (i.e., the time needed to dry the control (C) samples) was reduced in 34-53% by using ethanol as pre-treatments (34 ± 5% for E10, 47 ± 3% for E20, 53 ± 4% for E30). These reductions were like previously reported when ethanol was used as pre-treatment to convective drying. For example, 50% of time reduction was reported in apples immersed ethanol (95%, 14h) [11], 20% in bananas surface treated with ethanol [50], and 35% in guaco leaves treated by immersion in ethanol [51]. Moreover, high drying rates in ethanol-injected structured balls (mixed rice and soybean powders) samples [52] or pineapple slices dried in an ethanolic atmosphere [53] has been also found.

Regarding the application of US during drying, the acoustically assisted dried samples needed 41 ± 10% less time than the conventional dried ones. This intensification of the drying process by US application has been also previously reported. For example, 45% drying time reduction was reported in orange peel (40 °C, 1 m/s, assisted by US (90W)) [24], 48% in passion fruit peel (50 °C, 1 m/s, assisted by US 21.7 kHz, 30.8 kW/m^3) [39] or 46.1% in apple (50 °C, 1 m/s, assisted by US 30.8 kW/m^3) [54].

However, the effects of a combination of ethanol pre-treatments with the use of US during drying were highly significant being the observed reductions on drying time 55 ± 4% for E10US, 65 ± 7% for E20US, and 70 ± 2% for E30US. This means that the mass transfer accelerated by using ethanol pre-treatments was potentiated by the US application.

To evaluate and compare the effects of the different performed treatments, three mathematical models were used. The IR model was applied assuming negligible the external resistance to mass transfer (Eq. 3). Compared to the conventional drying experiments (C), every pre-treatment or the US application during drying increased the D_{eff} value identified (Table 2). However, as the %Var figures obtained, (lower than 94%) and the Figure 4 show, a considerable lack of fit was obtained when the IR model was

used, especially in the Control samples. This suggests the water transport was not only controlled by internal resistance but also, there was an influence of external resistance probably due to the low air velocity used [55]. In fact, in previous works carried out at similar dying conditions, diffusion model was not accurate to simulate the drying kinetics [54, 56]. In any case, the IR-model served as the first approach to improve the fitting of the IER-Model, where the external resistances were considered (Eq. 5).

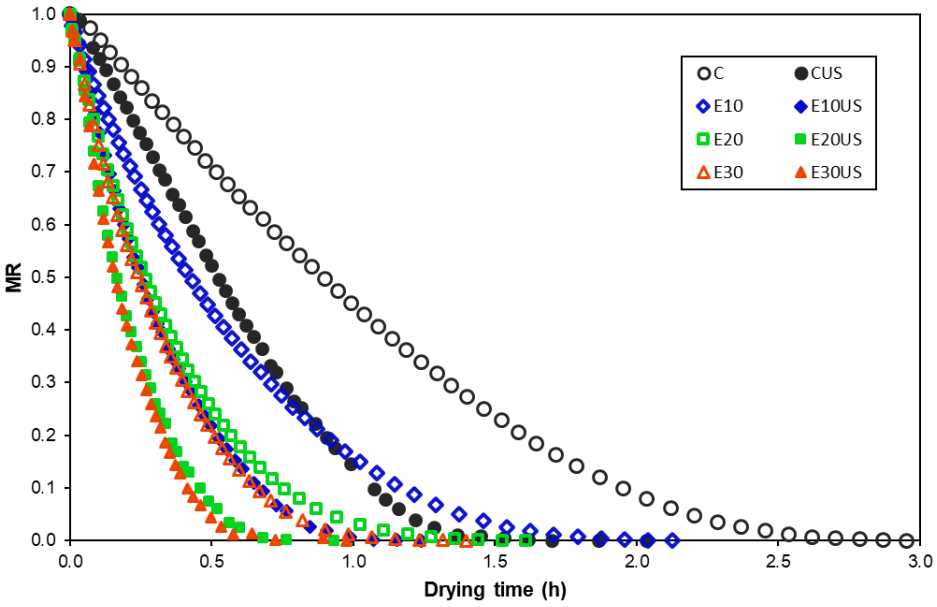

Figure 3. Dimensionless moisture ratio (MR). Each curve is representative of more than three replicates. Open figures are treatments of drying without US and those filled are with US.

The D_{eff} figures identified from the IER-Model were higher than those from IR-Model (Table 2). According to described by Vagenes and Marinos-Kouris [55], the D_{eff} from IR-Model implicitly includes both external and internal resistances where their combination results in lower values of D_{eff}. Therefore, the obtained D_{eff} and h parameters from IER-Model allows discriminating better the effect of using ethanol and/or US in the internal and external resistances respectively.

The convective mass transfer coefficient (h) increased for all treatments (Table 2) compared to control drying experiments.

When US was applied assisting the convective drying, it improved the identified h value (Table 2) compared to the control. This effect can be attributed to pressure variations, oscillating velocities and microstreaming, which reduce the boundary layer thickness and increase the water transfer to air phase [24]. This has been previously observed during drying of carrot cubes [57], persimmon [23], cassava and apple cubes

[58]. Different factors can influence the effect of US on mass transfer resistance, such as the air velocities (it is better at low air velocities (0.5 - 2 m/s) [23]) or mass load [57].

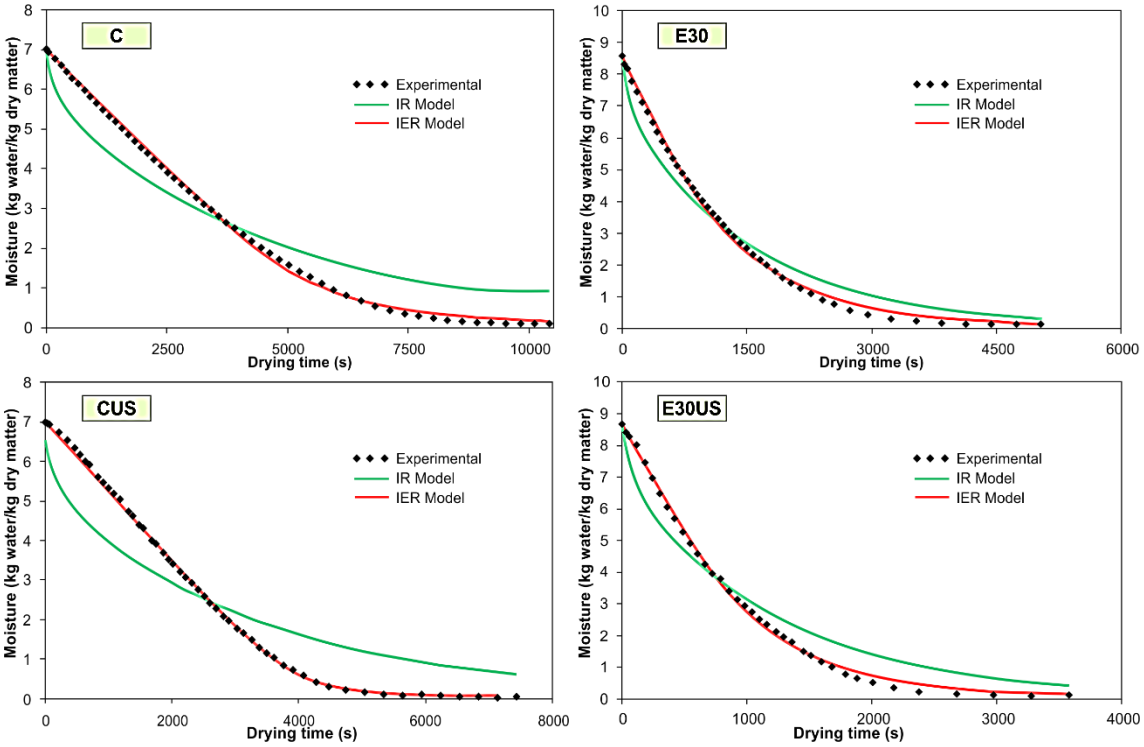

Figure 4. Drying kinetics of the C and E30 pre-treated samples dried with and without US modelled using both IR (green curve) and IER model (red curve).

However, the highest h values were found in the ethanol pre-treated samples. This means that the ethanol pre-treatment made easier the moisture transfer from the sample surface to the air phase. To the best of our knowledge, this is the first time the effect of ethanol pre-treatment on the external mass transfer coefficient is described. The ethanol application had more influence on decreasing the external resistance than the ultrasound. Thus, compared with conventional drying, while the US application increased the h value 55%, the pre-treatment with ethanol for 10 min increased more than 200% and for 30 min more than 300%. The external resistance is dependent on boundary layer thickness, which is affected by the sample shape, size and by the fluid circulation regime and properties [59, 60]. The air velocity, sample size and shape were the same for all treatments at the beginning of the drying process. However, the fluid properties were different in the ethanol pre-treated samples.

Table 2. Drying kinetics parameters of both IR and IER used models with their fitting. Different letters indicate significative differences (p< 5%) among treatments.

Treatment	IR-Model (Eq. 3)			IER-Model (Eq. 5)				Page Model (Eq. 6)			
	D_{eff} (x 10^{-10}, m^2/s)	R^2	%Var	h (x 10^{-3}, kg/ m^2 s)	D_{eff} (x 10^{-10}, m^2/s)	R^2	%Var	k (x 10^{-5}, 1/s)	n	R^2	%Var
C	1.83 ± 0.13^{a}	≥ 0.97	≥ 86.55	1.39 ± 0.04^{a}	6.22 ± 0.56^{ab}	≥ 0.99	≥ 99.82	1.12 ± 0.34^{a}	1.39 ± 0.03^{d}	≥ 0.99	≥ 99.50
CUS	2.94 ± 0.14^{ab}	≥ 0.96	≥ 84.38	2.16 ± 0.10^{a}	18.88 ± 0.79^{d}	≥ 0.99	≥ 99.91	0.66 ± 0.14^{a}	1.54 ± 0.03^{e}	≥ 0.99	≥ 99.67
E10	3.71 ± 0.53^{bc}	≥ 0.99	≥ 93.43	4.40 ± 0.76^{b}	5.48 ± 0.39^{a}	≥ 0.99	≥ 98.40	32.25 ± 14.17^{bc}	1.07 ± 0.05^{ab}	≥ 0.99	≥ 99.79
E10US	5.25 ± 0.62^{d}	≥ 0.98	≥ 80.16	6.09 ± 0.42^{c}	9.70 ± 0.79^{b}	≥ 0.99	≥ 99.66	19.94 ± 15.59^{ab}	1.24 ± 0.15^{c}	≥ 0.99	≥ 99.66
E20	4.55 ± 0.48^{cd}	≥ 0.99	≥ 90.60	6.16 ± 0.25^{c}	8.99 ± 0.70^{ab}	≥ 0.99	≥ 98.20	50.77 ± 8.35^{c}	1.05 ± 0.03^{a}	≥ 0.99	≥ 99.62
E20US	7.30 ± 0.60^{e}	≥ 0.98	≥ 91.05	8.25 ± 0.31^{d}	14.94 ± 0.85^{c}	≥ 0.99	≥ 98.01	41.67 ± 9.93^{bc}	1.15 ± 0.03^{abc}	≥ 0.99	≥ 99.56
E30	5.00 ± 0.51^{d}	≥ 0.98	≥ 87.41	5.84 ± 0.35^{c}	8.46 ± 0.47^{ab}	≥ 0.99	≥ 98.93	38.94 ± 9.02^{bc}	1.09 ± 0.03^{abc}	≥ 0.99	≥ 99.70
E30US	8.50 ± 0.68^{e}	≥ 0.98	≥ 89.72	9.13 ± 1.07^{d}	17.43 ± 3.25^{cd}	≥ 0.99	≥ 99.10	30.60 ± 3.96^{bc}	1.21 ± 0.02^{bc}	≥ 0.99	≥ 99.87

It is important to highlight that external resistance influence is more important in the first stage of drying. When ethanol is applied, different phenomena (related to structure and composition modifications) occurs, especially in the sample surface. The intercellular air is removed, the cell wall is thinning, some compounds are extracted and part of ethanol enters the sample [2, 6, 12-14]. These effects were related to improvement mechanisms occurring in the sample surface at the beginning of the drying process. Since the ethanol vapour pressure is higher than that of the water, the vaporization of ethanol could start almost instantly during drying. Then, the initial fluid (ethanol-water mixture) present on the sample surface became richer in water, but as it is a sequential process, there is still ethanol in the next layer of the tissue surface. A gradient surface tension is formed between the ethanol and water interface inside the sample, which promotes the water flow from inside the cells through the Marangoni effect [6]. At the same time, the flow is easier from the surrounding surface, since the cell wall is thinner, and intercellular air is absent offering lower resistance to flow. Then, the fluid can be fast transferred to the sample surface, and the vaporization to air phase occurred at higher rates. In fact, at the beginning of drying process, the vaporization rate of ethanol pre-treated samples for 30 min (0.95 g of fluid vaporized/min) was two times higher than the rate of vaporization of Control samples (0.4 g water vaporized/min).

As the drying processing time increases, the ethanol effects on the sample surface became less important. In this case, the influence of the structural modifications becomes significant in the diffusivity parameter (D_{eff}). Compared to control (C) the obtained D_{eff} parameter from IER-Model (Table 2) was similar ($p>0.05$) for every kinetics carried out with pre-treatments with ethanol (E10, E20 and E30). However, this value increases from 1.6 to 3 times for the treatments that included the US use.

This agrees with previously reported for apple drying, where D_{eff} increases from 1.3 to 2.4 times for all cases during convective drying (30 °C, 50 °C and 70 °C) assisted by US (18.5 and 30.8 kW/m^3) [54]. This demonstrates that US has an important effect in the internal resistance to mass transfer. The responsible mechanisms that improve the moisture removal from inside the sample are related to the alternative compressions and decompressions (“sponge effect”) produced by the US waves, which travels through samples promoting flow through the intercellular spaces and existing channels and can also create microscopic channels [61]. Besides, the “sponge effect” is more intense in porous structures, and apple tissue is considered a porous structure [58].

Furthermore, Sabarez, Gallego-Juarez and Riera [62] suggested that US impact is important mainly in the drying stage that is limited by internal resistance (i.e., the final stages of drying). This hypothesis was corroborated by Beck, Sabarez, Gaukel and Knoerzer [63], by applying US only in the final stages of a model food (water, cellulose,

starch and fructose drying), and even so, observing a significant reduction in drying time (more than 50%). The authors suggested there is a time lag after which the US accelerates the drying significantly (i.e., after free surface water has been evaporated) [63].

Regarding Peleg model parameters, it seems that the highest k value, the lower n value. In fact, compared to Control (C), higher k values and lower n values were obtained when ethanol pre-treatments were applied. The highest n value was observed in samples with US application. According to Simpson, Ramírez, Nuñez, Jaques and Almonacid [47], the n value is related to the "type of diffusion"; then at $n > 1$ a super-diffusive behaviour is attributed. In the present study, the highest n value (in samples with US application) coincide with the highest D_{eff} value observed in the same treatments, reinforcing D_{eff} as a parameter that considers not only the pure diffusion phenomenon but also other mass transfer mechanisms, such as capillarity. Our interpretation in previous works [2, 64] is that when $n \neq 1$, other mechanisms than a purely diffusive mass transfer are significant. Therefore, it can be suggested that the lower n values of ethanol pre-treatments are due to mechanisms associated with external mass transfer were more important, which were reflected by increasing the h values. In contrast, high n values when US was applied can be correlated with effects in the internal structure, which also was described by higher D_{eff} coefficients.

As conclusion, under the studied conditions, the ethanol pre-treatments and US application affect both external and external resistances. However, the ethanol showed more influence on decreasing the external one, while US, compared to ethanol pre-treatments, shows more influence on decreasing the internal resistance.

3.2. Projected area

The bidimensional projected area calculated in this study approached shrinkage and deformation obtained after performing ethanol pre-treatments and after drying process (Fig. 5). After ethanol pre-treatments, the projected area was slightly reduced (Fig. 5A). Compared with the fresh samples, the reduction was apparently the same in all dimensions, being higher for E30 pre-treatment, with 8.7% reduction. It is interesting to note that the E10 and E20 pre-treated samples showed less reduction, but the variation among samples area was higher than those of E30 samples - probably the pre-treatment time was not enough to affect all samples in the same manner.

After drying (Fig. 5B), all samples presented a reduction greater than 47% regarding their initial area (after pre-treatments). In contrast to ethanol pre-treatment, the US application had no significant effects on shrinkage ($p>0.05$). The samples pre-treated

with ethanol for 10 min presented the highest shrinkage in both cases dried without (E10) and with US application (E10US). As observed in Figure 5A, high variations among samples were obtained in this pre-treatment. Then, probably the ethanol did not affect homogeneously all the sample surface and species, remaining a more heterogeneous tissue. Therefore, this heterogeneous structure could originate different internal tensions during drying, which resulted in more shrunk material. The higher sample shrinkage could also influence the observed drying kinetics. Thus, D_{eff} value identified for this treatment was the lowest of all pre-treated samples (Table 2). According to [60] the D_{eff} is misleading because it is affected by shrinkage. The ethanol effects were more homogenous at higher pre-treatment time. Then, the samples pre-treated for 30 min presented a lower reduction of the projected area, with values in the range of the Control samples.

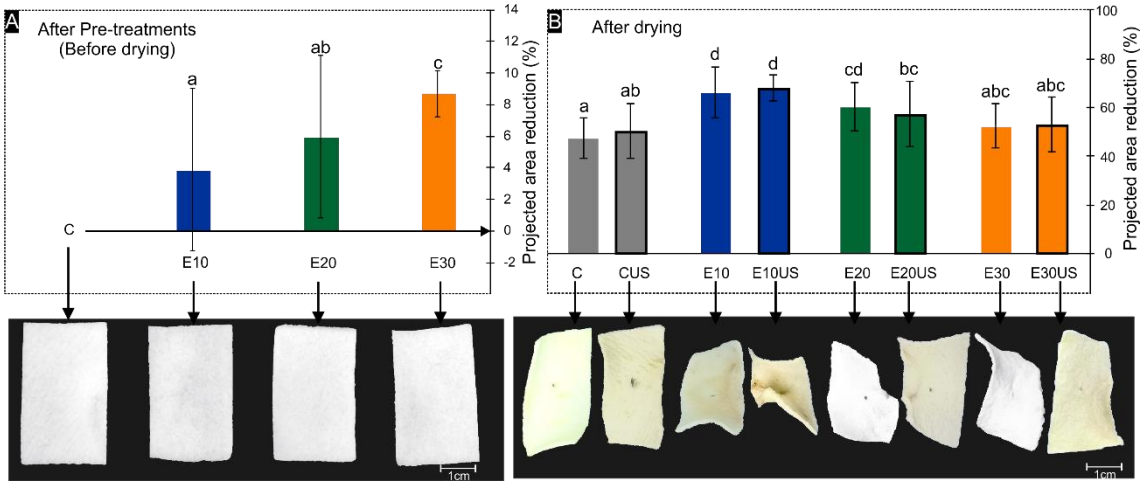

Figure 5. A: Projected area reduction after pre-treatments (related with the absolute shrinkage) and B: After dying (related with shrinkage and deformation of dried samples). Vertical bars are ± standard deviation and different letters indicate significant differences ($p<0.05$)

3.3. Rehydration

Figure 6 shows the rehydration kinetics for the Control and pre-treated samples dried with and without US. From the rehydration behaviour, no differences were observed between the samples dried with and without US (Figure 6). The ethanol pre-treatment increased the rehydration capacity, the longest pre-treatment time the greater water absorption. The application of US during drying only significantly affected the hydration of the samples pre-treated with ethanol for 10 min (E10US compared with E10). This could because as observed in Figure 3, the US had the highest effects on decreasing the drying time in this ethanol pre-treatment (10 min), when compared to

other pre-treatments. Therefore, the E10US compared with E10 samples experimented fewer drying alterations, which can be the reason for its best rehydration properties.

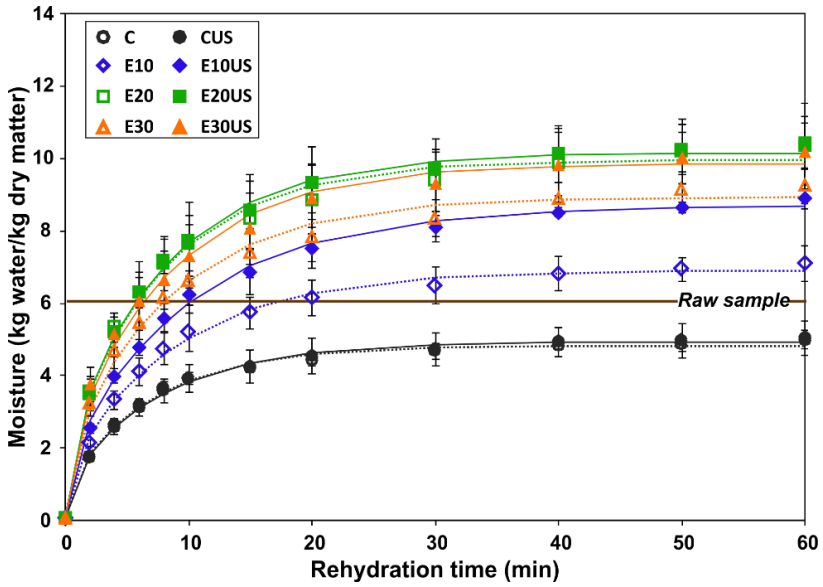

Figure 6. Rehydration kinetics of all treatments. Open figures are samples dried without US and filled are with US. Vertical bars are the ± standard deviation.

Table 3. Rehydration kinetics modelling. Identified parameters ± standard deviation. Different letters indicate significative differences (p<5%) among treatments.

Treatment	IR-model (Eq.3)			
	M_{eq} (kg water/ kg d.m)	D_{eff} (x 10^{-10}, m^2/s)	%Var	R^2
C	5.01 ± 0.28^{a}	8.48 ± 1.26^{a}	≥ 99.82	≥ 0.99
CUS	5.04 ± 0.47^{a}	8.15 ± 0.93^{a}	≥ 99.26	≥ 0.99
E10	7.09 ± 0.49^{b}	6.91 ± 1.12^{a}	≥ 98.88	≥ 0.99
E10US	8.88 ± 0.26^{bc}	6.11 ± 0.86^{a}	≥ 99.05	≥ 0.99
E20	10.32 ± 1.13^{c}	7.62 ± 2.02^{a}	≥ 97.63	≥ 0.98
E20US	10.33 ± 0.64^{c}	7.68 ± 1.25^{a}	≥ 99.14	≥ 0.99
E30	9.24 ± 0.49^{c}	7.02 ± 1.55^{a}	≥ 97.46	≥ 0.98
E30US	10.16 ± 0.99^{c}	7.12 ± 0.51^{a}	≥ 99.06	≥ 0.99

The modelling allowed to quantify the influence of the ethanol pre-treatment and US application in the hydration kinetics (Table 3). For ethanol pre-treated samples, the equilibrium moisture content was higher than the moisture of the controls (C and CUS) and even higher than the moisture of raw samples. This fact has previously reported in rehydration of apple [11], pumpkin [6], and scallion [12] which were pre-treated with ethanol. Table 3 shows the effective diffusion coefficient (D_{eff}) for all treatments, and no significant differences (p>0.05) were found among them. Similar results were found by Santacatalina, Soriano, Cárcel and Garcia-Perez [20] in ultrasonically assisted dried

eggplant rehydration, those authors reported no significant differences in the D_{eff} coefficient during rehydration of eggplant. The observed behaviour was probably a result of the balance between the driving forces and resistances to water absorption and its retention. That is the combined effects of the higher equilibrium moisture reached by ethanol pre-treated samples and their internal resistance increase as a consequence of sample shrinkage, probably resulting in no D_{eff} differences.

The high-water absorption of the dried apples using ethanol and US can be interesting for different purposes, for instance, to incorporate interesting compounds into the vegetable matrix, such as vitamins, minerals and antioxidant molecules.

3.4. Viscoelastic properties

Figure 7 shows the stress-relaxation behaviour of the raw samples (Fig. 7A), rehydrated samples after drying without (Fig. 7B) and with US application (Fig. 7C), and the comparison among these (Fig. 7D). It was observed that the raw samples show low stress decay and more residual elasticity. It suggests that the raw samples presented more elastic characteristics when compared with processed samples.

Two models were well fitted to the stress-relaxation experimental data, the Generalized Maxwell Model (GMM) (%Var ≥ 99 and R^2 ≥ 0.99) and Peleg Model (%Var ≥ 97 and R^2 ≥ 0.97) being the first which presented the best fit. The GMM was composed by two Maxwell elements and one residual spring (Eq.). The relaxation times (τ_1 and τ_2), modulus of elasticity (ξ_1 and ξ_2), viscosity (η_1 and η_2) of each Maxwell element and the residual elasticity (ξ_e) values are shown in Table 4.

A correlation among the structure and the Maxwell elements is possible to establish. According to Rojas and Augusto [6], Miano, da Costa Pereira, Miatelo and Augusto [65], the residual elasticity is related to the highest rigid structure- that is the lamella media; the first element (with their respective modulus ξ_1, τ_1) is associated with the cell structure; while the second element (with their respective modulus ξ_2, τ_2) is associated with the intercellular space structure. For all cases, this makes sense since the relaxation times of the cells (τ_1) was higher than the relaxation times of the intercellular spaces (τ_2), reflecting that the cells are more rigid than the intercellular spaces.

It was observed that the raw samples presented relaxation times (τ_1 and τ_2), elastic modulus (ξ_e, ξ_1, and ξ_2), and viscous modulus (η_1 and η_2) higher than those of the rehydrated samples. The relaxation time is a complex parameter, which is influenced by both elastic and viscous components, while the elastic and viscous modulus are related

to quality characteristics as its composition and texture attributes [66]. When compared with raw samples, the relaxation times of the C and CUS samples remains similar, but in ethanol pre-treated samples the τ_1 decreased up to 35%, and the τ_2 decreased up to 8%.

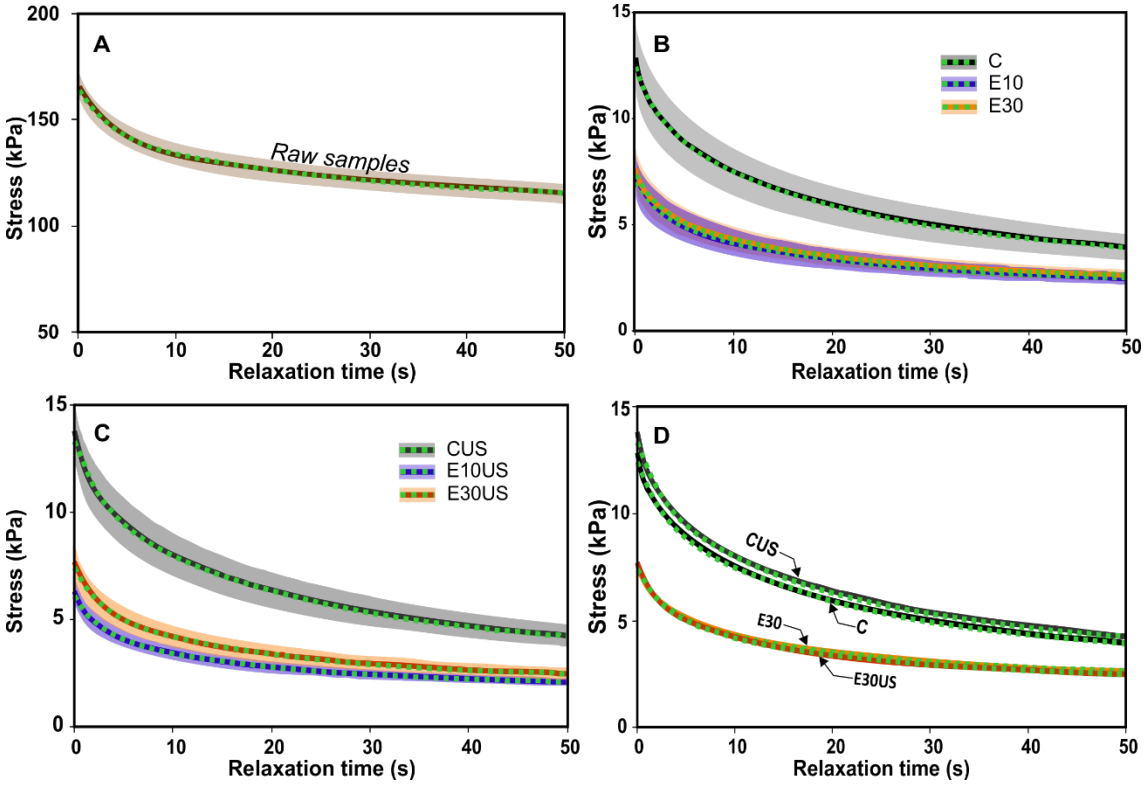

Figure 7. Stress-relaxation experimental data (dotted lines) fitted to the Generalized Maxwell Model (Eq. 8) (Straight lines). Shadow bands represent the confidence interval at 95%. A: Raw samples; B: Control (C) and ethanol pre-treated samples for 10 min (E10) and for 30 min (E30) dried and rehydrated; C: Non-pretreated samples dried with US application and rehydrated, (CUS) and ethanol pre-treated samples for 10 min (E10US) and for 30 min (E30US); D: Comparison among the control and ethanol pre-treated samples for 30 min, dried with (CUS and E30US) and without US (C and E30).

On the other hand, the elastic modulus for the raw samples was higher than that of the rehydrated samples. In fact, the structure and composition were modified during the drying contributing to decreasing the tissue elastic characteristics. This reduction was slightly more pronounced in samples pre-treated with ethanol. The same behaviour was observed in pumpkin samples pre-treated with ethanol, where the changes were attributed to structure modifications produced by the ethanol, which extracted and solubilized some components of the sample structure [6].

Table 4. Stress-relaxation parameters and fit criteria of the Generalized Maxwell Model (GMM) and Peleg Model application on the data obtained for the raw samples, and rehydrated samples, which were processed using the different treatments. Different higher case letters represent significative differences ($p<0.05$) of processed samples regarding the raw samples. Different lower-case letters represent significative differences ($p<0.05$) among processed samples.

Model Parameters		raw samples	Treatments							
			C	CUS	E10	E10US	E20	E20US	E30	E30US
Generalized Maxwell Model	τ_1	26.98 ± 2.68^{C}	22.23 ± 3.02^{Bb}	22.24 ± 3.36^{Bb}	19.45 ± 1.85^{Aa}	18.20 ± 1.65^{Aa}	17.54 ± 1.85^{Aa}	18.18 ± 2.09^{Aa}	19.26 ± 1.75^{Aa}	18.98 ± 3.16^{Aa}
	τ_2	2.69 ± 0.38^{B}	2.51 ± 0.32A^{Bb}	2.55 ± 0.20^{Bb}	2.46 ± 0.24^{ABab}	2.40 ± 0.31^{ABab}	2.20 ± 0.29^{Aa}	2.38 ± 0.37^{ABab}	2.43 ± 0.44A^{Bab}	2.43 ± 0.32^{ABab}
	ξ_e	441.22 ± 53.56^{B}	13.14 ± 3.34^{Aa}	14.08 ± 3.44^{Ab}	9.05 ± 1.60^{Ab}	7.81 ± 1.01^{Aa}	9.12 ± 1.47^{Aa}	8.70 ± 1.48^{Aa}	9.66 ± 2.13^{Aa}	9.07 ± 1.98^{Aa}
	ξ_1	137.44 ± 15.47^{C}	26.04 ± 7.59^{Bb}	27.69 ± 9.36^{Bb}	12.56 ± 4.83^{Aa}	10.15 ± 2.88^{Aa}	10.18 ± 4.41^{Aa}	11.54 ± 4.88^{Aa}	12.68 ± 5.23^{Aa}	12.92 ± 4.73^{Aa}
	ξ_2	80.09 ± 9.66^{D}	10.78 ± 1.53^{BCb}	11.85 ± 1.79^{Cb}	6.63 ± 1.18^{Aa}	6.60 ± 1.10^{Aa}	7.71 ± 1.71^{ABa}	7.32 ± 1.26A^{Ba}	7.33 ± 1.57^{ABa}	7.87 ± 1.02A^{Ba}
	η_1	3707.73 ± 544.68^{C}	598.18 ± 253^{Bb}	641.55 ± 305.50^{Bb}	251.76 ± 118.26^{Aa}	186.96 ± 61.59^{Aa}	182.80 ± 97.49^{Aa}	216.73 ± 114.22^{Aa}	250.14 ± 120.65^{Aa}	254.79 ± 134.66^{Aa}
	η_2	216.93 ± 46.47^{B}	27.27 ± 6.26^{Ab}	30.42 ± 6.34^{Ab}	16.466 ± 3.97^{Aa}	15.92 ± 3.68^{Aa}	17.04 ± 4.61^{Aa}	17.70 ± 4.97^{Aa}	18.16 ± 6.06^{Aa}	19.21 ± 4.05^{Aa}
	%Var	≥ 99.87	≥ 99.88	≥ 99.93	≥ 99.85	≥ 99.83	≥ 99.85	≥ 99.81	≥ 99.84	≥ 99.85
	R^2	≥ 0.99	≥ 0.99	≥ 0.99	≥ 0.99	≥ 0.99	≥ 0.99	≥ 0.99	≥ 0.99	≥ 0.99
Peleg Model	k_1	22.29 ± 2.43^{D}	10.92 ± 2.43^{Cc}	10.66 ± 2.54^{Cc}	8.94 ± 1.91^{BCbc}	7.61 ± 1.49^{ABab}	6.76 ± 1.84^{Aa}	7.64 ± 2.19^{ABab}	8.54 ± 2.20^{ABab}	7.99 ± 2.34^{ABab}
	k_2	2.96 ± 0.28^{C}	1.26 ± 0.05^{Aa}	1.27 ± 0.04^{Aab}	1.39 ± 0.11^{ABcd}	1.38 ± 0.08^{ABcd}	1.44 ± 0.13^{Bd}	1.39 ± 0.12^{ABcd}	1.40 ± 0.10^{Bcd}	1.35 ± 0.07^{ABbc}
	%Var	≥ 98.72	≥ 98.72	≥ 98.61	≥ 98.72	≥ 98.19	≥ 98.20	≥ 97.81	≥ 97.12	≥ 98.58
	R^2	≥ 0.99	≥ 0.99	≥ 0.98	≥ 0.98	≥ 0.98	≥ 0.98	≥ 0.98	≥ 0.97	≥ 0.98

As in the case of the elastic modulus, the viscous modulus of raw samples was higher than those of the rehydrated ones as a consequence of the structural modification during pre-treatment and drying combined with compositional modifications after rehydration. The water distribution during rehydration differs from their initial state and location (in the raw samples). Since the dried samples had cell walls damaged, the water during rehydration is highly distributed inside the intercellular spaces, and the cell-to-cell contact decreases [67]. Then, the samples present lower resistances to deformation and stress, their lower resistances to flow reflecting the lower viscous modulus.

Regarding the Peleg Model parameters, the k_2 parameter can be considered as "a representation of the solidity degree" being 1 for fluids, while infinite for solids [49]. Statistically, no significant differences ($p>0.05$) were evidenced among ethanol rehydrated samples, but their k_2 values were lower and differed from those of the raw samples. The k_2 values were closer to one in rehydrated samples, which means that they show a tendency to have more viscous than elastic character.

Therefore, as a conclusion, the viscoelastic parameters diminution reflects that during drying and rehydration the tissue loses its original properties and characteristics being more pronounced when pre-treatments was applied.

3.5. Antioxidant capacity and phenolic content

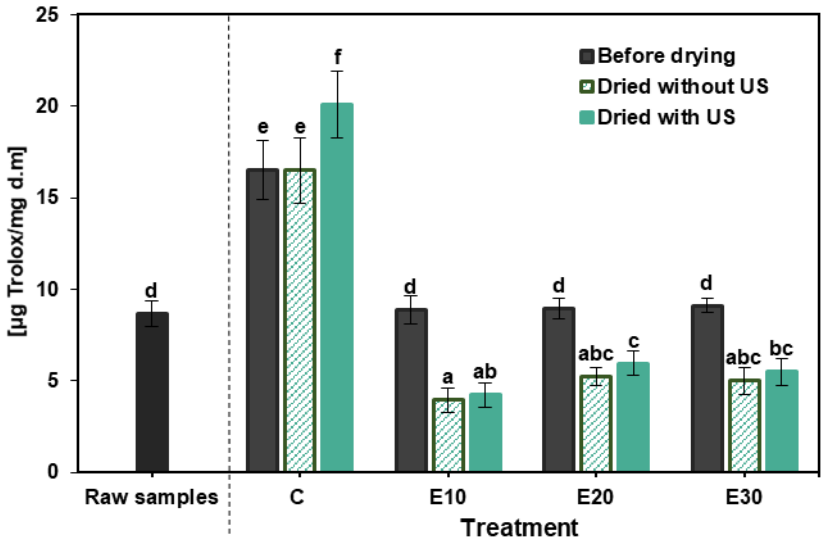

Figure 8. Antioxidant capacity (AC) measured in the raw samples, after ethanol pre-treatment (Before drying), and after drying without and with US application. Different letters indicate significative differences ($p<0.05$) among treatments.

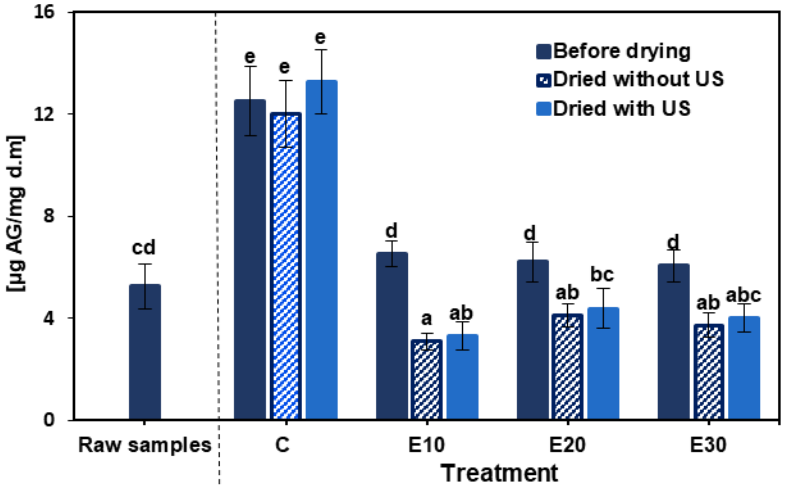

Figure 9. Total phenolic content (TPC) measured in the raw samples, after ethanol pre-treatment (Before drying), and after drying without and with US application. Different letters indicate significative differences ($p<0.05$) among treatments.

The raw apple (cv. Granny Smith) presented an AC of 8.68 ± 0.69 (µg Trolox/mg d.m). The obtained AC were in the range reported for fresh apple in previous works reported by Rodríguez, Santacatalina, Simal, Garcia-Perez, Femenia and Rosselló [54] (7.7 ± 1.7 µg Trolox/mg d.m by using the FRAP assay), and Santacatalina, Rodríguez, Simal, Cárcel, Mulet and García-Pérez [68] (12.9 ± 1.8 µg Trolox/mg d.m by using ABTS assay). Regarding the TPC, the value obtained was 5.24 ± 0.87 (µg AG/mg d.m) or 67.89 ± 13.23 (mg GAE/100g of fresh matter) was in the range reported by Santacatalina, Rodríguez, Simal, Cárcel, Mulet and García-Pérez [68] (10.2 ± 1.9 µg GAE/mg dm) and Vrhovsek, Rigo, Tonon and Mattivi [69] (between 66.2 and 211.9 mg/100 g of fresh matter depending on the apple variety).

These AC and TPC increased 1.9 and 2.4 times respectively (Fig. 8 and 9) after sample immersion in the citric and ascorbic acid solution (ca+aa solution). This was a necessary step due to the high activity of polyphenol oxidase (PPO) enzyme in apple [70], in order to prevent browning effects. In fact, the alternative to ca+aa solution treatment would be mild thermal processing (blanching). However, this process alters the apple structure, being thus preferred to avoid browning by using ca+aa solution. Since apple samples were thin, the used acids enter inside, then contributing to the quantified AC and TPC. In fact, due to the antioxidant characteristics of these acids, it was expected the AC increase. Moreover, it was also reported that ascorbic acid contributes to increase in the TPC measured value in a factor of 0.64 [71].

Compared to fresh sample, AC and TPC content decreased 46% and 50% respectively after ethanol pre-treatments. No significant differences ($p>0.05$) between the pre-treatments time tested were found. These effect of ethanol pret-reatment has

been also observed in other products and compounds such as the allicin content in garlic slices [13]. In any case, the AC and TPC content after pre-treatments were similar to those in the raw apple (figures 8 and 9). Therefore, a new treatment was conducted in order to evaluate if the observed reduction was associated to an extraction of the apple compounds during ethanol immersion or if it only extracted the ca+aa contents initially incorporated. Thus, an ethanol pre-treatment (E30, the largest pre-treatment time tested) was applied directly in the raw samples. In this case, the AC and TPC decreased by 37% and 42%. Consequently, the ethanol pre-treatment can extract not only the citric and ascorbic acids added but some apple antioxidant compounds.

Conventional drying did not affect AC and TPC of Control samples. Regarding samples dried with US (CUS), while TPC content was similar, AC was 21.8% higher than the samples before drying. It means that the application of US during drying could improve the antioxidant compounds extractability, increasing the quantified AC after drying. The obtained results differ from the previous study performed with apple dried with US application [54], were 39.1 ± 2.4% TPC loss was observed. It was related to the cellular damage induced by the combination of higher drying temperature (70 °C) and a greater US power applied (30. kW/m^3).

About the ethanol pre-treated samples, it was observed a significant decrease in the AC and TPC after drying. For the same ethanol pre-treatment, no significant differences ($p>0.05$) for AC and TPC were observed among samples dried without and with US application. Regarding the different ethanol pre-treatments tested, after drying, the lower AC retention (44%) was obtained using a pre-treatment for 10 min dried without US (E10), while the pre-treatment that showed better CA retention (67%) was the ethanol application for 20 min dried with US application (E20US). These samples also presented greater TPC retention, 71% (Figure 9).

The AC and TPC reduction after drying of the pre-treated samples can be related to different phenomena. Firstly, the pre-treatment can increase the exposition of compounds to the oxidation effect of drying air. In fact, the immersion in ethanol can remove the air in the tissues and change the cell walls of the porous structure, high surface area and thin geometry of apple samples[6], which can expose even more the internal constituents. Secondly, the slightly surface browning observed during drying of the pre-treated samples (but not in the control treatment) could indicate that the sample ethanol immersion can remove part of the ascorbic and citric acids previously added, allowing the activity of polyphenol oxidase (PPO). Once there is a direct relation between this enzyme activity and browning reaction, which decrease the phenolic content of apple [70, 72], its activity can partially explain the reduction of both AC and TPC.

Therefore, despite the reduction of the AC and TPC content of the fresh samples through the application of pre-treatments, the percentage retained after drying is still high and comparable with the percentages retained after applying different treatments or processes. For example, in apple cubes (8.8 mm side) after drying at low-temperatures (-10 °C to 10 °C), the total phenolic content retained ranged from 64.9% to 74%, but for all tested temperatures, these values decreased until ~ 59.2% retention when US was applied during drying [68]; while the AC retention was of about 24% to 53.9% for apple cubes dehydrated between -10 °C and 10 °C with US application of 25 and 50 W [73].

4. Conclusions

The combined application of ethanol pre-treatments or the ultrasonically assisted convective drying was evaluated. Both options reduced drying time (55 ± 4% in the case of US application and from 34 ± 5% to 53 ± 4% in the case of ethanol pre-treatments). However, the highest drying time reduction (70 ± 2%) was obtained when both techniques were simultaneously considered. From modelling, it was observed that the higher impact of ethanol pre-treatment was on the external mass transfer resistance, while the US mainly reduce the internal one. The pre-treatments did not significantly affect the sample shrinkage. After drying, samples shrinkage decreased as the ethanol pre-treatment time increased. Moreover, pre-treated samples reached great equilibrium moisture content after rehydration. Dried and rehydrated samples showed a decrease in both elastic and viscous characteristics, being more pronounced in ethanol pre-treated samples. The AC and TPC decreased after ethanol pre-treatments and after drying. In contrast, these were better preserved in samples dried with US application. Therefore, pre-treatments with ethanol highly accelerated the US-assisted drying, when compared to control samples, and no significant impact was observed in the sample shrinkage and viscoelasticity, with good rehydration properties.

5. Acknowledgement

The authors are grateful to the São Paulo Research Foundation (FAPESP, Brazil) for funding the project nº 2016/18052-5; to the National Council for Scientific and Technological Development (CNPq, Brazil) for the productivity grant of P.E.D. Augusto (306557/2017-7); to FONDECYT-CONCYTEC for the M.L. Rojas Ph.D. scholarship (grant contract number 087-2016-FONDECYT). Special thanks to the “Grupo de Análisis y Simulación de Procesos Agroalimentarios (ASPA)” and the MSc. Carlota Moreno for the support provided.

6. References

[1] S.B. Pawar, V.M. Pratape, Fundamentals of Infrared Heating and Its Application in Drying of Food Materials: A Review, Journal of Food Process Engineering 40 (2017) e12308-n/a.
[2] M.L. Rojas, P.E.D. Augusto, Ethanol and ultrasound pre-treatments to improve infrared drying of potato slices, Innovative Food Science & Emerging Technologies 49 (2018) 65-75.
[3] R.L. Monteiro, B.A.M. Carciofi, J.B. Laurindo, A microwave multi-flash drying process for producing crispy bananas, Journal of Food Engineering 178 (2016) 1-11.
[4] N.I. Lebovka, N.V. Shynkaryk, E. Vorobiev, Pulsed electric field enhanced drying of potato tissue, Journal of Food Engineering 78 (2007) 606-613.
[5] M.M.d. Oliveira, A.A.L. Tribst, B.R.d.C. Leite Júnior, R.A.d. Oliveira, M. Cristianini, Effects of high pressure processing on cocoyam, Peruvian carrot, and sweet potato: Changes in microstructure, physical characteristics, starch, and drying rate, Innovative Food Science & Emerging Technologies 31 (2015) 45-53.
[6] M.L. Rojas, P.E.D. Augusto, Ethanol pre-treatment improves vegetable drying and rehydration: Kinetics, mechanisms and impact on viscoelastic properties, Journal of Food Engineering 233 (2018) 17-27.
[7] Ó. Rodríguez, V. Eim, C. Rosselló, A. Femenia, J.A. Cárcel, S. Simal, Application of power ultrasound on the convective drying of fruits and vegetables: effects on quality, Journal of the Science of Food and Agriculture 99 (2019) 966-966.
[8] M.L. Magalhães, S.J.M. Cartaxo, M.I. Gallão, J.V. García-Pérez, J.A. Cárcel, S. Rodrigues, F.A.N. Fernandes, Drying intensification combining ultrasound pre-treatment and ultrasound-assisted air drying, Journal of Food Engineering 215 (2017) 72-77.
[9] M.L. Rojas, I. Silveira, P.E.D. Augusto, Ultrasound and ethanol pre-treatments to improve drying and rehydration of pumpkin, XII CIBIA 2019-Congresso Iberoamericano de Engenharia AlimentarFaro, 2019.
[10] E. Souza da Silva, S.C. Rupert Brandão, A. Lopes da Silva, J.H. Fernandes da Silva, A.C. Duarte Coêlho, P.M. Azoubel, Ultrasound-assisted vacuum drying of nectarine, Journal of Food Engineering 246 (2019) 119-124.
[11] T. Funebo, L. Ahrné, F. Prothon, S. Kidman, M. Langton, C. Skjöldebrand, Microwave and convective dehydration of ethanol treated and frozen apple – physical properties and drying kinetics, International Journal of Food Science & Technology 37 (2002) 603-614.
[12] X. Wang, Y. Feng, C. Zhou, Y. Sun, B. Wu, A.E.A. Yagoub, E.A.A. Aboagarib, Effect of vacuum and ethanol pretreatment on infrared-hot air drying of scallion (Allium fistulosum), Food Chemistry 295 (2019) 432-440.
[13] Y. Feng, C. Zhou, A. ElGasim A. Yagoub, Y. Sun, P. Owusu-Ansah, X. Yu, X. Wang, X. Xu, J. Zhang, Z. Ren, Improvement of the catalytic infrared drying process and quality characteristics of the dried garlic slices by ultrasound-assisted alcohol pretreatment, LWT (2019) 108577.
[14] M.L. Rojas, I. Silveira, P.E.D. Augusto, Improving the infrared drying and rehydration of potato slices using simple approaches: Perforations and ethanol, Journal of Food Process Engineering 42 (2019) e13089.
[15] M.A. Silva, A.M.P. Braga, P.H.S. Santos, Enhancement of fruit drying: the ethanol effect, Proceedings of the 18th International Drying Symposium (IDS 2012)Xiamen, 2012.
[16] F.A.N. Fernandes, S. Rodrigues, J.A. Cárcel, J.V. García-Pérez, Ultrasound-Assisted Air-Drying of Apple (Malus domestica L.) and Its Effects on the Vitamin of the Dried Product, Food and Bioprocess Technology 8 (2015) 1503-1511.
[17] J. Szadzińska, J. Łechtańska, R. Pashminehazar, A. Kharaghani, E. Tsotsas, Microwave-and ultrasound-assisted convective drying of raspberries: Drying kinetics and microstructural changes, Drying Technology (2018) 1-12.
[18] D. Colucci, D. Fissore, C. Rossello, J.A. Carcel, On the effect of ultrasound-assisted atmospheric freeze-drying on the antioxidant properties of eggplant, Food Research International 106 (2018) 580-588.

[19] F.A.N. Fernandes, S. Rodrigues, J.V. García-Pérez, J.A. Cárcel, Effects of ultrasound-assisted air-drying on vitamins and carotenoids of cherry tomatoes, Drying Technology 34 (2016) 986-996.
[20] J.V. Santacatalina, J.R. Soriano, J.A. Cárcel, J.V. Garcia-Perez, Influence of air velocity and temperature on ultrasonically assisted low temperature drying of eggplant, Food and Bioproducts Processing 100 (2016) 282-291.
[21] J. Corrêa, M. Rasia, A. Mulet, J. Cárcel, Influence of ultrasound application on both the osmotic pretreatment and subsequent convective drying of pineapple (Ananas comosus), Innovative Food Science & Emerging Technologies 41 (2017) 284-291.
[22] J. García-Pérez, C. Rosselló, J. Cárcel, S. De la Fuente, A. Mulet, Effect of air temperature on convective drying assisted by high power ultrasound, Defect and Diffusion Forum, Trans Tech Publ, 2007, pp. 563-574.
[23] J.A. Cárcel, J.V. García-Pérez, E. Riera, A. Mulet, Influence of High-Intensity Ultrasound on Drying Kinetics of Persimmon, Drying Technology 25 (2007) 185-193.
[24] C. Ortuño, I. Pérez-Munuera, A. Puig, E. Riera, J.V. Garcia-Perez, Influence of power ultrasound application on mass transport and microstructure of orange peel during hot air drying, Physics Procedia 3 (2010) 153-159.
[25] J. Cárcel, J. García-Pérez, J. Benedito, A. Mulet, Food process innovation through new technologies: Use of ultrasound, Journal of Food Engineering 110 (2012) 200-207.
[26] S. De la Fuente-Blanco, E. Riera-Franco de Sarabia, V.M. Acosta-Aparicio, A. Blanco-Blanco, J.A. Gallego-Juárez, Food drying process by power ultrasound, Ultrasonics 44, Supplement (2006) e523-e527.
[27] A.C. Miano, A. Ibarz, P.E.D. Augusto, Mechanisms for improving mass transfer in food with ultrasound technology: Describing the phenomena in two model cases, Ultrasonics Sonochemistry 29 (2016) 413-419.
[28] T.J. Mason, L. Paniwnyk, J.P. Lorimer, The uses of ultrasound in food technology, Ultrasonics Sonochemistry 3 (1996) S253-S260.
[29] J.V. García-Pérez, J.A. Cárcel, S. de la Fuente-Blanco, E. Riera-Franco de Sarabia, Ultrasonic drying of foodstuff in a fluidized bed: Parametric study, Ultrasonics 44, Supplement (2006) e539-e543.
[30] M.P. Martins, E.J. Cortés, V. Eim, A. Mulet, J.A. Cárcel, Stabilization of apple peel by drying. Influence of temperature and ultrasound application on drying kinetics and product quality, Drying Technology 37 (2019) 559-568.
[31] J. Schindelin, I. Arganda-Carreras, E. Frise, V. Kaynig, M. Longair, T. Pietzsch, S. Preibisch, C. Rueden, S. Saalfeld, B. Schmid, Fiji: an open-source platform for biological-image analysis, Nature methods 9 (2012) 676.
[32] L.E. Kurozawa, M.D. Hubinger, K.J. Park, Glass transition phenomenon on shrinkage of papaya during convective drying, Journal of Food Engineering 108 (2012) 43-50.
[33] P.O. Vargas, N.R. Pereira, A.O. Guimarães, W.R. Waldman, V.R. Pereira, Shrinkage and deformation during convective drying of calcium alginate, LWT 97 (2018) 213-222.
[34] M.A. Rao, J.F. Steffe, Viscoelastic properties of foods, Elsevier Applied Science New York1992.
[35] F.G.K. Vieira, G.D.S.C. Borges, C. Copetti, R.D.D.M.C. Amboni, F. Denardi, R. Fett, Physico-chemical and antioxidant properties of six apple cultivars (Malus domestica Borkh) grown in southern Brazil, Scientia Horticulturae 122 (2009) 421-425.
[36] R. Re, N. Pellegrini, A. Proteggente, A. Pannala, M. Yang, C. Rice-Evans, Antioxidant activity applying an improved ABTS radical cation decolorization assay, Free radical biology and medicine 26 (1999) 1231-1237.
[37] S. Rodrigues, F.A.N. Fernandes, J.V. García-Pérez, J.A. Cárcel, Influence of Ultrasound-Assisted Air-Drying and Conventional Air-Drying on the Activity of Apple Enzymes, Journal of Food Processing and Preservation 41 (2017) e12832.

[38] C. Moreno, C. Brines, A. Mulet, C. Rosselló, J. Cárcel, Antioxidant potential of atmospheric freeze-dried apples as affected by ultrasound application and sample surface, Drying Technology 35 (2017) 957-968.
[39] E.M.G.C. do Nascimento, A. Mulet, J.L.R. Ascheri, C.W.P. de Carvalho, J.A. Cárcel, Effects of high-intensity ultrasound on drying kinetics and antioxidant properties of passion fruit peel, Journal of Food Engineering 170 (2016) 108-118.
[40] S. Rodrigues, L.C.A. Silva, A. Mulet, J.A. Cárcel, F.A.N. Fernandes, Development of dried probiotic apple cubes incorporated with Lactobacillus casei NRRL B-442, Journal of Functional Foods 41 (2018) 48-54.
[41] F. Vallespir, Ó. Rodríguez, J.A. Cárcel, C. Rosselló, S. Simal, Ultrasound assisted low-temperature drying of kiwifruit: Effects on drying kinetics, bioactive compounds and antioxidant activity, Journal of the Science of Food and Agriculture 99 (2019) 2901-2909.
[42] Z. Erbay, F. Icier, A Review of Thin Layer Drying of Foods: Theory, Modeling, and Experimental Results, Critical Reviews in Food Science and Nutrition 50 (2010) 441-464.
[43] J. Bon, C. Rosselló, A. Femenia, V. Eim, S. Simal, Mathematical Modeling of Drying Kinetics for Apricots: Influence of the External Resistance to Mass Transfer, Drying Technology 25 (2007) 1829-1835.
[44] A. Vega-Gálvez, M. Miranda, C. Bilbao-Sáinz, E. Uribe, R. Lemus-Mondaca, Empirical modeling of drying process for apple (Cv. Granny Smith) slices at different air temperatures, Journal of Food Processing and Preservation 32 (2008) 972-986.
[45] J. Crank, The mathematics of diffusion, Oxford university press1979.
[46] G.E. Page, Factors Influencing the Maximum Rates of Air Drying Shelled Corn in Thin layers, Purdue University, Ann Arbor, 1949.
[47] R. Simpson, C. Ramírez, H. Nuñez, A. Jaques, S. Almonacid, Understanding the success of Page's model and related empirical equations in fitting experimental data of diffusion phenomena in food matrices, Trends in Food Science & Technology 62 (2017) 194-201.
[48] M. Peleg, Characterization of the stress relaxation curves of solid foods, Journal of Food Science 44 (1979) 277-281.
[49] M. Peleg, M.D. Normand, Comparison of two methods for stress relaxation data presentation of solid foods, Rheologica Acta 22 (1983) 108-113.
[50] J.L.G. Corrêa, A.M.P. Braga, M. Hochheim, M.A. Silva, The Influence of Ethanol on the Convective Drying of Unripe, Ripe, and Overripe Bananas, Drying Technology 30 (2012) 817-826.
[51] M.G. Silva, R.M.S. Celeghini, M.A. Silva, Effect of ethanol on the drying characteristics and on the coumarin yield of dried guaco leaves (Mikania laevigata SCHULTZ BIP. EX BAKER), Brazilian Journal of Chemical Engineering 35 (2018) 1095-1104.
[52] Y. Tatemoto, R. Mizukoshi, W. Ehara, E. Ishikawa, Drying characteristics of food materials injected with organic solvents in a fluidized bed of inert particles under reduced pressure, Journal of Food Engineering 158 (2015) 80-85.
[53] A.M.P. Braga, M.P. Pedroso, F. Augusto, M.A. Silva, Volatiles Identification in Pineapple Submitted to Drying in an Ethanolic Atmosphere, Drying Technology 27 (2009) 248-257.
[54] Ó. Rodríguez, J.V. Santacatalina, S. Simal, J.V. Garcia-Perez, A. Femenia, C. Rosselló, Influence of power ultrasound application on drying kinetics of apple and its antioxidant and microstructural properties, Journal of Food Engineering 129 (2014) 21-29.
[55] G.K. Vagenes, D. Marinos-Kouris, Drying kinetics of apricots, Drying Technology 9 (1991) 735-752.
[56] J.V. García-Pérez, C. Rosselló, J.A. Cárcel, S. De la Fuente, A. Mulet, Effect of Air Temperature on Convective Drying Assisted by High Power Ultrasound, Defect and Diffusion Forum 258-260 (2007) 563-574.
[57] J.A. Cárcel, J.V. Garcia-Perez, E. Riera, A. Mulet, Improvement of Convective Drying of Carrot by Applying Power Ultrasound—Influence of Mass Load Density, Drying Technology 29 (2011) 174-182.

[58] C. Ozuna, T. Gómez Álvarez-Arenas, E. Riera, J.A. Cárcel, J.V. Garcia-Perez, Influence of material structure on air-borne ultrasonic application in drying, Ultrasonics Sonochemistry 21 (2014) 1235-1243.
[59] M. Blasco, J.V. García-Pérez, J. Bon, J.E. Carreres, A. Mulet, Effect of Blanching and Air Flow Rate on Turmeric Drying, Food Science and Technology International 12 (2006) 315-323.
[60] A. Mulet, Drying modelling and water diffusivity in carrots and potatoes, Journal of Food Engineering 22 (1994) 329-348.
[61] J.V. García-Pérez, J.A. Cárcel, J. Benedito, A. Mulet, Power Ultrasound Mass Transfer Enhancement in Food Drying, Food and Bioproducts Processing 85 (2007) 247-254.
[62] H.T. Sabarez, J.A. Gallego-Juarez, E. Riera, Ultrasonic-Assisted Convective Drying of Apple Slices, Drying Technology 30 (2012) 989-997.
[63] S.M. Beck, H. Sabarez, V. Gaukel, K. Knoerzer, Enhancement of convective drying by application of airborne ultrasound – A response surface approach, Ultrasonics Sonochemistry 21 (2014) 2144-2150.
[64] M.L. Rojas, P.E.D. Augusto, Microstructure elements affect the mass transfer in foods: The case of convective drying and rehydration of pumpkin, LWT 93 (2018) 102-108.
[65] A.C. Miano, J. da Costa Pereira, B. Miatelo, P.E.D. Augusto, Ultrasound assisted acidification of model foods: Kinetics and impact on structure and viscoelastic properties, Food Research International 100 (2017) 468-476.
[66] W. Zhao, Y. Fang, Q.-A. Zhang, Y. Guo, G. Gao, X. Yi, Correlation analysis between chemical or texture attributes and stress relaxation properties of 'Fuji' apple, Postharvest Biology and Technology 129 (2017) 45-51.
[67] L. Mayor, R. Cunha, A. Sereno, Relation between mechanical properties and structural changes during osmotic dehydration of pumpkin, Food Research International 40 (2007) 448-460.
[68] J.V. Santacatalina, O. Rodríguez, S. Simal, J.A. Cárcel, A. Mulet, J.V. García-Pérez, Ultrasonically enhanced low-temperature drying of apple: Influence on drying kinetics and antioxidant potential, Journal of Food Engineering 138 (2014) 35-44.
[69] U. Vrhovsek, A. Rigo, D. Tonon, F. Mattivi, Quantitation of Polyphenols in Different Apple Varieties, Journal of Agricultural and Food Chemistry 52 (2004) 6532-6538.
[70] M. Murata, M. Tsurutani, M. Tomita, S. Homma, K. Kaneko, Relationship between apple ripening and browning: changes in polyphenol content and polyphenol oxidase, Journal of Agricultural and Food Chemistry 43 (1995) 1115-1121.
[71] D.K. Asami, Y.-J. Hong, D.M. Barrett, A.E. Mitchell, Comparison of the Total Phenolic and Ascorbic Acid Content of Freeze-Dried and Air-Dried Marionberry, Strawberry, and Corn Grown Using Conventional, Organic, and Sustainable Agricultural Practices, Journal of Agricultural and Food Chemistry 51 (2003) 1237-1241.
[72] M. Amiot, M. Tacchini, S. Aubert, J. Nicolas, Phenolic composition and browning susceptibility of various apple cultivars at maturity, Journal of Food Science 57 (1992) 958-962.
[73] J.V. Santacatalina, M. Contreras, S. Simal, J.A. Cárcel, J.V. Garcia-Perez, Impact of applied ultrasonic power on the low temperature drying of apple, Ultrasonics Sonochemistry 28 (2016) 100-109.

APPENDIX VII: Incorporation of microencapsulated hydrophilic and lipophilic nutrients into foods by using ultrasound as a pre-treatment for drying: A prospective study

ROJAS, M. L., ALVIM, I. D., & AUGUSTO, P. E. D. (2019).
ULTRASONICS SONOCHEMISTRY, 54, 153-161

Ultrasonics - Sonochemistry 54 (2019) 153–161

Contents lists available at ScienceDirect

Ultrasonics - Sonochemistry

journal homepage: www.elsevier.com/locate/ultson

Incorporation of microencapsulated hydrophilic and lipophilic nutrients into foods by using ultrasound as a pre-treatment for drying: A prospective study

Meliza Lindsay Rojas[a,*], Izabela Dutra Alvim[c], Pedro Esteves Duarte Augusto[a,b,*]

[a] Department of Agri-food Industry, Food and Nutrition (LAN), Luiz de Queiroz College of Agriculture (ESALQ), University of São Paulo (USP), Piracicaba, SP, Brazil
[b] Food and Nutrition Research Center (NAPAN), University of São Paulo (USP), Piracicaba, SP, Brazil
[c] Technology Center of Cereal and Chocolate, Food Technology Institute (ITAL), Campinas, SP, Brazil

ARTICLE INFO

Keywords:
Ultrasound
Microencapsulated nutrients
Iron
Carotenoids
Food matrix
Convective drying

ABSTRACT

The present work proposes using the ultrasound technology to incorporate microencapsulated nutrients during pre-treatments for drying of food products. Both hydrophilic and lipophilic nutrients were evaluated: incorporation of microcapsules of iron (obtained by spray drying using maltodextrin as wall material) and carotenoids (obtained by hot emulsification and solidification using hydrogenated palm oil as wall material). The ultrasound pre-treatment was applied in water and ethanol, where the microcapsules were dispersed, and food samples were immersed. Pumpkin and apple were selected as suitable food material to perform the iron and carotenoid incorporation, respectively. Ultrasound allowed more homogeneous iron incorporation in pumpkin. The iron content increased more than 1000% in pre-treated samples compared to control. In the same manner, carotenoid content increased in about 430% when ultrasound was applied. After drying, the carotenoid content decreased by 65% in control samples. However, better carotenoid retention was obtained after drying in ultrasound processed samples. The results show that pre-treatment with ultrasound can be used to incorporate nutrients into the food matrix, increasing not only the incorporated quantity but also promoting their preservation. Nevertheless, future studies must be performed to determine the nutrient bioavailability and bioaccessibility.

1. Introduction

The concern about nutritional deficiencies in population generates a growing interest in improving the nutritional quality of food. The purpose of fortification and/or enrichment of food is preventing or correcting a demonstrated deficiency (dietary, biochemical, functional and/or clinical) of one or more nutrients in the population or specific population groups. The international community is focused on the most prevalent deficiencies, such as Vitamin A, iodine and iron [1]. In addition to vulnerable groups (such as young children, elderly or pregnant women), nutritional requirements and/or deficiencies are affected by culture and lifestyle. For example, in athletes and vegetarians, iron deficiencies may increase.

Consequently, there is a growing demand for food fortification. Among many possibilities, such as genetic improvement or direct addition on formulated products, the incorporation of nutrients in structured foods, such as fruits and vegetables, is particularly difficult. The complex structure, different kind of tissues and cells, and the solubility behaviour of the nutrients can be cited as challenges to the mass transfer phenomena.

In this scenario, the ultrasound technology (US) has been proposed to improve different mass transfer unit operations, being thus a possibility to enhance the nutritional quality of foods. Moreover, this technology has been used as a pre-treatment for food drying, with the aim of improving the process and dry product properties/characteristics. Different fluids (medium in which the food is immersed) are used to transmit the acoustic waves to the food, such as water [2,3], osmotic solutions [4] or ethanol [5]. Therefore, in addition to improving drying, ultrasound pre-treatment can be used to incorporate compounds of interest (nutrients) into the food matrix, improving the nutritional quality of dry products. This work was developed considering this hypothesis.

Iron deficiency is the most prevalent nutritional deficiency in the world and the main cause of anemia [6,7]. Therefore, a diet rich in this mineral is recommended, while the administration of iron supplements, the fortification and/or enrichment of foods with this mineral are alternatives [8].

On the other hand, β-carotene, α-carotene and β-cryptoxanthin, are

* Corresponding authors at: Avenida Pádua Dias, 11 – Piracicaba/SP – 13418-900, Brazil.
E-mail addresses: mrojas@usp.br (M.L. Rojas), pedro.ed.augusto@usp.br (P.E.D. Augusto).

https://doi.org/10.1016/j.ultsonch.2019.02.004
Received 14 December 2018; Received in revised form 2 February 2019; Accepted 3 February 2019
Available online 05 February 2019

sources of provitamin A, of which β-carotene is the major provitamin A carotenoid. The health benefits of carotenoids once converted to vitamin A, including maintenance of normal eye health, epithelial function, embryonic development, and immune system function. As consequence, there is an increase of the demand for the addition of carotenoids into food products [9].

Different nutrients were used for food fortification under solution. For example, Fito, Chiralt, Betoret, Gras, Cháfer, Martínez-Monzó, Andrés and Vidal [10] incorporated controlled quantities of calcium and iron (using isotonic solutions of sucrose, iron gluconate and calcium gluconate) in the porous structure of fruit and vegetable. Deng and Zhao [11] used calcium solutions in apple. Lopez Barrera, Gaur, Andrade, Engeseth, Nielsen and Helferich [8], fortified vinegar by directly adding the iron into the vinegar. Rerkasem, Fukai and Huang [12] used iron solution to fortified parboiled rice, and Miano and Augusto [13] used iron solutions with and without US to incorporate iron in beans during its hydration.

However, among different challenges to incorporate nutrients into the food matrix, some common problems are nutrient degradation, sensorial changes in food products, and the different chemical affinities of nutrient and food products (affecting solubility).

Iron is susceptible to oxidation and it may produce adverse organoleptic changes (colour, odour and taste) in food products [7]. Similarly to iron, carotenoids are unstable and present multiple mechanisms of degradation [9]. However, differently to iron, carotenoids are not water soluble, which difficult their incorporation into food matrix. An alternative to prevent deterioration during processing, undesired organoleptic changes in fortified food, is the nutrient microencapsulation [9].

Different approaches have been used to incorporate encapsulated nutrients into food products. Bryszewska, Tomás-Cobos, Gallego, Villalba, Rivera, Taneyo Saa and Gianotti [7] used iron microcapsules for bread fortification and corroborated higher iron availability. Xu, Cheng, Liu and Zhu [14] evaluated the effect of encapsulated bioactive compounds in the degradation and oxidation of dried minced pork slices. In fortified milk, compared to no-encapsulated iron, the iron microcapsules results in higher accessibility since they were less affected by the presence of inhibitors [15]. These products are formulated/restructured or liquid, which facilitates the particle incorporation and distribution through the product. Furthermore, carotenoids were incorporated into pineapple [16] and into mango tissue [17] by using an emulsion as an osmotic agent composed, among others, by piquin pepper oleoresin, Arabic gum, sucrose and inulin. Therefore, oleoresin emulsions were directly used, but not previously elaborated microcapsules. In addition, the obtained osmotic dehydrated product is not a stable product being necessary to be dried to achieve microbiological stability. In fact, the authors freeze-dried the product impregnated with microcapsules, in special to allow its further evaluation. However, drying process was not evaluated. Recently, Vatankhah and Ramaswamy [18] studied the high pressure processing to impregnate a coconut oil emulsion into fruit tissues. However, the obtained impregnated products are high moisture and not microbiologically stable, being necessary to be dried.

In fact, an important concern is the impact of unit operations on the stability of nutrients in fortified foods, once the raw material is rarely stable and food processing is needed in order to guarantee both safety and stability. The degradation of nutrients is one of the main negative consequences of conventional drying processes. However, the use of US pre-treatments showed good results in preserve the nutrients naturally present in carrot [19,20] and papaya [4]. Therefore, probably the use of US could also contribute to preserving the incorporated nutrients.

Therefore, the present work will cover the incorporation of nutrient microcapsules inside a complex and natural food matrix by using US as pre-treatment for convective drying. In this work, two different nutrients (iron hydrophilic microcapsules and carotenoid lipophilic microcapsules) were incorporated in two food matrix (apple and pumpkin) using ultrasound, being also evaluated the nutrient preservation after convective drying.

2. Material and methods

2.1. Nutrients and raw material

The efficacy of nutrient fortification depends on many factors, such as the characteristics of the nutrient (type, status, encapsulation, solubility, particle size among others), and the characteristics of the food matrix (composition, structure, consumption form). In the design of fortified food, it is necessary to select the appropriate combination of fortificant and vehicle, taking into account the target population [21].

Different iron salts have been studied and incorporated into food products. Among these, the ferrous sulphate is cheap and efficiently absorbed [21], being chosen in the present work. Paprika oleoresin was used as a source of carotenoids such as capsanthin, capsorubin, β-carotene, zeaxanthin, and β -crypthoxanthin [22,23].

Ultrasound pre-treatments to improve food drying were already carried out using ethanol and water as wave transmission medium. The drying improvement is related to both structural changes and incorporation of solvent into the matrix. In this work, it was taken advantage of these pre-treatments to incorporate not only water and ethanol but also nutrients in the food matrix.

Two food products were selected to perform the experiments.

On the one hand, pumpkin (*Cucurbita moschata* Duch) due to its high carotenoid content, is considered a good source of β-carotene (known as a promotor of iron absorption). Therefore, this vegetable was selected to perform the iron incorporation experiments. Pumpkin cylinders of 1.5 cm diameter × 1 cm high were obtained from the same orange flesh part.

On the other hand, green apple (Var. Granny Smith) present low carotenoid content, thus being selected to perform carotenoid incorporation. The apple fruits were longitudinally cut in half, then slices of 0.2 cm thickness were obtained. After cutting, the slices were immediately blanched for 5 s using boiling water at 98.8 °C, followed by 30 s of cooling at T < 5 °C, in order to avoid browning.

2.2. Nutrient incorporation using pre-treatments for convective drying

Iron, in ferrous sulphate, is a hydrophilic nutrient, while carotenoids, in paprika oleoresin, are lipophilic nutrients. Therefore, different approaches of microencapsulation and incorporation into the food matrix (rich in water) are needed.

2.2.1. Hydrophilic nutrient: Iron microcapsules elaboration and incorporation

Iron hydrophilic microcapsules were produced by spray drying process, similarly to Alvim, Stein, Koury, Dantas and Cruz [24]. Iron microcapsules were prepared from a dispersion of maltodextrin (0.23 g/g dry matter) and ferrous sulfate (0.07 g/g dry matter) in filtered water. The mixture components were homogenized using a magnetic stirrer. Subsequently, the homogenised dispersion was dried using a laboratory scale spray-dryer (Mini Spray Dryer Labplant UK Ltd, model SD 06, Hunmanby, UK) with an atomizer nozzle of 1 mm diameter, atomization pressure of 4 bar and 150 ± 3 °C temperature inlet. The feed rate was adjusted to guarantee a temperature outlet of 80 ± 3 °C (variable flow rate up to 35.3 mL/min). Powdered microparticles presented an iron content of 4.35 ± 0.20 g/100 g and a particle mean diameter of 15.36 ± 0.23 μm (Fig. 1).

The microparticles mean diameter and size distribution were measured by laser diffraction, according to Fadini, Alvim, Ribeiro, Ruzene, Silva, Queiroz, Miguel, Chaves and Rodrigues [25]. The microscopy was carried out using an optical microscope (L100 Bioval, Curitiba) with a halogen lamp of 20 W coupled to a portable colour camera of 5 MP.

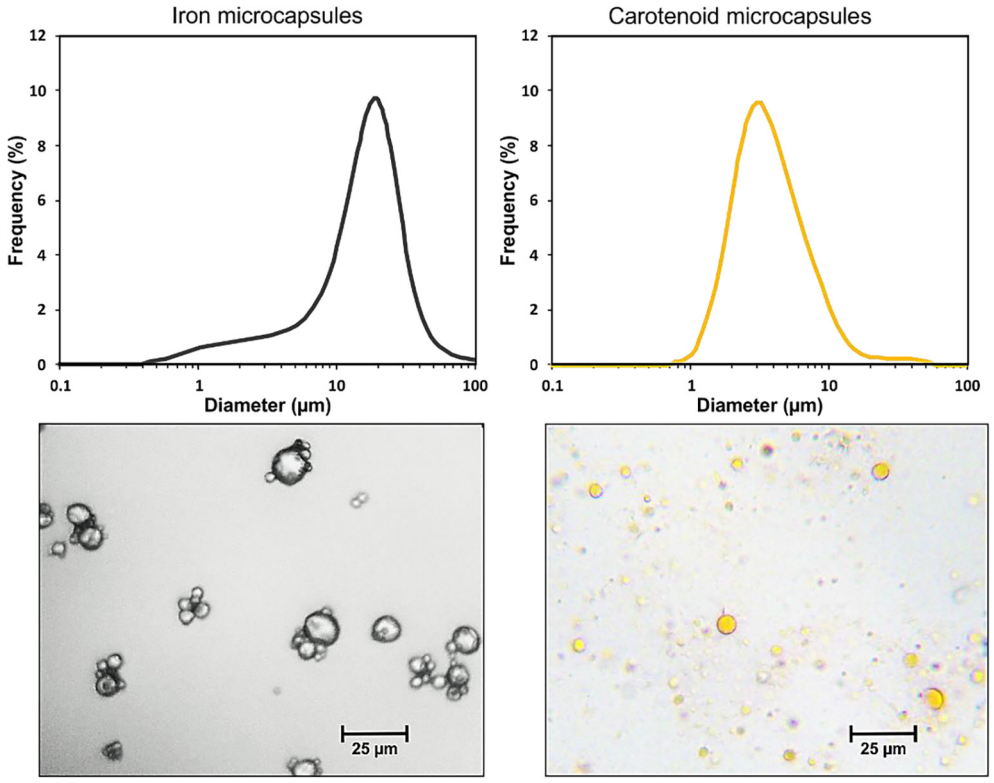

Fig. 1. Particle size distribution (up) and optical microscopy (down) of the used iron and carotenoid microcapsules.

Once both maltodextrin and ferrous sulphate are hydrophilic, water cannot be used as the medium to incorporate this nutrient into the food matrix. Therefore, ethanol was used to this. In fact, the ethanol incorporation into vegetables was already proposed to enhance drying process and product properties [5,26,27], being this an extra advantage of the present proposal. In addition to Control samples (without any pre-treatment), pumpkin cylinders (~140 g) were immersed in a glass beaker containing 500 mL of an ethanolic dispersion containing iron microcapsules (0.05 g/100 mL of ethanol) for 30 min, without (E) and with ultrasound application (E + US).

The E + US pre-treatment was performed using an ultrasonic bath containing 6 L of distilled water (Q13/25, Ultronique Brazil; frequency of 25 kHz), containing the glass beaker. The temperature was kept at 24–26 °C during processing using a heat exchanger inside the ultrasonic bath and an external water bath. The location of the samples inside the ultrasonic bath was evaluated by taking into account the good practices described by Vinatoru [28] to assure the highest ultrasonic intensity. The ultrasonic volumetric power was measured inside the glass beaker containing 500 mL of ethanol, through the calorimetric method [29,30]). The value of 80 W/L was determined.

After pre-treatment, the samples were rinsed superficially with 500 mL of ethanol to eliminate the superficial iron microcapsules, and the pre-treated samples were placed to dry according to the described in Section 2.3.

2.2.2. Lipophilic nutrient: Carotenoid microcapsules elaboration and incorporation

Carotenoid microcapsules were produced using a solid-lipid system that includes hot emulsification followed by cooling treatment (adapted from Jaspart, Bertholet, Piel, Dogné, Delattre and Evrard [31]. It was used a mixture of 100% hydrogenated palm oil A. Azevedo Óleos Vegetais, Itupeva Brazil) with melting point of 58.3 ± 0.2 °C, and paprika oleoresin (Citromax, Guarulhos, Brazil) (10 g/100 g of mixture). The palm fat was initially melted using a microwave (MTAS41, Midea, Joinville, Brazil) and then added with oleoresin under manual stirring until complete dispersion between the materials. The mixture was added to the heated water containing Tween 80 (Labsynth, Diadema, Brazil) (4 g/100 g of solution), maintained at 80 °C in a jacketed reactor (Lauda Thermal Bath ECOLINE RE 212, Lauda-Königshofen, Germany). The hot emulsification of that mixture was done using an ultraturrax (T 18 basic, IKA, Staufenim-Breisgau, Germany) at 15 000 revolutions per minute (rpm) for 15 min. The formed emulsion was immediately poured into chilled water at 7 ± 2 °C and stirred for 10 min until complete hardening of the particles (mechanical stirrer Lab Egg R11, IKA, StaufenimBreisgau, Germany). The formed emulsion of carotenoid microcapsules presented a total carotenoid content of 77.8 mg/100 g and a particle mean diameter of 3.11 ± 0.24 μm (Fig. 1).

The microparticles mean diameter, size distribution and microscopical evaluation were carried similarly to the iron microparticles.

Once both hydrogenated palm oil and paprika oleoresin are lipophilic, ethanol cannot be used as the medium to incorporate this nutrient into the food matrix. Therefore, water was used to this.

In addition to Control samples (blanched samples without any pre-treatment), apple slices (~60 g) were immersed in 1 L of an aqueous dispersion containing carotenoid microcapsules (100 g/L of water) for 30 min without (W) and with ultrasound application (W + US).

The same ultrasonic bath described above was used. The temperature of the sample was kept at 24–27 °C during the process using a heat exchanger inside the ultrasonic bath. The location of the samples inside the ultrasonic bath was by taking into account the good practices described by Vinatoru [28] to assure the highest ultrasonic intensity. However, the used volumetric power was 118 W/L – measured inside the polyethylene vessel containing 1 L of water by the calorimetric method). The volumetric power difference between both experiments is due to using other materials and conditions, such as volume of distilled water in the ultrasonic bath (4 L), geometry and material of containers, and microcapsule dispersion medium (water), mainly due to the difference of sample sizes and geometries.

After pre-treatment, the samples were rinsed superficially with 500 mL of distilled water to eliminate the superficial carotenoid

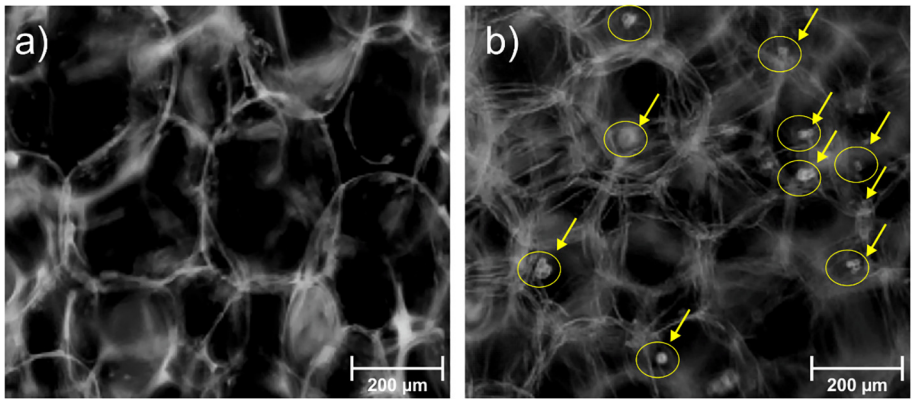

Fig. 2. Optical microscopy of the (a) *in-natura* pumpkin and (b) E samples (pumpkin cylinders treated for 30 min in ethanol containing iron microparticles.

microcapsules. Pre-treated samples were placed to dry according to the described in Section 2.3.

2.3. Drying

The drying process was performed using air at 50 °C and 0.8 ± 0.1 $m{\cdot}s^{-1}$ velocity, using an oven with circulation and air renewal (MA 035, Marconi, São Paulo, Brazil). On the one hand, the pumpkin samples were dried to a constant weight for the evaluation of the iron content. On the other hand, to evaluate the carotenoid content, the apple samples were dried up to a moisture of 25% w.b., to prevent effects of overdrying and facilitate the carotenoid extraction. The moisture during drying was controlled by mass balance using the moisture after pre-treatments and the sample mass along the drying time. The initial, after pre-treatments and after drying moisture contents were measured by completely drying crushed samples at 105 °C using a moisture analyser (MX-50, A&D Company, Tokyo, Japan).

2.4. Carotenoid quantification

The total carotenoid content was determined according to the spectrophotometric method described by Ordoñez-Santos and Ledezma-Realpe [32], Potosí-Calvache, Vanegas-Mahecha and Martínez-Correa [33] with some modifications. The solvent solution used for carotenoid extraction was composed by ethanol 99.5% (Êxodo Científica, São Paulo) and hexane 98.5% (Labsynth, São Paulo) in a proportion of 4:3 ethanol:hexane (determined after evaluation of different solvents and proportions).

For the control and pre-treated samples, ~ 0.7 g and for the dried samples, and ~0.25 g were weighed and placed in glass tubes (tightly capped and lined with aluminium foil for protecting it from oxygen and light). Then, 21 mL of solvent solution was added. The samples with solvent solution were crushed for 1 min using a rotor–stator homogenizer (Superohm, São Paulo). The homogenized samples were stirred at 250 rpm for 30 min using an orbital shaker cold bath (2 °C). After this, 2 mL of distilled water was added to each tube. They were stirred for 15 min and left at rest for 5 min to separate the phases (aqueous phase and hexanoic phase).

The absorbance of the hexane phase, which contained the extracted carotenoid), was read at 450 nm (FEMTO 600 S, São Paulo), using hexane to calibrate. The total carotenoid content was then calculated according to Eq. (1).

$$\frac{TC}{g} = \frac{A_{450} \times 536.85 \times V}{m \times 137.4} \quad (1)$$

where 536.85 g/mol is the molecular weight of β -carotene, V is the volume (mL) of hexane phase, m is the sample mass, and 137.4 mM^{-1} is the extinction coefficient for β -carotene in hexane.

2.5. Iron quantification

After performing the pre-treatments and drying process, dried pumpkin samples were milled using a stainless-steel analytical mill (IKA A11 basic analytical mill, Germany) before determining the iron content. The iron content was determined by an energy dispersive X-ray fluorescence spectrometer (Shimadzu EDX-720, Japan) following the methodology of Tezotto, Favarin, Paula Neto, Gratão, Azevedo and Mazzafera [34] and Paltridge, Milham, Ortiz-Monasterio, Velu, Yasmin, Palmer, Guild and Stangoulis [35].

2.6. Experimental design and statistical analysis

A completely randomised design (CRD) was conducted. All processes and analyses were performed at least 3 times. The analysis of variance (ANOVA) was carried out with a significance level of 5%. To determine statistical differences among means of treatments, Tukey test was used. To determine differences among the same treatment before and after drying, the T-test for two related samples (Paired-Samples T test) was used. Statistical analyses were determined using the IBM SPSS Statistics 23 software (IBM SPSS, USA).

3. Results and discussion

3.1. Iron incorporation

Fig. 2 shows the optical microscopy of the pumpkin *in-natura* and E samples (pumpkin cylinders treated for 30 min in ethanol containing iron microparticles). The microscopies of samples E + US (pumpkin cylinders treated for 30 min with US using ethanol containing iron microparticles) and dried products were not shown, due to severe structure modifications and the own colour of the pumpkin (deep orange) and microparticles (white), making difficult to identify de iron microcapsules. In Fig. 2b, iron microcapsules are highlighted inside the pumpkin tissue, which shows wrinkled cells as a consequence of ethanol.

In-natura pumpkin presented an iron content of 0.77 ± 0.04 g/100 g, which is in accordance with the reported by USDA [36], NEPA-UNICAMP [37] for different pumpkin species.

Considering that iron is not degraded by drying process, its quantity was determined after drying. Fig. 3 shows the iron content of control and pre-treated samples after drying, correcting the value to 25% wet basis (w.b) moisture. Compared to control samples, the iron content increased after pre-treatments in about 2186% for E and 1562% for E + US pre-treatments. No significant differences ($p > 0.05$) were obtained regarding the incorporated iron quantity with and without ultrasound (i.e., between E and E + US pre-treatments). However, the US improve the homogeneity of the added iron content – note that the standard deviation bar in Fig. 3 for E samples was higher, which is an

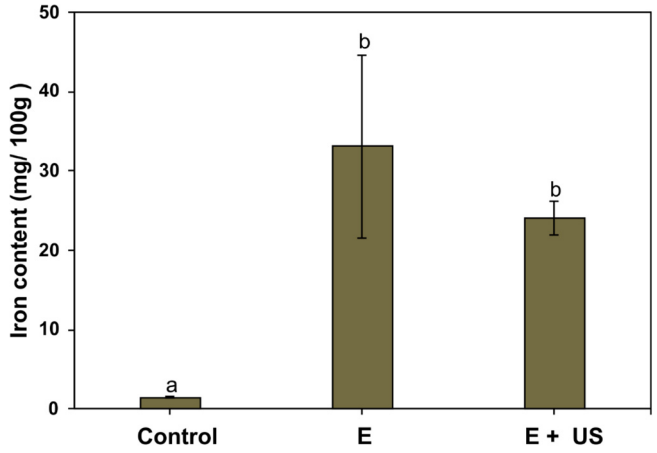

Fig. 3. Iron content of the dried Control and pre-treated samples (E and E + US), in mg per 100 g of sample corrected to a moisture of 25% w.b. Vertical bars are the ± standard deviation, different letters indicate significant differences ($p < 0.05$) among treatments.

interesting result from an industrial perspective.

In fact, when the iron microcapsules were added to ethanol, a tendency to form agglomerates was observed. Consequently, the iron incorporation could not be uniform among replicates. Furthermore, phase separation can take place. On the contrary, when US was applied, it allowed keeping the microcapsules uniformly dispersed in the ethanol during processing. It is worth mention that uniformity is an important characteristic for industrial processing.

The US application using ethanol medium to incorporate iron microcapsules is presented here for the first time.

Some previous studies used US to incorporate minerals into foods but using other medium and processes. For example, Deng and Zhao [11] by using osmotic solutions with calcium, evaluated the calcium incorporation in apple cylinders during osmotic dehydration assisted by US. Mashkour, Maghsoudlou, Kashaninejad and Aalami [38] studied the impregnation of iron in whole potatoes using US pre-treatment followed by vacuum impregnation. Compared to only vacuum impregnation, the iron content increased about 72% in samples pre-treated with US. On the other hand, Miano and Augusto [13] took advantage of the hydration process assisted by US to incorporate iron in beans. The samples processed with US increased iron content by 74% compared to those without US and 2659% compared to Control. The higher amount of iron incorporated in these studies was because they used iron solutions. However, the inconvenient of using iron in solutions are principally the possible changes of colour, flavour or interactions with other compounds of food. The colour of iron compounds is often a critical factor when fortifying lightly coloured foods [1]. In this work, any visual differences were identified among the pumpkin control and samples with iron incorporated (Fig. 6), probably due to its strong orange colour and the white colour of microparticles.

The iron content (Fig. 3) of pre-treated samples (E and E + US) varied from 24 to 33 mg/100 g at 25% w.b, which were similar or superior to the iron quantity reported in foods considered sources of iron. For example, the liver of chicken presents an iron content of 32.1 mg/100 g, spinach (5 mg/100 g), raw striped beans (16.4 mg/100 g) [37] – for comparison, their iron quantities were reported with moisture corrected to 25% w.b. However, the consumption of these products is made after any process and/or in higher moisture conditions, which decrease the amount of iron intake.

According to the Institute of Medicine [39], it is recommended a tolerable iron intake of 40 mg/day for children and adolescents while 45 mg/day for adolescents and adults. The amount in which the iron becomes toxic is difficult to express since it is related to the dietary reference values. These values are complex to define since it depends on different factors based on the population group (which determine specific requirements) and the ratio of intestinal iron absorption (which depends on the type of diet, iron status and genetic responses of the subject) [21]. Consequently, the iron amount reported in this work represents a possibility to counteract iron deficiency without risk of toxicity, since the enriched dry food here obtained presents an iron concentration in the same order of magnitude of natural food products. The obtained dry pumpkin could be consumed as is, as a snack, or after rehydration and/or cooking.

On the other hand, it is known that more important than iron quantity is its accessibility and availability. In this study, the composition of used food material (pumpkin) and microcapsules wall material (maltodextrin) suggests a good absorption of this mineral. Studies reported that ascorbic acid and carotenoids are enhancers of iron absorption [1,40,41]. It means that the absorption of iron is enhanced in a food that contains these compounds. As reported by Nawirska-Olszańska, Stępień and Biesiada [42], de Carvalho, Gomes, Godoy, Pacheco, do Monte, de Carvalho, Nutti, Neves, Vieira and Ramos [43], the pumpkin specie (*Cucurbita moschata*) presents a high carotenoid content, reflecting its intense orange colour. Additionally, the pumpkin species also contain ascorbic acid, from 2 − 10 mg/100 g [36,37]. Consequently, it can be suggested that the iron incorporated in pumpkin presents a great possibility of being absorbed.

The ultrasound can be stated as an alternative to obtaining food with better nutritional quality. It is worth mention that more studies are needed to optimize this amount, according to population requirements, as well as more studies are needed to understand the iron accessibility and availability in this specific food matrix.

The importance of this work lies in the demonstration that by using ultrasound, it was possible to incorporate this mineral into the pumpkin matrix, which due to its characteristics, suggests a good absorption of the incorporated iron.

3.2. Carotenoid incorporation

Fig. 4 shows the optical microscopy of the sample surfaces before and after drying. Regarding the images of samples after pre-treatment, the first row (50X magnification) allows cells to be visualized, while the second row (25X magnification) allows visualization of the tissue. In the W samples, small isolated and scattered carotenoid microcapsules were observed, while in the samples W + US, isolated microcapsules and carotenoid “globules” were observed in greater proportion.

Apparently, with the US application, the microcapsules that entered the tissue were grouped. This would be possible since US, while generates modifications in the structure of the tissue (channel generation, cell wall rupture, air extraction), could also generate modifications in the structure of the carotenoid microcapsules. A possibility is that, due to US effects during processing, the walls of some microcapsules were broken before entering the tissue, others were broken within the cells and others enter and remain as microcapsules. Subsequently, when the released carotenoids were inside the cell or intercellular spaces of the tissue, they were rearranged due to hydrophobic interactions forming the observed “globules”. These changes could cause the carotenoids to be more exposed to deteriorating conditions. However, this was not observed, through the retention of carotenoids after drying (explained below). Fig. 4 shows that it is a fact that US promotes the carotenoid incorporation inside the tissue. However, the order in which the product and microcapsule structure modifications occur still needs to be better studied.

After drying, it was difficult to observe the incorporated carotenoid microcapsules in W samples, due to the structural modifications. However, in the W + US samples, the carotenoid microcapsules were observed inside the apple tissue (Fig. 4).

Fig. 5 shows the total carotenoid content in apple slices, before drying (after pre-treatments) and after drying. The blanched samples (Control) presented a carotenoid content of 0.06 ± 0.01 mg/g dry

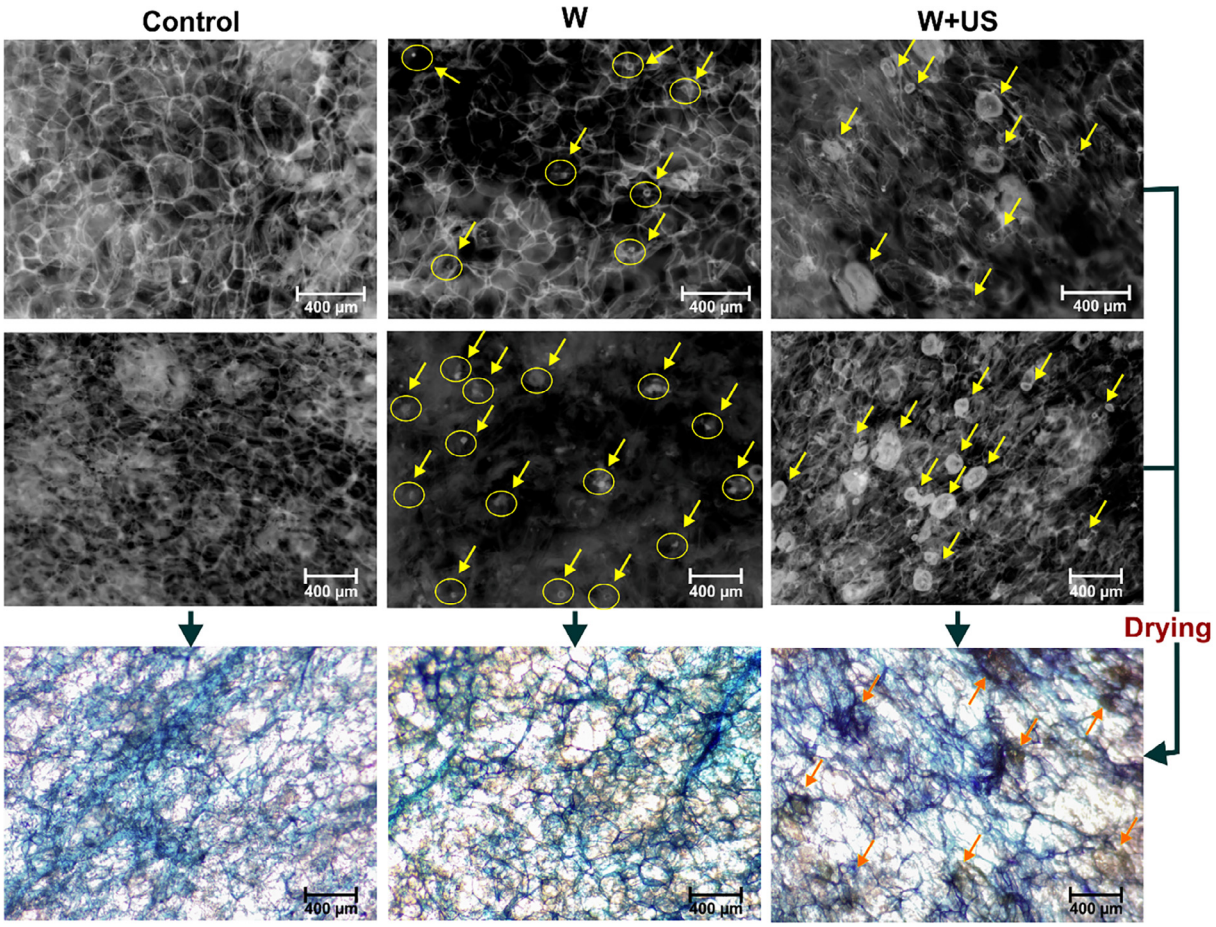

Fig. 4. Optical microscopy of apple samples after pre-treatments (up) and after drying (down). Images with negative filter allowed better visualization of carotenoid microcapsules after pre-treatments. Toluidine blue (0.1%) dye was used to mark cells and distinguish the carotenoid presence after drying. Arrows and circles indicate the carotenoid microcapsules or "globules". Control = *in-natura* apples after blanching; W = apple slices treated for 30 min in water containing carotenoid microcapsules; W + US = apple slices treated for 30 min in water containing carotenoid microcapsules under ultrasound. (For interpretation of the references to colour in this figure legend, the reader is referred to the web version of this article.)

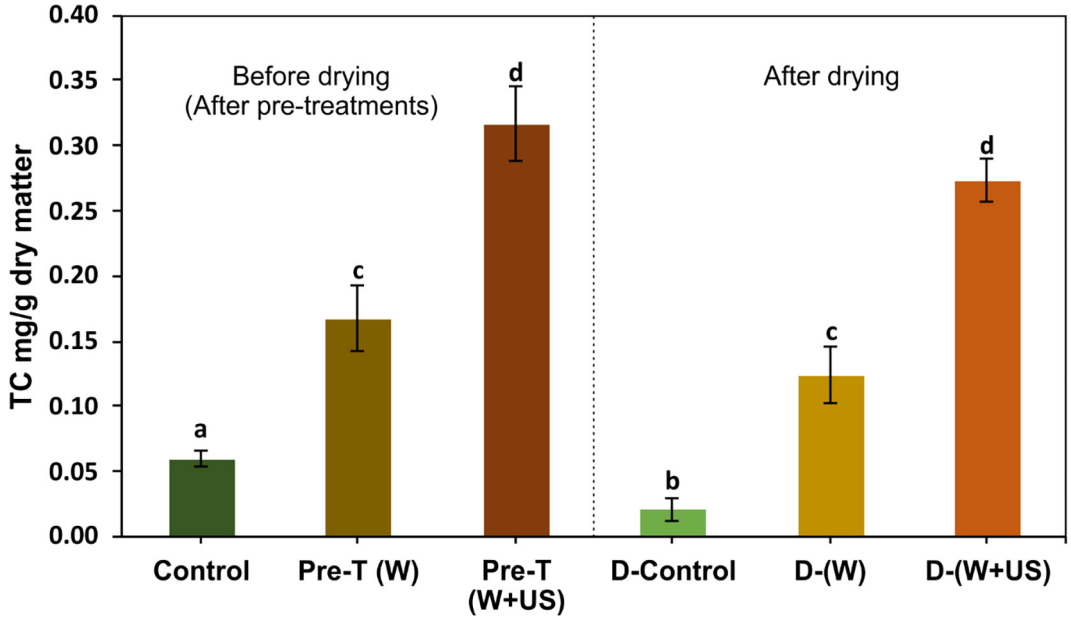

Fig. 5. Total carotenoid (TC) content before and after drying of the Control and pre-treated samples for 30 min without (W) and with US (W + US). Different letter indicates differences among treatments before, after drying, and differences between the same treatment before and after drying ($p < 0.05$).

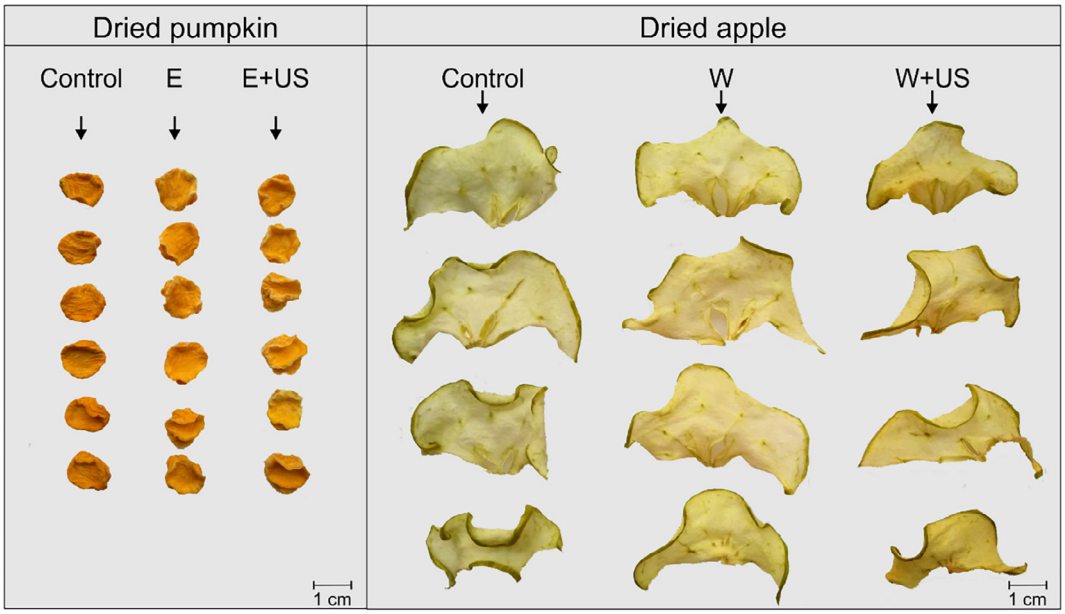

Fig. 6. Pumpkin and apple samples obtained after pre-treatments and drying.

matter of the flesh part, which is in accordance with the expected. Among the different apple cultivars, the yellow and red skinned apples are those that present higher carotenoid content (from 10 − 30 μg/g of dry flesh) in their flesh part [44]. The used apple cultivar (Granny Smith) is one of the non-red apple cultivar that presents the lowest carotenoid content [45].

A great increase in carotenoid content was observed after pre-treatments, with significant differences among these ($p < 0.05$). The obtained carotenoid content after pre-treatments was higher than those reported for the flesh part of pineapple, acerola or sweet potato, for example [46], which is remarkable.

In fact, compared to control, the samples immersed in the carotenoid microcapsules dispersion without US (W) increased their carotenoid content in about 181%, while, this increase was about 430% in samples processed with US (W + US). As far as we known, no studies have been conducted to incorporate carotenoid microcapsules using US processes. The obtained carotenoid increase was higher than the reported during osmotic dehydration process, in which pineapple [16] and mango samples [17] were impregnated with a carotenoid emulsion containing piquin pepper oleoresin. It was affirmed that carotenoids were incorporated into intercellular spaces of pineapple tissue, increasing the β-carotene content in 28%. However, although a partial dehydration is observed during osmotic dehydration, the obtained product is still unstable from a microbial view – highlighting the importance of studying the drying process.

When US was applied in solid foods, it causes different effects on the medium as a consequence of acoustic waves travel [3,47–51]. Based on these effects, different mechanisms occurring simultaneously, and they could be considered as the responsible for carotenoid incorporation in the apple matrix:

- The US generates acoustic streaming, increasing the convection of the dispersion containing the carotenoid microparticles, then promoting the contact of microparticles with apple surface.
- The US generates alternating compression and expansion of the tissue (the so called “sponge effect”), expelling the intercellular air and incorporating the fluid; then, the fluid and the microparticles could be incorporated inside the intercellular spaces.
- The US, trough acoustic cavitation and micro-jets, generates microchannels and cell wall disruption; then, the fluid and the microparticles could be incorporated inside the cells.

After drying, the carotenoid content decreased by 65% in Control samples (Fig. 5). Carotenoids are sensitive compounds, which are degraded by different oxidation mechanisms induced by heat, light, oxygen, interactions with radical species, enzymes, among others [9,20]. Consequently, a carotenoid content reduction is expected after hot-air drying as well as in other processes. Carotenoid content reduction of 27% was observed in carrot slices convectively dried (60 °C, 0.3 $m.s^{-1}$) [20], 40% of total carotenoid reduction was observed in papaya slices after thermal processing [52], and 29% of total carotenoid reduction in peach after freezing process [53].

In contrast with the control treatment, the carotenoid content of the apple slices incorporated with microparticles was reduced only 26% in W samples, and 14% in W + US samples (Fig. 5). Results suggest that despite the original structure modification of the microcapsules, the observed “globules” probably present the same rearranged wall as the original microcapsules, and it offers a protective effect with less degradation compared to the carotenoids naturally present. The final quantity in the dried samples, even considering the partial degradation, can still be considered high – highlighting the obtained results.

Furthermore, as observed, the carotenoid retention was higher when ultrasound was used. It is a relevant result, demonstrating that ultrasound is an interesting technology not only to incorporate carotenoid into foods but also to better retain it after drying. Different possibilities can be considered for promoting the carotenoid retention in samples processed with US:

- The control samples and pre-treated samples needed longer drying time than W + US samples, which needed ~20% less time to reach 25% moisture. It implies that, by using ultrasound, samples are less exposed to deteriorating conditions, then better retaining the carotenoid content.
- The carotenoid incorporated in the W samples probably remain principally in the intercellular spaces of the superficial sample regions; therefore, they were more susceptible to deterioration.
- The carotenoid in the W + US samples was probably incorporated more inside the tissue and maybe inside the cells, being more protected of deteriorating conditions during drying process, then decreasing the carotenoid degradation.

Fig. 6 shows the dried pumpkin and apple samples produced with the different performed treatments. In the pumpkin iron enriched samples, no visual differences were observed, while in the carotenoid enriched apples a slight orange coloration was appreciated compared to the control samples – however nothing so significant as to detract from the visual quality of the product.

3.3. Final consideration

This work shows an innovative possibility where the nutritional quality of the product could be improved by taking advantage of the pre-treatments with the use of US, which were originally made to improve drying [54]. It was demonstrated that the use of US increases the incorporation of nutrients regardless of the type of nutrient, either hydrophilic or lipophilic.

However, it should be mention that despite the objective was fulfilled, this work does not intend to be a reference from the nutritional point of view. Consequently, this work does not propose that the ferrous sulfate is the best source of iron for humans, that the paprika oleoresin is the best source of carotenoids for humans, that the evaluated wall materials are the best choice from a nutritional point of view, nor recommend the incorporation of nutrients in this way as a nutritional politic.

Even so, we highlight the importance of this work as a prospective study of using the microencapsulation and ultrasound technologies to obtain products with better quality, taking advantage of the process characteristics.

In fact, this work is the first step for future research.

Future studies must be performed to determine if the incorporated nutrients are bioavailable and bioaccessible, through different conditions of storage. Not only iron and carotenoids but also other nutrients and functional components can be incorporated into a different kind of food matrix, also considering different microcapsules (that must be optimized). In addition, ultrasound can be used for accelerating this process.

Therefore, an easier, cheaper and efficient way of food fortification or enrichment can be developed, and ultrasound can be a protagonist.

4. Conclusions

Fortified or enriched foods could be produced using US pre-treatment and microencapsulated nutrients. The performed pre-treatments allowed higher iron incorporation in pumpkin. US resulted in products with more homogeneous nutrient incorporation. Additionally, carotenoid microcapsules were incorporated in apple using US. Not only the incorporated carotenoid quantity was higher when US was used, but also better carotenoid retention was obtained after drying. The results show that pre-treatment with US can be used with a double purpose: both to improve drying (that has already been demonstrated) as well as to incorporate nutrients and obtain a high quality product. The obtained results are useful both from an industrial and academic perspective.

Acknowledgements

The authors are grateful to the São Paulo Research Foundation (FAPESP, Brazil) for funding the project n° 2016/18052-5; to the National Council for Scientific and Technological Development (CNPq, Brazil) for the productivity grant of P.E.D. Augusto (306557/2017-7); and to FONDECYT-CONCYTEC (Peru) for the M.L. Rojas Ph.D. scholarship (grant contract number 087-2016-FONDECYT).

Declarations of interest

None.

References

[1] FAO, Food Fortification: Technology and Quality Control, in: F.a.A.O.o.t.U. Nations (Ed.) FAO Food And Nutrition Paper – 60, Rome, 1996.
[2] C. Ricce, M.L. Rojas, A.C. Miano, R. Siche, P.E.D. Augusto, Ultrasound pre-treatment enhances the carrot drying and rehydration, Food Res. Int. 89 (2016) 701–708.
[3] A.C. Miano, M.L. Rojas, P.E.D. Augusto, Structural changes caused by ultrasound pretreatment: direct and indirect demonstration in potato cylinders, Ultrason. Sonochem. (2018).
[4] P.M. Azoubel, M. da Rocha Amorim, S.S.B. Oliveira, M.I.S. Maciel, J.D. Rodrigues, Improvement of water transport and carotenoid retention during drying of papaya by applying ultrasonic osmotic pretreatment, Food Eng. Rev. 7 (2015) 185–192.
[5] M.L. Rojas, P.E.D. Augusto, Ethanol and ultrasound pre-treatments to improve infrared drying of potato slices, Innovative Food Sci. Emerg. Technol. 49 (2018) 65–75.
[6] H. Tapiero, L. Gaté, K.D. Tew, Iron: deficiencies and requirements, Biomed. Pharmacother. 55 (2001) 324–332.
[7] M.A. Bryszewska, L. Tomás-Cobos, E. Gallego, M. Villalba, D. Rivera, D.L. Taneyo Saa, A. Gianotti, In vitro bioaccessibility and bioavailability of iron from breads fortified with microencapsulated iron, LWT 99 (2019) 431–437.
[8] E.C. Lopez Barrera, S. Gaur, J.E. Andrade, N.J. Engeseth, C. Nielsen, W.G. Helferich, Iron fortification of spiced vinegar in the Philippines, J. Food Sci. 83 (2018) 2602–2611.
[9] C.S. Boon, D.J. McClements, J. Weiss, E.A. Decker, Factors influencing the chemical stability of carotenoids in foods, Crit. Rev. Food Sci. Nutr. 50 (2010) 515–532.
[10] P. Fito, A. Chiralt, N. Betoret, M. Gras, M. Cháfer, J. Martínez-Monzó, A. Andrés, D. Vidal, Vacuum impregnation and osmotic dehydration in matrix engineering: application in functional fresh food development, J. Food Eng. 49 (2001) 175–183.
[11] Y. Deng, Y. Zhao, Effect of pulsed vacuum and ultrasound osmopretreatments on glass transition temperature, texture, microstructure and calcium penetration of dried apples (Fuji), LWT – Food Sci. Technol. 41 (2008) 1575–1585.
[12] B. Rerkasem, S. Fukai, L. Huang, Key factors affecting Fe density in Fe-fortified-parboiled rice: parboiling conditions, storage duration, external Fe-loading rate and genotypic differences, Food Chem. 123 (2010) 628–634.
[13] A.C. Miano, P.E.D. Augusto, The ultrasound assisted hydration as an opportunity to incorporate nutrients into grains, Food Res. Int. 106 (2018) 928–935.
[14] L. Xu, J.-R. Cheng, X.-M. Liu, M.-J. Zhu, Effect of microencapsulated process on stability of mulberry polyphenol and oxidation property of dried minced pork slices during heat processing and storage, LWT 100 (2019) 62–68.
[15] C. Gupta, P. Chawla, S. Arora, S.K. Tomar, A.K. Singh, Iron microencapsulation with blend of gum arabic, maltodextrin and modified starch using modified solvent evaporation method – Milk fortification, Food Hydrocolloids 43 (2015) 622–628.
[16] E.I. Salazar-López, M. Jiménez, R. Salazar, E. Azuara, Incorporation of microcapsules in pineapple intercellular tissue using osmotic dehydration and microencapsulation method, Food Bioprocess Technol. 8 (2015) 1699–1706.
[17] J. Jiménez-Hernández, E.B. Estrada-Bahena, Y.I. Maldonado-Astudillo, Ó. Talavera-Mendoza, G. Arámbula-Villa, E. Azuara, P. Álvarez-Fitz, M. Ramírez, R. Salazar, Osmotic dehydration of mango with impregnation of inulin and piquin-pepper oleoresin, LWT – Food Sci. Technol. 79 (2017) 609–615.
[18] H. Vatankhah, H.S. Ramaswamy, High pressure impregnation of oil in water emulsions into selected fruits: a novel approach to fortify plant-based biomaterials by lipophilic compounds, LWT 101 (2019) 506–512.
[19] L. Wang, B. Xu, B. Wei, R. Zeng, Low frequency ultrasound pretreatment of carrot slices: effect on the moisture migration and quality attributes by intermediate-wave infrared radiation drying, Ultrason. Sonochem. 40 (2018) 619–628.
[20] A. Rawson, B.K. Tiwari, M.G. Tuohy, C.P. O'Donnell, N. Brunton, Effect of ultrasound and blanching pretreatments on polyacetylene and carotenoid content of hot air and freeze dried carrot discs, Ultrason. Sonochem. 18 (2011) 1172–1179.
[21] R. Blanco-Rojo, M.P. Vaquero, Iron bioavailability from food fortification to precision nutrition. A review, Innovative Food Sci. Emerg. Technol. (2018).
[22] E. Uquiche, J.M. del Valle, J. Ortiz, Supercritical carbon dioxide extraction of red pepper (Capsicum annuum L.) oleoresin, J. Food Eng. 65 (2004) 55–66.
[23] D. Hornero-Méndez, J. Costa-García, M.I. Mínguez-Mosquera, Characterization of carotenoid high-producing Capsicum annuum cultivars selected for paprika production, J. Agric. Food. Chem. 50 (2002) 5711–5716.
[24] I.D. Alvim, M.A. Stein, I.P. Koury, F.B.H. Dantas, C.L.D.C.V. Cruz, Comparison between the spray drying and spray chilling microparticles contain ascorbic acid in a baked product application, LWT-Food Sci. Technol. 65 (2016) 689–694.
[25] A.L. Fadini, I.D. Alvim, I.P. Ribeiro, L.G. Ruzene, L.B.D. Silva, M.B. Queiroz, A.M.R.D.O. Miguel, F.C.M. Chaves, R.A.F. Rodrigues, Innovative strategy based on combined microencapsulation technologies for food application and the influence of wall material composition, LWT 91 (2018) 345–352.
[26] M.L. Rojas, P.E.D. Augusto, Ethanol pre-treatment improves vegetable drying and rehydration: kinetics, mechanisms and impact on viscoelastic properties, J. Food Eng. 233 (2018) 17–27.
[27] M.A. Silva, A.M.P. Braga, P.H.S. Santos, Enhancement of fruit drying: the ethanol effect, in: Proceedings of the 18th International Drying Symposium (IDS 2012), Xiamen, 2012.
[28] M. Vinatoru, Ultrasonically assisted extraction (UAE) of natural products some guidelines for good practice and reporting, Ultrason. Sonochem. 25 (2015) 94–95.
[29] T.J. Mason, D. Peters, Practical Sonochemistry: Power Ultrasound Uses and Applications, PHorwood Publishing Limited, 2004.
[30] A.R. Jambrak, T.J. Mason, L. Paniwnyk, V. Lelas, Ultrasonic effect on pH, electric conductivity, and tissue surface of button mushrooms, brussels sprouts and

cauliflower, Czech J. Food Sci. 25 (2007) 90–100.
[31] S. Jaspart, P. Bertholet, G. Piel, J.-M. Dogné, L. Delattre, B. Evrard, Solid lipid microparticles as a sustained release system for pulmonary drug delivery, Eur. J. Pharm. Biopharm. 65 (2007) 47–56.
[32] L.E. Ordoñez-Santos, D.P. Ledezma-Realpe, Lycopene concentration and physico-chemical properties of tropical fruits, Food Nutr. Sci. 4 (2013) 758.
[33] D.C. Potosí-Calvache, P. Vanegas-Mahecha, H.A. Martínez-Correa, Convective drying of squash (Cucurbita moschata): influence of temperature and air velocity on effective moisture diffusivity, carotenoid content and total phenols, DYNA 84 (2017) 112–119.
[34] T. Tezotto, J.L. Favarin, A. Paula Neto, P.L. Gratão, R.A. Azevedo, P. Mazzafera, Simple procedure for nutrient analysis of coffee plant with energy dispersive X-ray fluorescence spectrometry (EDXRF), Scientia Agricola 70 (2013) 263–267.
[35] N.G. Paltridge, P.J. Milham, J.I. Ortiz-Monasterio, G. Velu, Z. Yasmin, L.J. Palmer, G.E. Guild, J.C.R. Stangoulis, Energy-dispersive X-ray fluorescence spectrometry as a tool for zinc, iron and selenium analysis in whole grain wheat, Plant Soil 361 (2012) 261–269.
[36] USDA, National, nutrient database for standard reference legacy release, in, agricultural research service from the united states department of, Agric. Maryland (2018).
[37] NEPA-UNICAMP, Tabela brasileira de composição de alimentos/Brazilian table of food composition., in, Campinas-SP, 2011, p. 161.
[38] M. Mashkour, Y. Maghsoudlou, M. Kashaninejad, M. Aalami, Effect of ultrasound pretreatment on iron fortification of potato using vacuum impregnation, J. Food Process. Preserv. (2018) e13590.
[39] P.O.M. Institute of Medicine, Iron, in: Dietary Reference Intakes for Vitamin A, Vitamin K, Arsenic, Boron, Chromium, Copper, Iodine, Iron, Manganese, Molybdenum, Nickel, Silicon, Vanadium, and Zin, National Academies Press, Washington (DC), 2001.
[40] R. González Urrutia, Biodisponibilidad del hierro, Revista costarricense de salud pública 14 (2005) 6–12.
[41] M.N. García-Casal, Carotenoids increase iron absorption from cereal-based food in the human, Nutr. Res. 26 (2006) 340–344.
[42] A. Nawirska-Olszańska, B. Stępień, A. Biesiada, Effectiveness of the fountain-microwave drying method in some selected pumpkin cultivars, LWT 77 (2017) 276–281.
[43] L.M.J. de Carvalho, P.B. Gomes, R.L.D.O. Godoy, S. Pacheco, P.H.F. do Monte, J.L.V. De Carvalho, M.R. Nutti, A.C.L. Neves, A.C.R.A. Vieira, S.R.R. Ramos, Total carotenoid content, α-carotene and β-carotene, of landrace pumpkins (Cucurbita moschata Duch): a preliminary study, Food Res. Int. 47 (2012) 337–340.
[44] R. Delgado-Pelayo, L. Gallardo-Guerrero, D. Hornero-Méndez, Chlorophyll and carotenoid pigments in the peel and flesh of commercial apple fruit varieties, Food Res. Int. 65 (2014) 272–281.
[45] P. Kumar, S. Sethi, R.R. Sharma, S. Singh, S. Saha, V.K. Sharma, M.K. Verma, S.K. Sharma, Nutritional characterization of apple as a function of genotype, J. Food Sci. Technol. 55 (2018) 2729–2738.
[46] E.N. Ellong, C. Billard, S. Adenet, K. Rochefort, Polyphenols, carotenoids, vitamin C content in tropical fruits and vegetables and impact of processing methods, Food Nutr. Sci. 6 (2015) 299.
[47] K. Yasui, Chapter 3 - dynamics of acoustic bubbles, in: F. Grieser, P.-.K. Choi, N. Enomoto, H. Harada, K. Okitsu, K. Yasui (Eds.), Sonochemistry and the Acoustic Bubble, Elsevier, Amsterdam, 2015, pp. 41–83.
[48] R.K. Gould, Rectified diffusion in the presence of, and absence of, acoustic streaming, J. Acoust. Soc. Am. 56 (1974) 1740–1746.
[49] T.Y. Wu, N. Guo, C.Y. Teh, J.X.W. Hay, Theory and fundamentals of ultrasound, Advances in Ultrasound Technology for Environmental Remediation, Springer, 2013, pp. 5–12.
[50] A.C. Miano, A. Ibarz, P.E.D. Augusto, Mechanisms for improving mass transfer in food with ultrasound technology: describing the phenomena in two model cases, Ultrason. Sonochem. 29 (2016) 413–419.
[51] J. Cárcel, J. García-Pérez, J. Benedito, A. Mulet, Food process innovation through new technologies: use of ultrasound, J. Food Eng. 110 (2012) 200–207.
[52] M.P. Cano, B. de Ancos, G. Lobo, M. Monreal, Effects of freezing and canning of papaya slices on their carotenoid composition, Zeitschrift für Lebensmittel-Untersuchung und Forschung 202 (1996) 279–284.
[53] A. Oliveira, E.M.C. Alexandre, M. Coelho, R.M. Barros, D.P.F. Almeida, M. Pintado, Peach polyphenol and carotenoid content as affected by frozen storage and pasteurization, LWT – Food Sci. Technol. 66 (2016) 361–368.
[54] Ó. Rodríguez, V. Eim, C. Rosselló, A. Femenia, J.A. Cárcel, S. Simal, Application of power ultrasound on the convective drying of fruits and vegetables: effects on quality, J. Sci. Food Agric. 98 (2018) 1660–1673.

APPENDIX VIII: Simple abstracts (English, Português, Castellano, Valencià)

Simple abstract

Food drying has been used since ancient times to store and to have disponible products for longer periods. However, in the present time the processes normally used by the industries demand a great amount of energy, and the food obtained also present some problems (for example, the degradation of nutrients). The present Thesis intends to propose improvements to these problems, by studying the application of ethanol, high power ultrasound and mechanical perforations (emerging technologies) as pre-treatments to the drying process. These technologies have been applied to improve different types of drying processes and different food properties. The results obtained show that, by using the proposed technologies, the food products dry much faster, thus reducing the energy consumption, and the products obtained have better characteristics. For example, they absorb more water and quicker, and retain better the nutrients. Furthermore, by using the technologies proposed, it was also possible to incorporate nutrients into foods that were dried, thus obtaining products with better nutritional quality.

Resumo simples

A secagem de alimentos tem sido utilizada desde tempos antigos para armazenar e dispor de alimentos por períodos mais longos. No entanto, atualmente, os processos normalmente utilizados pelas indústrias apresentam elevado consumo energético, e os alimentos obtidos podem apresentar problemas (por exemplo, a degradação de nutrientes). A presente Tese pretende propor melhorias para esses problemas através da aplicação de etanol, ultrassom de alta potência e perfurações mecânicas (tecnologias emergentes) como pré-tratamentos para o processo de secagem. Essas tecnologias foram aplicadas para melhorar diferentes processos de secagem e diferentes propriedades nos produtos. Os resultados obtidos demonstram que, utilizando as tecnologias propostas, é possível que os alimentos sequem muito mais rápido, reduzindo o consumo de energia e os produtos obtidos tenham melhores características. Por exemplo, eles absorvem mais água e mais rapidamente, e retêm melhor os nutrientes. Ainda, utilizando as tecnologias propostas, também foi possível incorporar nutrientes nos alimentos secos, obtendo produtos com melhor qualidade nutricional.

Resumen sencillo

El secado de alimentos se utiliza desde tiempos antiguos para poder almacenar y disponer de productos por mayor tiempo. Sin embargo, en la actualidad los procesos normalmente utilizados por las industrias aún demandan de mucha energía, y el alimento obtenido presenta también problemas (por ejemplo, la degradación de nutrientes). La presente tesis pretende proponer mejoras a estos problemas mediante la aplicación de etanol, ultrasonido de alta potencia y perforaciones mecánicas (tecnologías emergentes) como tratamientos previos al proceso de secado. Estas tecnologías fueron aplicadas para mejorar diferentes tipos de procesos de secado y diferentes propiedades de los alimentos. Los resultados obtenidos demostraron que mediante el uso de las tecnologías propuestas se consiguió que los alimentos sequen mucho más rápido, disminuyendo por lo tanto el consumo energético, además, los productos obtenidos presentaron mejores características. Por ejemplo, absorben más agua, no se deforman, y retienen mejor sus nutrientes. Por otro lado, utilizando las tecnologías propuestas también se logró incorporar nutrientes a los alimentos que fueron secados, obteniendo entonces productos con mejor calidad nutricional.

Resum senzill

L'assecat d'aliments s'utilitza des de temps antics per a poder emmagatzemar i disposar de productes per major temps. No obstant això, en l'actualitat els processos normalment utilitzats per les indústries encara demanden de molta energia, i l'aliment obtingut presenta també problemes (per exemple, la degradació de nutrients). La present tesi pretén proposar millores a aquests problemes mitjançant l'aplicació d'etanol, ultrasò d'alta potència i perforacions mecàniques (tecnologies emergents) com a tractaments previs al procés d'assecat. Aquestes tecnologies van ser aplicades per a millorar diferents tipus de processos d'assecat i diferents propietats dels aliments. Els resultats obtinguts van demostrar que mitjançant l'ús de les tecnologies proposades es va aconseguir que els aliments assequen molt més ràpid, disminuint per tant el consum energètic, a més, els productes obtinguts van presentar millors característiques. Per exemple, absorbeixen més aigua, no es deformen, i retenen millor els seus nutrients. D'altra banda, utilitzant les tecnologies proposades també es va aconseguir incorporar nutrients als aliments que van ser assecats, obtenint llavors productes amb millor qualitat nutricional.